Author:
Alvino, Valeria V

Title:
Preclinical studies of swine pericytes for treatment of congenital and adult cardiac disease

PRECLINICAL STUDIES OF SWINE PERICYTES FOR TREATMENT OF CONGENITAL AND ADULT CARDIAC DISEASE

VALERIA VINCENZA ALVINO

A dissertation submitted to the University of Bristol in accordance with the requirements of the degree of Philosophiae Doctor in the Department of Translational Health Sciences, Bristol Medical School, Bristol

December 2019

43,037 words

ABSTRACT

Background. We have previously reported that it is possible to use human pericytes obtained from remnants of palliative surgery in neonatal patients with congenital heart disease to engineer animal-derived prosthetic grafts. The working hypothesis is that pericytes isolated from cardiac tissue at the occasion of palliation can be expanded and incorporated in prosthetic grafts forming a living tissue implantable for definitive correction of the heart defect. In order to obtain proof of concept in an *in vivo* large animal model, we sought to use autologous swine cardiac pericytes as a surrogate of the human cell product, thereby surmounting the problem of immune rejection of xenogeneic cells. This thesis illustrates the progressive steps of the manufacture process of a swine cardiac pericyte engineered vascular conduit and the first demonstration of implantation in a piglet pulmonary artery.

Methods and Results. The first step consisted of an adaptation of the isolation/expansion procedure previously set up for human cardiac pericytes using swine customized reagents. Neonatal human and swine CPs were similar in terms of cardiac anatomical localization and antigenic profile following isolation using immunomagnetic beads and culture expansion. Like human pericytes, swine surrogates form clones after single cell sorting, secrete angiogenic factors and extracellular matrix proteins, and support endothelial cell migration and network formation *in vitro*. Seeded and unseeded (control) vascular CorMatrix® patches were kept under static culture conditions for five days, and then, were shaped into a conduit to reproduce a vessel and incubated in a bioreactor system under a perfused flow for one or two weeks. Immunohistochemistry studies showed the viability and integration of swine pericytes into the outer layer of the conduit. Acellular or pericyte-engineered conduits were implanted in two 9-week old piglets to replace the left branch of the main pulmonary artery. After four months, the anatomical and functional integration of the grafts was assessed by Doppler echocardiography and cardiac magnetic resonance imaging. The extracellular matrix remodeling, vascularization and microcalcifications were evaluated by immunohistochemistry.

Conclusions. This work demonstrates the feasibility of using neonatal swine cardiac pericytes for the reconstruction of a pulmonary artery branch in a piglet model. These results pave the way to novel tissue engineering solutions for correction of congenital heart disease using autologous cardiac pericytes

DEDICATIONS AND ACKNOWLEDGMENTS

My first heartfelt thanks are to my supervisor Professor Paolo Madeddu. You have been a guide, a teacher and a mentor. You supported me day by day with enthusiasm and passion, making yourself a great inspiration to me. Thank you for believing in me and in the project, for supporting and pushing me when needed, for letting me grow and develop my own skills and knowledge by giving me the opportunity to make mistakes and learn from these.

I would like to express my gratitude to Professor Massimo Caputo, without you and your decision to trust and rely on a person you didn't know I would never start working at the BRI, the opportunity you gave me is a precious gift and I am very grateful for this.

Thank you to my colleagues and friends Helen, Elisa, Sadie and Iker. My journey in research has started with you guys, you have thought me a lot and helped me to manage stressful situations in the lab. I would like to thank our core technicians, Paul and Jan, and other colleagues and clinicians on the level 7 Research floor that it would be difficult to list here.

A special thanks to my fabulous husband, Nando who has encouraged me in the difficulties of life during our fourteen years together and supported me in the hardest parts of my work. Without your help, all this would have been very tough. Thank you!

Finally, a huge thank you to my parents for the continuous support and belief in me. All I have done and every single step that brought me here at this point is because you have given me the huge opportunity to do so, and I know how much effort both of you put into this. Thank you, mum and dad!

AUTHOR'S DECLARATION

I declare that the work in this dissertation was carried out in accordance with the requirements of the University's Regulations and Code of Practice for Taught Postgraduate Programmes and that it has not been submitted for any other academic award. Except where indicated by specific reference in the text, this work is my own work. Work done in collaboration with, or with the assistance of others, is indicated as such. I have identified all material in this dissertation which is not my own work through appropriate referencing and acknowledgement. Where I have quoted from the work of others, I have included the source in the references/bibliography. Any views expressed in the dissertation are those of the author.

SIGNED: …… DATE: ……..

PLAGIARISM DECLARATION

I declare that some of the text used in this thesis has been taken from the published papers "**Alvino, VV** et al. 2020. *In vitro preclinical testing of pericyte-engineered grafts for the correction of congenital heart defects*" and "**Alvino, VV**. et al. 2018. *Transplantation of allogeneic pericytes improves myocardial vascularization and reduces interstitial fibrosis in a swine model of reperfused acute myocardial infarction*. J Am Heart Assoc." I declare that the text utilised was written by my supervisor and by myself.

SIGNED BY FIRST AUTHORS: …….. DATE: ……..

SIGNED BY SENIOR AUTHOR: …….. DATE: ……..

I also declare that some of the text used in this thesis has been taken from the published review "Avolio E., **Alvino, VV.** et al. 2017. *Perivascular cells and tissue engineering: current applications and untapped potential.* Pharmacol Ther" and from the published paper "Avolio, E., **Alvino VV**. et al. 2015. *Expansion and characterization of neonatal cardiac pericytes provides a novel cellular option for tissue engineering in congenital heart disease*" in which I contributed for writing and experiments, respectively.

SIGNED BY FIRST AUTHORS: …….. DATE: ……..

SIGNED BY SENIOR AUTHOR: …….. DATE: ……..

TABLE OF CONTENTS

LIST OF FIGURES

LIST OF TABLES

LIST OF ABBREVIATION

A

ACC	American college of cardiology
ACE	Angiotensin converting enzyme
ACHD	Adult congenital heart disease
AHA	America heart association
ALP	Alkaline phosphatase
ANG 1/2	Angiopoietin 1/2
APCs	Adventitial saphenous vein pericytes
ASD	Atrial septal defect
AVCD	Atrioventricular canal defect

B

BBB	Blood-brain-barrier
BCA	Bicinchoninic acid assay
bFGF	Basic fibroblast growth factor
BM	Bone marrow
BNP	Brain natriuretic peptide
BRB	Blood-retinal-barrier
BSA	Bovine serum albumin

C

CABG	Coronary artery bypass graft
CALP	Calponin
CDCs	Cardiosphere-derived cells
CHD	Congenital heart disease
CM	Conditioned media
CMR	Cardiovascular magnetic resonance
CNIC	Centro National de Investigations Cardiovasculares
CNS	Central nervous system
COL	Collagen
CPCs	Cardiac progenitor cells
CPs	Cardiac pericytes
CT	Computer tomography

D

DAPI	4’,6-diamidin-2-fenilindolo
DMEM	Dulbecco’s modified Eagle medium
DMD	Duchenne muscular dystrophy
DMSO	Dimethyl sulfoxide
DPBS	Dulbecco’s phosphate buffered saline
DPX	Distyrene plastyciser xylene
DT	Doubling time

E

EBM-2	Endothelial basal medium-2
ECM	Extracellular matrix
ECs	Endothelial cells
EDTA	Ethylenediaminetetraacetic
EdU	5-ethynyl-2’-deoxyuridine
EGM-2	Endothelial cell growth media-2
ELISA	Enzyme linked immunosorbent assay
eNT	ectonucleotidase
EPCs	Endothelial progenitor cells
ESCs	European Society of Cardiology
EthD-1	Ethidium-homodimer-1
EVG	Elastic tissue-Van Gieson’s

F

FACS	Fluorescent activated cell sorting
FBS	Foetal bovine serum
FDA	Food and drug administration
FMO	Fluorescent minus one

G

GAG	Glyocosamminoglycan
GFP	Green fluorescent protein
GFs	Growth factors
GMP	Good manufacturing practice

H

H&E	Hematoxylin and Eosin
hCPs	Human cardiac pericytes
HF	Heart failure
HLHS	Hypoplastic left heart syndrome
hNB CPs	Human new-born cardiac pericytes
HUVECs	Human umbilical cord vein endothelial cells

I

ICC	Immunocytochemistry
ID	Internal diameter
IF	Immunofluorescence
IHC	Immunohistochemistry
IL-10	Interleukin-10
iPSCs	Induced pluripotent stem cells

L

LA	Left atrium
LAD	Left anterior descending
LPA	Left pulmonary artery
LV	Left ventricle

M

MHRA	Medicines and Healthcare products Regulatory Agency
MI	Myocardial infarction
MMP	Metalloproteinases
MPA	Main pulmonary artery
mRNA	Messenger ribonucleic acid
MSCs	Mesenchymal stem cells
MW	Molecular weight

N

NG2	Neural/glial antigen 2

O

OCT	Optimal cutting temperature
OCT-4	Octamer-binding transcriptional factor 4
OD	Optical density
ODI	Outer diameter
OX-LDLs	Oxidized low-density lipoproteins

P

PA	Pulmonary artery
PAD	Peripheral artery disease
PAGE	Polyacrylamide gel electrophoresis
PB	Post-bioreactor
PBMNCs	Peripheral blood mononuclear cells
PBS	Phosphate buffered saline
PCL	Polycaprolactone
PCR	Polymerase chain reaction
PDA	Patent ductus arteriosus
PDGFRβ	Platelet-derived-growth factor receptor beta
PET	Positron emission tomography
PFA	Paraformaldehyde
PGA	Poly-glycolic acid
PLLA	Poly-lactic acid
PS	Post-static
PTFE	Polytetrafluoroethylene
PVDF	Polyvinylidene difluoride

R

RA	Right atrium
RAS-MAPK	Rasopathy-mitogen-activated protein kinase
RG5S	Regulator G-protein signalling 5
RNA	Ribonucleic acid
RPM	Rotation per minute
RV	Right ventricle
RVEF	Right ventricular ejection fraction
RVOT	Right ventricular outflow tract

S

sCPs	Swine cardiac pericytes
SD	Standard deviation
SDS	Sodium dodecyl sulphate
SEM	Standard error of the mean
SIS-ECM	Swine intestinal submucosa extracellular matrix
SMMHC11	Smooth muscle myosin heavy chain 11
SMTN	Smoothelin
SOP	Standard operating procedure
SOX-2	Sex determing region Y
SNB CPs	Swine new-born cardiac pericytes
sPAECs	Swine pulmonary artery endothelial cells
SV	Saphenous vein

T

T-MSCs	Thymus-mesenchymal stem cells
TAGLN	Transgelin
TBS-T	Tris-buffered saline- Tween-20
TE	Tissue engineering
TEVG	Tissue engineering vascular graft
TGFβ1	Transforming growth factor beta 1
Tie-2	Tyrosine kinase with Immunoglobulin-like and EGF-like domains 2
TOF	Tetralogy of Fallot

U

UBC-MNCs	Umbilical cord-mononuclear cells
UCM	Unconditioned media
UV	Ultraviolet

V

VECs	Valve endothelial cells
VEGF	Vascular endothelial growth factor
VEGFR2	Vascular endothelial growth factor receptor 2
VICs	Valve interstitial cells

VSD	Ventricular septal defect
VSMCs	Vascular smooth muscle cells

W

WB	Western blot

α

α-SMA	Alpha-smooth muscle actin

1 Introduction

1.1 Congenital heart disease

Congenital heart disease (CHD) is the most common type of birth disorders and it was defined by *Mitchell SC et al* as "a gross structural abnormality of the heart or intrathoracic great vessels" (Mitchell et al. 1971).

In the last decades there was a remarkable improvement in the surgical techniques for correction of different forms of CHD. Yet, a definitive solution is rarely achieved especially in patients with complex malformations. Therefore, the goal of the present work is to investigate the possibility of improving current prostheses by engineering them with cardiac pericytes. The rationale is that these cells will confer the prosthesis with the properties of a living tissue capable of adapting to the recipient immediately upon implantation and of remodelling long term in synchrony with the heart growth.

This thesis comprises a description of the clinical problem, the rationale of tissue engineering, experimental methodology, results and discussion in the light of current knowledge. I also report data of a published study, where I firstly demonstrated the identity of human and swine pericytes and the feasibility of using them for the treatment of ischemia in a swine model of reperfused myocardial infarction (MI).

1.1.1 Epidemiology

Although there is negligible variation among the population-based statistical studies, in the UK the prevalence of CHD is ~ 1% of live births, with a similar prevalence worldwide, and the incidence is ~ 5000 babies born annually (Avolio et al. 2015a; Triedman and Newburger 2016; Bouma and Mulder 2017).

The introduction of cardiopulmonary bypass in 1950s allowed efficient treatments of simple and complex forms of CHD becoming a standard practice, available worldwide, in the care of these defects. These procedures have improved dramatically the long-term survival bringing a new class of CHD patients called adults with congenital heart disease (ACHD). For the treatment of simple defects, research is focused on the procedure to increase the efficacy, safety and to provide high-quality life to infants and children living particularly in countries with limited healthcare centres and budget. On the other end of the spectrum of disease severity, the outcomes continue to improve in patients with complex malformations (**Figure 1-1**) (Erikssen et

al. 2015). Considering all complex defects, cumulative survival to 16 years of age in patients underwent surgery in 1971 to 1989 was ~ 60% versus ~ 85% in 1990 to 2011. Childhood survival is now well established even in the most complex forms of CHD, such as, univentricular heart syndrome. However, as the early benefits of cardiac intervention and surgical repair in childhood have become routine, the flip side of the improved long-term survival is the presence of many CHD complications emerged in adulthood. The percentage of CHD-related deaths occurring in different age-group, by period of death, are shown in **Figure 1-2** (Knowles et al. 2012). Infants comprised >50% of CHDs until the period 1979-1983, but now they represent ~ 20% of all CHD deaths. On the other hand, ~ 20% of CHD deaths between 1959 and 1973 were adults, whereas most deaths now occur within this age-range. The exact long-term efficacy of different CHD therapies is hard to compare overtime because of the constant evolution of different strategies of therapy and the long-life expectation. In addition, the evolution of these treatments may delay the complication onset making difficult the comparison of the efficacy of different treatments (Triedman and Newburger 2016).

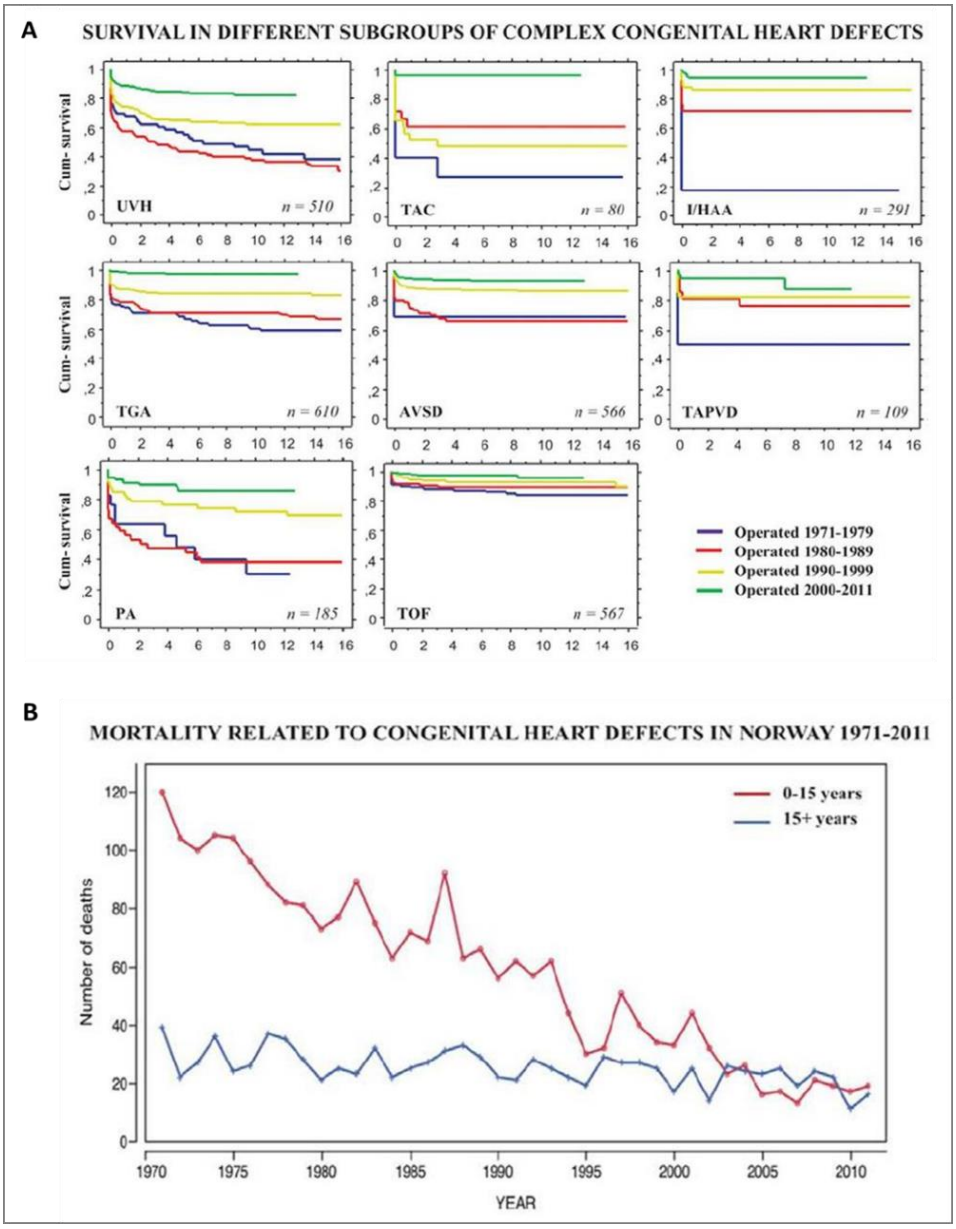

Figure 1- 1. A. Post-operative survival until 16 years old for complex CHD. *Abbreviations*: AVSD= atrioventricular septal defects; I/HAA= interrupted or hypoplastic aortic arch; PA= pulmonary atresia; TAC= truncus arteriosus communis; TAPVD= totally anomalous pulmonary venous drainage; TGA= transposition of the great arteries; TOF= tetralogy of Fallot; UVH= univentricular hearts. B. Mortality related to CHD in Norway between 1971-2011. Figure source: Erikssen et al., 2015, American Heart Association (AHA), Inc.

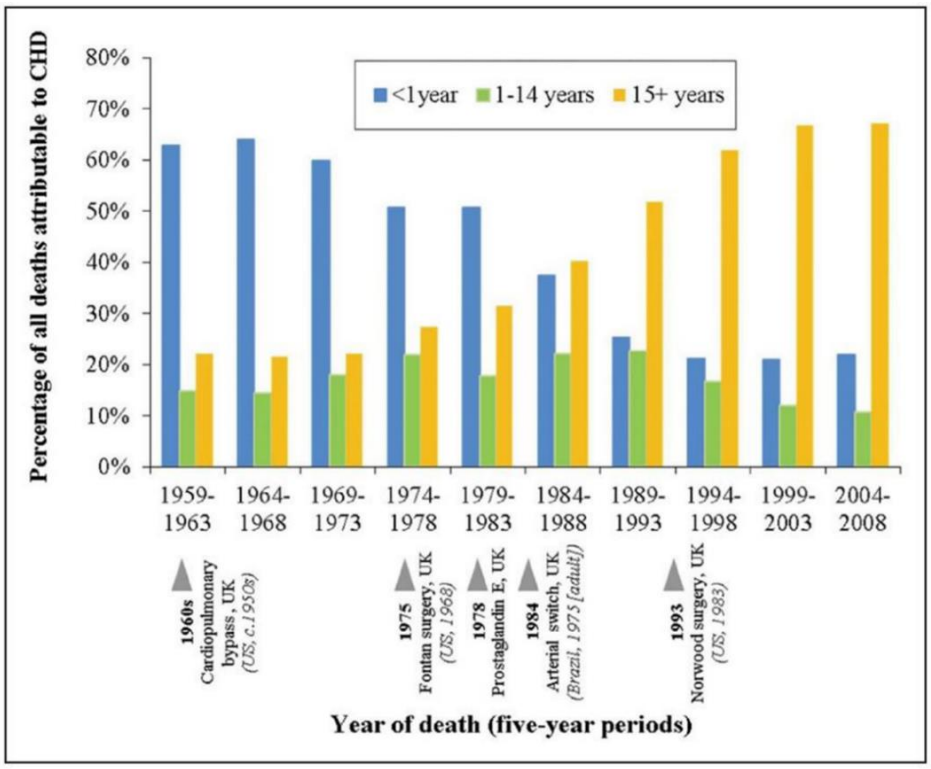

Figure 1- 2. Percentage of all the deaths for CHD in England and Wales between 1959 and 2008 assessed in three groups of age. Figure source: Knowles et al., 2012, Archives of disease in childhood, British Medical Journal (BMJ).

1.1.2 Classification of congenital heart disease

1.1.2.1 Healthy heart anatomy and function

The heart is a muscle tissue which pumps blood throughout our body. It has four anatomical chambers: two upper chambers which are right atrium (RA) and left atrium (LA), and two lower chambers which are right ventricle (RV) and left ventricle (LV). These chambers are separated by a septum. Blood flows inside the chambers *via* four different valves. The function of the valves is to open and close to allow blood flowing in only one direction.

- Tricuspid valve, which connects the RA and RV
- Pulmonary valve, which connects the RV and pulmonary artery (PA)
- Mitral valve, which connects LA and LV
- Aortic valve located between LV and aorta

The normal blood flow cycle follows the route body-heart-lungs-heart-body. Deoxygenated blood coming from the systemic circulation returns to the heart and enters the RA and flows in the RV through the tricuspid valve. Using a low pressure, RV pumps blood into the PA through

the pulmonary valve. Then, blood goes to the lungs to become oxygenated. From lungs, oxygenated blood flows into the LA and, from here, passes into LV *via* mitral valve. Under high pressure, blood is pumped into the aorta which, in turn, takes blood for the systemic circulation.

1.1.2.2 Heart development for the understanding of congenital heart defects

Recent molecular heart development studies unravelled the basic developmental mechanisms of normal and abnormal cardiovascular development. In order to understand what it has been previously discussed about the post-natal heart anatomy, a brief step back to the foetal development and to the formation of the three germ layers will be necessary.

During the 1st week of embryonic life, fertilized egg develops into blastocyst and implants in the mother's uterus. During the 2nd week of embryonic development, the implanted blastocyst penetrates deeper in the uterine wall and primitive placenta begins to form. At the 3rd week, a primitive umbilical cord develops. Furthermore, at this stage blastocyst develops in three-layer disks: endoderm (inner layer), mesoderm (middle layer), and ectoderm (out layer). Specific body systems will develop from each layer. The mesoderm gives rise to heart, vascular system, dermis, muscle, sex glands, lymph glands, kidney, connective tissue, blood cells, and subcutaneous tissue (Moorman et al. 2003).

Early in the development, the primitive heart in the form of a cardiac crescent develops as two tubes called first and second heart field constituted by progenitor cardiogenic mesodermal cells. These two tubes merge as one single tube which begins to swell and develops into various anatomical features of the heart. Heart begins to beat by the 3rd week of development. In normal cardiac development, the cardiac tube will twist and turn on itself in a rightward direction, this is called "dextral looping". This results in the RV developing on the right side of the heart and LV developing on the left side of the heart. Abnormal looping in a leftward direction is called "levo looping". This results in the RV developing on the left side of the heart, and LV developing on the right side of the heart (Kloesel et al. 2016).

Entering the 4th week of the embryonic life, the atrial and ventricular septum begin to form. The atrial septum grows in layers and includes tissues, such as, septum primum, septum secundum and endocardial cushion tissue. The latter is in the middle of the heart and from it rises tricuspid valve, mitral valve, part of the atrial and ventricular septum. Septum primum grows downward between RA and LA and it eventually fuses with endocardial cushion. The septum secundum grows in parallel with septum primum. Both septa develop with holes in them to create a

passageway from blood to flow from RA to LA through the foramen ovale. If the pressures on the RA are higher than pressures on the LA, the passage will stay open to allow blood to flow from right to left side. Errors may occur during atrial separation in secundum atrial septal defect (ASD), opening in the middle of atrial septum and produced when the tissue of septum primum does not reach the septum secundum adequately to close completely the wall, or when a tiny hole is left in the septum primum as the tissue is grown. In primum ASD, the hole is in the lower part of the atrial septum near the tricuspid and mitral valves. It results in problems of growth of the endocardial cushion tissue. Defects here are often associated with defects in the mitral and tricuspid valves. The most severe form of this alteration is atrioventricular canal defects (AVCDs). The aorta and PA develop from a single tubular structure, the truncus arteriosus. Two areas of a ticker tissue project into the lumen of this tube on the right and left side, as they continue to grow, these regions meet and fuse to form a septum which takes a spiral course through the end of this tube. This septum divides the truncus arteriosus into two vessels, the aorta and PA. The conal tissue involved in the separation of the truncus arteriosus also directs the placement of the aorta and PA over their ventricles.

By the 5^{th} week of embryonic life, the ventricular septum continues to grow, the muscular portion of ventricular septum develops from bulb ventricular flange, which is derived from the differential growth of primitive ventricle and bulbus cordis, and the membranous septum develops from the endocardial cushion tissue. Conal tissue contributes to the complete closure of the septum between the aortic and pulmonary valves.

By the 6^{th} and 7^{th} weeks of embryonic life, the ventricular septum completely separates into RV and LV. Errors may occur during the ventricular septation: muscular defects can occur in any portion of the muscular septum, for instance small defects close on their own as the tissues develop; membranous defects allocated behind the septal leaflets of tricuspid valve; sub-pulmonary defects are caused by deficiency of canal septum; AVCDs are caused by defects in the endocardial cushion tissue of the atrioventricular septum.

The aorta, PA and their branching vessels are formed by the brachial arch arteries. Initially there are six pairs of brachial arch arteries. The first, second and fifth pairs disappear forming ligaments which hold the heart in place. The third aortic arch forms the common carotid artery and internal carotid arteries. The fourth carotid arch forms part of the final aortic arch and the proximal portion of the right subclavian artery, the sixth carotid arch forms the proximal branch of PA, the ductus arteriosus, and provides pulmonary blood flow *via* the branch and develops lung buds. Alterations occurring in the arch formation result in different cardiac defects, such as, coartaction of the aorta, interrupted aortic arch, aortic atresia, patent ductus arteriosus

(PDA), and vascular ring. By the 8th week of embryonic development, the heart resembles the post-natal heart in structure and functions, and it will continue to grow and develop over the next 30th and 32nd weeks (**Figure 1-3**) (Moorman et al. 2003; Gittenberger-de Groot et al. 2005; Kloesel et al. 2016).

Genetic reasons are responsible of the different errors occurring in the foetal cardiac development. However, non-genetic factors may contribute to the disruption of the normal heart development. In the following paragraphs, the genetic and non-genetic factors determing the development of the heart congenital malformations will be better explained (Mahler and Butcher 2011; Kloesel et al. 2016).

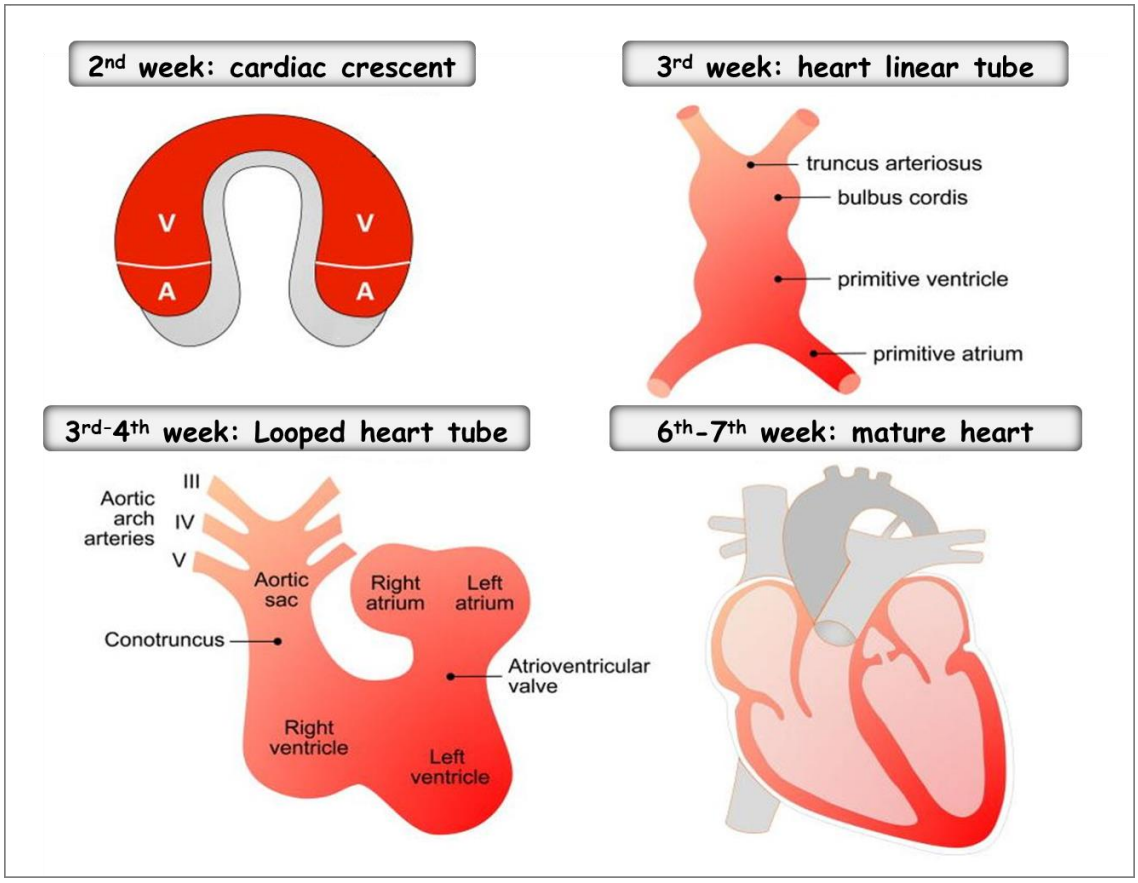

Figure 1-3. Schematic representation of cardiac development at different stages of the embryonic life. Figure source adapted in modified version from Kloesel at al., 2016, Anesth Analg.

1.1.2.3 Single and complex forms of congenital heart defects

Common types of CHD include valve defects, atrial and ventricular septal defects, stenosis of the aorta and pulmonary artery and heart muscle defects. These alterations are presented as *single*

defects, characterized by the presence of a "hole" in the internal wall of the heart, the septum, connecting the chambers, and *complex defects*, characterized by the lack of one or more chambers or valves and responsible of the lack of blood oxygenation and circulation, heart failure (HF) and death (Woodward 2011; Sun et al. 2015).

Single CHD are characterized by holes in the septum of the heart. The most common ones are atrial septal defects (ASD) and ventricular septal defect (VSD).

- Atrial septal defect (ASD)

It is the presence of a hole separating the upper chambers of the heart (atria). In this condition, oxygenated blood in the left-side of the heart mixes with deoxygenated blood coming from the systemic circulation.

- Ventricular septal defect (VSD)

It is the presence of the hole separating the lower chambers of the heart (ventricles). The septum normally closes before birth, so that when baby is born, oxygenated blood cannot mix with deoxygenated blood. In VSD patients, deoxygenated and oxygenated blood mixes, flowing through the hole from the LV to RV and exits the lung arteries. If the hole is large, the excess of blood pumped in the lung arteries forces the heart and lungs to work with more strength, the RV may become hypertrophic and lungs become congested (Geva et al. 2014; Sun et al. 2015).

Complex CHD are characterized by mixed lesions occurring at the same time. The most common ones are Tetralogy of Fallot (TOF) and univentricular heart syndrome or hypoplastic left heart syndrome (HLHS).

- Tetralogy of Fallot (TOF)

Characterized by concomitant and different malformations:

- Pulmonary stenosis, due to the narrowing of the pulmonary valve and right ventricular outflow tract (RVOT) resulting in a reduction of blood flow to the lung;
- VSD, due to a hole between LV and RV;
- RV hypertrophy, characterized by a ticker muscle because of the extra effort that the heart makes to pump blood into the narrowed pulmonary outflow tract;
- Overriding aorta, located between RV and LV and resulting in the exiting of deoxygenated blood from the RV through the aorta into systemic circulation (Woodward 2011).

- Univentricular heart syndrome or hypoplastic left heart syndrome (HLHS)

It is another complex and severe abnormality characterized by hypoplasia of the LV, aorta, mitral and aortic valves, the presence of ASD, and a PDA. Blood cannot properly flow into the LV and it passes through the ASD from the LA to the RA and then, enters the RV. The RV guides the

systemic circulation through the ductus. The hypoplastic LV is vital only because of the PDA-dependent circulation. Before birth, the ductus is open and allows blood to bypass its entry into the lungs as the foetus receives oxygenated blood from maternal placenta which is delivered through the umbilical cord. After birth, the blood must receive oxygen from the lungs and the ductus closes within few days. If the ductus is still open, the blood is unable to flow into the lung to become oxygenated. Patients with univentricular heart syndrome require a palliative intervention within few days from birth which consists of using a stent holding the ductus open and allow blood to be pumped into the aorta and systemic circulation (**Figure 1-4**) (Tchervenkov et al. 2006; Barron et al. 2009).

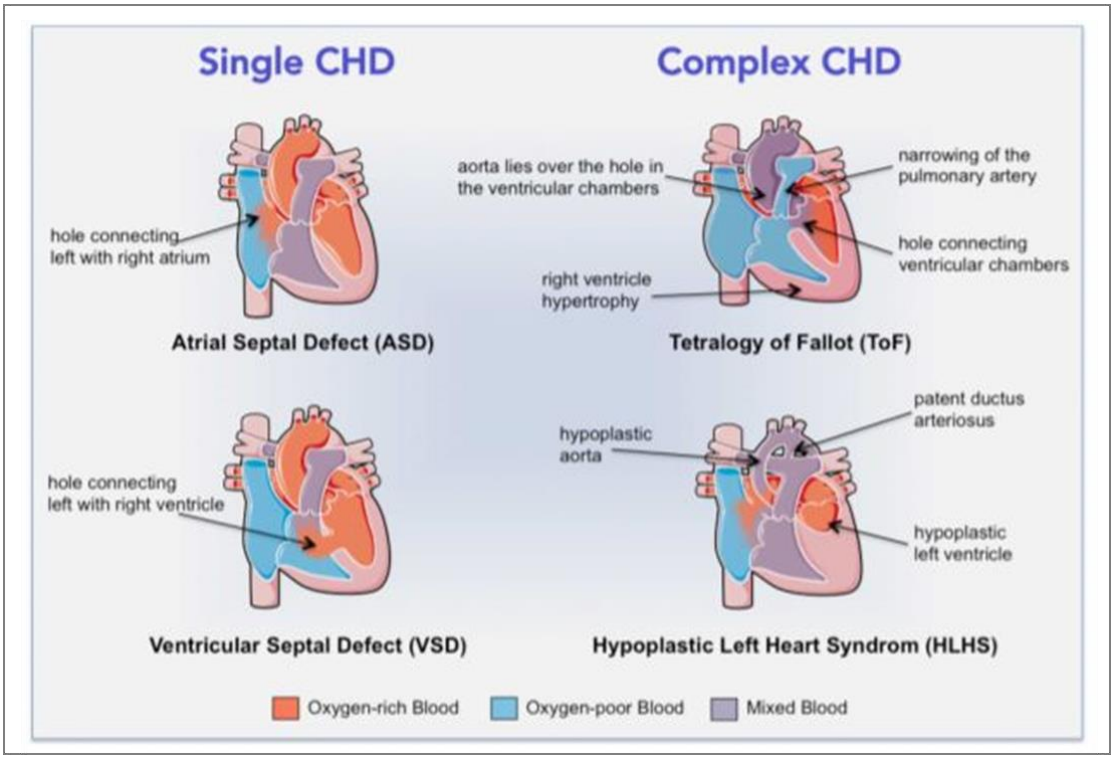

Figure 1- 4. Single and complex congenital heart malformations. Single CHD: Atrial and ventricular septal defects (ASD and VSD) display the presence of a hole connecting the left with right atrium or ventricle. Complex CHD: Tetralogy of Fallot (TOF) showing four concomitant types of abnormalities: overriding aorta, narrowing of the pulmonary artery (PA), right ventricle hypertrophy and VSD; Univentricular heart syndrome or hypoplastic left heart syndrome (HLHS) characterised by hypoplastic left ventricle, aorta, valve alteration, VSD and patent ductus arteriosus (PDA). Figure source: Avolio et al., 2015, Frontiers in Cell and Developmental Biology.

1.1.2.4 Cyanotic and acyanotic congenital heart defects

The distinction between *cyanotic* and *acyanotic* forms of CHD refers to the direction of blood flow when is diverted from one side to another of the heart (shunt).

Cyanotic forms of CHD are characterized by reduced oxygen levels and occurs when deoxygenated blood mixes with oxygenated blood obviating the lungs and enter the systemic circulation. Patients with right-to-left shunts have cyanotic alterations, such as, in TOF and HLHS. *Acyanotic forms* of CHD occur when blood flows from left-to-right side of the heart. ASD is an example of acyanotic lesion, where blood is shunted through the ASD from the LA to the RA. Therefore, oxygenated blood coming from the lungs to the LA, diverts (shunt) to the RA and mixes with deoxygenated blood coming from the systemic circulation, triggering an increased volume load in the RV. In most ASD, the oxygen saturation levels result normal and without symptoms. However, patients with large left-to-right shunts have so much blood in the pulmonary artery that develop a pulmonary congestion or pulmonary hypertension. This condition affects the oxygen level and the patient develops cyanosis with classic symptoms, such as, bluish skin, lips and nails (Woodward 2011; Ossa Galvis and Mendez 2019; Rao 2019).

1.1.2.5 Genetic and non-genetic causes of congenital heart defects

The aetiology of the most CHD is unknown. Although advanced genetic progresses have been made by scientists and physicians, only 30% of patients has CHD on genetic bases (Zaidi and Brueckner 2017). This explains that CHD are presumably the consequences of the interactions between multiple genes and environment. Maternal diabetes, phenylketonuria, obesity, infections, alcohol, Rubella and use of thalidomide and retinoic acid are reported to be one of the risk factors. Studies supporting the theory of a genetic contribution showed an increased risk for first degree relatives, monozygotic twins and families with consanguinity (Oyen et al. 2009; Herskind et al. 2013). Different mutations have been identified in CHD patients which involve alterations in molecules modifying chromatin, regulating the proliferation and differentiation pathways and activating cardiac gene transcription. For instance, damaging and missense mutations were identified in genes which participate in the methylation and ubiquitination process of the histone octamer and chromatin (Triedman and Newburger 2016). Mutations were found in NOTCH signalling pathway, fundamental in the cardiac development as it controls the cell proliferation and differentiation. For instance, alterations in NOTCH-ligand, JAGGED1 and NOTCH2 receptor are responsible of Alagille syndrome characterized by liver

disease, altered kidney development and CHD defects, such as TOF. Furthermore, aberrant variant of NOTCH1 is associated with CHD. Mutations in genes involved in RAS-Mitogen-Activated Protein Kinase (RAS-MAPK) pathway are responsible of Noonan syndrome and associated with CHD, such as, pulmonary stenosis (De Backer et al. 2019). Another class of altered genes in CHD are cardiac transcription factors, such as, NK2-5 which is involved in the heart development during the embryogenesis, and triggers structural defects, and Tbx5 leading Holt-Oran syndrome associated with cardiac alterations. These factors act together for the transactivation of different cardiac developmental factors and this cooperative mechanism explains the presence of different CHD. Variant of the cardiac transcription factor GATA4 is associated to simple and complex forms of CHD.

Future collaborations between cardiologists, geneticists, surgeons, and biologists will bring the identification of new CHD mutations. This discover will pave the way to improve the care of patients through an early diagnosis and specific therapies (Triedman and Newburger 2016).

1.1.3 Natural evolution of congenital heart disease

The successful diagnosis and therapy management of CHD led the population of ACHD to grow dramatically. In the United States, among 1.3 million of CHD patients, the adults represent 60% (more than the total CHD population). This explains that nowadays even patients with severe forms of the disease, which are identified by high mortality during childhood, have much longer life expectation. Comparing ACHD group with the general population, the mortality of ACHD is drastically high (Verheugt et al. 2010). Results from the CONCOR study in Netherlands, showed that ~ 0.6% of ACHD patients died because of the presence of late complications for cardiac causes. The 26% died for chronic HF and 19% died for unknown sudden death. Among the 23% who died for non-cardiovascular causes, 14% died for pneumonia, and 9% died for malignant diseases (**Figure 1-5**) (Triedman and Newburger 2016).

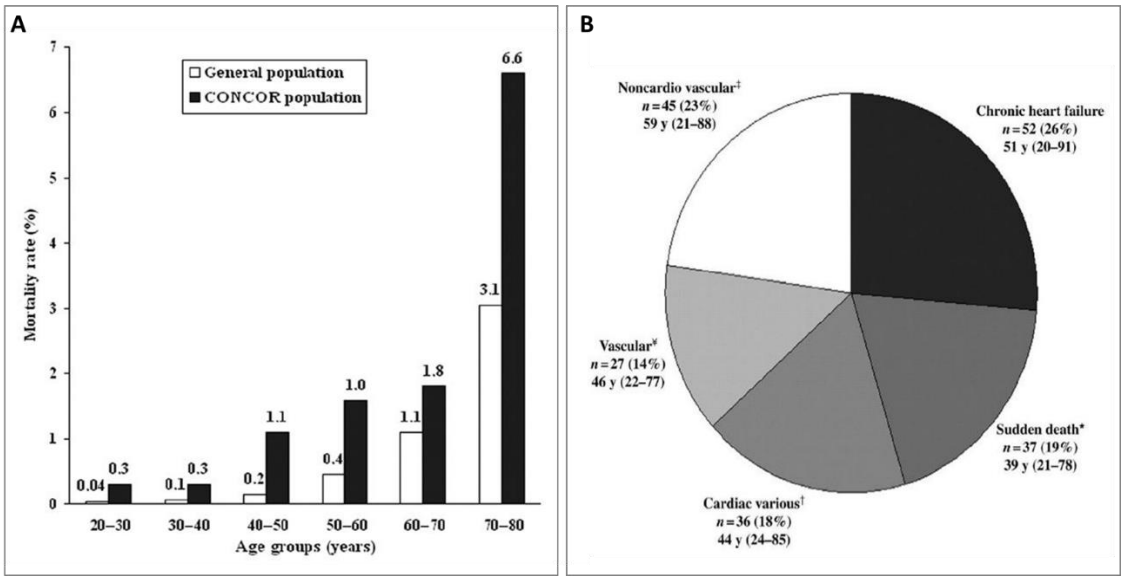

Figure 1-5. A. CONCOR study on ACHD mortality in the general Dutch population. B. Causes of death in 197 ACHD patients. Chronic heart failure (HF) (26%), and sudden death (19%) were recorded most often. Figure source: Verheugt et al., 2010, Oxford Journal and European Society of Cardiology (ESC).

HF represents a major problem in the CHD population that survive in adulthood. It occurs in ~ 26% of adult patients by the age of 30, and its incidence increases with the age (Norozi et al. 2006). This complication is not limited to severe forms of CHD. Patients with lower-complexity lesions, which represent the majority of ACHD, have higher burden of adverse cardiovascular events relative to the general population with hazard ratios ranging from 2 for acute coronary syndrome to 13 for HF (Saha et al. 2019). The pathogenesis of HF in ACHD is a multifactorial process, with altered myocardial structure and perfusion, cardiac injury following open-chest surgical interventions, insufficient myocardial protection during bypass and RV overload resulting from residual anatomical defects and graft failure (Budts et al. 2016). Medical therapies are based on pathophysiologic mechanisms which are mainly focused on canonical signalling pathway, such as, the renin-angiotensin-aldosterone and the adrenergic system (Miyamoto et al. 2014; Andersen et al. 2016). Nevertheless, recent trials using Angiotensin II receptor blockers or Angiotensin converting enzyme (ACE) inhibitors, failed to show any beneficial effect on the primary endpoint of ventricular function (Hsu et al. 2010; van der Bom et al. 2013). Therefore, further research is needed to optimize current treatment guidelines (Wehman and Kaushal 2015; Kaushal et al. 2017).

Arrhythmia is the most frequent long-term complications in CHD and responsible of morbidity and mortality in the adult life. ACHD patients may develop different arrhythmias. Intra-atrial re-

entrant tachycardia is a common mechanism of arrhythmia causing disabling symptoms which lead hypotension, syncope, and cardiac arrest. Atrial fibrillation is caused by hemodynamic stress in the atrium associated with aortic stenosis, mitral valve malformation and non-repaired univentricular dysfunction. The incidence of arrhythmia generally occurs after surgery and increases with the age of the patient. Ventricular arrhythmias are not frequent in CHD young patients (until ~ 20 years old), but adult patients with VSD, TOF and ventricular dysfunction develop serious ventricular tachycardia and they die. The medical and pacemaker therapies, together with catheter ablation intervention, are the opportunities to reduce the incidence of arrhythmias (Andersen et al. 2016; Bouma and Mulder 2017).

Endocarditis infection represents another late complication in ACHD patients. Its incidence appears the same in the past 40 years in the general CHD population (Tleyjeh et al. 2005; DeSimone et al. 2015). However, in ACHD the incidence has been increased because of the implantation of prostheses (patches, valves, conduits). Currently, the incidence of endocarditis in children with CHD ranges between ~ 1% and 12% per 1000 patients annually (Morris et al. 1998). The mortality associated with this infection is reduced from 9% to 7% in the last 20 years, presumably due to improved diagnosis, surgical intervention and medical therapy with antibiotics (Niwa et al. 2005; Di Filippo et al. 2006).

Old ACHD patients may present comorbidities, such as, hypertension, hyperlipidaemia, and diabetes mellitus. These comorbidities impact on the cardiac structure and function and increase the risk of ventricular dysfunction and HF (Bhatt et al. 2015).

A big challenge consists to improve the knowledge on the diagnosis, treatment and regular follow-up on young and adult patients, focusing on the early signs and symptoms which trigger these complications.

1.1.4 Diagnosis and therapy of congenital heart disease

Diagnostic procedures

The advanced clinical procedures in the management of CHD patients has improved the survival significantly in neonates, children and adults.

Echocardiography for the prenatal diagnosis of CHD has made substantial progresses as it has improved the counselling with the parents, set up a consultation procedure between the clinicians, improved the diagnosis and treatment of complications and it has provided an imaging guidance for prenatal interventions (Jone and Schowengerdt 2009). Although some new

techniques are still waiting to be validated on large scale in CHD patients, transthoracic and transoesophageal echocardiography are hugely improving in terms of quality of imaging.

Cardiovascular magnetic resonance (CMR) is superior than other imaging techniques because it performs better images of complex anatomical structures and function of the heart. Using more advanced hardware and software, CMR also provides a quantitative evaluation of heart physiology.

Likewise, CMR, *computer tomography (CT)* allows the evaluation of extra-cardiac structures, like arteries and assesses their anatomy and functions in ACHD patients with a low dose of radiation (Wiant et al. 2009; Bret-Zurita et al. 2014).

Positron emission tomography (PET) has been used for research studies for the assessment of physiological, pathological and metabolic mechanisms. It is used also in the clinical setting for the prognosis of patients, to assess inflammation in patients with endocarditis, and to evaluate new therapies.

Three-dimensional (3D) printing uses data of the patients obtained from CT and CMR to print and reconstruct layer by layer the heart and the vessels. This allows to assess complex and pathological structures, plan surgical intervention, facilitate the counselling with the patient, and teach the students (Anwar et al. 2017).

Some *biomarkers* are used for the diagnosis of CHD progression toward HF. Brain natriuretic peptide (BNP), is expressed by cardiomyocytes, has vasodilatory effects and alleviates the signs of HF. Although it is increased in adults with CHD, it is hard to draw a conclusion because the values change in different patients. Troponins are specific cardiac biomarkers which identify myocardial alterations. They are released in patients with myocardial infarction (MI), chronic HF, and pulmonary hypertension. Galectin, Cystatin C, Growth differentiation factor 15 and Procalcitonin are biomarkers that still need to be evaluated before being placed into the routinely clinical setting (Bouma and Mulder 2017).

Therapies

The surgical approaches for the correction of CHD can be *one-step* or *multiple-step* surgery. Indeed, the one-step therapy is the best option and it is often used to repair single forms of CHD where it is possible to close holes present in the heart with sutures or patches, to repair or substitute a valve, to relieve obstructed arteries and to restore blood flow to the vessels (Avolio et al. 2015a; Sun et al. 2015). Complex forms of CHD require multiple-step surgery for the repair of structural defects.

Among CHD surgical interventions, it is possible to distinguish *palliative* and *reparative* procedures. Palliation, which means relief, is used to modify and improve heart defects and

reduce the disorders in babies, infants and children who are physically too weak for a reparative or corrective surgery. Surgical palliation aims to reduce cyanosis, weaken symptoms of HF, establish blood flow and pressure into the vessels through a shunt procedure prior to later repair. This procedure allows baby to grow up, gain weight and stabilize the hemodynamic before a definitive repair. TOF patients require palliation before a reparative surgery. The aim of definitive repair in these patients, is to hinder the obstructions which interfere with the route of blood flow from the RV to the PA and close the VSD. The surgeon reconstructs the RVOT which is obstructed through the resection of muscle bundles using a patch, performs a valvectomy of obstructed valve and pulmonary arterioplasty (Henaine et al. 2012; Avolio et al. 2015a). HLHS patients require an urgent palliative surgery within few days from birth to hold their ductus arteriosus open to avoid the risk of death that would occur without any treatment (Barron et al. 2009). The possibility of using a minimally invasive therapeutic approach is given by *transcatheter intervention* and still not available for the majority of the patients (Mahle et al. 2008; Kenny and Hijazi 2017). However, when either treatments are not possible, the heart transplantation becomes the only option. Since the donor availability is very limited, this radical option is addressed to a very few cases.

The improvement in survival has increased the number of ACHD and related complications. There is an urgent need to standardize a clinical-educational program in the transition phase between adolescents and adults to allow young patients to become more skilled about their disease and reducing the probability of delaying CHD care (diagnosis, complication assessment, therapy) in adulthood (Mackie et al. 2018). American College of Cardiology (ACC) and American Heart Association (AHA) member committee in 2018 have provided clinical guidelines with all the recommendations for the management of adults with CHD (Stout et al. 2019). This guideline is a complete revision of previous 2008 ACC/AHA guidelines and focuses only on the care of ACHD. This because of the successful diagnosis and treatment strategies employed in babies and children with this disease which have brought to a high prevalence of the adult population. ACHD patients require specific needs and cardiologists must be specifically trained for their care in ACHD centre. Recently European Society of Cardiology (ESC) working group published a position paper with the recommendation for the transcatheter intervention in ACHD highlighting the issues of its allocation on national scale and how to train the surgeons to reach a standard recognition as ACHD interventionists (Chessa et al. 2019). This process is slow because it will require infrastructures, expertise of different cardiologists for each procedure enabling to train the future ACHD interventionists.

1.2 New therapies

1.2.1 Definition and classification of prostheses

The etymology of the word prosthesis derives from the Ancient Greek *prosthesis*, meaning "addition, application, attachment". Prostheses are used as patches, conduits or valves in the daily CHD reparative surgery and they can be biological tissues or synthetic material. In the current paragraph and following ones, different names are used to indicate the word prosthesis, such as, graft or scaffold.

Biological prostheses or *bio-prostheses* derive from human or animal tissue and include homografts, autografts and xenografts. Alongside the xenografts, there are swine intestinal submucosa extracellular matrix (SIS-ECM) grafts, of which the different forms are listed and described below. *Synthetic prostheses* are Gore-Tex® and mechanical valves.

- Biological prostheses or Bioprostheses

- Homografts or allografts are vascular conduits or valves derived from human cadavers and simulate the native valve by maintaining its morphology. They are used for aortic and pulmonary valve replacement and for RVOT reconstruction. *Advantages*: no chemical cross-linking agent treatment and good mechanical and hemodynamic properties. *Disadvantage*: limited availability and immune reaction if the decellularization process for the removal of native cells is not complete, cryopreservation and thawing processes of these grafts lead deterioration of their structure (Neumann et al. 2013). Decellularized homografts have been used as a good option to the cryopreserved homografts as the deterioration process is lower (Cebotari et al. 2011; Ruzmetov et al. 2012).
- Autografts are autologous tissues (valve or pericardium) derived from the patient. Usually autologous pulmonary valve is used in TOF patients to reconstruct the RVOT. *Advantages*: growth potential in parallel with the body growth (Simon et al. 2001; Al-Halees et al. 2002). *Disadvantages*: tendency to dilatation leading aortic valve regurgitation (Dohmen et al. 2002) and the difficulty to handle the autologous pericardium because of rolling, making the surgical interventions harder and slower (Pok and Jacot 2011).
- Xenografts are derived from animals, such as, swine and bovine, they are usually swine valves and bovine pericardium employed for valve replacement (Yap et al. 2013). They can be used as stentless valves entirely fabricated from swine aortic valves and bovine pericardium and, as stented valves which are mounted on a metallic or polymeric stent

(Pibarot and Dumesnil 2009). *Advantages*: unlimited supply and swine valves provide an appropriate anatomical structure when implanted. *Disadvantage*: lack growth potential and the decellularization process triggers calcification and stenosis (Avolio et al. 2015a).

- Swine intestinal submucosa extracellular matrix (SIS-ECM) grafts are approved by Food and Drug Administration (FDA), and are decellularized prostheses obtained from a proprietary decellularization technique which generates a ~ 100 µm-tick membrane for preclinical and clinical uses. *Advantages*: superior biological activity compared to other prostheses, easy handling and durability, remodelling and regeneration potential without the risk of deterioration, immunologically inert, high mechanical properties, homing of the host cells (Pok and Jacot 2011; Iop et al. 2018). The biocompatibility of SIS-ECM with a native tissue results from the presence of matrix proteins, mainly collagen type I (~ 90%) and less collagen type II, IV, V and VI, and laminin, fibronectin, glycosaminoglycan (GAG), such as, hyaluronic acid and heparan sulphate which prevent the formation of the scar during the healing phase. The presence of growth factors (GFs) and integrins lead a positive remodelling of the graft. Preclinical studies on different animals showed promising outcomes (Iop et al. 2018). The first use of SIS-ECM in cardiovascular application was to generate a dog sub-aortic model which resulted in a good vascular implantation with neovascularization process and without infections or hyperplasia observed (Badylak et al. 1989). SIS-ECM was used as a patch in cardiovascular application for abdominal aorta repair in green fluorescent protein (GFP) transgenic rodents. The results showed optimal engraftment, endothelialization, without inflammation or calcification (Padalino et al. 2012). Furthermore, these grafts have been employed as a patch for carotid artery repair in a sheep model. Although an initial narrowing was observed, the artery returned to normal and new remodelling with collagen deposition and re-endothelialization were observed (Fallon et al. 2012). One preclinical study showed negative outcomes in the same animal species where the graft induced dilatation, stenosis, rupture and aneurysm formation (Pavcnik et al. 2009). SIS-ECM have been used in clinical practice for pediatric CHD surgery showing the safety and feasibility of the grafting without calcification or death after implantation (Scholl et al. 2010; Quarti et al. 2011; Witt et al. 2013). The use of SIS-ECM in the urgency medicine for the brachiocephalic arterial trunk reconstruction showed the feasibility and safety of using a promptly graft in a young patient underwent an emergency intervention (Eckhauser et al. 2013). SIS-ECM grafts have been used in experimental studies for complex CHD malformations as valve conduits and in clinical studies for tricuspid valve

repair. However, recent studies on valve reconstruction for CHD highlighted the negative outcomes of SIS-ECM showing the strong inflammatory activity, fibrosis and calcification of the explanted graft (Zaidi et al. 2014; Rosario-Quinones et al. 2015; Mosala Nezhad et al. 2017). The high inflammatory response was possibly associated to the high sensitivity with the epitope α-gal present on swine tissue and not in the human counterpart. SIS-ECM grafts are fabricated by CorMatrix® Cardiovascular, Inc regenerative biotechnology company in different forms: Cor™Patch, Cor™Tricuspid and Cor™Pediatric.

- Cor™Patch is commercially available and designed for epicardial and intramyocardial use, for congenital cardiac and vascular repair, for intraventricular repair and arterial and valve repair. The structure of ECM allows angiogenesis and growth of the host cells after implantation.
- Cor™Tricuspid is a decellularized ECM stentless valve used for tricuspid valve disease. It is not commercially available, and it does not require anticoagulation and anti-calcification therapy.
- Cor™Pediatric is a decellularized stentless valve, used for investigational studies and it is not commercially available. It provides support and continuity to the atrioventricular tract in pediatric population and is supplied in different sizes. It is resistant to calcification and it might require a short-term anticoagulant treatment.
- Other SIS-ECM grafts used for non-cardiovascular applications are Oasis® (Healthpoint, Ldt, US), Surgisis®, which has been suspended from the clinical trial because of asymptomatic pseudoaneurysms reported after using this graft, Durasis®, and Stratasis®, all produced by Cook Biotech, US, and Restore® (DePuy, West Chester, PA, US).

- Synthetic prostheses

- Gore-Tex® is a polytetrafluoroethylene (PTFE) material available as a patch or conduit and used for RVOT obstruction (Allen et al. 2002). *Advantages*: durability. *Disadvantages*: unable to grow with the patient's heart, low remodelling capacity, loss of mechanical properties over time and association with high risk of infections (Pok and Jacot 2011).
- Mechanical valves are designed as monoleaflets, bileaflets and caged ball valves. Monoleaflet valves have one disk attached by central and lateral metallic support. Bileaflet valves consist of two disks attached to a metallic ring. Caged ball valves are made of metallic cage, a silastic ball and a circular ring. These valves are no longer used.

Advantages: optimal durability. *Disadvantages*: risk of thromboembolism and thrombosis, long-term anticoagulant therapy, risk of haemorrhage. On the other hand, bioprosthetic valves have low risk of thromboembolism but a limited durability due to their deterioration. The high risk of thromboembolism is due to type of prosthesis, position of the implanted valve, tendency to form a thrombus, risk factor associated to the patient and anti-thrombotic therapy (**Figure 1-6**) (Pibarot and Dumesnil 2009).

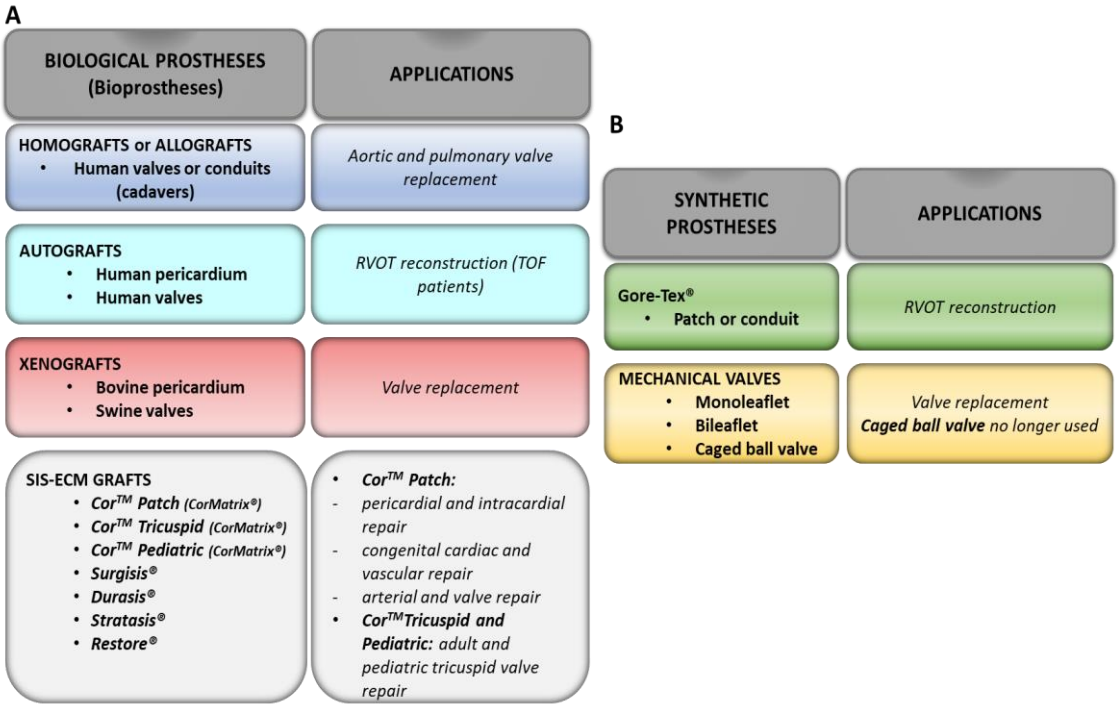

Figure 1-6. Cartoon displaying the classification and use of different prostheses used for cardiovascular and non-cardiovascular therapy. A. Biological prostheses or bioprostheses. B. Synthetic prostheses. *Abbreviations*: CHD= congenital heart disease; RVOT= right ventricular outflow tract; SIS-ECM= swine intestinal submucosa-extracellular matrix; TOF= tetralogy of Fallot.

1.2.2 Balanced *versus* unbalanced remodelling of the bioprostheses

In all bioprostheses ECM contributes to the mechanical support, cell communication, proliferation, differentiation and angiogenesis within the tissue where it is implanted. The "constructive" remodelling of a bioprosthesis is regulated by a perfect balance between synthesis and degradation of all its components without incurring in the loss of its integrity. The degradation process begins with the healing process (scar formation) and with a newly tissue formed. Different processes may lead the physiological degradation of the prostheses. Firstly,

the proliferation of monocytes and their differentiation in macrophages M2 type rather than M1 type. This class of macrophages stimulates the remodelling and the integration of the graft inside the native tissue *via* GFs, such as, interleukin-10 (IL-10) and transforming growth factor beta 1 (TGFβ1). Macrophages M1 type induce the release of proteolytic acidic enzymes, such as, Metalloproteinases (MMP), which together with GFs, induce the degradation of the graft (Iop et al. 2018). M1 macrophages are more involved in the inflammatory pathways and secretion of proinflammatory cytokines which stimulate inflammation and fibrosis. M2 macrophages, are involved in the anti-inflammatory pathways where trophic factors are secreted for a perfect balance between proliferation, differentiation, cell death and angiogenesis for the ingrowth of the native tissue (Piterina et al. 2009). Another process could be the release of vascular endothelial growth factor (VEGF) and TGFβ1 following the degradation of the graft. Furthermore, the degradation products of the graft are released into the circulation which recruit progenitor cells from the bone marrow (BM) through paracrine mechanisms. Circulating BM cells migrate to the site of graft implantation and support the angiogenesis process (Iop et al. 2018).

However, the loss of integrity of a bioprosthesis shifts the remodelling process from a balanced to an unbalanced mechanism, causing a deterioration. One of the mechanism responsible of the deterioration of a bioprosthesis is the decellularization procedure used during the fabrication of the graft to prevent immune response from the host tissue. Decellularization is a process which eliminates cells from the graft and preserves its original structure. Different methods have been used for the cell removal, such as, enzymatic lysis with trypsin, detergent method with sodium dodecyl sulphate (SDS), freeze drying, chemical treatment with glutaraldehyde and a mix of enzymatic and chemical methods (Rieder et al. 2004; Schmidt et al. 2007). Usually, decellularization with glutaraldehyde allows protein cross-links and stabilization of collagen deposition providing tensile strength, elasticity and resistance to deterioration. However, the improvement of these characteristics in the graft, comes at a price. Bioprosthetic valves are the most affected ones from the decellularization process after implantation. Structural valve deterioration represents a huge restriction for the *in vivo* integrity and durability of the prostheses. In order to understand how the bioprosthetic valves can be deteriorated, a brief description of the valve structure is reported in this paragraph. Valves are characterized by three layers: fibrosa (outflow layer), spongiosa (central layer) and ventricularis (inflow layer) (Schoen 2008; Jover et al. 2018), and each layer has a different ECM composition and organization. The main two cell populations resident in the valves are valve endothelial cells (VECs) and valve interstitial cells (VICs). VECs are well characterized for their differential phenotypes and gene

expression. They control permeability and establish paracrine contacts with VICs (Chen and Simmons 2011). VICs are heterogenous mesenchymal cell type similar to vascular smooth muscle cells (VSMCs) and fibroblasts which interact with the ECM displaying a high phenotypic plasticity. This confers to the valves the capacity to preserve their integrity and function and participate in the reparative processes (Liu et al. 2007; Schoen 2008). The removal of VICs from the bioprosthetic valves during the decellularization process, make them very prone to degeneration as these cells secrete ECM proteins and have contractile properties like VSMCs. (Pibarot and Dumesnil 2009; Avolio et al. 2015a; Jover et al. 2018) Furthermore, tissue fixation with glutaraldehyde cause calcium ion influx and cell membrane damage which together with phospholipids act as hydroxyapatite nucleation sites. Molecules from the host and a stress environment trigger the growth of calcium crystals and the release of degradation products of the graft induces activation of the immune response (humoral and cellular). Atherosclerosis mechanism also contributes to this unbalanced remodelling mechanism with the deposition of oxidized low-density lipoproteins (ox-LDLs), followed by monocyte recruitment and their differentiation in macrophages with M1 phenotype. M1 macrophages with ox-LDL produce foam cells which trigger release of pro-inflammatory cytokines, collagen alteration, osteogenic differentiation of native endothelial cells (ECs) and BM circulating cells, which are recruited from the circulation (**Figure 1-7**). Deterioration is a cumulative event because calcium crystals adhere, accumulate and spread on the ECM by forming nodules which interfere with the bioprostesis structure and function (Pibarot and Dumesnil 2009; Avolio et al. 2015a; Jover et al. 2018).

Structural valve deterioration is the most frequent cause of re-intervention for valve replacement in patients with bioprostheses. The disease associated with the bioprosthesis deterioration is called *bioprosthetic valve disease* rather than *valve heart disease* or *valve structural disease* (Jover et al. 2018). One of the mechanisms responsible of this condition is the decellularization treatment during the manufacture of the grafts. Other risk factors associated with the degeneration are the age of the patient, valve position (failure due to the position in the mitral rather than in the aortic position), hypertension, ventricular hypertrophy and hyperparathyroidism. Mechanical valves might be an option, as they are not limited by the deterioration as for the bioprostheses and are durable. However, they have a high risk to develop thromboembolism and thrombosis. After implantation, patient requires anticoagulation treatment. The use of mechanical valves in children and adolescents with congenital valve disease would require these anticoagulants which it is not appropriate for an active lifestyle.

Although valve replacement is a gold standard in patients with bioprosthetic valve disease, it is not a definitive therapy and an ideal valve prosthesis does not exist yet. A possible option might be the use of anti-calcifying agents (Schoen 2008). Alternatively, the seeding of VICs in the decellularized bioprosthetic valves may overcome the issue associated with their elimination during the decellularization process because these cells would produce and secrete ECM and natural components to prevent structural deterioration.

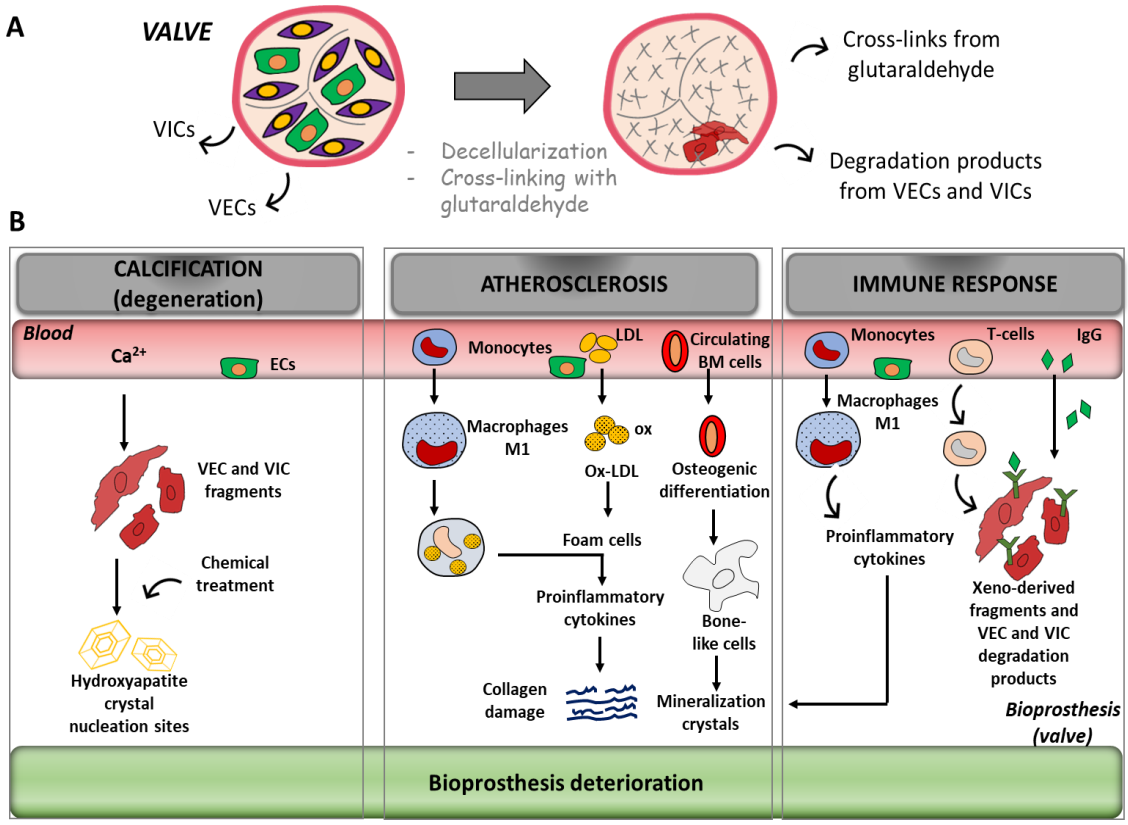

Figure 1-7. Deterioration of bioprosthetic valves following decellularization process. A. Valve structure and resident cells. Cross-links from glutaraldehyde and degradation products in the valve. B. Calcification, atherosclerotic and immune response processes in the bioprostheses. *Abbreviations*: ECs= endothelial cells; IgG= immunoglobulin G; LDL= low density lipoprotein; M1= macrophages type 1; ox= oxidized; VECs= valve endothelial cells; VICs= valve interstitial cells.

1.3 Cell therapy

1.3.1 Dispersed cells, *in vitro* and *in vivo* tissue engineering

Cell therapy offers an alternative solution to the current and standard medical and pharmacological treatments and the only answer to the different diseases that cannot be otherwise treated with the conventional surgical procedures. Three different cell-based therapy approaches have been described: *cell therapy with dispersed cells*, *cell therapy with in vitro tissue engineering (TE)*, and *cell therapy with in vivo TE*.

- Dispersed cell therapy

It is characterized by the injection of dispersed cells in the area of injury to promote the regeneration of the tissue and possibly to restore its function. There are different cell delivery methods which allow their distribution and retention in the damaged heart and are intracoronary, intramyocardial, intravenous and epicardial injection. The therapeutic effect of the injected cells occurs through cell-cell direct contact, differentiation in cardiovascular cells and paracrine mechanisms by releasing soluble GFs which have protective and regenerative effects on the surrounding cells, despite these cells are not directly involved in the formation of newly tissue through the differentiation process. A recent trial identifies vesicles, called exosomes, which are secreted by cardiosphere-derived cells (CDCs), as important elements for the regeneration and protection of the damaged heart. The presence of specific microRNAs in these vesicles, exerts the same regenerative and functional effects produced when CDCs are injected alone into the heart (Krause et al. 2010; Ibrahim et al. 2014).

Recently cell therapy with dispersed cells has been applied for the correction of CHD. In complex forms of CHD which would require heart transplantation to treat end-stage of HF, cell therapy is the first realistic treatment possible (Bernstein and Srivastava 2012). One of the most complex defects which might have benefits from stem cell therapy is univentricular heart syndrome or HLHS, characterized by a hypoplastic LV, mitral and aortic valves and narrowing of the aorta. The underdeveloped LV is unable to pump blood into systemic circulation and if this condition is not treated, becomes fatal. The current therapy consists of three palliative procedures at different stages of the child. At the end of the palliation, the systemic circulation is aided by the RV and deoxygenated blood flows passively into PA vasculature. However, the RV, which guides the systemic circulation through the ductus arteriosus, is exposed to HF. In the absence of curative treatments, stem cell therapy may be an innovative strategy to treat RV dysfunction responsible of HF and prevent this complication. Different stem cell therapies have been employed for univentricular dysfunction in preclinical and clinical studies.

- Preclinical studies have highlighted the mechanisms by which stem cells act in the damaged tissue reaching the conclusion that both stem cells and paracrine mechanism are involved in the regeneration of the injured myocardium. Recent preclinical studies have used large animal models which simulate the univentricular dysfunction typical of human patients. The proposed approach was the induction of the RV pressure and /or volume overload. In a 4-month-old sheep model, the RV volume overload was generated by implanting a patch between the RVOT and main PA (MPA). Then, autologous umbilical cord mononuclear cells (UBC-MNCs) and control medium were injected into the RV of myocardium. After 3 months from the injection, sheep treated with cells showed higher RV diastolic function compared with controls (Yerebakan et al. 2009). In a Yorkshire swine model, RV pressure overload was induced with PA banding. Then, human mesenchymal stem cells (MSCs) and control medium, were injected intramyocardially. One month after the injection, swine treated with cells had less RV dilatation and the RV function was improved (Wehman et al. 2016; Wehman et al. 2017). Swine animal model underwent PA banding and injected with cardiac progenitor cells (CPCs) showed reduced fibrosis and increased vascular density in the RV compared to control (Wehman et al. 2017).
- One of the first clinical studies with dispersed cell therapy was the intracoronary injection of CDCs in patients with univentricular dysfunction. After few months from the injection, patients treated with CDCs showed an improvement of right ventricular ejection fraction (RVEF) and reduction of RV hypertrophy (Ishigami et al. 2015). Other clinical trials are testing the injection of autologous UBC-MNCs in univentricular dysfunction at the II stage of the palliative intervention, while another clinical trial is evaluating the injection of human allogeneic MSCs in the same patients in terms of safety and efficacy (Kaushal et al. 2017; Ambastha et al. 2018; Bittle et al. 2018).

- *In vitro* TE therapy

TE offers a promising solution through the production of an irreplaceable material which uses a 3D biologic or synthetic scaffold incubated with stem or progenitor cells and differentiated cells to support a therapy through regeneration, remodelling and growth mechanisms (Cheema et al. 2012; Smit and Dohmen 2015). Scaffold is a template for cell adhesion and new tissue creation. In fact, its infiltration by cells after implantation leads the formation of a living tissue which matches perfectly in the host's tissue. Seeded cells aid the homing of host's cells *via* chemoattractant GFs. TE has been used initially to regenerate tissues, such as, trachea, oesophagus and skeletal muscle. *Vacanti et al.*, in 1994 performed the first TE production of

tracheal cartilage (Vacanti et al. 1994). Further, TE has been applied also in cardiovascular field. Some previous investigations in adult patients proposed that dispersed cells, when injected alone, might dye after implantation into the heart and that their regeneration capacity is due to release of their paracrine GFs. However, this kind of therapy does not have advantages in patients with CHD who need additional material working as a delivery system to address cells specifically to the injured site. For heart and vessels, these materials are found in forms of patches, conduits or valves. Stem cells perform better when incorporated in the bioprostheses, such as, pericardium, valves, ECM scaffolds (SIS-ECM) that can grow and remodel together with native heart (Bertipaglia et al. 2003; Scholl et al. 2010; Dean et al. 2012; Kalfa and Bacha 2013; Smit and Dohmen 2015). Before the implantation, cellularized TE scaffold must grow *in vitro*. Firstly, they are primed in static culture, then, they are grown and matured using a bioreactor which maintains cells in culture providing nutrient supply and gas exchanges which in turn, control and regulate the interaction between the cells and TE scaffold (Carrier et al. 1999; Hecker and Birla 2007; Huang et al. 2016; Stephenson and Grayson 2018). Preclinical and clinical investigations have showed the potential of tissue engineering vascular graft (TEVG) with stem cells for a definitive repair of complex forms of CHD which can be diagnosed before and after birth. For these patients, time of diagnosis is fundamental to plan a surgical intervention with a TEVG and according to that, it is possible to have two scenarios. If the diagnosis is made before birth, stem cells are collected from uterus with non-invasive techniques, expanded and seeded on the TEVG, ready to be implanted after birth during a definitive surgical intervention without the need of the palliative step. Induced pluripotent stem cells (iPSCs) are suitable for this aim. Furthermore, stem cells from the umbilical cord can be collected at birth and used for patients who do not require an urgent palliation at birth. If the diagnosis is made after birth, cells can be isolated from a leftover tissue of a palliative procedure, expanded and seeded into the TEVG which will be surgically implanted during a definitive open-chest surgery (Avolio et al. 2015a). A schematic representation is displayed in **Figure 1-8**. The advantage of using stem cells or progenitor cells may derive from their commitment to generate the main cell population in the heart, such as, cardiomyocytes, ECs and VSMCs.

- *In vivo* TE therapy

Although in vitro TE has generated constructs which simulate the *in vivo* microenvironment using bioreactors, resembling the physiological condition of the body after an *ex-vivo* culture is hard. After implantation, TE scaffold is deficient of its own vascular structure to maintain cell survival, proliferation and production of ECM. Thus, the implanted scaffold only relies on the newly vascular structures coming from the surrounded native tissue and this brings to limited

long-term results in preclinical and clinical therapeutic studies. To overcome this issue, new studies are supporting the *in vivo* TE therapy which uses patient's body as a bioreactor to seed scaffolds (bioprostheses like valves or ECM), seeded with or without cells or GFs to induce the self-regeneration capacity of the tissue. This strategy allows the body to provide a continuous boost between exogenous and endogenous cells and GFs (through direct and paracrine mechanisms), to generate a niche for the growth of the tissue. Furthermore, this strategy often obviates excessive manipulation of cells during *in vitro* culture, ensuring that the cells retain their functional properties. Recent investigations of bone scaffold fabrication with *in vivo* TE approach, have shown promising results and demonstrated efficacy in the reconstruction of the bone in different bone-related diseases (Huang et al. 2016; Stephenson and Grayson 2018).

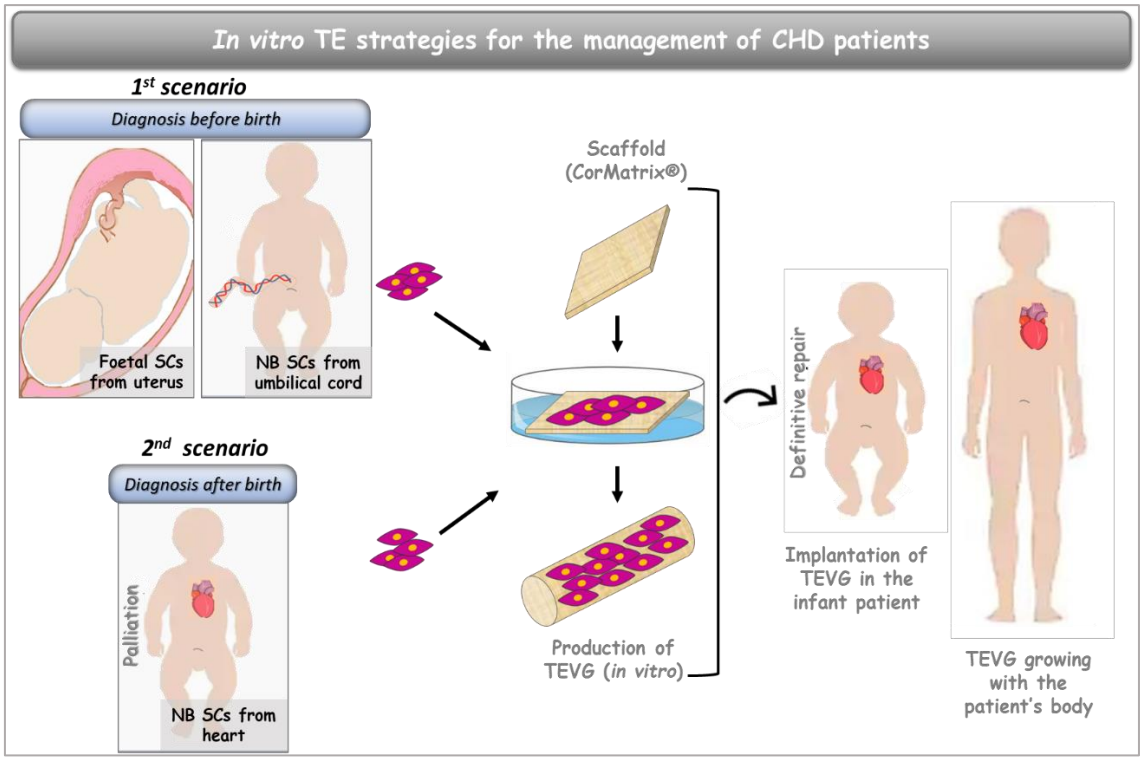

Figure 1-8. Schematic illustration of TE strategies for the management of new-born and infant patients with complex forms of CHD. Based on time of diagnosis, stem cells can be collected before birth or after birth. If the diagnosis is made before birth, stem cells from uterus can be collected, used to create a TEVG, following static culture and an in vitro bioreactor system, and implanted in the infant patient for a definitive and corrective surgery. Stem cells from the umbilical cord can be isolated after birth if the baby does not require an urgent palliative surgery. If the diagnosis is made after birth, stem cells from heart can be collected during a first palliative intervention, expanded and seeded into a TEVG which is implanted in the infant patient during a definitive open-chest surgery. *Abbreviations*: CHD= congenital heart disease;

NBs= new-born; SCs= stem cells; TEVG= tissue engineering vascular graft. Figure adapted in a modified version from Madeddu et al., 2019, Front. Cardiovasc. Med.

1.3.2 Properties of an ideal cellularized tissue-engineering graft

To optimize a TE graft is important to make two main decisions about the graft itself and the cells which are going to repopulate the bioengineered graft. The graft used in cardiovascular surgical application should possess an intact structure, enabling the exogenous and endogenous cell infiltration and providing new vasculature and blood flow within the tissue (Cheema et al. 2012; Fallahiarezoudar et al. 2015). The result is a new tissue characterized entirely by patient's cells capable of remodelling in response to physiological stimuli (Butcher et al. 2011; Dean et al. 2012).

An ideal TEVG, in the forms of patches, valves or conduits, used to repair complex forms of CHD, such as, TOF and HLHS should have the following features:

- *Growth potential*, the implanted graft should grow and enlarge together with the patient's body;
- *Durability*, the implanted graft should be durable until the all life-course of the patient and resist to the hemodynamic stimuli happening in the body;
- *Availability in different sizes*, according to needs of repairing heart in babies, children or adults;
- *Pliability*, the graft should have a reversable deformation;
- *No immunogenicity*, a decellularized scaffold should prevent the immune response from the host. Alternatively, the seeding of MSCs with immunomodulatory properties, confers the graft this important aspect;
- *No thromboembolism, no anticoagulation treatment*, the cellularized scaffold should prevent the formation of thrombi and the formation of emboli in the circulation. In case of valve repair in children with CHD, the use of mechanical valves in association with anticoagulant therapy is not indicated. Alternatively, the seeding of ECs or endothelial progenitor cells (EPCs) into the scaffold may prevent the risk to develop thromboembolism.
- *Low incidence to deterioration*, the decellularization with glutaraldehyde, exposes the graft to the structural deterioration. Bioprosthetic valves may undergo deterioration because this process eliminates the main cell component resident in the valves, the VICs

which maintain the structure of the graft. The seeding of exogenous VICs into the valves may reduce this incidence;

- *Resistance to calcification*, the risk of calcification in children is higher than in adults, as in young patient the mobilization of calcium triggered by bone remodelling, increase the calcification mechanism. Anti-calcifying agents or the seeding of VICs into the bioprosthetic valves may reduce the risk associated to the treatment with cross-linking agents (Butcher et al. 2011; Pok and Jacot 2011);
- *Mechanical resistance*.

1.3.3 *In vitro* cellularization and growth of the tissue-engineered graft

The understanding of cellularization effects on a TEVG and the method of cell seeding are very important. In the previous paragraph, we explained the properties of graft engineered with cells. Here, the method of seeding and the culture conditions of the engineered graft will be explained. Multicellular organisms need a 3D-culture environment to provide structural integrity, to identify functional barriers and to establish specific microenvironments. Although cell biologists have been isolating and expanding monolayer of cells in a 2D-environment, to engineer tissues, it is fundamental the integration of cell biology with TE materials to grow cells in a 3D-environment. A 2D-plastic substrate restrains cell attachment only in a planar direction with an apical and basal cell polarity and a secretion of GFs in the culture media. A 3D-scaffold, such as, an ECM substrate owns cell polarity in planar and transversal way without any restriction. The ECM structure allows the secretion and distribution of concentrated GFs. Integrins and receptors lead the cell attachment and secretion of newly ECM elements. The release of GFs and other bioactive components enhances different cell functions, such as, proliferation, migration and differentiation (Hussey et al. 2018). The **Figure 1-9** displays the cell growth on a 2D-plastic dish and the interaction between cells and ECM-based 3D-scaffold.

The seeding into the scaffold, attachment, infiltration and the distribution are one of the matters of discussion in TE. Dai and colleagues found that a static culture condition was a simple method of seeding which did not require any advanced laboratory equipment and specific culture reagents. Cells were seeded on top of a planar or flat scaffold, cell growth media was added to the plastic dish and placed in the incubator for further analysis. Moreover, the cells were not uniformly distributed, and the infiltration rate was low resulting in a high number of cells in the surface of the graft. The low rate was explained by the occurrence of air bubble into the flat graft that only a low-pressure culture system could improve the cell performance. This

mechanism used a pump which drew the air contained in the scaffold allowing the cells and the media to penetrate. This method reduced the cell viability and the function of the scaffold (Dai et al. 2009). Another cell seeding system is the centrifugation. Briefly, when the cells are seeded, an intermediate spin force is applied to allow the cells moving in the middle of the graft. However, there are two issues with this method: the centrifugation affects the viability and functionality of the cells and then during the centrifugation an overlapping of the scaffold pieces does not ensure a uniform cell distribution (Godbey et al. 2004). The perfusion culture condition uses a bioreactor which maintains the cells in culture for short- and long-term and allows their infiltration and uniform distribution providing nutrient supply and gas exchanges in the 3D structure. This system uses a dynamic flow which simulates the physiological *in vivo* conditions where the blood provides all the nutrients and ensures the perfusion of the cellularized structure. The functional features of a bioreactor system are the O_2, CO_2, temperature, pressure, PH and nutrients, such as, glucose and these factors regulate the remodelling of the cells and ECM proteins into the graft (Carrier et al. 1999; Hecker and Birla 2007).

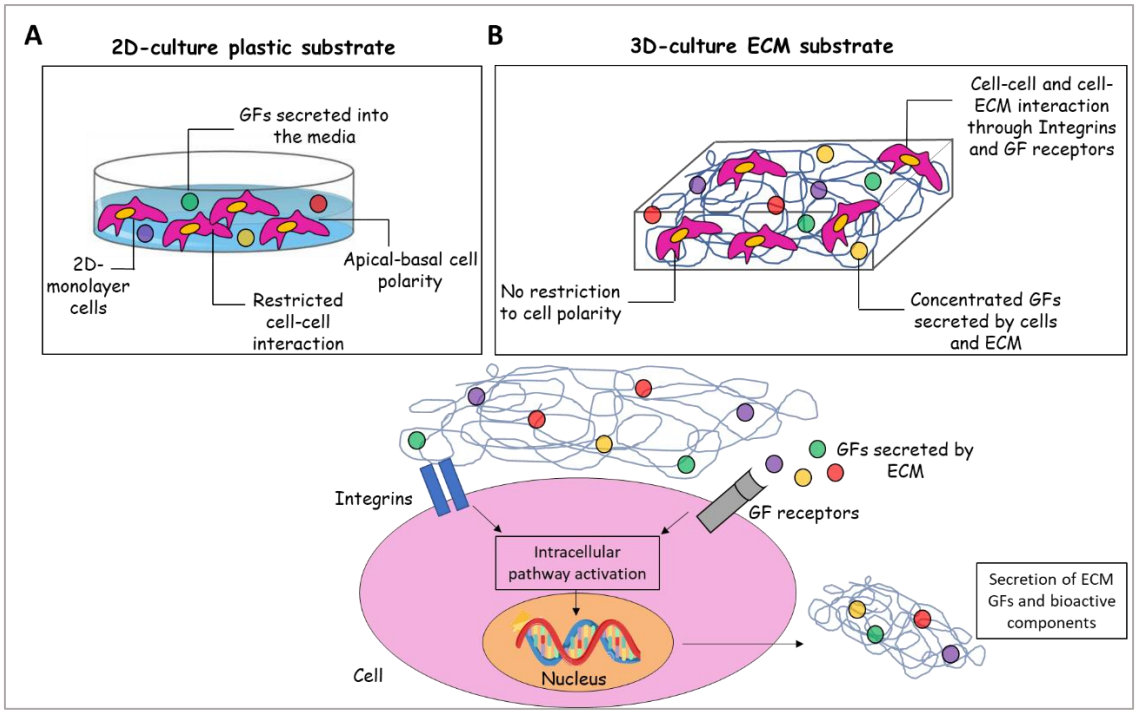

Figure 1-9. 2D- and 3D- cell growing substrates. A. In a 2D- plastic environment, cells are attached as monolayer in a planar direction and forced to maintain an apical and basal polarity only. Cell-cell interactions is also restricted. The GFs are secreted by the cells and propagated in the media. B. In a 3D-scaffold, cells receive all the stimuli from different directions of the ECM and no polarity restriction is present. A gradient of concentrated GFs is released by the cells and ECM and this involves integrins and receptors, which, in turn, activate an intracellular signalling

pathway. In the nucleus, genes are transcribed, and new ECM elements are synthesized and secreted. *Abbreviations*: ECM= extracellular matrix; GF= growth factor; 2D= 2-dimensional

1.4 Pericytes: major players in vasculogenesis and angiogenesis

1.4.1 Definition, localization, characterization and function

Pericytes were characterized for the first time by Charles-Marie Benjamin Rouget in 1873 and described as mural cells or Rouget cells located in the basement membrane of capillaries and venules (Bergers and Song 2005). These cells surrounded the vessels and because of their perivascular localization (*peri*, around and *cyto*, cell), they were named pericytes by Karl Wihelm Zimmerman. They contribute to the formation, maturation and stabilization of the existing blood vessels and promotion of angiogenesis. Furthermore, they have been considered fundamental players also in the repair mechanisms conferring a potential target for different therapies. Pericytes surround and encircle the ECs of capillaries, arterioles and venules, and establish different types of contacts in the area where the basement membrane is absent. These areas facilitate the communication between cells and are called peg-sockets which contain gap-, tight- and adherent- junctions. Pericyte density in the abluminal area of the vessels ranges around 10% and 50% in different tissues. For instance, the frequency of pericytes to ECs in the skeletal muscle is 1:100, in the central nervous system (CNS) and retina is 1:1. A possible explanation is due to pericyte contribution to the formation of blood-brain-barrier (BBB) and blood-retinal-barrier (BRB) (Shepro and Morel 1993; Armulik et al. 2005). In this these tissues pericyte coverage is fundamental to protect them from toxic factors coming from the circulation. Furthermore, in CNS, pericytes work as regulators of hypoxic and hypoglycemic environment which regulate the adaptive response necessary to maintain the homeostasis and to protect weak neurons. In the kidney, pericytes constitute 30% of the total cell population and regulate the ultrafiltration at the level of glomerulus (Armulik et al. 2005; Ferland-McCollough et al. 2017). Pericyte morphology is different beside the tissues. It ranges from the elongated, flatted and stellate shaped cells covering a large area of the abluminal vessels in CNS to rounded mesangial cells covering a small area of vessels in kidney. The large and small blood vessels (arteries and veins), are characterized by three structural layers. *Intima* layer (inner layer), represents the internal luminal side of the vessels where the ECs reside and work as regulator of vascular permeability, tone, and recruitment of blood cells. *Media layer* where the VSMCs are located, regulating the contractility of the vessels and the production of ECM. Then, *adventitial*

layer (out layer), is characterized by fibroblasts, stromal and progenitor cells which are involved mainly in the production and secretion of ECM and organized together in a microenvironment which is defined vasculogenic niche. Pericytes are still a debated cell population among scientists. At first, microvascular pericytes have been considered cells surrounding ECs from capillaries and venules of different tissues. However, recent studies found a new population of pericytes, defined adventitial pericytes or adventitial pericytes-like cells surrounding the adventitial layer of arterioles in the veins and arteries, and sometimes found in the *vasa vasorum* of large vessels. Thus, due to their localization, they are also named macrovascular pericytes (**Figure 1-10**) (Campagnolo et al. 2010; Avolio et al. 2015c; Avolio and Madeddu 2016).

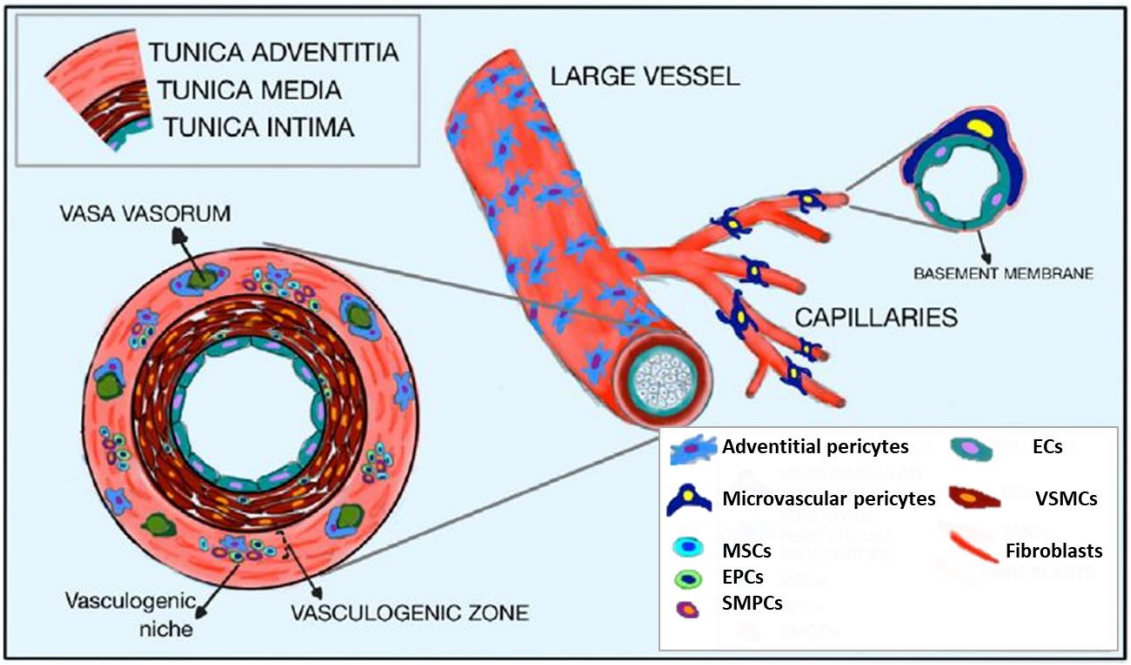

Figure 1-10. Vascular progenitor or vascular stem cells distributed in in the large vessels. *Abbreviations*: ECs= endothelial cells; EPCs= endothelial progenitor cells; MSCs = mesenchymal stem cells; SMPCs= smooth muscle progenitor cells; VSMCs= vascular smooth muscle cells. Figure source: Avolio and Madeddu., 2016, Vascular Pharmacology.

Microvascular and macrovascular pericytes can be considered stem cells, likewise MSCs, they have proliferative and clonogenic capacities, they express stemness antigens and have a multilineage differentiation potential *in vitro* (Crisan et al. 2008). For all these aspects, pericytes are defined progenitor of MSCs. Although microvascular and macrovascular pericytes share similar phenotypes and functions, some biological features are different. Furthermore, it is very difficult to delineate the difference between pericytes, MSCs and VSMCs because of the similar

antigenic characteristics. A universal consensus will be necessary to establish the similarities and differences between cell populations which share pericyte properties. Regardless of tissue source, microvascular pericytes have *in vitro* and *in vivo* different markers, such as, platelet-derived growth factor receptor β (PDGFRβ), neural/glial antigen 2 (NG2), CD44, ecto nucleotidase eNT/CD73, CD105, CD90, vimentin, and regulator G-protein signalling 5 (RGS5) (Covas et al. 2008; Crisan et al. 2008; Armulik et al. 2011). The transcription factors encoding for stemness and multipotency have been reported expressing by pericytes in few cases, and they have octamer-binding transcription factor 4 (OCT4), sex determing region Y (SOX2) and homeobox NANOG (Campagnolo et al. 2010; Avolio et al. 2015c). Alongside microvascular pericytes, there are two subpopulations which show some *in situ* antigenic differences based on the expression of CD146 and CD34. The first one is CD146+/NG2+ and CD34-/CD31-/CD45-, the second one is CD34+/NG2+ and CD146-/CD31-/CD45- (Campagnolo et al. 2010; Avolio et al. 2015c; Chen et al. 2015; Avolio et al. 2017). Compared to microvascular pericytes, adventitial or macrovascular pericytes are less studied. They have been found in the saphenous vein (adventitial saphenous-vein pericyte-APCs), cardiac vessels, thoracic aorta and arteries and veins from different tissues. They are CD34+/NG2+ and CD146-/CD31-/CD45- and express PDGFRβ, NG2 and the typical MSC markers, such as, CD44, CD90, eNT/CD73, and CD105. These cells may represent real vascular stem cells due to their primitive behaviour to act as progenitor or ancestor cells of different cell types, like MSCs. This theory is also supported by their multipotent phenotype CD34+ and CD31-/CD146- (Campagnolo et al. 2010; Corselli et al. 2012). Furthermore, these cells might be also progenitor of microvascular pericytes, however, further studies need to be undertaken (Crisan et al. 2008; Crisan et al. 2012). Our team have demonstrated that APCs exerted a great regenerative potential in mouse model of limb ischemia and acute MI (Campagnolo et al. 2010; Katare et al. 2011; Iacobazzi et al. 2014; Avolio et al. 2015b; Gubernator et al. 2015). Perivascular cells share different properties with other vascular resident cells, such as, MSCs, ECs and VSMCs. This might cause confusion derived by the fact that pericytes, *in situ*, are CD34+, antigen which is lost during culture and expansion of cells. Therefore, pericytes can be identified according to these criteria: morphology, co-expression of two or more markers, *in situ* localization, gene and protein expression and functional properties. A typical functional assay which allows to distinguish pericytes from MSCs, is Matrigel tube formation assay where pericytes promote and stabilize the networks created by the ECs (Campagnolo et al. 2010; Armulik et al. 2011; Dar et al. 2012; Avolio et al. 2015c).

1.4.2 Cardiac pericytes

Recently pericytes have been studied also in the heart. In such a vascularized organ, these cells are abundant, and their role in the tissue homeostasis and physiopathology has led the researcher to better study this cell population. Their role in the cardiac homeostasis is due to their intermediation between the blood system and vascular endothelium with cardiomyocytes and interstitial cells. To date, Cardiac pericytes (CPs) have been isolated from foetal heart, post-natal heart and post-mortem heart. Microvascular pericytes which share the same morphology as perivascular pericytes, have been isolated from adult explanted hearts using a Percoll density-gradient centrifugation. Expanded CPs expressed NG2, PDGFRβ, α-smooth muscle actin (α-SMA), calponin (CALP), and connexin-43 but they are also positive for alkaline phosphatase (ALP) (Nees et al. 2012). *Péault B.* has isolated microvascular pericytes from heart of foetus and adult post-mortem. After the isolation, expanded cells were NG2+/ PDGFRβ+/CD146+ and CD34-/CD45-, with mesenchymal lineage differentiation capacity. In addition, they were unable to differentiate in cardiomyocytes *in vitro* and *in vivo* in a murine MI model (Chen et al. 2015). In 2015, our team isolated and characterized microvascular and adventitial pericytes from remnants of heart biopsies of CHD new-born patients undergoing palliative surgery. *In situ*, these cells were CD34+/NG2+/PDGFRβ+ and CD31-/CD146-. *In vitro*, these cells loose CD34 antigen as reported for pericytes isolated from saphenous vein of patient undergoing coronary artery bypass grafting (CABG). They showed stemness markers, such as, SOX2, NANOG and OCT4, they were clonogenic and able to differentiate in mesenchymal lineage, but not in cardiomyocytes. They support the in vitro angiogenesis and release proangiogenic factors (Avolio et al. 2015c) (**Table 1-1**). Cardiac pericytes regulate and stabilize the angiogenesis and vessel permeabilization through direct (cell-cell) and indirect (paracrine mechanism) interactions with ECs. In some circumstances, pericytes move from a quiescent phase to an activated or angiogenic phase, triggering specific events, such as, migration and proliferation, maturation, coverage of ECs, secretion of GFs and ECM remodelling. At the same time proliferation, migration and angiogenic capacity of ECs are regulated by pericytes. Regardless the source, the pericyte-EC crosstalk is controlled by Angiopoietin 1/Tie2 signalling required for the EC and vessel stabilization. Angiopoietin 1 (ANG1) is expressed by pericytes whilst the antagonist, angiopoietin 2 (ANG2), and its receptor Tyrosine kinase with immunoglobulin-like and EGF-like domains 2 (Tie2) are expressed by ECs. ANG2 acts as an autocrine modulator of ANG1/Tie2 signalling by inhibiting ANG1/Tie 2 in the ECs, triggering vessel destabilization. Different studies have demonstrated that Tie2 is also expressed by pericytes and ANG2 produced by ECs, acts paracrinally on pericytes and in this way it contributes to the vessel

destabilization (Armulik et al. 2005; Ferland-McCollough et al. 2017; Teichert et al. 2017). Furthermore, the interaction ECs-pericytes is also controlled by VEGF-A/ VEGFR2 (vascular endothelial growth factor receptor 2) signalling which regulates the EC survival, vessel stabilization and angiogenesis sprouting (Darland et al. 2003; Chang et al. 2013). PDGF-BB/PDGFRβ signalling regulates pericyte recruitment and proliferation and vessel stabilization (Stratman et al. 2010; Fuxe et al. 2011). N-cadherin/N-cadherin and Jagged1/NOTCH signalling control pericyte recruitment, vessel maturation and stabilization, and sprouting (Tillet et al. 2005; Tattersall et al. 2016).

Source	Antigenic characteristics	References
Microvascular pericytes (heart)	*In situ*: NG2+/PDGFRβ+/CD146+ and CD34-/CD45- *In vitro*: CD34+	*Péault et al., 2015*
Microvascular and adventitial pericytes (heart)	*In situ*: CD34+/NG2+/PDGFRβ+ and CD31-/CD146- *In vitro*: CD34-	*Madeddu et al., 2015*
Adventitial or macrovascular pericytes from saphenous vein (APCs)	*In situ*: CD34+/NG2+/PDGFRβ+ and CD31-/CD146- *In vitro*: CD34-	*Madeddu et al., 2010*

Table 1-1. Antigenic characteristics of CPs obtained from cardiac biopsies and saphenous vein. *Abbreviations:* CD= cluster of differentiation; NG2= neural/glial antigen 2; PDGFRβ= platelet-derived growth factor β.

1.4.2.1 Application of cardiac pericytes for congenital heart disease using tissue-engineering applications

CPs are raising considerable attention for cardiovascular reparative field and particularly in congenital heart structural malformations. The reasons of using CPs for cardiac repair are numerous. For instance, they are pleiotropic, angiogenic and safe cells. They do not form tumours which are associated with the use of iPSCs. However, prior to starting a clinical phase trial, it is fundamental to undertake teratoma studies according to the international consensus guidelines. These cells have abundant secretome containing many cytokines and GFs that induce tissue regeneration and angiogenesis *via* paracrine signalling and containing chemoattractant factors which recruit CPs and other cells to the damaged area. An important aspect to consider when choosing the best cell component for cell therapy is the number of cells that can be obtained from a tissue biopsy. CPs are more abundant than other stem or progenitor cells in the heart, and it is possible to yield millions of cells after their *in vitro* expansion by starting from ~ 100 mg of biopsy obtained from leftovers of CHD neonatal or infant patients undergoing palliative treatment (Avolio et al. 2015c). Furthermore, CPs are considered immunotolerant, for that reason they are preferred for an allogeneic transplantation if there is no time for the patient to wait for an autologous transplantation. Thus, the main approach for the definitive correction of complex forms of CHD is cell therapy with autologous CPs. Although pericytes isolated from non-cardiac tissues, such as, saphenous vein may be preferred for the easy access to the vein, CPs may be characterized by a higher plasticity and committed to differentiate in all the cardiovascular cell lineage due to their organ specificity (Avolio and Madeddu 2016). Nonetheless, due to pericyte heterogenicity, this is still to be investigated. For instance, the lack of their *in vitro* electrical activity might suggest that after transplantation, these cells do not cause arrhythmias (Avolio et al. 2015c). Due to their vasculogenic and angiogenic properties, these cells can be a valid candidate for the repair of structural alterations of vessels and cardiac muscle. They are compatible with the used scaffolds clinically certified, such as, SIS-ECM manufactured by CorMatrix® company. For all these aspects CPs may be an optimal cell source for TEVG reconstruction in patients with complex CHD lesions (**Figure 1-11**). This thesis illustrates a study evaluating the use of a TEVG engineered with swine allogeneic CPs. Results have been published in JAHA (Alvino et al. 2020).

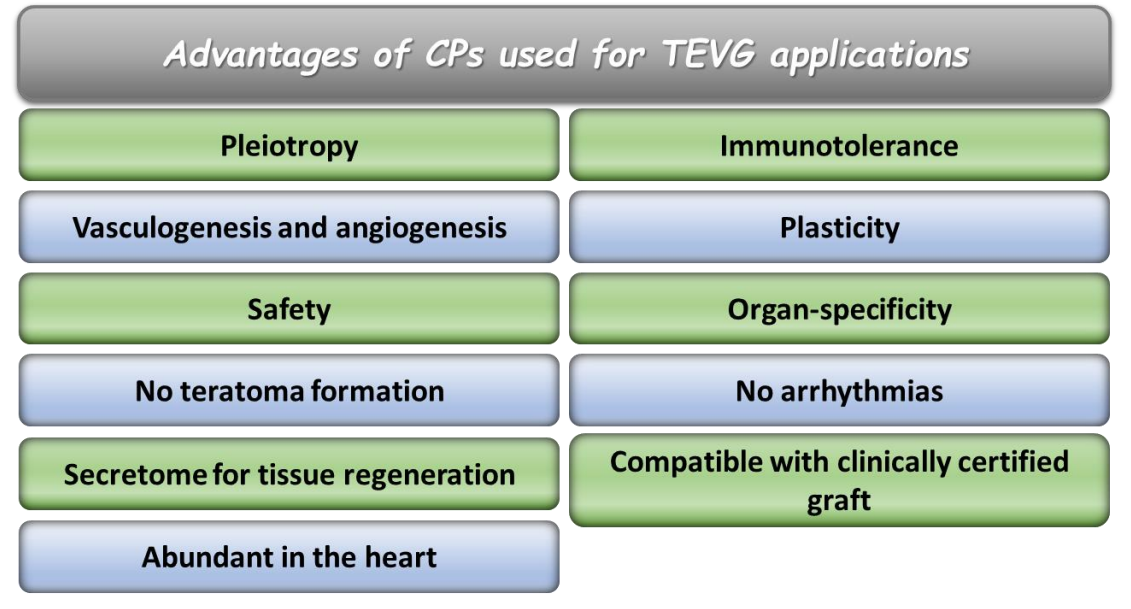

Figure 1-11. List of different advantages of using CPs seeded in a bioprosthesis for CHD definitive correction. *Abbreviations*: CPs= cardiac pericytes; TEVG= tissue-engineered vascular graft.

1.5 *In vitro* and *in vivo* models of cardiac diseases

Every therapy must show safety and efficacy before its application in human patients. Different therapeutic tests can be performed in different models: *in vitro* cell models, *in vitro* simulators, *in vitro* organoids and *in vivo* animal models (small and large animals). In biomedical research studies the general aim is to understand the human body and the physiological and pathological alterations which may affect its anatomy and function to undertake prevention or curative therapies. Thus, it is fundamental to start looking for the best way to simulate what happens in human patients by using the perfect *in vitro* and *in vivo* models. *In vitro* models are the "core" of biomedical research studies. There are different *in vitro* models used, depending on the number of cell type that can be yielded from different sources, the material replicated to obtain a cell preparation (tissue biopsy), and the culture system (suspension or adherent cultures and 2D- or 3D- systems).

- *In vitro* cell models

Historically, *in vitro* models were cells cultured in a 2D-plastic dish. Nowadays, cells are grown also in more complex 3D-structures, which provide structural and functional integrity and establish a better and dynamic cell microenvironment. *In vitro* cell models show many benefits, such as, easy pharmacological treatments, genetic modifications, small sample size and relatively low costs. Indeed, results from *in vitro* cell studies require to be investigated and validated in *in vivo* animal models prior to approaching to human situation. However, the

translational outcomes from the benchside to bedside is very hard because of a limited overlap between animals and humans. Although in the future the abrogation of *in vivo* animal model will be unlikely, the *in vitro* models are gaining always much interest in the global research field (Jonsson et al. 2016). Their importance is increasing with some initiatives, like, 3Rs (Replacement, Reduction, Refinement) which regulates the use of animals in a more controlled and ethical manner. The first "R" refers to replacement of the animals with other alternative techniques, such as, cultured cells. The second "R" indicates the reduction of the number of animals to employ in the experimental procedure without interfering with the good quality of data. The third "R" is for refinement to improve the quality of animal life in all the experimental stages (Cabrera-Pérez et al. 2016).

- *In vitro* simulators

Nowadays, simulators are gaining much interest for training and educational purposes. Hydraulic and computational simulators have been employing in cardiovascular field due to the complexity of this system. They can be tailored on patient's clinical parameters to simulate a specific physiopathological condition and they can make or support a clinical decision, by simulating a specific therapy to check the reaction of the patient. Nonetheless, simulators are a relatively new area of research and the test will require more studies from different investigators, such as, clinicians, biologists, bioinformaticians, and engineers.

- *In vitro* organoids

The concept of maintaining cells in 3D-environment is born because cells cultured in a conventional 2D-flat system perform differently than the cells in an *in vivo* environment. In these 2D-culture systems, cells are unable to mimic the dynamic complexity of an in vivo system. The possibility of using cells in a 3D-structure to simulate the native tissue or organ, could reproduce better the physiological and pathological mechanisms, and processes that, in some circumstances, cannot be produced in the body due to ethical issues or its scarcity. In addition, the use of this system may help to reduce the cost, time and work for the animal studies. Recently 3D-structures, called organoids, have been employed as *in vitro* models of human organs to understand physiological and pathological mechanisms. To date, brain, pancreas, intestine, lung, prostate and tumour organoids have been generated (Lancaster and Huch 2019). In the future organoids may be used in many research fields, such as, diseases, drug production, developmental biology, and regenerative and personalized medicine. An organoid resembles an organ and should satisfy some criteria: *i.* its 3D-structure should retain all the characteristics of the tissue which has been modelled; *ii.* it should contain different cell types as in the native organ; *iii.* It shows some of the specialized functions of the native tissue; *iv.* Self-organization

(self-assembly, self-patterning, self-morphogenesis), like in the native tissue (Sasai 2013a; Sasai 2013b). From blood, skin and urine samples collected from patients it is possible to obtain somatic cells that can be reprogrammed by adding transcription or reprogramming factors, to obtain human iPSCs which are employed for the generation of organoids (Long et al. 2018). Different iPSCs have been obtained from human cardiac heart diseases, such as, cardiomyopathy, cardiomyopathy associated to Duchenne muscular dystrophy (DMD), arrythmias, cardiac hypertrophy and MI. The creation of cardiac organoids can be a challenge due to the complex environment constituted by different types of cells that can be associated to specific diseases. Recent studies are trying to generate cardiomyocyte organoids derived from iPSCs. In addition, iPSCs isolated from a specific patient can be differentiated not only in cardiomyocytes but also in cardiac fibroblasts, and ECs, so that they can be used to create an organoid which represents the specific physiological and pathological characteristics of that patient. For instance, in the heart, fibroblasts are responsible for the remodelling of cardiac tissue through the synthesis and secretion of ECM and contribute to the electrical properties of the heart isolating the upper and lower chambers of the heart. ECs regulate the contractility of cardiomyocytes, they are oxygen and nutrient transporters and are controller of vasomotor tone. For all these aspects, these cells (cardiomyocytes, ECs and fibroblasts) may be cultured together to generate a human cardiac functional organoid. Different TE techniques have been developed to create 3D-cardiac tissue organoids and mimic heart physiology. The first one attempts to create tissue models by seeding cells in moulded hydrogel with collagen, Matrigel, fibrin and other biomaterials. The final organoid can be used to measure the contractile force. The second technique uses cell sheets cultured on a heat responsive 2D-surface. Then, different sheets are collected and mounted with the alternative to include vascular structures which are harvested from the animals, or to include supporting scaffolds. The third method uses the gravity to allow the sediment of cells and produce the organoids (hanging-drop system), which contains thousands of cells (Zuppinger 2016; Nugraha et al. 2019).

- *In vivo* animal models

Although the different *in vitro* models represent a pillar in the biomedical research to study physiological and pathological mechanisms of a disease and to track quickly a therapeutic compound, many human pathologies rely on having appropriate *in vivo* models to study the state of a disease and develop a specific therapy (Dottori et al. 2012). Animal preclinical models propose to recreate this condition aiming to test therapies that will be reproduced in the future clinical trials on the human patients. Small animal models, such as, mice and rats, are often used in cardiovascular research, as they are cost-effective, they have easy handling and housing

(maintenance in small cages), short gestation, they can be genetically manipulated to generate transgenic animals and short life- span which allows the investigators to follow the natural history of disease in a reasonably short time. MI mouse model is the most used to simulate an infarct. In MI patients the mortality is quite high and those ones who survive have a heart-pump alteration. Cardiomyocytes are irreversible affected, and the medical therapy helps to relieve the symptoms (Andersen et al. 2014). In order to create a MI model, living mouse is sedated with isoflurane chamber or by injecting anaesthetics followed by a short cooling time in ice water. In order to maintain the anesthesia under hypothermic conditions and perform the surgery, the animal is positioned on a cool bag in the right lateral position, the skin is cut, the thorax at the level of the 4^{th} intercostal space, and the left anterior descending (LAD) artery is ligated. Induced MI is highlighted by the light pallor in the heart below the ligation after the sutures. Then, the thorax and skin are closed, and mouse is placed on a warm-heated plate for its recovery (Katare et al. 2011; Dayan et al. 2012; Porrello et al. 2013; Avolio et al. 2015b; Camacho et al. 2016). Another model of peripheral artery disease (PAD) is the hindlimb ischemia mouse model. It consists in the surgical ligation of the proximal and femoral artery, followed excision of the vessels bringing the occlusion of the blood flow and induction of limb ischemia (Niiyama et al. 2009; Padgett et al. 2016). Despite small rodents are commonly used to recapitulate some phenotypic characteristics of the human heart diseases, these models do not simulate all their characteristics. According to phylogenetic properties, mouse and human are very distant each other and all the physiological and pathological mechanisms and responses to different therapies, such as, pharmacological treatments or specific cell therapies are not predictable. In addition, mouse and human have different heart anatomy, coronary structures, capillary density, and cardiac mechanical properties. Since mice are small-sized animals, imaging studies, and blood sampling procedure result complicated (Darland et al. 2003; Mestas and Hughes 2004; Libby 2015; Tsang et al. 2016). All these aspects limit the possibility of obtaining clear and significant experimental results for the future therapies in humans.

1.5.1 Large animal models and preclinical applications with tissue-engineered vascular grafts.

Despite no animal model replicates exactly the *in vivo* characteristics of the human being, to increase the robustness of the data and to better predict the clinical scenario, large animal models are always more used as a solid preclinical tool for future human translational studies (Epstein et al. 2017). The advantages of these animals are numerous, such as, long life span,

immunology characteristics similar to humans, large material to manipulate for the experimental procedures and high yields of cells obtained from the isolation. Particularly, swine animals have cardiovascular similarity with humans for heart size, heart physiology, hemodynamic parameters and contractility, tolerance to complex and invasive interventions and suitability for imaging studies (Harding et al. 2013; Tsang et al. 2016). Currently swine model studies are gaining much interests in cardiovascular field for cell therapy with dispersed cells and for TE vascular applications. In the latter, swine become patently necessary when testing an intracardiac or vascular graft (in forms of patches, conduits, valves or stents), and biomedical devices. The lack of similarity between human and mouse in vascular dimensions and hemodynamic parameters make these rodents poor models for TEVG evaluation (Swartz and Andreadis 2013). Nonetheless, the use of a large animal faces some limitations, such as, rapid growth which makes difficult the adult animal handling, high costs for husbandry maintenance and for experimental procedures. In fact, swine studies are expensive from both time and financial perspectives and most laboratories cannot afford them. Nonetheless, because they are conducted in closer setting with human conditions, than those ones performed in rodent models, the efficacy and safety require a preclinical and confirmation also in a large animal model. Swine animal is the most suitable model for the TEVG in CHD repair (Iop et al. 2014; Mosala Nezhad et al. 2017). Some models have been created to reproduce the clinical scenario of complex forms of CHD, such as, TOF (Albertario et al. 2019; Ghorbel et al. 2019). Piglets have been used for many reasons, to simulate a pediatric CHD situation, their quick growth allows the monitor of the implanted TEVG with a fast pace. Optimal TEVG procedure requires integration, remodelling and functionality of the graft, which depends on the regenerative capacity of the recipient animals determined by the age. In fact, neonatal or young swine, represent optimal recipient for these purposes (Swartz and Andreadis 2013). Furthermore, it is possible to obtain a young swine bred littermates from the same husbandry to undertake paired experimental procedures and allogeneic cell transplantation studies without incurring in the immune response and rejection of the recipient swine. An equivalent cell product from a swine littermate allows the use of a TEVG with allogeneic cells as an alternative to autologous procedure.

Prof *M. Caputo* has surgically created some models which reflect complex CHD malformations. The first one is a young swine model which reproduces the clinical scenario of TOF/pulmonary atresia with hypoplastic native left and right PA and major aorto-pulmonary collaterals. Surgical PA branch and pulmonary valve replacement are the only alternative treatment by using a TEVG conduit (CorMatrix®) and pulmonary valve repair with autologous swine pericardium. In this animal model, a left posterolateral thoracotomy is performed, the proximal and distal parts of

the left pulmonary artery (LPA) are clamped, and a ~ 3 mm LPA is resected to accommodate the TEVG conduit (CorMatrix®, ~ 10 mm long and ~ 6 mm diameter) with or without cells (**Figure 1-12**) (Ghorbel et al. 2019). The second one is a swine model which recreates the clinical scenario of TOF with RV dysfunction and where the reconstruction of the RVOT (pulmonary valve not included) is required. Briefly, piglet heart is exposed through median sternotomy and cardiopulmonary bypass is then established by cannulation of the inferior and superior vein cava and the ascending aorta. An incision of ~ 4 cm in length is made over the RVOT and below the pulmonary valve annulus, leaving the pulmonary valve intact. The cut is closed using a TEVG patch (CorMatrix®) with or without cells (Albertario et al. 2019). Currently, Prof *Caputo* is creating new two surgical approaches to simulate TOF patients with pulmonary atresia requiring MPA and pulmonary valve substitution. In the first case, ~ 8 mm MPA is excised on the beating heart just above the pulmonary valve and up to the pulmonary artery bifurcation, and the TEVG conduit (CorMatrix®) is implanted as interposed graft. Pulmonary valve is repaired with autologous swine pericardium. In the second case, a longitudinal incision starting from the MPA across the pulmonary valve annulus is created into the RVOT and the TEVG conduit (CorMatrix®) is sutured into place on an empty beating heart. Pulmonary valve is substituted with a different material.

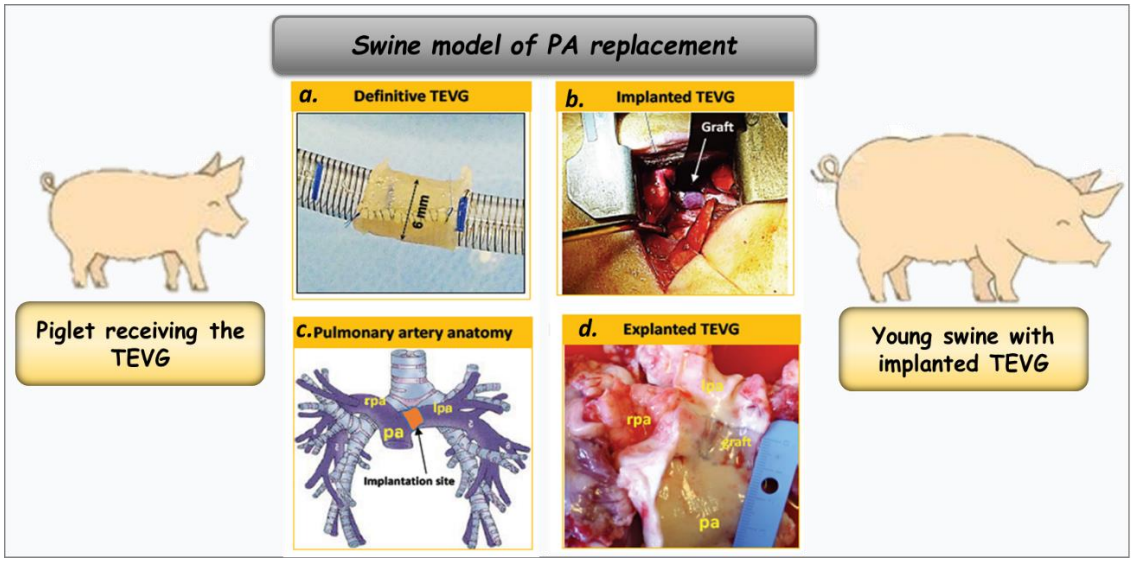

Figure 1-12. Schematic representation of a swine model of PA reconstruction. Piglet ready to receive a TEVG conduit (a.), which is implanted around a branch of PA which has been previously resected (b.); Figure panel showing the anatomical area of TEVG implantation; (c.); Explanted TEVG and native PA (d.) when the pig has grown. *Abbreviations*: PA= pulmonary artery; lpa= left pulmonary artery; mpa= main pulmonary artery; TEVG= tissue engineering vascular graft. Figure adapted in a modified version from Ghorbel et al., 2019, Biomaterials.

Different small and large animal models have been tested using TEVG to evaluate the safety and feasibility of the intervention before translational studies. During these procedures, grafts were seeded with progenitor or mature cells and further implanted into the animal model. Some examples are listed in the **Table 1-2**.

Preclinical model	Cells seeded	Graft used	Outcomes	References
1. Rat	Xenogeneic skeletal pericytes	Poly(ester-urethane) urea scaffold	Implanted into abdominal aorta, pericyte populated the graft, ECs, SMCs, collagen remodelling	*He et al.*, 2010
2. SCID mice	Xeneogenic BM-MNCs	PGA scaffold	Implanted in vena cava as interposed graft, organized layer of ECM, ECs and SMCs resembling native tissue	*Roh et al.*, 2010
3. Lamb	Autologous BM-MNCs	PGA scaffold	Implanted in vena cava as interposed graft, graft patent and increased in volume, no aneurism dilatation	*Brennan et al.*, 2008
4. Lamb	Allogeneic BM-MNCs or MSCs	Decellularized swine pulmonary conduit	Implanted into PA, re-endothelialisation, BM-MSC valves with ECM remodelling, BM-MNC valves with inflammatory cell infiltration	*Vincentelli et al.*, 2007
5. Sheep	Autologous BM-MSCs	PGA/PLLA	Implanted into PA, graft comparable to native tissue	*Sutherland et al.*, 2005
6. Dog	Allogeneic BM-MNCs	Copolymer covered by PLLA	Implanted into vena cava, no stenosis, graft showing ECs and SMCs	*Matsumura et al.*, 2003b
7. Sheep	Autologous ECs	Decellularized bioprosthetic valves	Implanted into RVOT, no calcification, ECs and fibroblasts in the graft	*Dohmen et al.*, 2006

Table 1-2. Preclinical animal models for TEVG application. *Abbreviations:* BM-MNCs= bone marrow mononuclear cells; ECs= endothelial cells; ECM= extracellular matrix; MSCs= mesenchymal stem cells; PA= pulmonary artery; PGA= poly(glycolic acid); PLLA= poly(lactic acid); SCID=sever combined immunodeficient. References: 1.(He et al. 2010); 2.(Roh et al. 2010); 3.(Brennan et al. 2008); 4.(Vincentelli et al. 2007); 5.(Sutherland et al. 2005); 6.(Matsumura et al. 2003b); 7.(Dohmen et al. 2006).

1.5.2 Clinical application with tissue engineered graft for congenital heart disease.

Currently the synthetic biodegradable polymers are the most used in clinical TEVG to produce scaffolds seeded with autologous human cells. These grafts are poly-lactic acid (PLLA), poly-glycolic acid (PGA) and polycaprolactone (PCL) and are easily manipulated and found on the market (Butcher et al. 2011; Avolio et al. 2015a). The transplantation of a TEVG in a pediatric patient with univentricular heart syndrome and pulmonary atresia, was performed in 2001.

Autologous cells were isolated from peripheral vein, expanded and seeded into a PLLA and PCL conduit graft, strengthened with PGA to degrade within six weeks. Twenty-eight weeks after implantation, the graft was not occluded and no dilatation was observed (Shin'oka et al. 2001). Twenty-four weeks later, the same research group implanted a PLLA/PCL graft seeded with BM-MNCs in CHD children. The results revealed the absence of obstruction (Matsumura et al. 2003a). *Naito et al*., have demonstrated the successful implantation of synthetic polymeric grafts seeded with saphenous vein-derived cells in an adolescent CHD patient (Naito et al. 2003). Four years later, *Shin'oka et al*., implanted synthetic polymeric grafts cellularized with BM cells. After sixteen months from the implantation, the TEVG was patent and no thrombosis was observed (Shin'oka et al. 2005).

Although these promising clinical outcomes in CHD young patients, the performance of the TEVGs requires deeply investigation. The TE synthetic polymers are prone to degradation (PGA: ~ 3 months and PLLA/PGA: ~ 3 years), altering the mechanical properties of the construct and making difficult the long-term follow-up studies.

2 Aim and objectives of the thesis and experimental plan

In the following chapters, I show the material, methods and results of my work during the three-year PhD course.

- **Cell-graft-based therapy for the treatment of complex CHD**

The aim of the project is to combine the CP-based therapy with a new delivery system as an alternative to the current biological and synthetic prostheses employed in pediatric surgery for the correction of CHD.

One major problem in the repair of congenital heart defects is that prosthetic grafts can only remodel through the repopulation by invading cells from neighbour tissues and the blood circulation. This spontaneous reparative process is not rapid enough to prevent a progressive mismatch between the graft and recipient's heart. In the complex form of CHD, such as, TOF, a palliative "shunt" operation becomes necessary to allow to direct blood flow to the lungs and relieve cyanosis before the definitive correction (Yuan and Jing 2009). This temporal window may provide a scope for expanding cardiac cells (CPs) from surgery leftovers obtained from the palliation, to generate living prostheses. Prostheses endowed with immediate growing capacity ahead of implantation could be better suited to match the rapid growth of the baby's heart than the currently available acellular grafts which without a bioactive component are prone to degeneration. For this study, swine animal model becomes a fundamental preclinical tool to reproduce the clinical scenario of a baby, infant or child with complex and severe forms of CHD, like TOF.

In the next chapters, I describe a new study aimed at testing the feasibility of implanting swine CPs engineered with a TE vascular conduit (CorMatrix®), in a four-week-old swine using the same procedure employed to reconstruct branch PAs in CHD patients. Autologous human CPs (hCPs), represent the final cellular product (Avolio et al. 2015c) for clinical application. However, as CPs are considered immunotolerant, they may be used for an allogeneic transplantation if there is no time for the baby patient to wait for an autologous transplantation with the vascular conduit. Thus, we used allogeneic CPs isolated from littermates of the recipient swine after the demonstration of antigenic and functional similarities with hCPs.

This project consists of three objectives: *Objective 1*, set-up isolation and expansion protocols to generate stocks of quality assured swine CPs and demonstrate the equivalence with human CPs according to antigenic and functional properties; *Objective 2*, encompasses the seeding of swine CPs into a TEVG and provides a proof of their viability, ECM remodelling and unchanged phenotype following two different *in vitro* culture systems; *Objective 3*, provides a proof-of-

concept of feasibility and efficacy of the pericyte-TEVG in the swine TOF model and histological assessment of the explanted grafts (**Figure 2-1**).

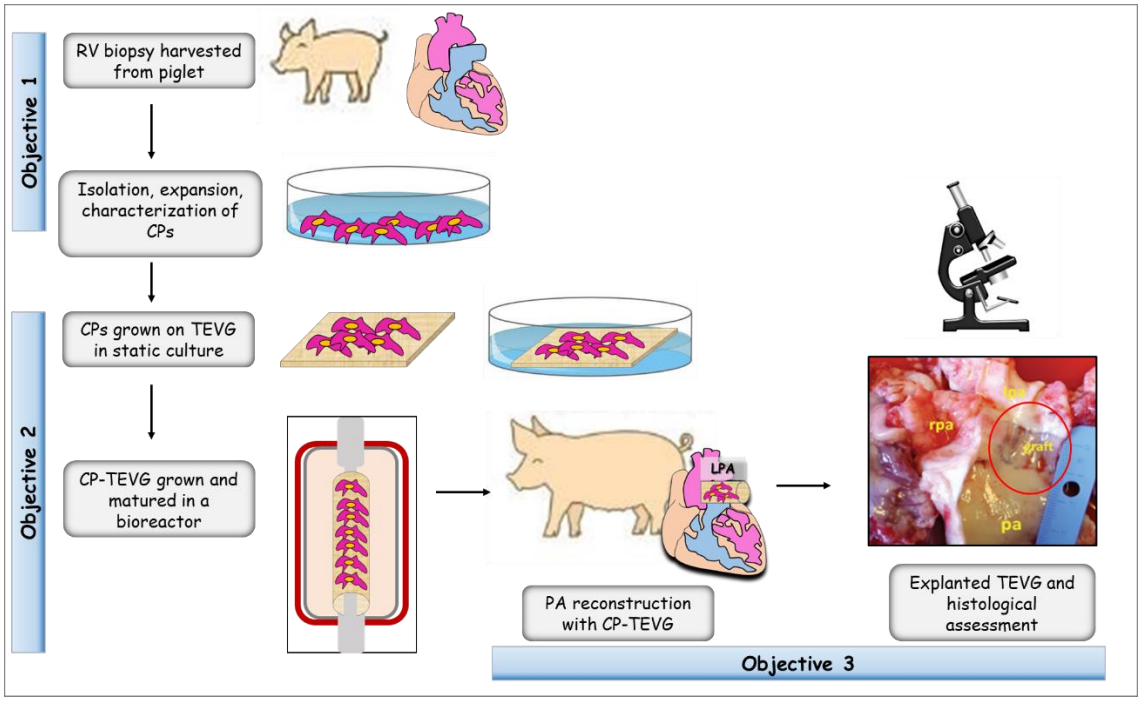

Figure 2-1. Schematic representation of the three main objectives in the project. *Abbreviations*: CPs= Cardiac pericytes; ECM= extracellular matrix; LPA= Left pulmonary artery; PA= pulmonary artery; RV= right ventricle; TEVG tissue engineering vascular graft.

3 Rationale of the study

3.1 Preclinical testing of pericyte-engineered grafts for the correction of congenital heart defects

In this chapter, I report the first preclinical trial with swine CPs delivered with a TEVG conduit in a swine model of CHD to obtain proof of feasibility and efficacy of PA reconstruction before asking the permission for a future clinical trial. The results of the study are submitted for publication in the JAHA (Alvino et al. 2020). Previous studies for cardiovascular repair are based on a therapy with dispersed cells injected into myocardium to restore the whole cardiac muscle vascularization and contractility. For instance, this has been demonstrated in our previous publication where we used swine APCs for the therapy of acute MI in an adult MI model (Alvino et al. 2018). The above therapy is not suitable to repair and reconstruct a large vessel in patients with CHD. It is necessary to use a compatible and absorbable biomaterial which is implanted and integrated perfectly with the patient's body and grown with it. Most of the prostheses currently used are not durable and required to be replaced at some point, by exposing child and adult patients to multiple surgical interventions (Perloff and Warnes 2001; Yuan and Jing 2009; Said and Burkhart 2014; Rosario-Quinones et al. 2015). Here, the ECM-based graft (CorMatrix®) cellularized with CPs overcomes these issues (Scholl et al. 2010; Nelson et al. 2016; Woo et al. 2016). We tried to use autologous swine CPs (sCPs) at first, then, because of the difficulties associated with cardiac harvesting procedure, we have decided to use allogeneic cells obtained from a swine littermate.

4 Material and methods

4.1 Ethics

Animal experiments were performed in accordance with the "Guide for Care and Use of Laboratory Animals" published by the National Institutes of Health in 1996 and conforming to the "Animals (Scientific Procedures) Act" published in 1986. The protocol was covered by the UK Home Office ethical approval PPL 30/3019 and PF6E6335D. The report of experimental data follows the ARRIVE (Animal Research: Reporting of In Vivo Experiments) guidelines (Kilkenny et al. 2010).

4.2 Swine Cardiac Pericyte processing

The Good Manufacturing Practice (GMP) compliant-SOP for the isolation, expansion, characterization and functional activity of human new-born cardiac pericytes (hNB CPs) has been described previously (Avolio et al. 2015c). The *in vitro* protocols used for swine new-born CPs (sNB CPs) has been reported in this manuscript according to the previous publication (Avolio et al. 2015c).

4.2.1 Preparation of swine newborn cardiac pericytes

Four-weeks old Large white/Landrace piglets (UK registered breeder) were terminally anesthetized with Euthatal for the collection of cardiac tissue and blood *via* an indwelling jugular vein cannula for the isolation of peripheral blood-mononuclear cells (PB-MNCs) and extraction of serum used in the culture media for sCP expansion. In some experiments, commercial swine heat-inactivated serum (Sigma-Aldrich, UK) was used in alternative to the piglet serum. Cardiac samples (from 20 mg up to 200 mg biopsy) were processed using a modification of the GMP-compliant-standard operating procedure (SOP) previously employed for the isolation/expansion and characterization of CPs from the neonatal human hearts (**Table 4-1**). Briefly, cardiac biopsies were minced in small pieces and digested with 0.45 WU/mL/g Liberase enzyme for 2 hours, at 37°C. Cell strainers (70µm, 40 µm and 30 µm pores) were used to to remove clumps of cells and tissue after enzymatic digestion. Single cell suspensions of immunomagnetically-sorted CD31- and CD34+ cells were cultured in the incubator at 21% O_2 and 5% CO_2 and onto dishes coated with 1% (w/v) swine gelatin (Sigma-Aldrich, UK) in endothelial cell growth media-2 (EGM-2) supplemented with 10% heat-inactivated swine serum and 1% (v/v) penicillin and streptomycin (**Figure 4-1**). Adherent sCP colonies appeared after 7-10 days of culture and were passaged to

new culture dishes once they reached 80-90% of confluence. At P2, cells were split for further expansion or generation of frozen stocks.

Swine CP code	Weight (g)	Experimental use
240617 A	0.9	Immunohisto-cytochemistry, PCR, ELISA, Migration assay w/o anti-Tie2
080717 A	0.08	Immunohisto-cytochemistry, PCR, Matrigel-co, Migration assay w/o anti-Tie2
080717 B	0.08	Immunocytochemistry, FACS, PCR, Matrigel-co/CM, ELISA, Migration assay without anti-Tie2, EdU assay
060917 A	0.09	Immunocytochemistry, GC-viability-DT, Clonogenic assay, PCR, Matrigel-co, ELISA
060917 B	0.09	GC-viability-DT, FACS, Matrigel-co/CM, ELISA, Migration assay without anti-Tie2, EdU assay
060917 C	0.09	Immunocytochemistry, GC-viability-DT, Clonogenic assay
140618 A	0.2	PCR, Matrigel-CM, Migration assay-anti-Tie2, EdU assay
190618 A	0.013	Immunocytochemistry, Matrigel-CM, Migration assay-anti-Tie2, EdU assay
240718 A	0.01	Immunocytochemistry

Table 4-1. Code of donor newborn swine and analysis performed on corresponding cardiac samples and isolated cells. *Abbreviations*: DT= Doubling Time; ELISA= Enzyme-Linked Immunosorbent Assay; FACS= Flow Activated Cell Sorting; GC= Growth Curve; PCR= Polymerase Chain Reaction; Tie2= Tyrosine kinase with immunoglobulin-like and EGF-like domains 2.

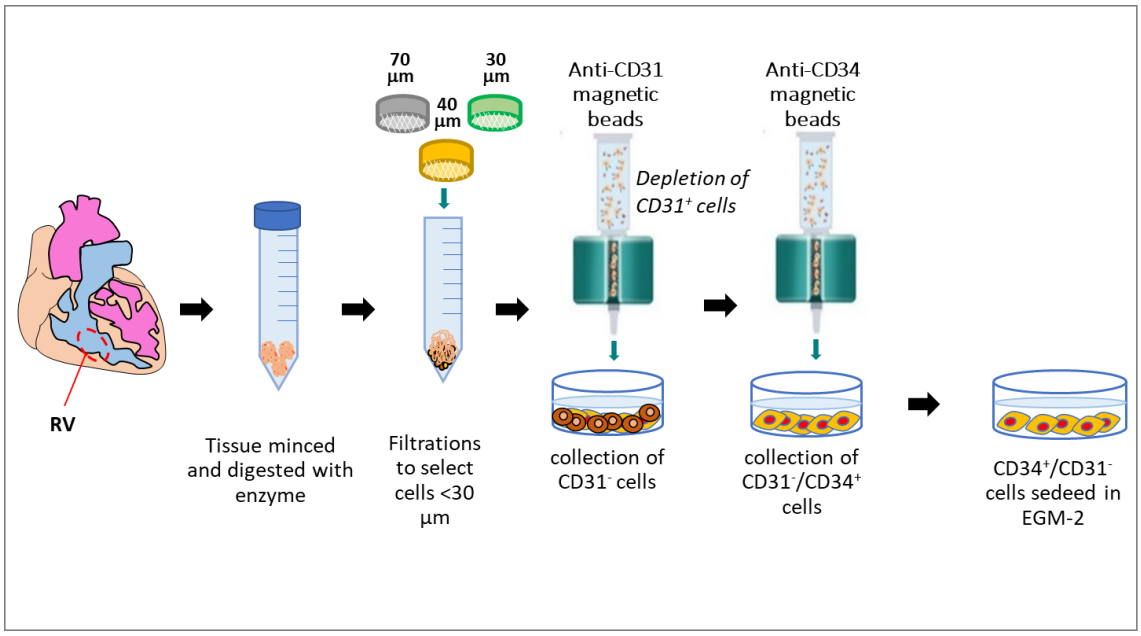

Figure 4-1. Scheme of swine NB CP isolation. Right ventricle (RV) small biopsy was harvested from a four-week-old pig, minced in small pieces and digested with Liberase enzyme. The neutralized enzyme solution was passed through the filters for the selection of <30 µm cells. CD31-/CD34+ cell fraction was obtained from immunomagnetic separation with microbeads (anti-CD31 and anti-CD34). The first colonies appeared after 7-10 days of culture in EGM-2. *Abbreviations*: CD= cluster of differentiation; EGM-2= endothelial cell growth media-2.

4.3 Assessment of new-born cardiac pericyte features

A series of comparative studies were performed to assess the purity of cells isolated from swine heart biopsy and to verify their similarity to hCPs. The cells were studied at P5/6, using from 3 to 7 biological replicates (run in triplicate) unless otherwise specified.

4.3.1 Growth curves, viability and doubling time

For the cell quality control, three fresh or frozen-thawed sCP lines were seeded onto a pre-coated 6-well plate, in EGM-2 at a density of 3,000/cm^2. They were detached with 1xTrypsin/EDTA at 4, 5, 6, 7 and 8 days of culture and counted using Trypan Blue exclusion method to assess the cell expansion, viability and duplication time.

4.3.2 *In situ* localization and antigenic characteristics

4.3.2.1 Immunohistochemistry and immunocytochemistry studies

In order to determine if available antibodies identify pericytes in their typical perivascular localization, cardiac tissue samples (N=2) were harvested, washed in 1x phosphate buffered saline (PBS) and fixed in 4% (w/v) paraformaldehyde (PFA) for 16 hours, at +4°C. After one wash in 1xPBS, fixed samples were placed in 30% (w/v) sucrose for 48 hours, at +4°C and embedded in Optimal Cutting Temperature compound (OCT compound, VWR, UK). Eight-micron-thick sections were cut using the Cryostat STAR Nx50 (Thermo Fisher, UK) at -20°C. Frozen sections were fixed in ice-cold glacial Acetone (Fisher, UK) for 5 minutes, at -20°C. Fixed cells were kept air-dried for 15 minutes and hydrated in 1xPBS for 10 minutes. Non-specific binding sites were blocked with 5% (v/v) foetal bovine serum (FBS) in 1xPBS for 30 minutes, at +20°C. Double staining combinations of anti-swine NG2 (NovusBio, UK)/anti-human CD31 (R&D systems ,UK) and anti-swine CD34 (Abcam, UK)/anti-human CD31 primary antibodies were used for the *in situ* localization of CPs. After a 16 hours incubation, at +4°C in the above blocking solution, sections

were washed twice in 1xPBS and incubated with secondary antibodies (Alexa Fluor 568-conjugated anti-rabbit IgG, Alexa Fluor 647-conjugated highly cross-adsorbed anti-mouse IgG, Alexa Fluor 488-conjugated anti-rabbit, IgG – all Invitrogen, UK) diluted 1:200 in the blocking solution for 1 hour, at +20°C, in the dark. The nuclei were counterstained with 4',6-diamidino-2-phenylindole (DAPI) 1:1000 in 1xPBS for 2 minutes, at +20°C, in the dark. The sections were washed twice in 1xPBS and mounted with Fluoromount G mounting media (Invitrogen, UK). Immunofluorescent images were taken using 10x and 20x objectives of Zeiss Observer.Z1 microscope and Zen pro software. Primary, secondary antibodies and concentrations used in immunohistochemistry (IHC) are listed and described in the **Table 4-2**.

For immunocytochemistry (ICC), expanded cells (N=7 biological replicates run in triplicate) were fixed with 4% (w/v) PFA for 10 minutes, at +4°C, washed once in 1xPBS and incubated with the blocking solution. For the detection of intracellular antigens, cells were permeabilized with 0.1% (v/v) Triton X-100 for 10 minutes, at +4°C. Cells were incubated with the indicated primary antibodies (16 hours, at +4°C) and appropriate secondary antibodies (1:200, Alexa Fluor 488-conjugated anti-rabbit or anti-mouse IgG – all Invitrogen, UK) for 1 hour, at +20°C, in the dark. The nuclei were counterstained with DAPI. Slides were mounted with Fluoromount G and the images were taken at 200x and 400x magnification using Zeiss Observer.Z1 microscope. Zen pro software was utilized to compose and overlay the images. Secondary antibody controls by eliminating primary antibodies were used (images not shown). Swine pulmonary artery endothelial cells (sPAECs) were used as positive control for endothelial cell markers. Primary and secondary antibodies used in ICC are listed and described in the **Table 4-2**. The antibody concentrations in IHC and ICC were used according to those ones applied for hCPs.

4.3.2.2 Flow cytometry assessment

In order to assess the antigenic characteristics of sCPs, fluorescent activated cell sorting (FACS) was employed. To optimize the FACS analysis and exclude the occurrence of background, a single-step staining – fluorescent minus one (FMO) protocol was adopted on three sNB CP lines and on sPAECs for the endothelial cell antigen control. The FMO methodology is recommended in multiple fluorescence studies, like the ones used here, to ensure that any spread of the fluorochromes into the channel of interests is properly identified. Cells ($1x10^6$, N=3 biological replicates), were washed in 1x Dulbecco's phosphate buffered saline (DPBS) and treated with 1xtrypsin/ethylenediaminetetraacetic (EDTA). Then, they were washed, spun at 400xg, for 10 minutes, at +4°C and re-suspended in FACS staining buffer containing 1% (w/v) bovine serum

albumin (BSA), 1 mM (v/v) EDTA and 0.1% (w/v) sodium azide followed by blocking of non-specific binding with 10% (w/v) BSA in 1xDPBS. Next, $2x10^5$ cells/tube were incubated with pericytes, mesenchymal and endothelial antibodies fluorophore-conjugated for 30 minutes, at +4°C, in the dark and in FACS buffer. For the detection of endothelial marker CD31, cells were washed twice in FACS buffer. Swine PAECs were used as positive control for endothelial antigens CD31 and CD146. Swine PB-MNCs were used as positive control for the hematopoietic marker CD45. In addition, a Fixable Viability Dye eFluor780 was used to label dead cells and exclude them from the gating strategy. Prior to sample acquisition, the cells were fixed with 1% (v/v) PFA in 1xPBS. FACS antibodies used in flow cytometry are listed in the **Table 4-3**.

Marker	Technique	Permeabilization	Reactivity	I antibody source and dilution	II antibody source
α-SMA	ICC	Yes	Human/Swine	Sigma, 1:400	Sigma, Cy3-conjugated
CALP	ICC, IHC	Yes	Human/Swine	Abcam, 1:100	Invitrogen, A488 goat α-rabbit
CD31	ICC	Yes	Swine	Abcam, 1:20	Invitrogen, A488 goat α-rabbit
CD31	IHC	No	Human	R&D, 1:50	Invitrogen, A488 highly adsorbed goat α-mouse
CD34	IHC	Yes	Swine	Abcam, 1:100	Invitrogen, A488 goat α-rabbit
eNT/CD73	ICC	Yes	Swine	R&D, 1:10	Invitrogen, A488 donkey α-sheep
CD146	ICC	Yes	Human/Swine	Abcam, 1:100	Invitrogen, A488 goat α-rabbit
GATA-4	ICC	Yes	Human	Abcam, 1:100	Invitrogen, A488 goat α-rabbit
NANOG	ICC	Yes	Human	Abcam, 1:100	Invitrogen, A488 goat α-mouse
NG2	ICC, IHC	No	Swine	NovusBio, 1:50	Invitrogen, A488 goat α-rabbit

OCT-4	ICC	Yes	Human/Swine	Abcam, 1:100	Invitrogen, A488 goat α-rabbit
PDGFRβ	ICC	Yes	Swine	GeneTex, 1:100	Invitrogen, A488 goat α-mouse
SMMHC11	ICC, IHC	Yes	Human/Swine	Abcam, 1:100	Invitrogen, A488 goat α-rabbit
SMTN	ICC, IHC	Yes	Human/Swine	Santa-Cruz, 1:100	Invitrogen, A488 goat α-mouse
SOX2	ICC	Yes	Human/Swine	Merck Millipore, 1:100	Invitrogen, A488 goat α-rabbit
TAGLN	ICC, IHC	Yes	Human/Swine	Santa-Cruz, 1:50	Invitrogen, A488 goat α-mouse
VE-CADHERIN	ICC	Yes	Human/Swine	Santa-Cruz, 1:50	Invitrogen, A488 goat α-mouse
Vimentin	ICC	Yes	Human	Abcam, 1:400	Invitrogen, A488 goat α-rabbit

Table 4-2. Primary and secondary antibodies used in immunohisto-cytochemistry studies of sNB CPs. *Abbreviations*: CALP= Calponin; CD= Cluster of Differentiation; eNT= Ecto-5-nucleotidase; GATA-4= Transcription binding factor-4; NANOG= Homeobox protein NANOG; NG2=Neural/Glial antigen 2 proteoglycan; OCT-4= Octamer binding transcription factor 4; PDGFRβ=Platelet-Derived Growth Receptor β; SMA= Smooth Muscle Actin; SMMHC11= Smooth Muscle Myosin Heavy Chain 11; SMTN= Smoothelin; SOX-2= Sex determining region Y-box 2; TAGLN= Transgelin; VE-CADHERIN= Vascular Endothelial Cadherin.

Marker	**Permeabilization**	**Reactivity**	**Antibody source and dilution**	**Fluorophores**
CD31	No	Swine	Serotec, 1:80	PE
CD44	No	Swine	eBioscience, 1:20	APC
CD45	No	Swine	Serotec, 1:25	FITC
eNT/CD73	No	Swine	R&D, 1:10	Invitrogen, APC-conjugated donkey α-sheep
CD90	No	Swine	eBioscience, 1:20	PE-Cy7
CD105	No	Swine	LifeSpan, 1:5	PE
CD146	No	Swine	Serotec, 1:60	FITC

PDGFRβ	No	Swine	Biolegend, 1:25	PE
Dye eFluor780	No		eBioscience, 1:1000	APC-Cy7

Table 4-3. Antibodies used in flow cytometry studies on sNB CPs. *Abbreviations*: APC=Allophycocyanin; APC-Cy7= Allophycocyanin-Cy7; CD=Cluster of Differentiation; FITC=Fluorescein isothiocyanate; PE=Phycoerythrin; Pe-Cy7= Phycoerythrin-Cy7.

4.3.3 Clonogenic assay

The single-cell coning was performed on two sNB CP lines at P3, using a motorized device connected to the flow cytometry sorter (Influx™ BD, US). Sorted cells were placed into each well of a 96-well culture plate and cultured up to four weeks in EGM-2 media for the quantification of colonies generated from a single cell. A comparative assay between fresh and frozen-thawed sCPs was performed to assess if both conditions allow the generation of clones.

4.3.4 Gene expression assessment

Total ribonucleic acid (RNA) was obtained from cultured sCPs and reverse-transcribed using a High Capacity RNA-to-cDNA kit (Invitrogen, UK). The reverse transcription-polymerase chain reaction (PCR) was performed using the first-strand cDNA with TaqMan fast Universal PCR Master Mix and on a Quant Studio 6 Flex Real-Time PCR system for the following angiogenic genes: VEGF-A, Angiopoietin 1 (ANG1, Life Technologies, UK), Angiopoietin 2 (ANG2, Life Technologies, UK). The messenger ribonucleic acid (mRNA) expression level was determined using 2-ΔΔCt method. Swine PAECs were used as control of angiogenic factors. The TaqMan probes used in the molecular biology studies are listed in the **Table 4-4**.

Gene	Species	Assay ID
ANG1	Swine	Ss03391075_m1
ANG2	Swine	Ss03392362_m1
PPIA (housekeeper)	Swine	Ss03394782_g1
VEGF-A	Swine	Ss0339390_m1

Table 4- 4. TaqMan probes in the molecular biology studies. *Abbreviations*: ANG1= Angiopoietin 1; ANG2= Angiopoietin 2; PPIA= Peptidyl-Prolyl-Isomerase A; VEGF-A= Vascular Endothelial Growth Factor-A.

4.3.5 Angiogenic factor expression

Anti-human enzyme-linked immunosorbent assay (ELISA) kits (R&D Systems, UK) were used to measure the levels of VEGF-A, ANG1, ANG2 and basic Fibroblast Growth factor (bFGF) proteins in the conditioned media (CM) from sCPs (N=4 biological replicates run in triplicate) which were cultured in a T25 flask in 2.5 mL endothelial basal medium-2 (EBM-2) (serum and growth factor-free media), for 48 hours in the incubator. Swine PAECs were used as control. The optical density (OD) of each well was determined using a Dynex Opsys MR microplate reader set to 450 nm.

4.3.6 Network formation

The capacity of sCPs to form networks on Matrigel matrix basement membrane was assessed using sCPs or sPAECs alone or both in co-culture. In addition, the network formation capacity of sPAECs was assessed following stimulation with sCP-CM or unconditioned media (UCM). Briefly, cells (sCPs to sPAECs at a 2:5 ratio, N=4 biological replicates run in triplicate), were seeded in the µ-slides for angiogenesis (Ibidi, UK) on top of 10 µL thin-coated Matrigel in EBM-2 or sCP-CM for 6 hours. Prior to seeding, sCPs were stained with the long-term cell tracker Dil (TRITC-conjugated, red fluorescence, Thermo fisher, UK) to visualise CPs when forming network structures with sPAECs. Briefly, cell growth media was removed, and the cells were incubated with 1:1000 (v/v) Dil, for 5 minutes, at +37°C, protected from light. Cells were incubated with the dye for further 15 minutes, on ice and washed carefully with 1xDPBS. Media was added and cells were placed into the incubator for few hours for recovery prior to Matrigel assay. The network formation was assessed by taking images under brightfield and immunofluorescence (IF), using 5x objective and the length of networks was measured using the free software Imagej. Representative images were also taken using 10x objective.

4.3.7 Chemotactic activity – Endothelial cell migration assay

Next, the capacity of sCP-CM to exert chemoattractant effects and to induce the migration of sPAECs was tested. The latter (187,500 cells/cm^2) were seeded on Transwell cell culture insert equipped with 8 µm pore size polycarbonate membranes (Corning, UK) in EBM-2 media. The migration of sPAECs through the membrane was stimulated by adding 500 µL of sCP-CM to the bottom of the same wells. In parallel, EBM-2 basal media or EBM-2 supplemented with 100 ng/mL of swine recombinant VEGF-A (Cambridge Bioscience, UK) were used to assess spontaneous and growth factor directed migration. In a separate assay, an antagonist of tyrosine kinase with Immunoglobulin-like and EGF-like domains 2 kinase receptor (anti-Tie2, 7.5 µm

diluted in dimethyl sulfoxide - DMSO, Abcam, UK) was used to contrast the effect of the sCP-CM on migration. DMSO alone (7.5 µM, Sigma, UK), was used as vehicle. After 16-hour incubation at +37 °C in the incubator, the polycarbonate membranes were washed in 1xDPBS and scraped with a cotton swab to remove non-migrating cells. Migrating cells at the bottom side of the filter were assessed by Giemsa and DAPI staining. For the Giemsa staining, the membranes were fixed in 4% (w/v) PFA and 100% (v/v) Methanol. Giemsa stain solution was added for 1 hour, at +20°C, in the dark. For staining of the nuclei, the membranes were washed in 4% (w/v) PFA and incubated with 1:1000 (v/v) DAPI for 2 minutes, at +20°C, in the dark. In either case, membranes were washed twice in 1xPBS, carefully removed from the inserts with a scalpel and mounted with DPX (Distyrene, Plastyciser, Xylene, Sigma-Aldrich, UK) mounting media on top of the slides for the visualization of the cells and nuclei, respectively. Membranes were analysed with an epifluorescent microscope at 200x magnification; 10 fields were randomly acquired, and cells counted. Migrated cells were expressed as percentage of total seeded cells. A schematic representation of migration assay is shown in the **Figure 4-2**.

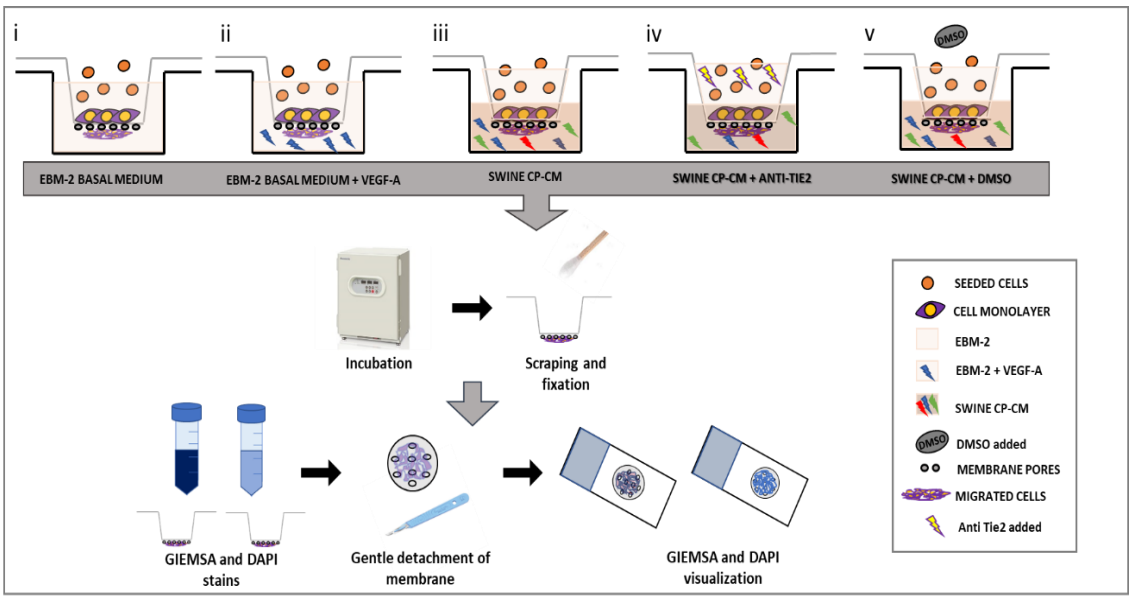

Figure 4-2. Chemotactic activity of sNB CPs. Migration of sPAECs in a transwell cell culture system. Different culture conditions were displayed: i. Cells seeded in EBM-2 basal medium; ii. EBM-2 with 10 ng/mL VEGF-A; iii. swine CP-CM (containing all GFs released by CPs); iv. sCP-CM with anti-Tie2; v. sCP-CM with DMSO. *Abbreviations*: CPs= cardiac pericytes; CM= conditioned media; DMSO= dimethyl sulfoxide; EBM-2= endothelial cell basal medium-2; Tie2= tyrosin kinase with immunoglobulin-like and EGF-like and EGF-like domains 2; VEGF-A= vascular endothelial growth factor-A.

4.3.8 Endothelial cell proliferation

The capacity of sPAECs to proliferate in the presence of sCPs and sCP-CM was assessed by Click-iT™ EdU (5-ethynyl-2'-deoxyuridine) Cell Proliferation Kit for imaging, Alexa Fluor™ 488 dye (Thermo fisher, UK), using UCM and sCP-CM media. Briefly, sCPs were labelled with Dil according to manufacturer's instructions prior to seeding for the assay. Swine PAECs and sCPs (sCPs to sPAECs at a 2:5 ratio, N=4 biological replicates, run in triplicate), were seeded into 96-multiwell-plate plastic dishes and the EdU was incubated for a minimum of 16 hours with 100 µL EBM-2 and sCP-CM. Cells were fixed in 4% (w/v) PFA and the membranes were permeabilized using 0.1% (v/v) Triton X-100. The EdU detection reagents were added to the wells for 30 minutes and an anti-swine CD31 primary antibody (Abcam, UK) was incubated for 16 hours, at +4 °C, protected from light. A secondary antibody was used to detect sPAECs stained with CD31 antigen. Cells were incubated with 1:10000 HOECHST 33342 for 3 minutes, at +21 °C, protected from light. Fluorescent images were taken using a fluorescent microscope and 10 fields were acquired randomly using 20X magnification objective. Proliferative sPAECs were counted as a percentage of total sPAECs seeded.

4.4 Tissue Engineering studies

4.4.1 Static culture of cardiac pericytes onto CorMatrix

For the cellularized vascular grafts employed during the surgical procedures for the correction of CHDs, pieces of extracellular matrix (ECM®, CorMatrix®, Cardiovascular, Sunnyvale, CA) were primed with EGM-2 media for 48 hours, at +37°C, and then, seeded with 20,000 sCPs/cm^2 at P5 and cultured for 5 days in a 48-multiwell-plate. To adhere the ECM at the bottom of the wells, sterile cell crown inserts (Sigma-Aldrich, UK) were used. The CM was then collected and the cellularized ECMs were cut in three pieces: one was fixed in 4% (w/v) PFA for 16 hours, at +4°C and embedded in paraffin for histological studies, while the other two pieces were OCT-embedded for frozen section preparation and snap-frozen for molecular biology and protein analysis. Nine biological replicates were examined unless otherwise specified.

4.4.2 Dynamic culture of cardiac pericytes onto CorMatrix

After completion of the 5-days static culture (5-days PS), sCP-seeded CorMatrix® was further grown in a 3D CulturePro™ Bioreactor (TA instruments, US) to overcome the limitations

associated with the traditional static culture conditions. Non-seeded CorMatrix® was used as control. The bioreactor system is composed of a peristaltic pump (Masterflex L/S digital 07528-20), a silicone tubing (3/175mm (1/8”) internal diameter (ID), 6.35mm (1/4“) outer diameter (ODI)) to connect the various compartments of the chamber, a pump cassette tubing (PharMed BPT tubing, 2-stop, 2.79 mm ID) compatible with Ismatec, IDEX Health & Science GmbH (SC0736)) to withstand the cyclic action of the pump and perfuse the all system, a single or multi-chamber stand for sample setup, and six 3DCulturePro bioreactor chambers. Every single 3DCulturePro bioreactor chamber consists of two separated compartments (chamber-A and chamber-B). Chamber-A has the function of reservoir while chamber-B is designed to host the scaffold. The flow rate is determined by the rotation per minute (RPM) selected on the pump interface and by the ID of the pump cassette tubing: with the ID of 2.79 mm and RPM range of 3-300, the flow rate can be set between 1.1 and 100 ml/min (**Figure 4-3**). All the components were designed to withstand laboratory procedures, autoclavable sterilization (cycle of 121°C for 30 min), and long period in incubators. The flat seeded-ECM was stitched in a conduit-shape to the rotating arm of the bioreactor with cells facing the external (abluminal) side of the conduit. The latter was filled with EGM-2 media supplemented with 10% (v/v) swine serum, 1% (v/v) penicillin and streptomycin and maintained in the incubator at +37°C. Seven and fourteen days later (7- and 14-days PB), the CMs were collected and the conduits were unstitched and cut in three pieces: one was fixed in 4% (w/v) PFA and paraffin-embedded and the other two pieces were frozen for OCT-embedding and for RNA and protein analysis. Four biological replicates were examined unless otherwise specified. A schematic representation of TE approach by using pericyte engineered grafts (PEGs) following static and dynamic culture environment is shown in **Figure 4-4**. The list of swine PEGs and specific experimental usage in the CorMatrix® and *in vivo* studies is reported in the **Table 4-5**.

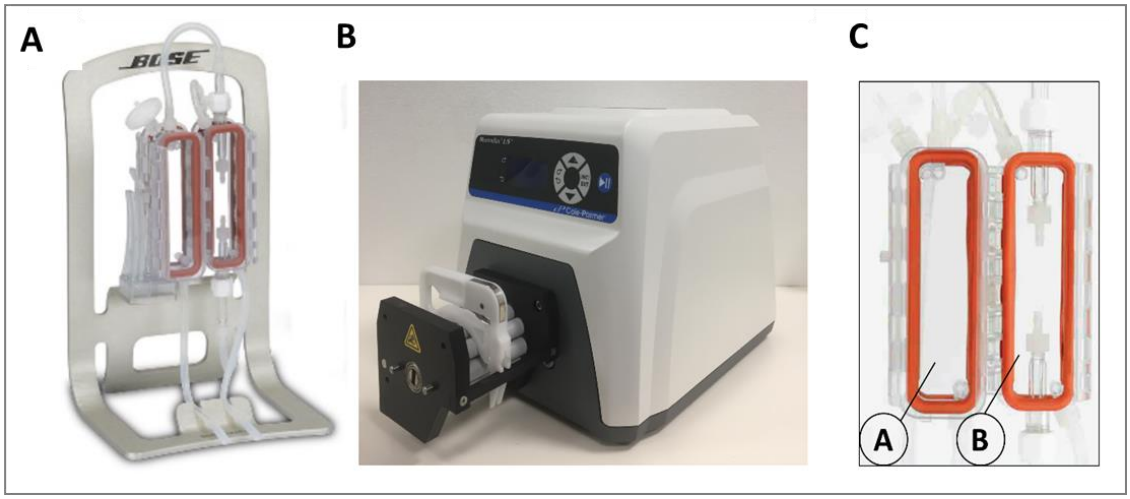

Figure 4-3. 3DCultureProTM perfusion Bioreactor. A. Perfusion bioreactor on a single chamber-stand; B. peristaltic pump; C. 3DCulturePro Bioreactor Chambers.

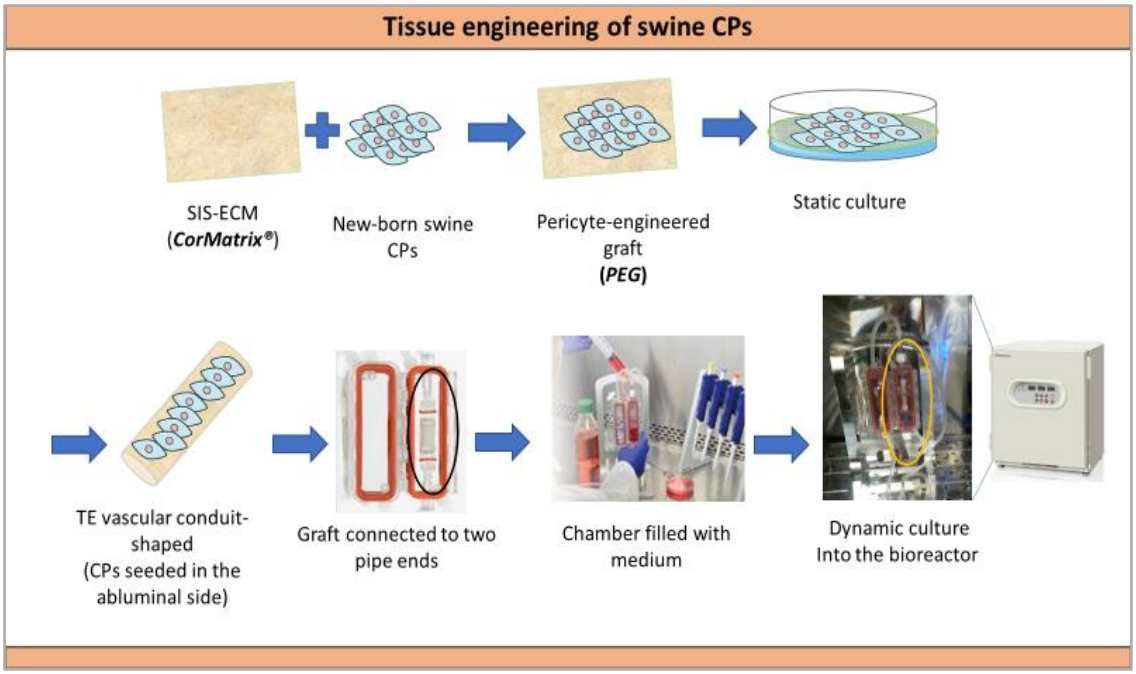

Figure 4-4. TE of sNB CPs. Cells seeded on top of swine decellularized intestinal submucosa (CorMatrix®) and cultured in a flat and static environment up to 5 days; A cellularized conduit-shaped matrix stitched to the rotating arms of a bioreactor, filled with media and grown up to 7- and 14- days in the incubator. *Abbreviations*: CPs= cardiac pericytes; ECM= extracellular matrix; PEG= pericyte engineered graft; SIS= swine intestinal submucosa; TE= tissue engineering.

Swine code	Post-static	Post-dynamic	In vivo
240617A	H&E, EVG, Collagen, Proliferation, Apoptosis, NG2 and VSMC markers	H&E, EVG, Collagen, Proliferation, Apoptosis, NG2, VSMC markers	
080717A	Collagen		
080717B	Viability, H&E, EVG, Collagen, Proliferation, Apoptosis, NG2 and VSMC markers	Viability, H&E, EVG, Collagen, Proliferation, Apoptosis, NG2 and VSMC markers	
060917A	H&E, EVG, Collagen, Proliferation, Apoptosis, NG2 and VSMC markers	H&E, EVG, Collagen, Proliferation, Apoptosis, NG2, VSMC markers	
060917B	H&E, EVG, Collagen, Proliferation, Apoptosis, NG2 and VSMC markers	H&E, EVG, Collagen, Proliferation, Apoptosis, NG2, VSMC markers	

191217A	Viability		
140618A	Viability, H&E, EVG, Collagen, Proliferation, Apoptosis, NG2 and VSMC markers	Viability	Engraftment
190618A	Viability, H&E, EVG, Collagen, Proliferation, Apoptosis, NG2 and VSMC markers	Viability	Engraftment
240718A	Viability, H&E, EVG, Collagen, Proliferation, Apoptosis, NG2 and VSMC markers	Viability	Engraftment
050918A	H&E, EVG, Collagen, Proliferation, Apoptosis, NG2 and VSMC markers		Engraftment
050918B	H&E, EVG, Collagen, Proliferation, Apoptosis, NG2 and VSMC markers		Engraftment
30.01.19A			Engraftment
30.01.19 B	Viability	Viability	Engraftment
Unseeded Graft	Viability, H&E, EVG, Collagen, Proliferation, Apoptosis, NG2 and VSMC markers	Viability, H&E, EVG, Collagen, Proliferation, Apoptosis, NG2, VSMC markers	Engraftment

Table 4- 5. Pericyte engineered grafts (PEGs) and *in vitro* and *in vivo* studies. *Abbreviations*: Elastic tissue Van Gieson's; H&E= Hematoxylin and Eosin; EVG=; NG2= neural/glial antigen 2; VSMC= vascular smooth muscle cells.

4.4.3 Immunohistochemistry of cardiac pericytes onto pericyte-engineered grafts

Histological assessment of the graft structure – To obtain a general layout of the cell and interstitial collagen distribution within the CorMatrix graft, 8 µm-thick frozen sections were stained with hematoxylin and Eosin (H&E), elastic tissue-Van Gieson's (EVG) using a Shandon Varistan 24-4 slide stainer (Thermo Fisher, UK) and Azan Mallory according to the manufacturer's instructions. Slides were mounted with DPX and covered with coverslips. Images were acquired at 10x and 20x objectives using Zeiss Axio Observer.Z1 with Zen Blue software (Carl Zeiss Microscopy, LLC, US).

Viability and apoptosis – Cells were detached from the CorMatrix graft by enzymatic digestion and cytospun for 5 minutes, at 500 rpm, at +20°C on top of slides using EZ double cytofunnelTM (Thermo Fisher, UK) and a cytospin machine (Cytospin 4, Thermo Fisher, UK). Slides were fixed

with 4% (w/v) PFA for 10 minutes, at +4°C and used for apoptosis assessment. Two different enzymes were used for cell detachment: 1xtrypsin/EDTA up to 5 minutes, at +37°C and 1xAccutase (Biolegend, UK) up to 10 minutes, at +37°C. Viability was determined with Trypan Blue exclusion method and apoptosis with Apoptag Red In situ Apoptosis Detection kit (Millipore, UK). As a positive control for apoptosis, sCPs were treated with 15 µM (v/v) of Hydrogen Peroxide (H_2O_2 Sigma, UK) in ddH_2O for 1 hour, at +37°C. In addition, cell viability was assessed *in situ* (without detaching cells from the graft), at 5-days PS and 7-days PB using a Viability/Cytotoxicity immunofluorescent kit (Thermo Fisher, UK). Saponin (Sigma-Aldrich, UK) treated samples were used as positive controls (0.1% (w/v) saponin in ddH_2O, for 10 minutes). Pieces of cellularized graft were washed in 1xDPBS and incubated with 2 µM Calcein, 4 µM Ethidium-homodimer-1 (EthD-1) in 1xDPBS, for 30 minutes, at +37°C, in the dark. For the visualization of the nuclei, 1:1000 (v/v) HOECHST 33342 in 1xPBS was added and 80% (v/v) of Glycerol in 1xPBS was used for live imaging.

Proliferation – After fixation in glacial acetone and permeabilization with 0.1% (v/v) Triton X-100, frozen sections were stained with anti-swine Ki67 primary antibody (Abcam, UK) in the blocking solution (5% (v/v) FBS in 1xPBS) for 16 hours, at +4°C. Alexa Fluor 568-conjugated IgG anti-rabbit was used as secondary antibody. After washes in 1xPBS, DAPI and Fluoromount G were used for the visualization of the nuclei and the imaging, respectively as previously described.

Expression of mural cell markers – The effect of the engraftment on the expression of pericyte and Vascular Smooth Muscle Cell (VSMC) markers. Eight-µm-thick sections from frozen samples were cut and fixed in ice-cold Acetone for 5 minutes, at -20°C. Sections were kept air-dried for 15 minutes and re-hydrated in 1xPBS. Non-specific binding sites were blocked using 5% (v/v) FBS in 1xPBS. Sections were incubated with anti-human and anti-swine NG2, α-SMA (Sigma-Aldrich, UK), CALP (Abcam, UK), transgelin (TAGLN, Santa-Cruz, UK), smoothelin (SMTN, Santa-Cruz, UK) and smooth muscle myosin heavy chain 11 (SMMHC11, Abcam, UK) primary antibodies for 16 hours, at +4°C. Secondary antibodies were incubated for 1 hour, at +20°C, in the dark. The nuclei were counterstained with DAPI and slides were mounted with Fluoromount G.

Immunofluorescent and brightfield images of representative grafts were taken using 10x and 20x objectives using Zeiss Observer.Z1 microscope and with Zen pro software. A swine LPA, a saphenous vein (SV) and RV biopsy specimen served as control tissues for all the above stainings.

4.5 *In vivo* implantation of vascular graft conduits engineered with cardiac pericytes

4.5.1 Study design and surgical procedure

Surgical procedures were performed with swine under general anesthesia (Ketamine®/Midazolam®/Dexmedetomidine®, Isoflurane®) and neuromuscular blockade (Pancuronium Bromide®). Details of the operation were reported previously (Ghorbel et al. 2019). Briefly, a left postero-lateral thoracotomy was performed in two 4-week-old sister Landrace female pigs. The proximal and distal part of the LPA was resected to accommodate the conduit-shaped graft (10 mm long and 6 mm diameter). One piglet received a conduit cellularized with sCPs from a sister piglet and cultured under static (5 days) and dynamic (7 days) conditions. The other pig was implanted with an unseeded conduit also maintained under static and dynamic conditions. Animals were recovered under intense postoperative monitoring for the initial 24 hours. Analgesics (Paracetamol® and Morphine®) and antibiotics (Cefuroxime®) were administered during this period according to the needs. Surgical procedures were performed by Prof and surgeon *Caputo M*.

4.5.2 Cardiac functional parameters

Imaging studies were performed using a two-dimensional Doppler Echocardiography system (VividQ, GE, Healthcare, UK) and a cardiac magnetic resonance 3-T scanner (Siemens Healthcare, Erlangen, Germany) at baseline and 4 months after implantation. Then, swine were euthanized by an overdose of IV pentobarbitone according to the surgical facility standard protocols.

4.6 Immunohistochemistry of vascular graft conduits

Four months after implantation, swine were sacrificed, and grafted LPAs were harvested and stored in 1xPBS on ice until transported to the laboratory. Tissues were either snap-frozen in OCT or fixed in 4% (w/v) PFA before OCT and paraffin inclusion for immunohistochemistry analysis.

For a general overview of the grafted LPA, cells and elastin content, 8 µm-thick frozen sections were stained with H&E and EVG using a Shandon Varistan 24-4 slide stainer. Slides were mounted with DPX mounting medium and coverslips were used to preserve the grafts for the imaging.

The occurrence of microcalcifications was assessed using Silver staining kit acc. to Von Kossa and Nuclear fast red-aluminium sulphate solution 0.1% (Merck Millipore, UK). Briefly, sections were incubated with 1% (v/v) silver nitrate solution under ultraviolet (UV) light for 20 minutes, at +20°C. After washes in distilled H_2O, the un-reacted silver was removed with 5% (v/v) sodium thiosulphate for 5 minutes, at +20°C. Slides were washed once, counterstained with 0.1% (v/v) nuclear fast red solution for 5 minutes, at +20°C and mounted with DPX and coverslips.

Collagen fibres and interstitial fibrosis were assessed with Azan Mallory solution on 5-µm-thick paraffin-embedded sections according to manufacturer's instructions.

All the images were taken using Zeiss Observer.Z1 microscope with 2.5x and 10x objectives and tiling parameters of the Zen pro software were used to cover the whole grafted LPA.

ECs in the intima and mural cells in the tunica media and adventitia of the LPA and graft were recognized using anti-human CD31 (1:50), anti-swine NG2 (1:50) primary antibodies and anti-swine α-SMA cy3-conjugated (1:400) for 16 hours, at +4°C. After two washes in 1xPBS, frozen sections were incubated with Alexa Fluor 647-conjugated highly adsorbed anti-mouse IgG and Alexa Fluor 488-conjugated anti-rabbit IgG secondary antibodies (all 1:200, for 1 hour, at +20°C). SMA antibody was incubated as last already cy3-conjugated. Slides were stained with 1:1000 (v/v) DAPI in 1xPBS and mounted with Fluoromount G for the imaging. Representative images were taken with 10x and 20x objectives using Zeiss Observer.Z1 microscope and Zen pro software.

4.7 Statistical analysis

Average values are plotted with group size value shown in figure legends. Statistical significance for differences between experimental groups was determined using Student's t-test when comparing two groups and ANOVA with post-hoc when comparing more than two groups. Values were expressed as means±standard error of the mean (SEM) or standard deviation (SD). Probability values (P) <0.05 were considered significant. Results from the in vivo feasibility study are reported in a descriptive format.

5 Results

5.1 Isolation, expansion and characterization of swine cardiac pericytes

5.1.1 Viability, growth curves and doubling time

Here, an adapted SOP previously employed for the isolation and expansion of human CPs was used to evaluate if an equivalent cell product could be obtained from swine cardiac biopsy. The main modification of the procedure was the substitution of 2% (v/v) heat-inactivated FBS with 10% (v/v) heat-inactivated swine serum and the use of 1% swine gelatin as coating material of culture dishes. Fifteen sNB CP lines were successfully isolated and expanded from small cardiac biopsies as small as 0.01 g weight (lowest limit of success). The swine cell lines used for in vitro and in vivo studies are reported in the Material and methods, **Tables 4-1** and **4-5**. The cells had a typical spindle-shape morphology (**Figure 5-1A-B**). They grew quickly in culture with an average doubling time (DT) of 44.5±7.6 hours (using fresh-expanded cells) and 41.7±4.6 hours (using frozen and thawed-expanded cells). From the initial seeding number (30,000 cells in a 6-multiwell plate, 3,000/cm^2), sCPs reached the final counts of ~600,000 (fresh-expanded cells) and ~450,000 (thawed-expanded cells) at 8 days of culture (**Figur 5-1C**). The viability was consistently >90% in all the samples examined (fresh-expanded cells 98±1.1; thawed-expanded cells 95±1.6) (**Figure 5-1D**).

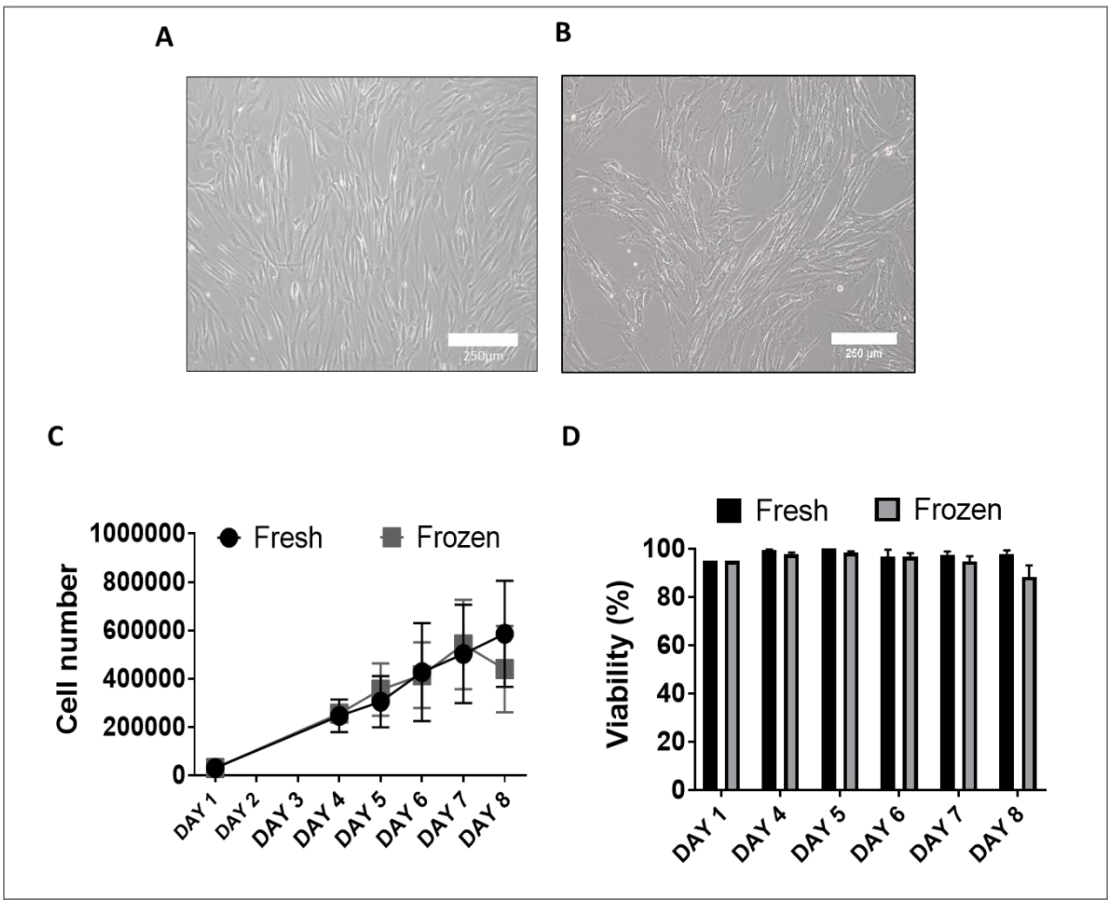

Figure 5-1. Morphology, growth rates and viability of CPs. A and B. Phase-contrast microscopy image of human (A) and swine (B) CPs (x100 magnification; scale bar=250 µm). C and D. Graphs showing the growth curves (C) and the viability (D) of 3 swine CP lines (n=3) seeded at 3,000/cm2 at day 1 and detached and counted at day 4, 5, 6, 7 and 8 of culture. Values are expressed as mean±SEM. Error bars in the graphs show the variability of the data and indicate the error in the above measurement.

5.1.2 Immunohistochemical localization of swine cardiac pericytes

IHC assessment confirmed the perivascular localization of swine CPs in the cardiac tissue. A combination of antibodies was used for cell-type *in situ* localization. CD31+/CD34+ ECs were typically found around the lumen of capillaries and arterioles. Moreover, here, CD31-/CD34+/NG2+ cells were identified around capillaries (**Figure 5-2A**) and especially within the external lamellae of the arterioles (**Figure 5-2B**).

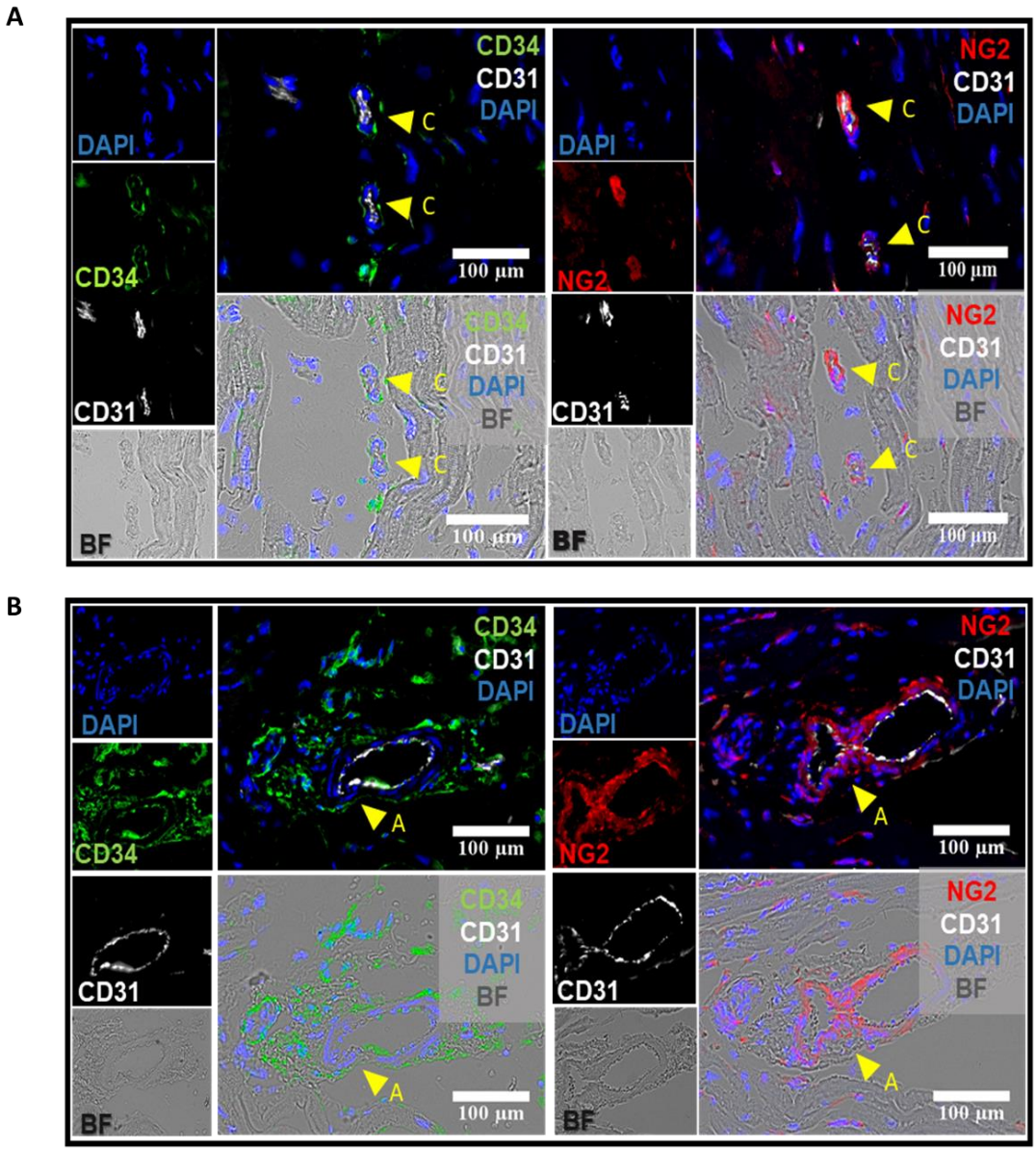

Figure 5- 2. In situ localization of swine CPs. A and B. IF and BF images showing the localization of CD31-/CD34+/NG2+ CPs in swine hearts around the small vessels - capillaries (A) and larger vessels - arterioles (B). A combination of specie-specific primary antibodies was used on the same field of two consecutive eight-µm-thick sections. Inserts showing anti-CD34 labelled with green fluorescence, anti-NG2 in red and anti-CD31 in pseudo-white colour. Nuclei are recognised by blue fluorescence of DAPI. Arrows indicate CPs around capillaries and arterioles. Images taken at x200 magnification, n=2 sample size, scale bar=100 µm. *Abbreviations*: A= Arterioles; BF= Brightfield; C= Capillaries; CD=cluster of differentiation.

5.1.3 Antigenic profile of swine cardiac pericytes by immunocytochemistry

The similarity of the two cell products was confirmed by ICC analysis showing the percentage of positive cells to the marker of total nuclei. The results displayed high expression of the lineage antigens NG2 (100±0.01%), PDGFRβ (100±0.01%), mesenchymal antigen eNT/CD73 (100±0.01%) and non-lineage marker Vimentin (100±0.01%). They were positive for the cardiac transcription factor GATA-4, and stemness markers SOX-2 and OCT-4 (all 100±0.01%) but negative for NANOG, and the endothelial markers CD31 and VE-cadherin. When looking at markers that identify VSMCs, ICC revealed that sCPs expressed α-SMA (97.1±1.0%) and CALP (96.7±1.0%). These two markers have a low-intermediate contractile specificity and they are not expressed only by VSMCs (Liu et al. 2013). Swine CPs were negative for TAGLN, SMTN and SMMHC, the last two ones are highly specific for the contractile VSMCs. Moreover, the positive expression for Ki67 (22.8±4.0%) confirmed proliferative activity of sCPs (**Figure 5-3**).

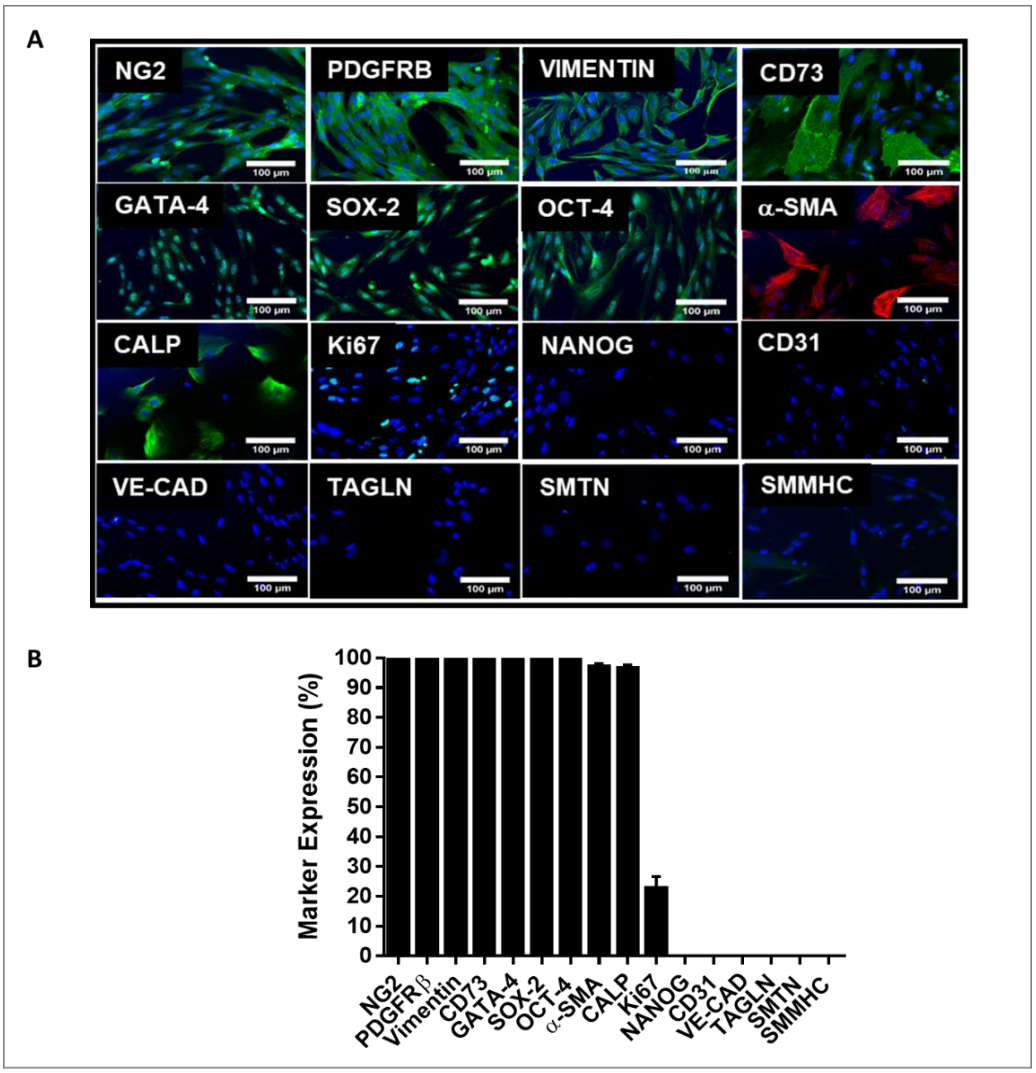

Figure 5-3. Antigenic characteristics by IF of swine CPs. ICC microphotographs showing the expression of NG2, PDGFRβ, eNT/CD73, Vimentin, GATA-4, SOX-2 and OCT-4. Cells are negative for NANOG and the EC markers CD31 and VE-cadherin. Swine CPs are positive for α-SMA and CALP and negative for TAGLN, SMNTN and SMMHC. The expression of Ki67 is indicative of proliferating cells. DAPI (blue) identifies nuclei. Magnification x200, n=7 sample size, scale bar=100 µm. Values in the bar graph are represented as mean±SEM. Fluorescence is normalised by total nuclei counted. *Abbreviations:* CD= cluster of differentiation; CALP= calponin; NG2= neural/glial antigen 2; OCT4= octamer-binding transcriptional factor 4; PDGFRβ= platelet-derived-growth factor beta; SMA= smooth muscle actin; SMMHC= smooth muscle myosin heavy chain; SMTN= smoothelin; SOX-2= sex deteming region Y; TAGLN= transgelin.

5.1.4 Flow cytometry characterization of swine cardiac pericytes

Furthermore, FACS analysis indicated that, like hCPs, cardiac-derived swine cells abundantly expressed PDGFRβ, the mesenchymal markers CD105, CD90, CD44, eNT/CD73, while being negative for CD146, CD31 and the hematopoietic marker CD45. Swine PAEC and PB-MNC positive controls were found positive for the expression of CD146, CD31 and CD45, respectively in ICC and FACS studies (**Figure 5-4**). While ICC visualises the marker expression in the cytoplasm, membrane or nucleus of the cell, FACS allows to select distinct cells by size and granularity, it excludes dead cells using gating strategy, and it identifies also a weak expression of the detected antigen.

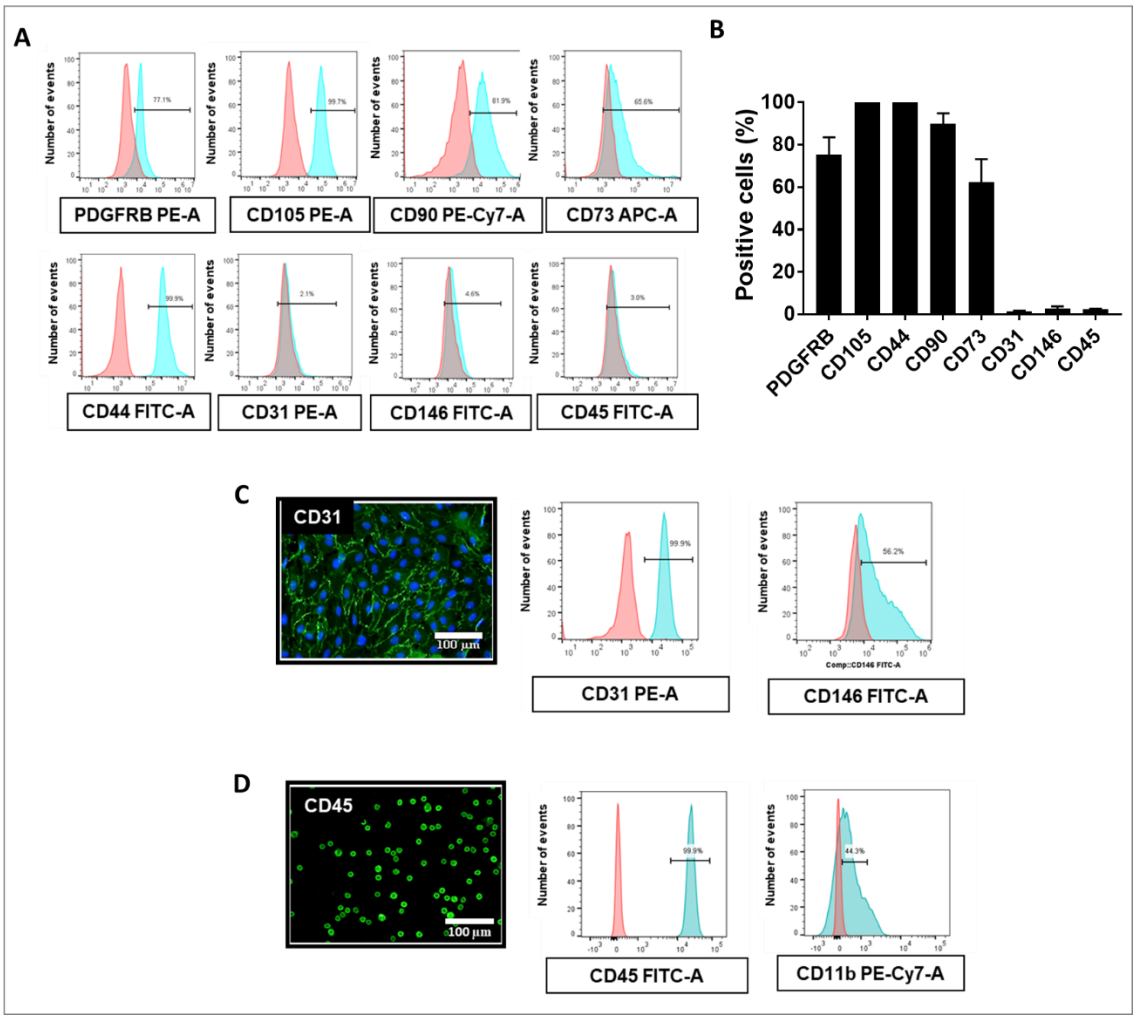

Figure 5-4. Antigenic characteristics by FACS of swine CPs. A and B. Representative graphs and histograms of each surface marker. Negative control staining profiles are shown by the red histograms, whereas specific antibody staining profile are shown by light blue histograms. Bar graph shows the mean±SEM values of n=3 biological replicates. C and D. IF images and histograms are also shown for sPAECs and sPB-MNCs. *Abbreviations:* APC-A=Allophycocyanin-area; CD= cluster of differentiation; FITC-A=Fluorescein isothiocyanate-area; PDGFRβ= platelet-derived-growth factor beta; PE-A=Phycoerythrin-area; Pe-Cy7-A= Phycoerythrin-Cy7-area.

5.2 Clonogenic potential

Two biological replicates were sorted as single cells and cultured in 96 multiwell-plates (**Figure 5-5A**). Two weeks later, 4.6% (11/240) and 9.2% (22/240) of freshly processed cells formed the first colonies. The same cell lines underwent the clonogenic assay after a cycle of freezing and thawing. In this experiment, colonies were generated by the two cell lines with a frequency of 7.9% (19/240) and 21.3% (51/240), respectively. Of these primary colonies, 0.8% (2/240) and

1.3% (3/240) from fresh cell lines and 0.8% (2/240) and 5.4% (13/240) from thawed cell lines could be further expanded in culture. **Figure 5-5B** showed that sCPs were able to generate clones from a single cell and that these clonogenic cells maintained the original phenotype as assessed by ICC.

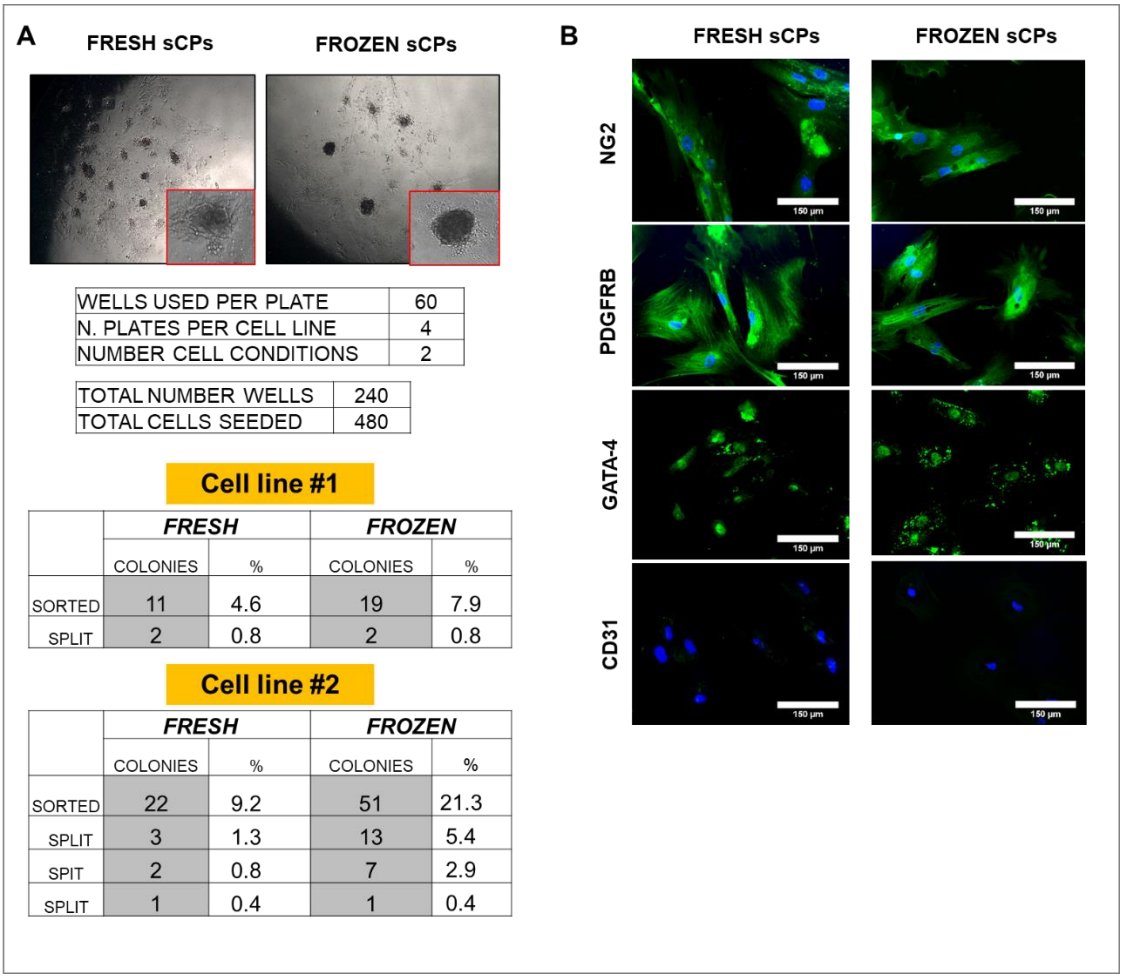

WELLS USED PER PLATE	60
N. PLATES PER CELL LINE	4
NUMBER CELL CONDITIONS	2

TOTAL NUMBER WELLS	240
TOTAL CELLS SEEDED	480

Cell line #1

	FRESH		*FROZEN*	
	COLONIES	%	COLONIES	%
SORTED	11	4.6	19	7.9
SPLIT	2	0.8	2	0.8

Cell line #2

	FRESH		*FROZEN*	
	COLONIES	%	COLONIES	%
SORTED	22	9.2	51	21.3
SPLIT	3	1.3	13	5.4
SPIT	2	0.8	7	2.9
SPLIT	1	0.4	1	0.4

Figure 5-5. Clonogenic capacity of swine CPs. A. Phase-contrast images showing the formation of the first colonies after two weeks from the cell sorting. As indicated from the tables, two fresh cell lines formed an average of 6.9% small colonies and two thawed cell lines gave rise to an average of 14.6% colonies. The second cell line formed new colonies after multiple passaging. B. IF images of colonies from fresh and thawed cells confirm the positivity for NG2, PDGFRβ and GATA-4 and the absence of CD31 antigen. Magnification x200, n=2 for fresh cell lines and n=2 for thawed cell lines, scale bar=150 µm. *Abbreviations*: CD= cluster of differentiation; NG2= neural/glial antigen 2; PDGFRβ= platelet-derived-growth factor beta; sCPs= swine cardiac pericytes.

5.3 Angiocrine properties

5.3.1 Angiocrine factors

Genes involved in the mechanism of angiogenesis were tested. Quantitative PCR analysis of angiogenic gene transcripts in five sCP lines showed these cells express more VEGF-A and ANG1 but less ANG2 than control sPAECs (**Figure 5-6A**). A similar pattern was observed comparing the levels of those angiogenic factors in the CM. For instance, VEGF-A in sCP-CM was 11.3 pg/hr/10^6 cells compared to VEGF-A in sPAEC-CM (0.03 pg/hr/10^6 cells). ANG1 in sCP-CM was 240.8 pg/hr/10^6 cells and not secreted by sPAEC-CM. ANG2 in sCP-CM was 11 pg/hr/10^6 cells and in sPAEC-CM was 38.9 pg/hr/10^6 cells. Basic FGF in sCP-CM was 11.1 pg/hr/10^6 cells and not secreted by sPAEC-CM. This result was in line with previous findings which explain the role of ANG1/2 pathway in pericyte-EC cross-talking (Armulik et al. 2005; Ferland-McCollough et al. 2017; Teichert et al. 2017). In addition, bFGF protein levels were remarkably higher in CM of sCPs compared with sPAECs (**Figure 5-6B**). Therefore, this angiocrine profile resembles the described paracrine phenotype of hCPs (Avolio et al. 2015c).

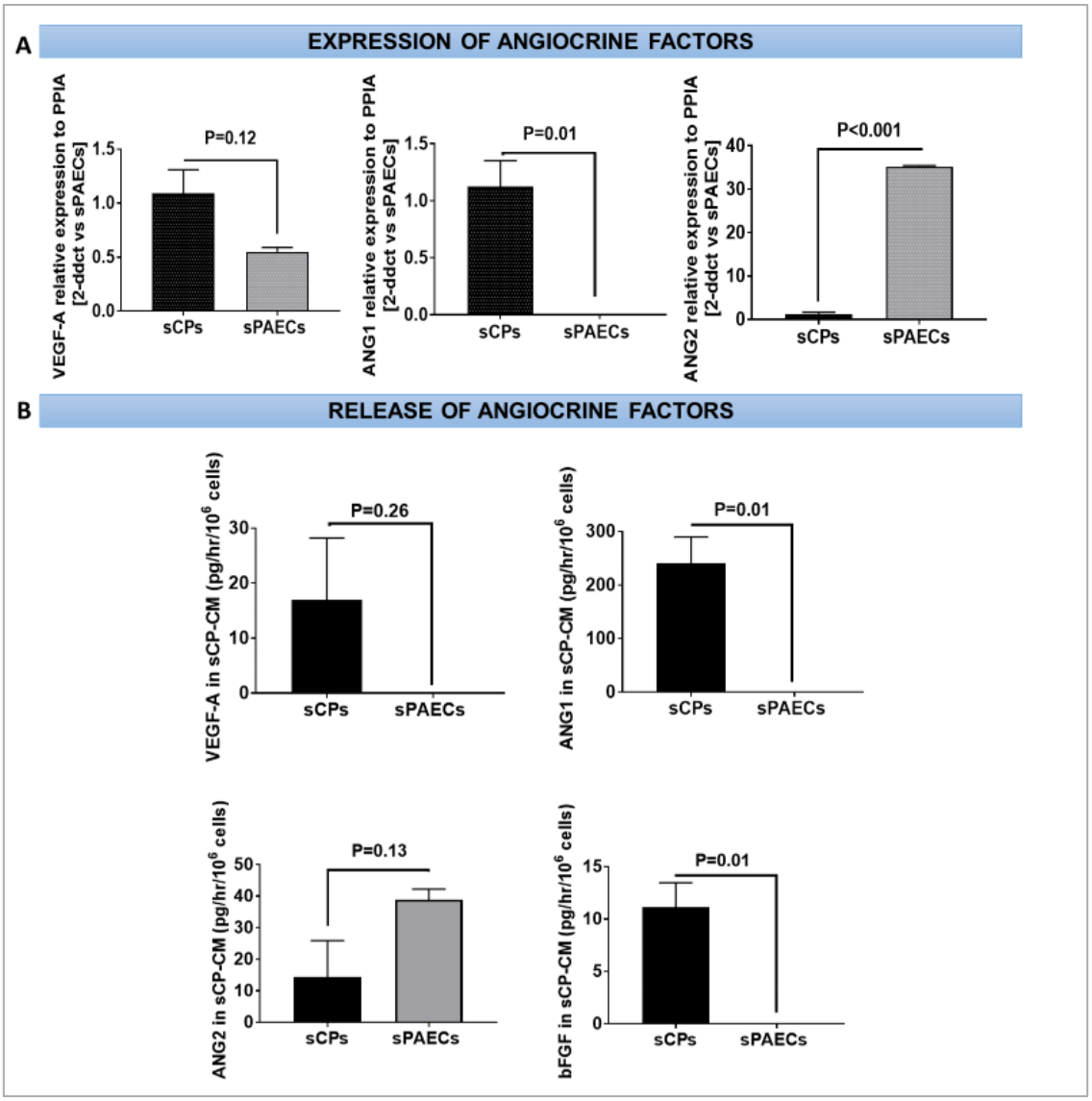

Figure 5-6. Expression and secretion of angiogenic factors by sCPs. A. Bar graphs show the expression of VEGF-A (P=0.1 vs sPAECs), ANG1 (*P=0.01 vs sPAECs) and ANG2 (**P=0.001 vs sPAECs) in n=4 sCP cell lysate. B. Bar graphs show the level of VEGF-A (P=0.26 vs sPAECs), ANG1 (*P=0.01 vs sPAECs), ANG2 (P=0.1 vs sPAECs) and bFGF *P=0.01 vs sPAECs) in the sCP-CM. *Abbreviations*: ANG1= angiopoietin 1; ANG2= angiopoietin 2; bFGF= basic fibroblast growth factor; PPIA= peptidylprolyl isomerase A; sCPs= swine cardiac pericytes; sPAECs= swine pulmonary artery endothelial cells; VEGF-A= vascular endothelial growth factor-A.

5.3.2 Proangiogenic activity

One of the important features of hCPs consisted of their ability to modulate the angiogenesis either *via* direct contact with ECs, or *via* paracrine mechanisms, by transferring GFs to ECs.

Therefore, an endothelial tube formation assay (Matrigel) was performed to investigate if sCPs also share the capacity to promote endothelial cell networks *in vitro*. In this set up, both sCPs (**Figure 5-7A**) and their CMs (**Figure 5-7B**) led to a potentiation of the network forming capacity of sPAECs used as an angiogenic target for sCPs here (sPAECs+sCPs *P=0.02; sCP-CM *P=0.01). Moreover, the sCP secretome exerted superior proangiogenic activity as indicated by the length of tubes expressed in mm (sPAECs+sCP-CM= 28.2 mm±2.3 vs sPAECs+sCPs= 11.1 mm±1.2). This occurred as higher specificity of the sCP-derived paracrine factors for sPAECs.

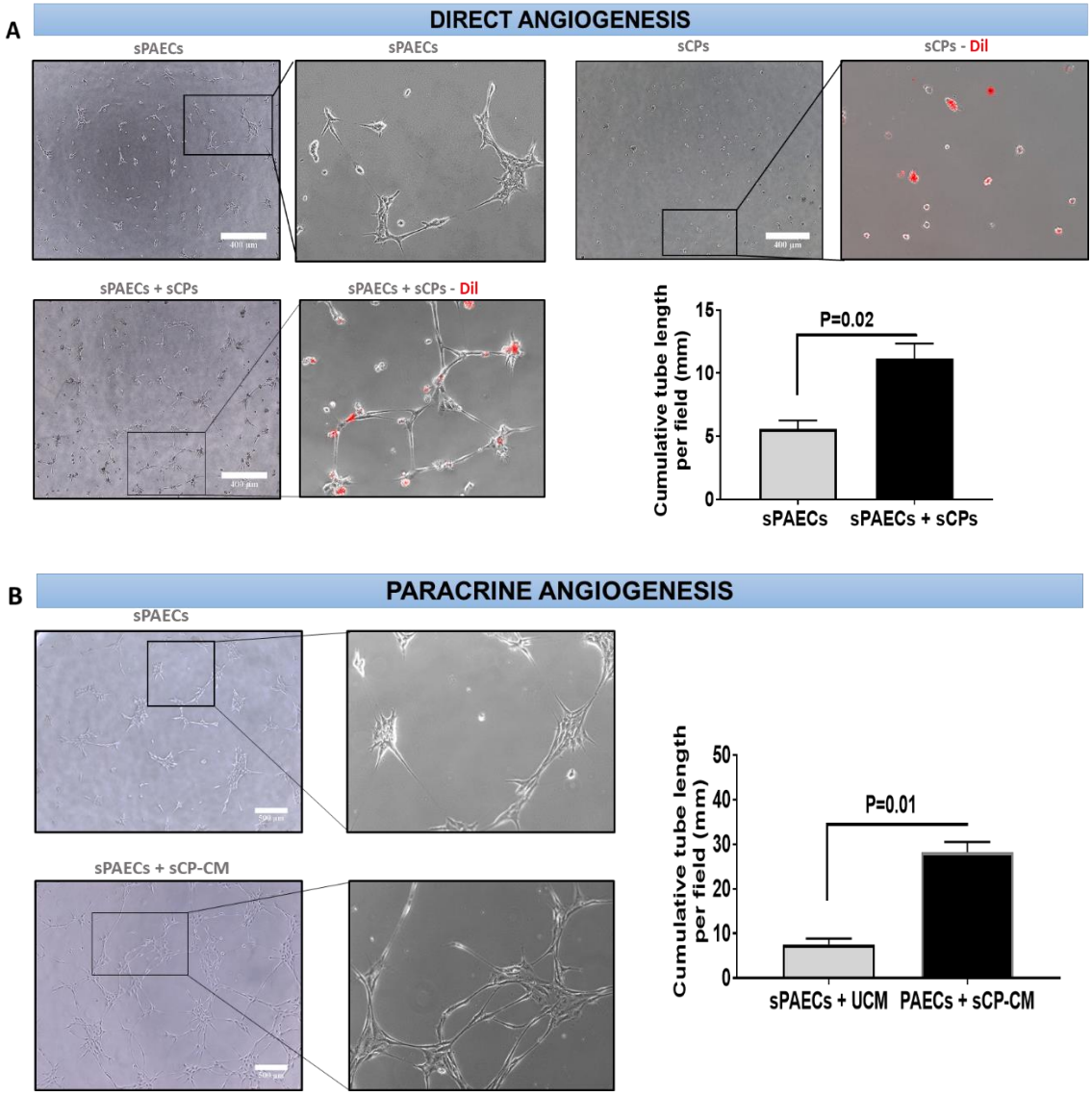

Figure 5-7. Direct and paracrine angiogenic activity of sCPs in a Matrigel assay. A. Representative phase-contrast images of network formation by sPAECs and sCPs cultured alone or in combination (sCPs to sPAECs at a 2:5 ratio) on Matrigel substrate. Swine CPs were stained with DiI (red fluorescence) to assess the ability to cooperate with sPAECs in forming tube structures. Bar graphs showing the cumulative tube length (mm) per field. B. Representative phase-contrast

images of network formation by sPAECs cultured on Matrigel in the presence of unconditioned medium (UCM) or sCP-CM. Bar graphs showing the cumulative tube length per field. Values are expressed as mean±SEM, n=4 per each group. *Abbreviations*: CM= conditioned media; sCPs= swine cardiac pericytes; sPAECs= swine pulmonary artery endothelial cells; UCM= unconditioned media.

5.3.3 Chemotaxis - Endothelial cell migration assay

The recruitment of sPAECs is a property instrumental to the promotion of *in vivo* endothelialization of the TE vascular conduit. In order to examine whether GFs secreted by sCPs could exert chemoattractant effects on sPAECs, a migration assay with sPAECs and sCP-CM was performed. Results of this assay, where migrated sPAECs were examinated using DAPI or Giemsa stainings, revealed that sCP-CM increased the rate of sPAEC migration by ~2-fold compared to EBM-2 basal medium or EBM-2 supplemented with VEGF-A only (EBM-2 vs sCP-CM *P<0.01; EBM-2+VEGF-A vs sCP-CM *P<0.05) (**Figure 5-8A-C**). Interestingly, the addition of an anti-Tie2 kinase receptor antagonist inhibited the chemotactic effect of the sCP-CM, thus suggesting ANG1 signalling is involved in sPAEC attraction (EBM-2 vs sCP-CM *P=0.01; sCP-CM vs sCP-CM+antiTie2 *P<0.05; sCP-CM+antiTie2 vs sCP-CM+DMSO *P<0.01) (**Figure 5-8D-F**).

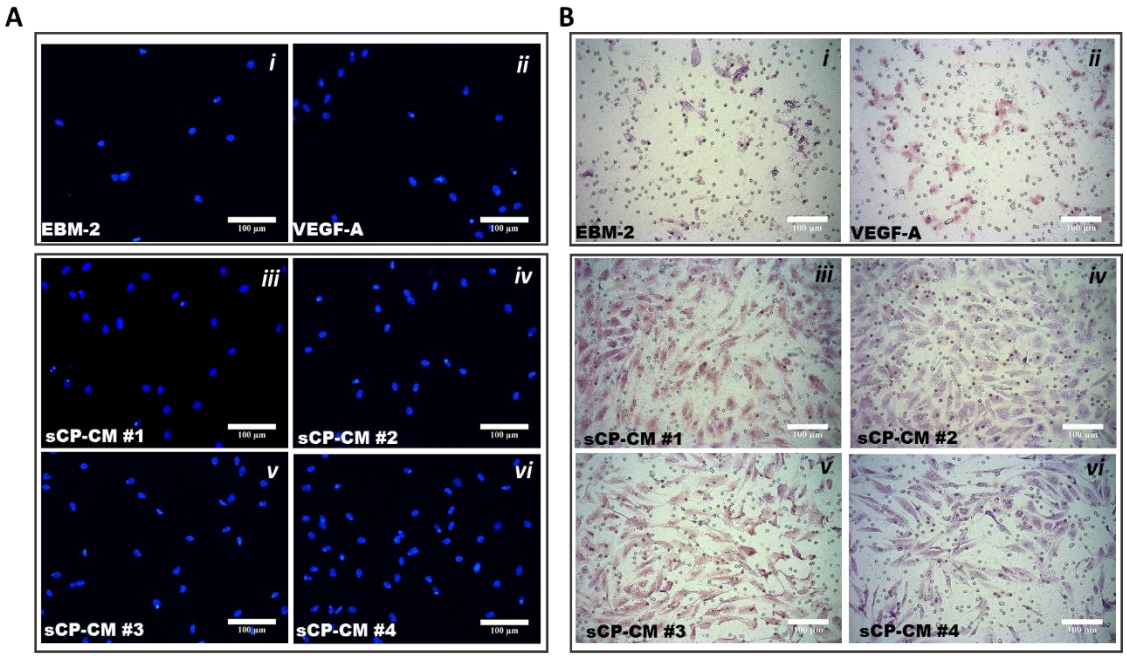
A
i
ii
EBM-2
VEGF-A
iii
iv
sCP-CM #1
sCP-CM #2
v
vi
sCP-CM #3
sCP-CM #4
B
i
ii
EBM-2
VEGF-A
iii
iv
sCP-CM #1
sCP-CM #2
v
vi
sCP-CM #3
sCP-CM #4

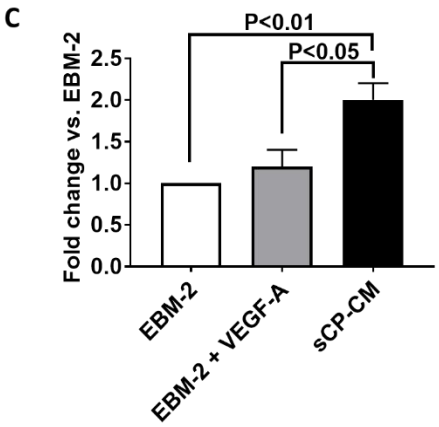
C
P<0.01
P<0.05
Fold change vs. EBM-2
2.5
2.0
1.5
1.0
0.5
0.0
EBM-2
EBM-2 + VEGF-A
sCP-CM

D

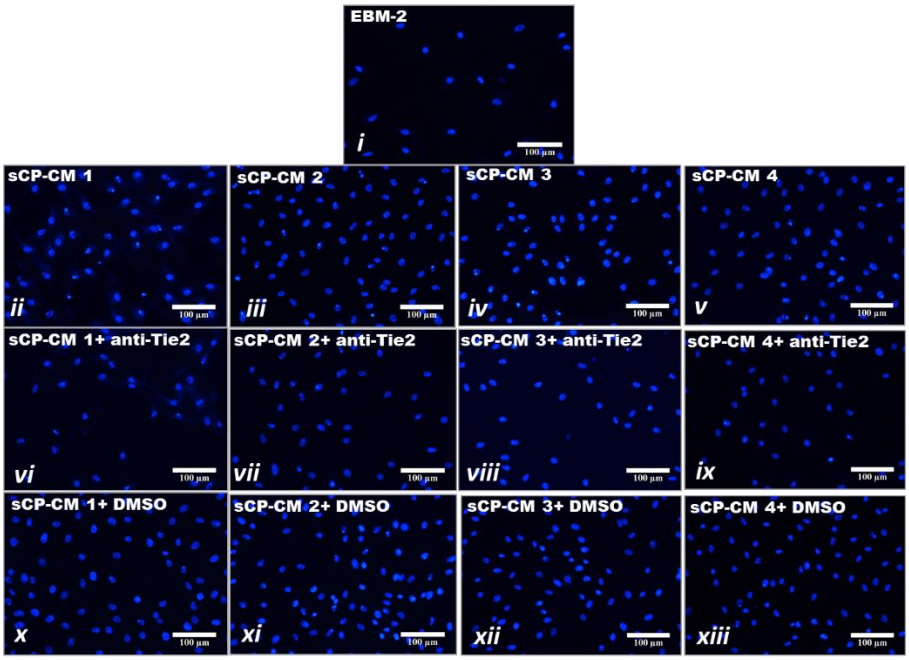
EBM-2
i
sCP-CM 1
ii
sCP-CM 2
iii
sCP-CM 3
iv
sCP-CM 4
v
sCP-CM 1+ anti-Tie2
vi
sCP-CM 2+ anti-Tie2
vii
sCP-CM 3+ anti-Tie2
viii
sCP-CM 4+ anti-Tie2
ix
sCP-CM 1+ DMSO
x
sCP-CM 2+ DMSO
xi
sCP-CM 3+ DMSO
xii
sCP-CM 4+ DMSO
xiii

E

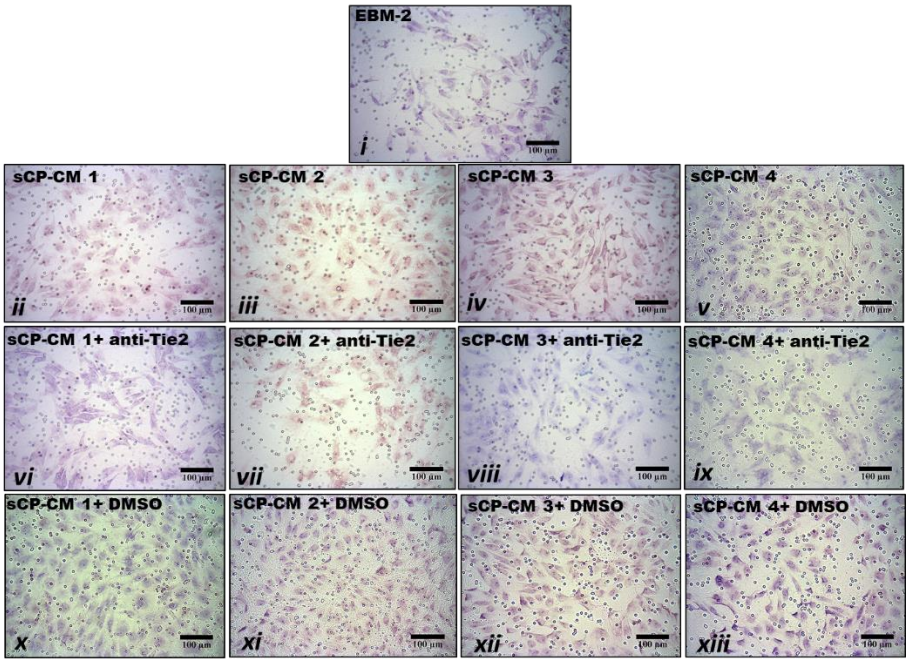
EBM-2
i
sCP-CM 1
ii
sCP-CM 2
iii
sCP-CM 3
iv
sCP-CM 4
v
sCP-CM 1+ anti-Tie2
vi
sCP-CM 2+ anti-Tie2
vii
sCP-CM 3+ anti-Tie2
viii
sCP-CM 4+ anti-Tie2
ix
sCP-CM 1+ DMSO
x
sCP-CM 2+ DMSO
xi
sCP-CM 3+ DMSO
xii
sCP-CM 4+ DMSO
xiii

F

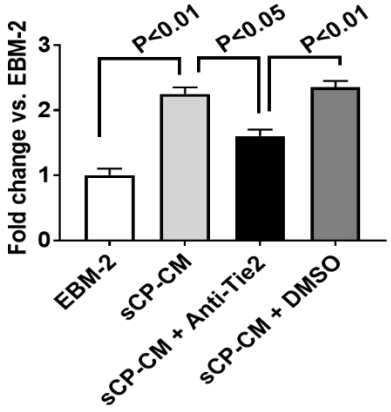
P<0.01
P<0.05
P<0.01
Fold change vs. EBM-2
0
1
2
3
EBM-2
sCP-CM
sCP-CM + Anti-Tie2
sCP-CM + DMSO

Figure 5-8. Chemotactic activity of factors secreted by swine cardiac pericytes. A-C. In a migration assay the sCP-CM enhanced the migration of sPAECs. Representative images of migrated cells stained by DAPI (A) or Giemsa (B) following stimulation with EBM-2 (i), VEGF-A (ii, 100 ng/mL), or CM from four sCP lines (iii-vi). Images acquired using a x200 magnification. C. Bar graph showing the fold change of migrated cells vs. EBM-2 basal media. N= 4, data are expressed as mean ± SEM. D-F. Effect of Tie-2 inhibitor (7.5 μM) on the chemotactic activity of sCP-CM. Representative images of migrated cells stained by DAPI (D) or Giemsa (E) following stimulation with EBM-2 (i), CM from four sCP lines (ii-v), or CM from the same sCP lines added with a Tie2 antagonist (vi-ix) or its vehicle (x-xiii, DMSO). Images acquired using a x200 magnification. G. Bar graph showing the fold change of migrated cells vs. EBM-2 basal media. Data are expressed as mean ± SEM. *Abbreviations*: CM=conditioned media; DMSO= dimethyl sulfoxide; EBM-2= endothelial cell basal medium-2; sCPs= swine cardiac pericytes; Tie2= Tyrosine kinase with immunoglobulin-like and EGF-like domains 2; VEGF-A= vascular endothelial growth factor-A.

5.3.4 Proliferation of swine pulmonary artery endothelial cells

In addition, the stimulation of sPAEC proliferation from sCPs and their secretome were tested (**Figure 5-9A-B**). Results indicate that the abundance of EdU positive sPAECs was not increased by co-culturing them with sCPs or exposing them to sCP-CM (72.8±2.6% and 69.6±2.3% *vs*. 66.2±2.3% in sPAECs alone, P=0.29 for both comparisons). Considering this data in the light of the Matrigel and transwell assay results, we speculate that sCPs exert proangiogenic effects through the stimulation of sPAEC migration and the stabilization of newly formed sPAEC networks, which would be otherwise subjected to spontaneous regression in the Matrigel assay.

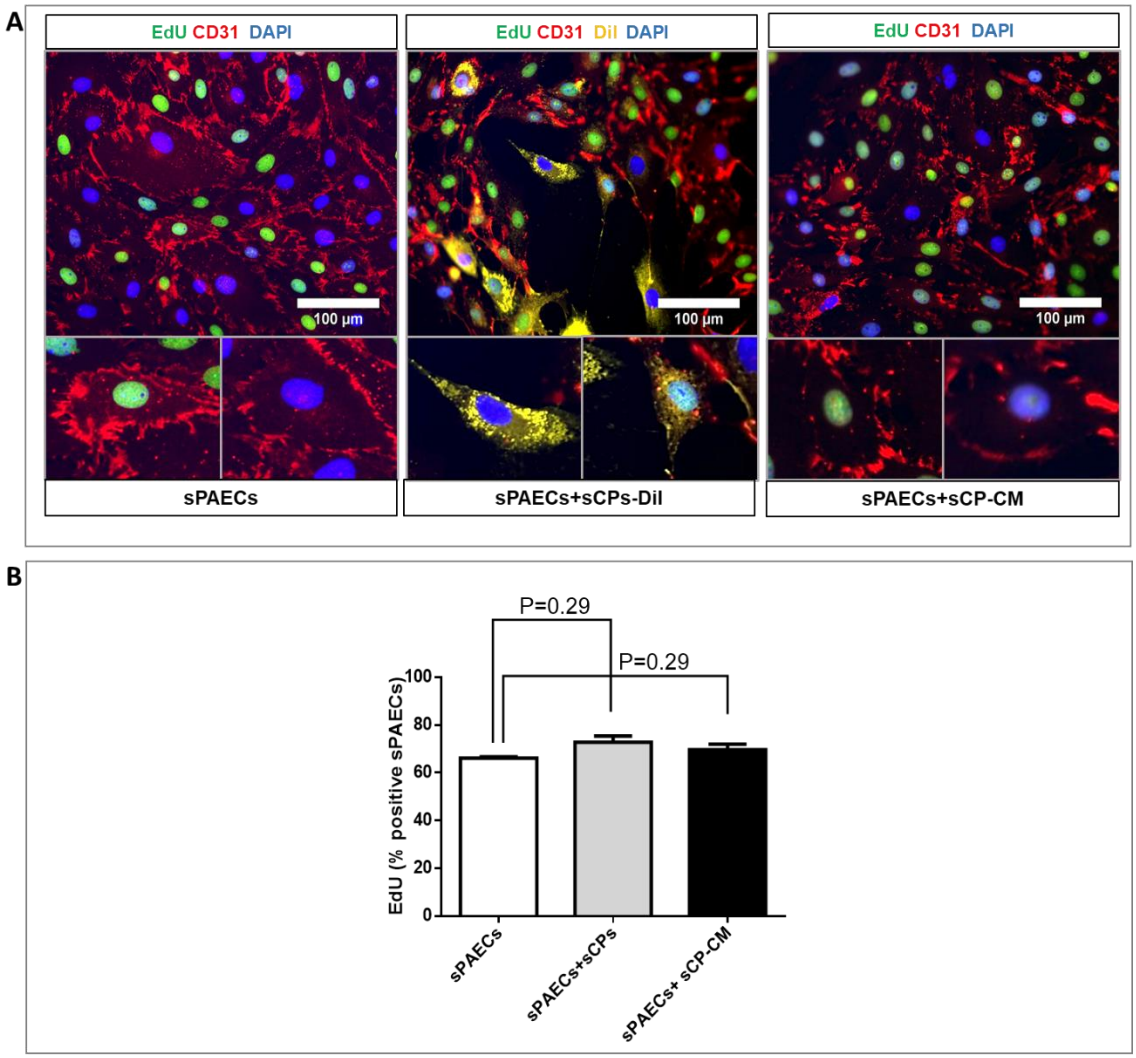

Figure 5-9. Proliferation of sPAECs (EdU proliferation assay). A. Representative IF images of proliferating sPAECs following co-culture with sCPs and sCP-CM. Swine PAECs are stained with anti-CD31 (red fluorescence) and sCPs with the long-term cell tracker DiI (yellow fluorescence). Images acquired using 200X magnification. B. Bar graph displaying the percentage of EdU positive sPAECs following stimulation with sCPs and sCP-CM. N=4, data are mean±SEM. *Abbreviations*: CD= cluster of differentiation; CM= conditioned media; EdU=5-ethynyl-2'-deoxyuridine; sCPs= swine cardiac pericytes; sPAECs= swine pulmonary artery endothelial cells;

5.4 Tissue engineering studies of swine cardiac pericytes

Next, sCPs were seeded at 20,000/cm^2 on CorMatrix®, a clinically approved graft material, and seeded and unseeded control grafts were cultured as "patch" for 5 days under static condition. In additional experiments, the two systems were transferred as conduits from the static condition to a flow bioreactor for a period of 1 or 2 weeks of dynamic culture.

5.4.1 Histological analysis of pericyte-engineered grafts

Figure 5-10 shows representative images from the histology and IHC analyses performed on grafts harvested at the end of each of the above culture stages. Staining with H&E documented that seeded cells adhered to the surface of the scaffold forming a thicker layer at 14 days post-dynamic culture as compared to post-static culture. No cells were detected in the unseeded matrix (**Figure 5-10A**). In seeded scaffolds, fibres of elastin (EVG, **Figure 5-10A**) and Collagen (COL, **Figure 5-10B**) were clearly detected in proximity of the cell-seeded area and across the matrix, with the signal intensity being stronger as compared with unseeded grafts. Freshly collected LPA was used for comparison. The bar graph shows that there was a progressive increase in the collagen content throughout the culture period of the cellularized graft, which peaked at 14 days of the dynamic conditioning in the bioreactor (**Figure 5-10B**). At this stage, the initial gap in collagen content between the CorMatrix® and native LPA was almost completely abrogated.

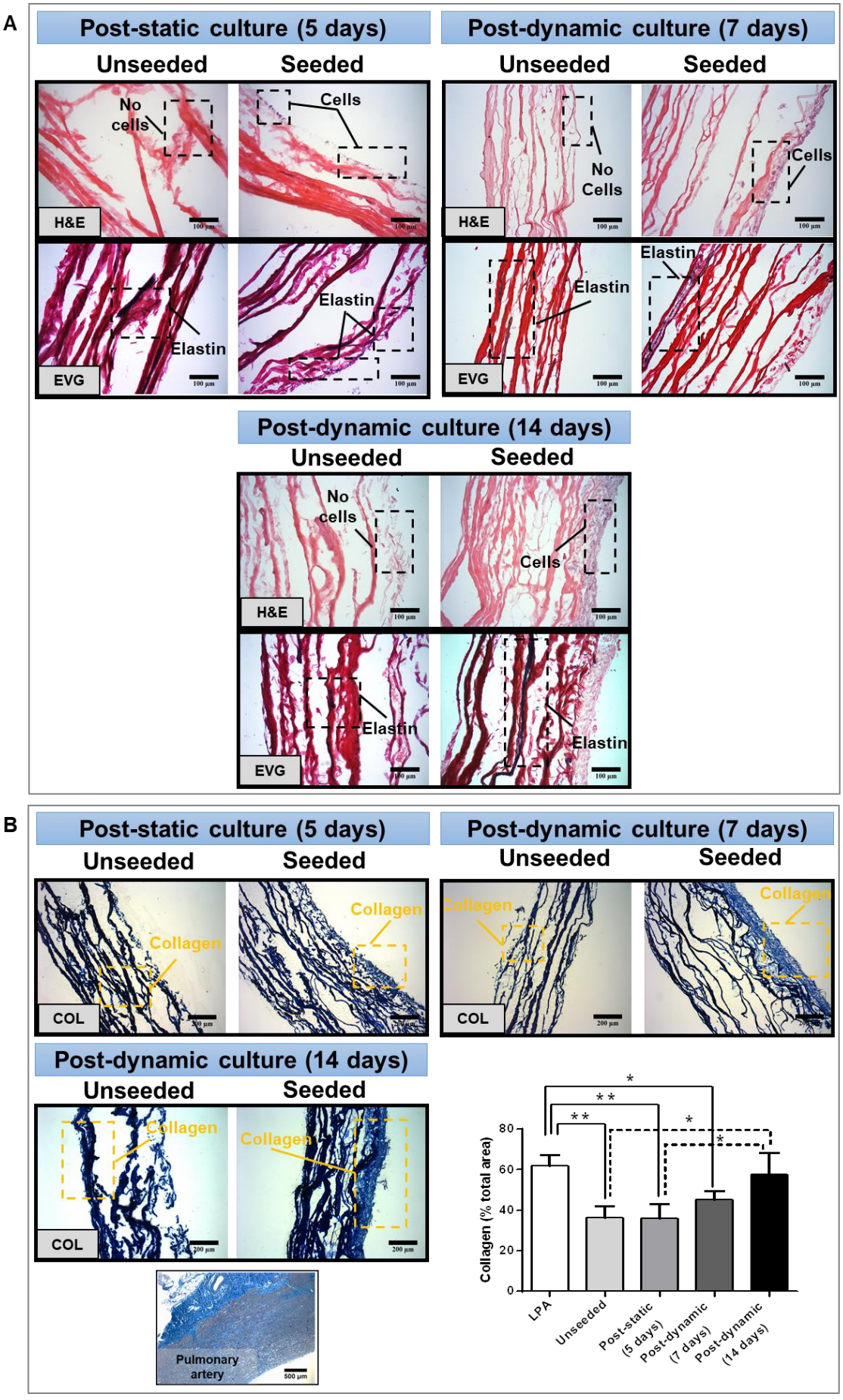
A
Post-static culture (5 days)
Unseeded
Seeded
No cells
Cells
H&E
Elastin
EVG
Post-dynamic culture (7 days)
Unseeded
Seeded
No Cells
Cells
H&E
Elastin
EVG
Post-dynamic culture (14 days)
Unseeded
Seeded
No cells
Cells
H&E
Elastin
EVG
B
Post-static culture (5 days)
Unseeded
Seeded
Collagen
COL
Post-dynamic culture (7 days)
Unseeded
Seeded
Collagen
COL
Post-dynamic culture (14 days)
Unseeded
Seeded
Collagen
COL
Pulmonary artery
Collagen (% total area)
LPA
Unseeded
Post-static (5 days)
Post-dynamic (7 days)
Post-dynamic (14 days)

Figure 5-10. Histochemistry of CorMatrix® seeded with swine CPs. *A.* Cells and nuclei staining with H&E and Elastic fibres staining with EVG; B. COL staining with Azan Mallory and quantification of grafts and LPA. These staining are performed following 5-days PS (n=9) and 7- and 14-days PB (n=5). Magnification x200, scale bar= 100 µm; Magnification x100, scale bar=200 µm. *Abbreviations*: COL= Collagen; EVG= Elastic fibres Van Gieson's; H&E= Hematoxylin and Eosin; PS= Post-Static; PB= Post-Bioreactor.

5.4.2 Immunohistochemistry analysis of pericyte-engineered grafts

The evaluation of cell viability after the seeding in a 3D-culture system and prior to implantation is fundamental to test their efficacy in the preclinical study. Viability was assessed *in situ* with a viability/cytotoxicity IF kit as well as using Trypan blue exclusion method after cell detachment from the matrix, using Trypsin or Accutase enzymes, and cytospin. Positive controls were treated with saponin or H_2O_2. Cells showed a consistently high viability in situ (95.8±2.2% post-static, PS; 92±1.6% post-bioreactor, PB) and >90% after detachment with both enzymatic methods and length of conditioning time (**Figure 5-11A-B**). Results of TUNEL assay documented low apoptosis levels after cell detachment with both enzymatic treatments (3.4±2.4% Trypsin PS and 5.1±3.1% Accutase PS; 0.5±0.4% Trypsin PB and 5.6±1.7% Accutase PB). Immunofluorescent images also showed low apoptotic cells compared to H_2O_2 (**Figure 5-11C-D**).

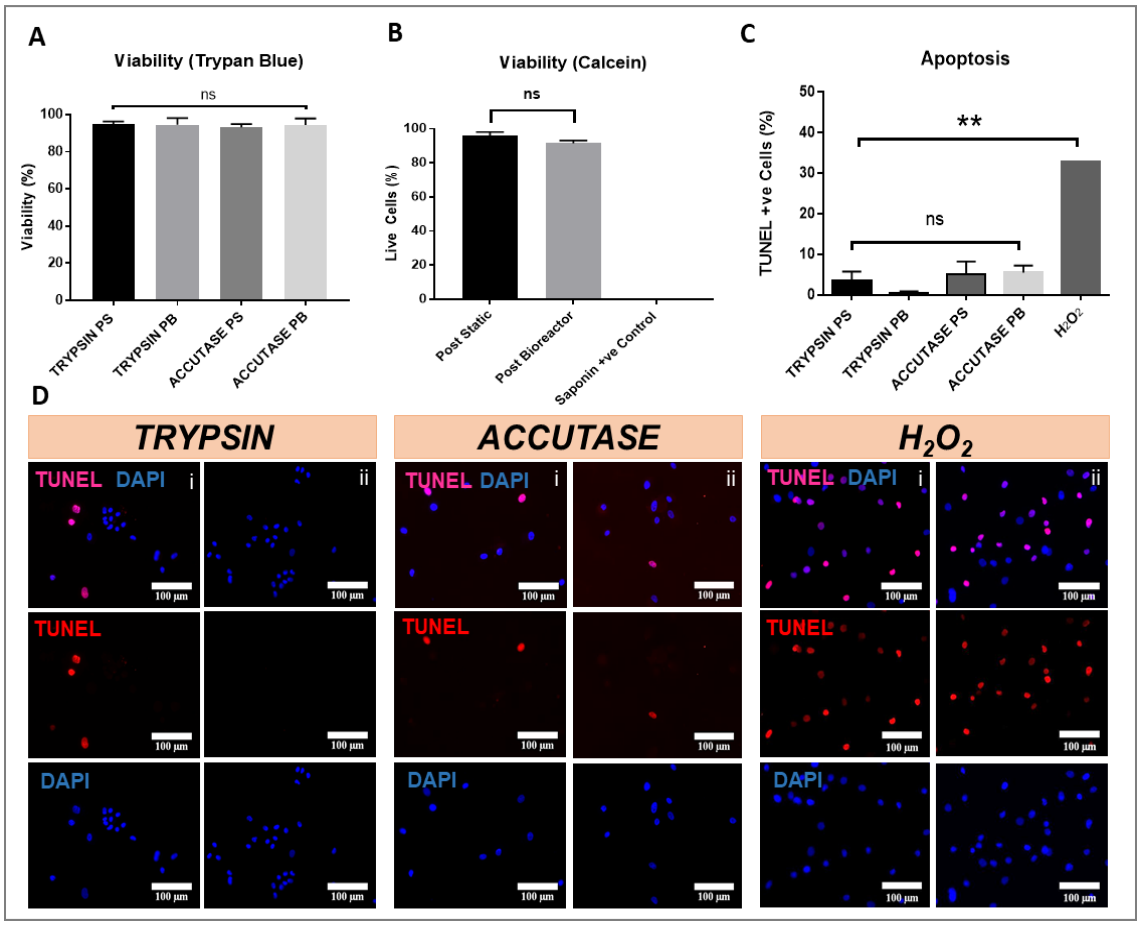

Figure 5-11. Cell viability and Apoptosis of CorMatrix® engineered with swine CPs. A. Trypan Blue exclusion method shows high viability of swine CPs after detaching from the matrix with two enzymatic methods at the end of static and dynamic culture. B. The data was confirmed using Calcein staining of the grafts. Saponin was used as a control cytotoxic agent. C&D. Apoptosis was assessed by the TUNEL assay. Bar graph showing results and representative IF microscopic images displayed single and merged channels of two different fields in the same sample (i-ii, blue=DAPI, red- TUNEL, merge= DAPI+/TUNEL+). Magnification x200, scale bar= 100 µm. Data are expressed as mean±SEM of 4 biological replicates (n=4); **P=0.001 vs H2O2. *Abbreviations*: PB= post-bioreactor; PS=post-static; +ve= positive vehicle.

Quantitative analysis of cell proliferation revealed 8.9±8.0% of total cells expressed Ki67 at 5-days PS. The frequency of proliferating cells decreased following dynamic culture (5.4±1.0% 7-days PB and 2.1±1.4% 14-days PB). However, due to the large variability of the measure, the change in proliferation did not reach statistical significance. No Ki67 staining was detected in the unseeded graft (**Figure 5-12A-B**).

A

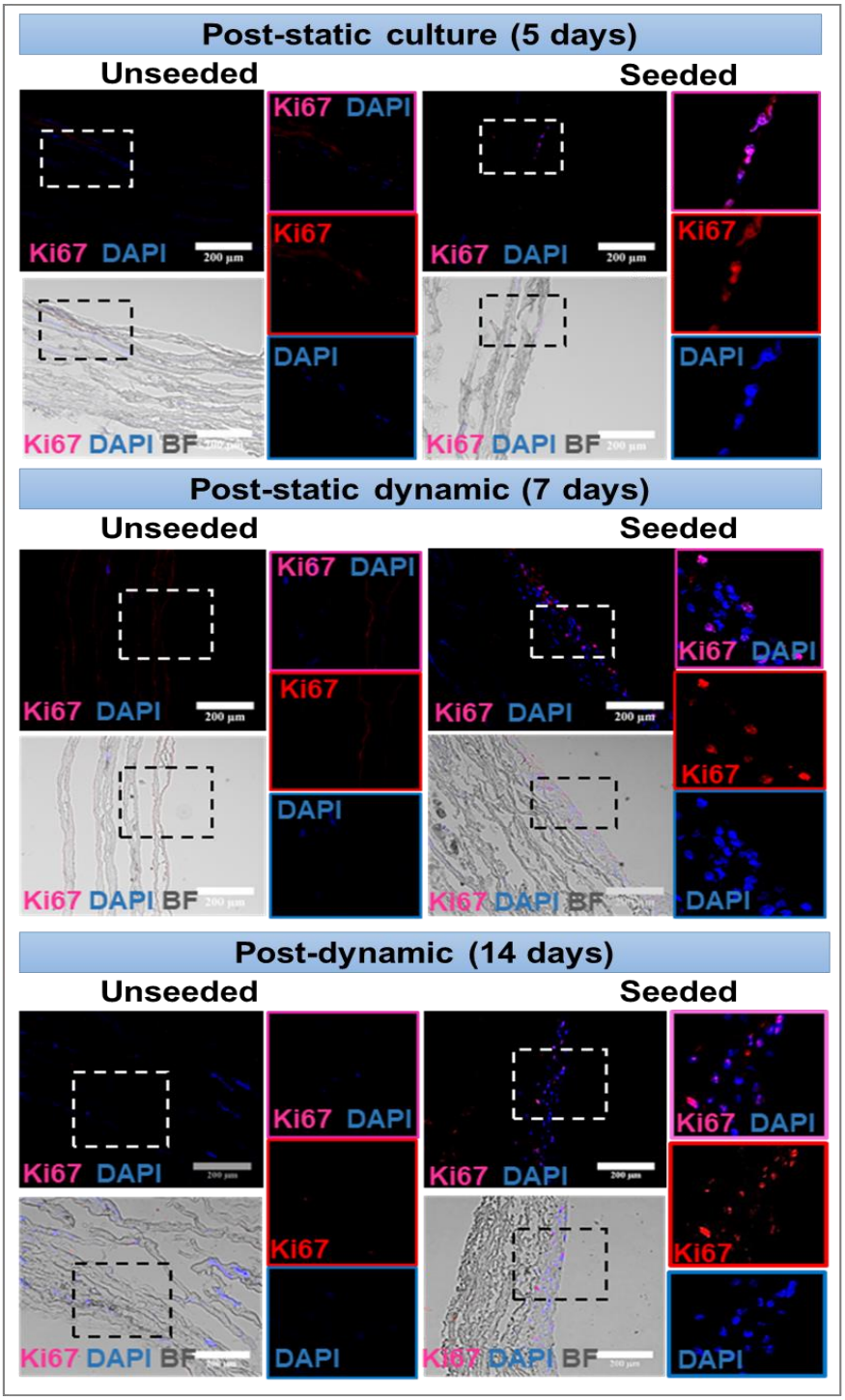
Post-static culture (5 days)
Unseeded
Seeded
Ki67 DAPI
Ki67
DAPI
Ki67 DAPI BF
200 µm
Post-static dynamic (7 days)
Unseeded
Seeded
Post-dynamic (14 days)
Unseeded
Seeded

B

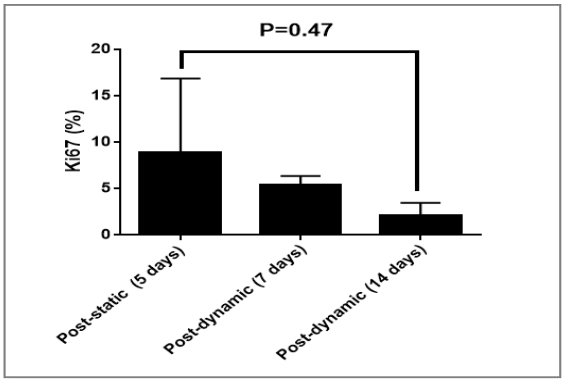
P=0.47
Ki67 (%)
20
15
10
5
0
Post-static (5 days)
Post-dynamic (7 days)
Post-dynamic (14 days)

Figure 5-12. Proliferation of CorMatrix® grafts engineered with swine CPs. A. Representative IF and BF images of proliferation assessed by Ki67 staining. Fluorescent images are displayed as single and merged channels in the side panels (blue= DAPI, red=Ki67, merge= DAPI+/Ki67+). No staining was detected in the unseeded grafts in the different experimental conditions. Magnification x100, n=4 sample size, scale bar= 200μm. Single and merged panels displayed staining at higher magnification. B. Bar graph showing the proliferation following static and dynamic cultures (P=0.47).

Next, sCPs were tested to assess if they maintain their original phenotype or acquire additional markers after culture the PEGs under static conditions and subsequent application of flow in the bioreactor. As expected, control unseeded conduits did not show any positive staining for the studied markers, thus confirming to be acellular. Seeded grafts collected at the end of the static culture showed few NG2-expressing cells, with this antigenic cell phenotype being remarkedly more abundant after application of flow but maintaining the original location at the seeded surface of the conduit (**Figure 5-13A**). A similar pattern was observed for the other natively expressed antigens α-SMA, (**Figure 5-13B**), CALP (**Figure 5-13C**), whereas cells in the grafts as patches and in the conduits were negative for TAGLN (**Figure 5-13D**), SMTN (**Figure 5-13E**) and SMMHC (**Figure 5-13F**), thus indicating they did not acquire a mature muscular phenotype with transfer from plastic into the conduit.

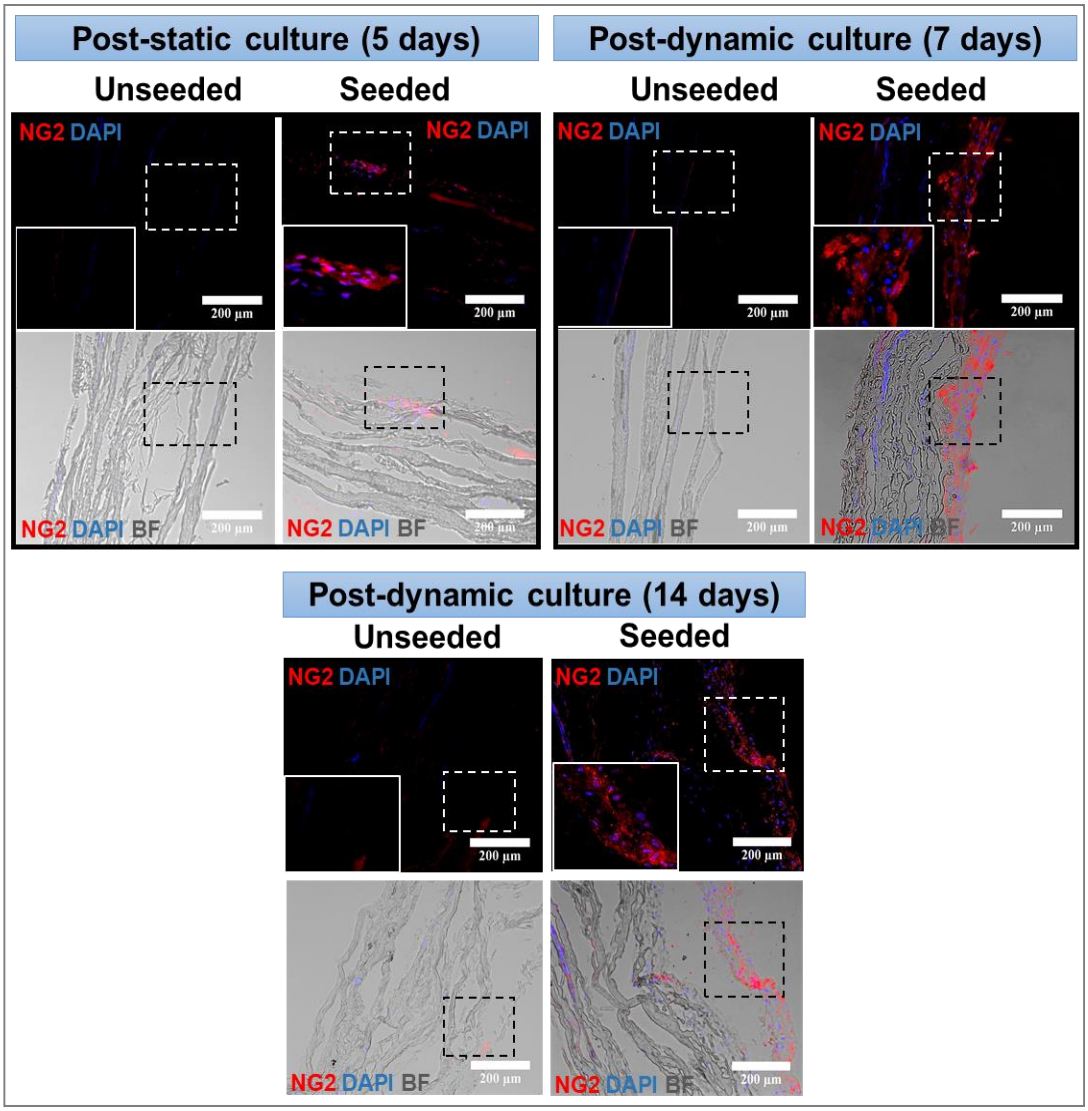

Figure 5-13. Immunohistochemistry of CorMatrix® grafts seeded with swine CPs. IF and BF images showing PEGs collected at 5-days PS (n=9) and 7- and 14-days PB (n=5) cultures which were positive for NG2 (A), α-SMA (B), CALP (C) and were negative for TAGLN (D), SMTN (E) and SMMHC (F). Magnification x100, scale bar= 200µm. Merge channels also shown in the small panels at higher magnification. Red=all the above markers; blue=DAPI. BF=Brightfield. *Abbreviations*: BF= brightfield; CALP= calponin; NG2= neural/glial antigen 2; SMA= smooth muscle actin; SMMHC= smooth muscle myosin heavy chain; SMTN= smoothelin; TAGLN= transgelin.

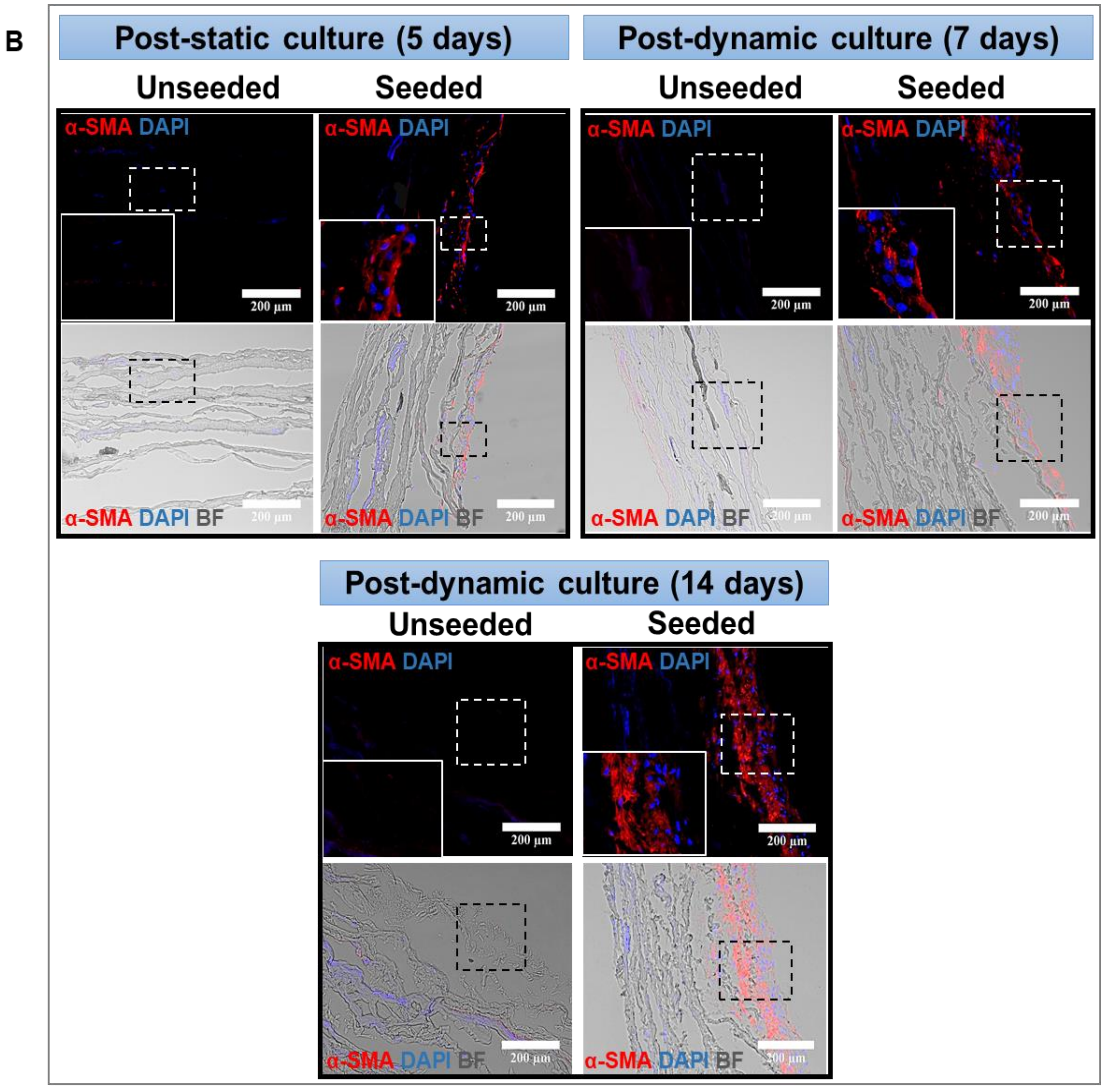

Figure 5-13 (continued).

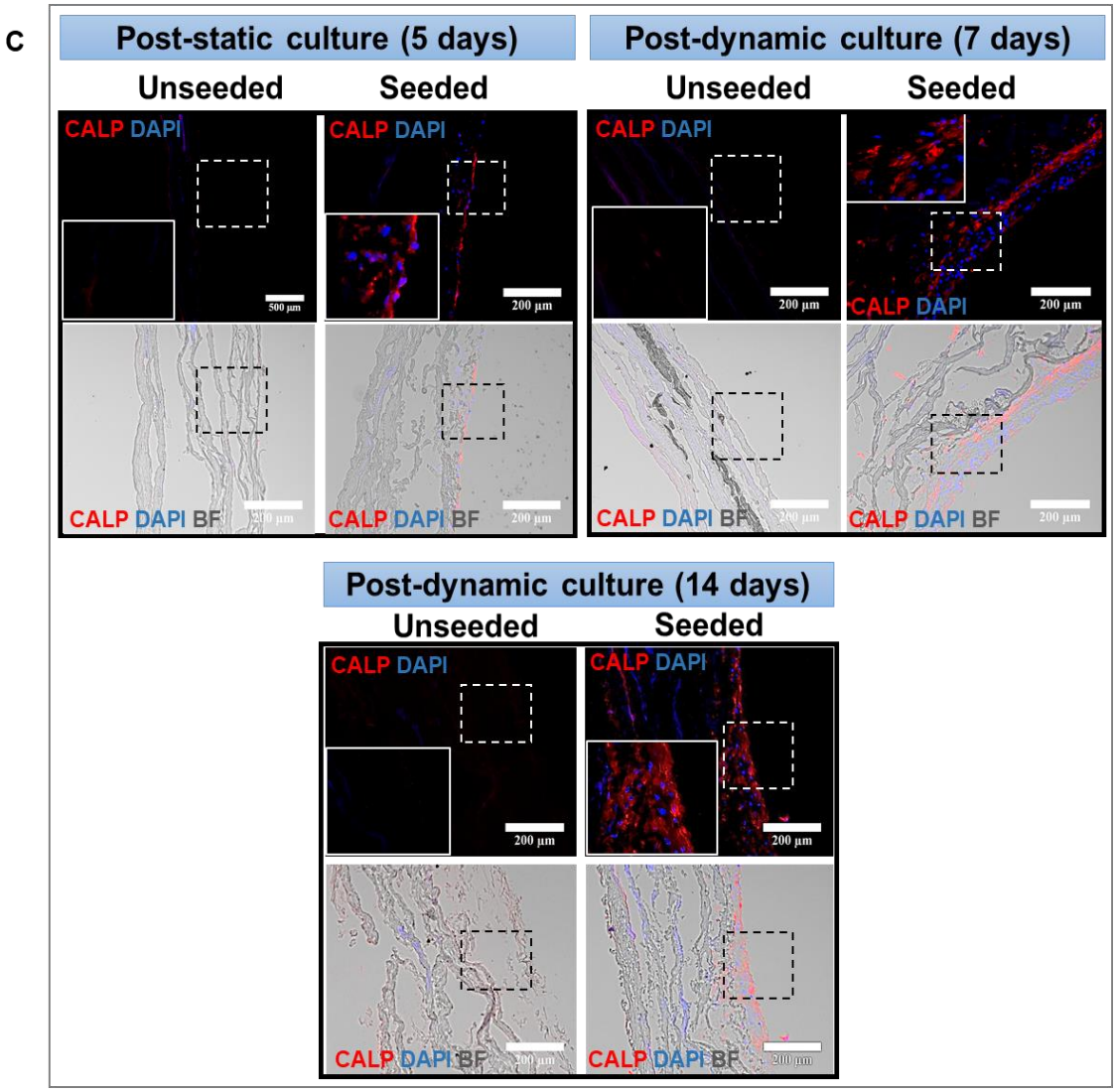

Figure 5-13 (continued).

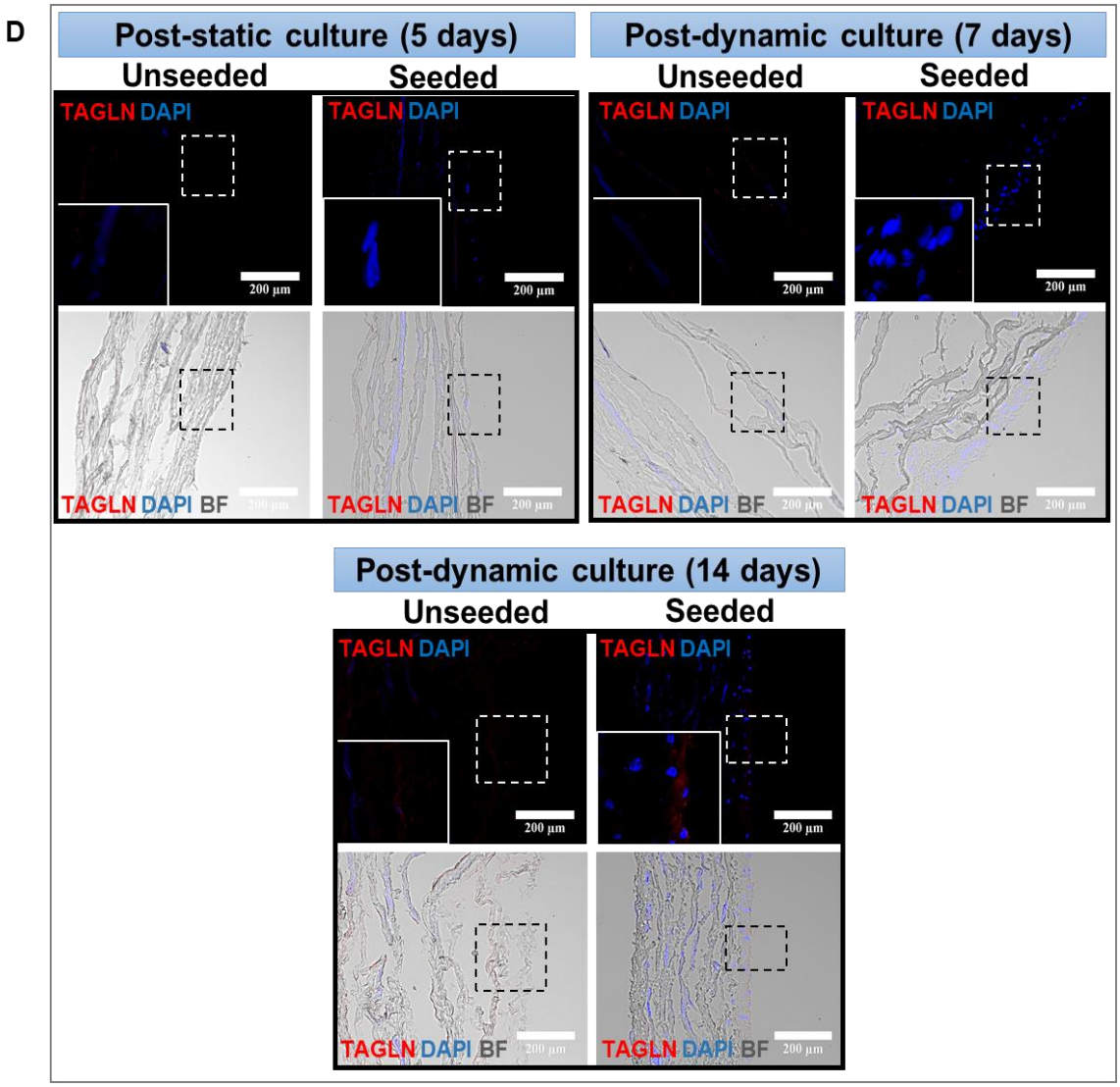

Figure 5-13 (continued).

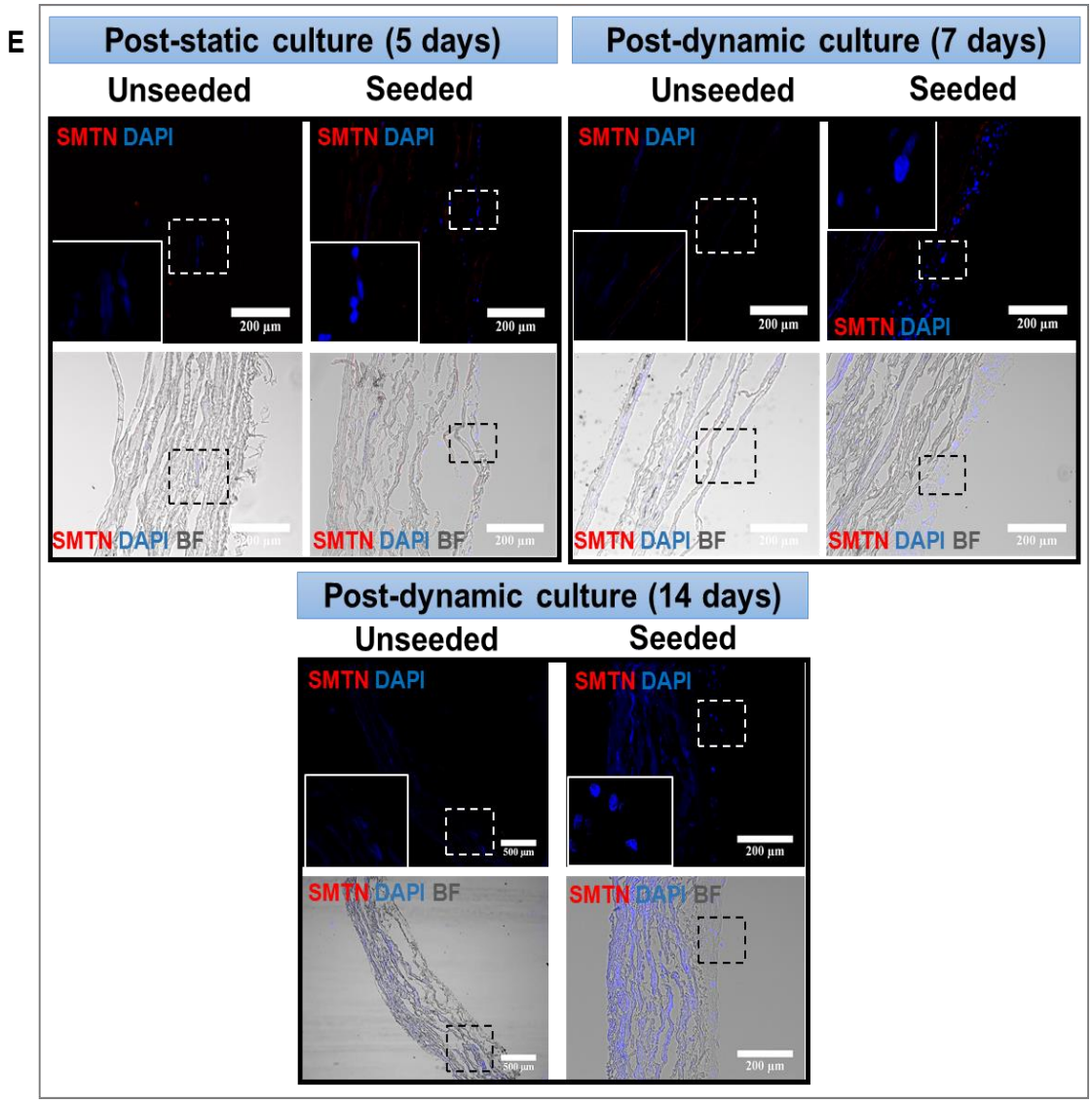

Figure 5-13 (continued).

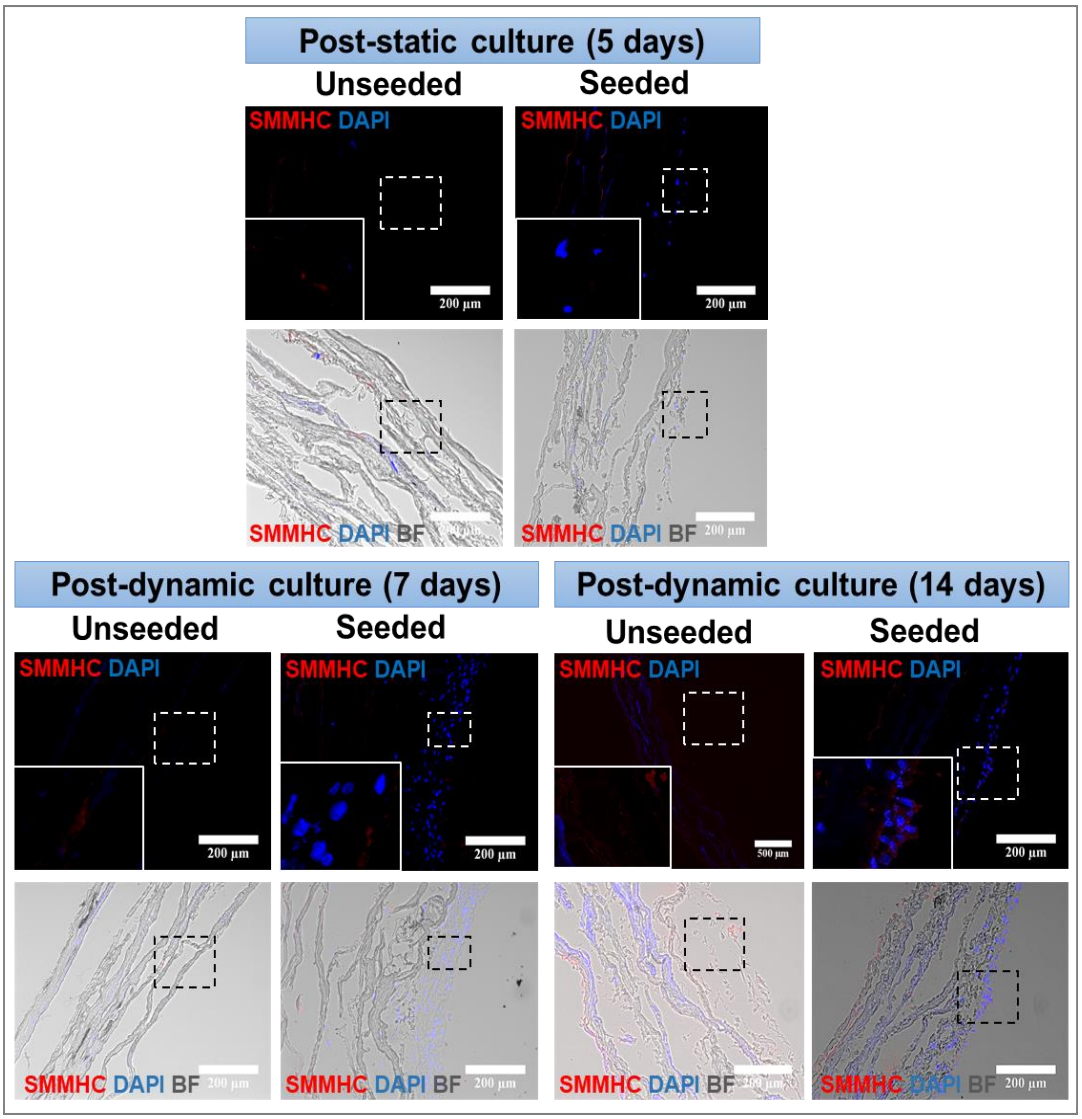

Figure 5-13 (continued).

5.5 *In vivo* implantation of vascular conduits engineered with cardiac pericytes

Finally, a feasibility study was performed on two four-week-old sister weaner piglets underwent LPA surgical replacement with seeded or unseeded CorMatrix® conduits, respectively. Following static and dynamic culture conditions, the grafts used for the *in vivo* studies (20 mmx30 mm) were re-shaped by the surgeon to create a conduit of ~ 10 mm long and ~ 6 mm diameter. The small branch of LPA was resected to accommodate the TEVG with or without cells (**Figure 5-14**). Both animals survived the experimental period and showed similar growing curves.

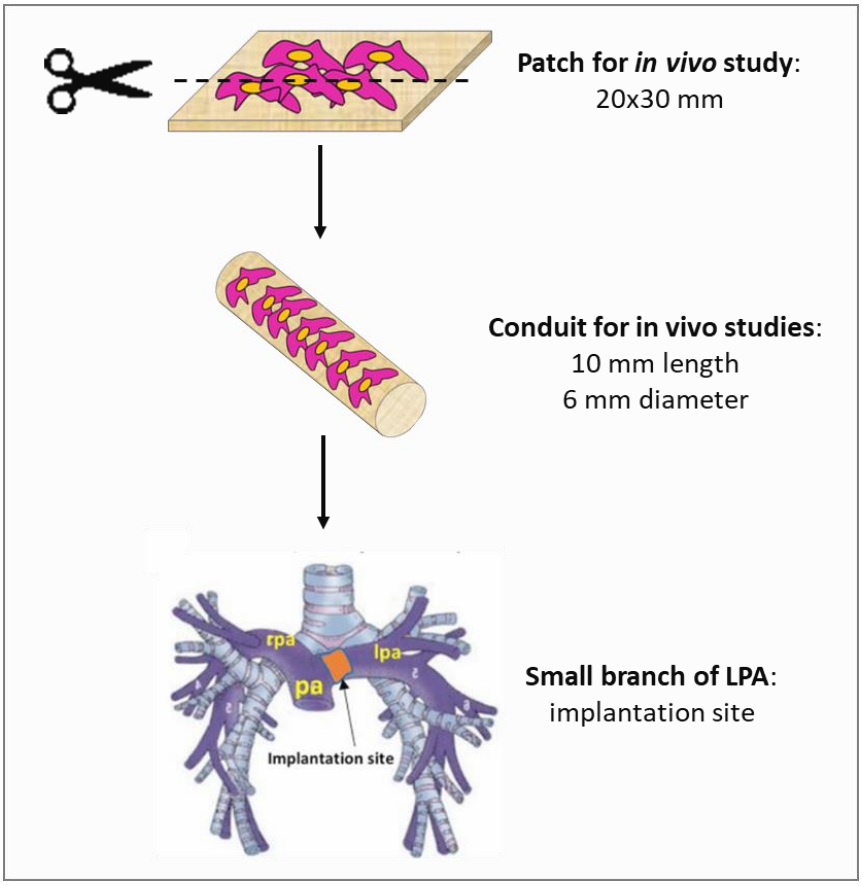

Figure 5-14. Diagram displaying the characteristics of the TEVG used for in vivo studies. Following static and dynamic culture conditions, cellularized or non-cellularized graft of 20 mm x 30 mm was cut and re-shaped to create a new conduit of 10 mm length and 6 mm diameter. The small branch of LPA was resected, and the conduit sutured around the proximal and distal LPA of the animal.

5.6 Cardiac magnetic resonance and Doppler analysis

Figure 5-15 showed representative images of Doppler and CMR which confirmed the patency of grafted LPA in both pigs transplanted with seeded and unseeded grafts. **Table 5-1** reports the individual blood flow velocity at different times of follow-up, with values within the normal range for both animals. The imaging and related analyses were provided by the imaging department based at the Veterinary School of Langford (Bristol).

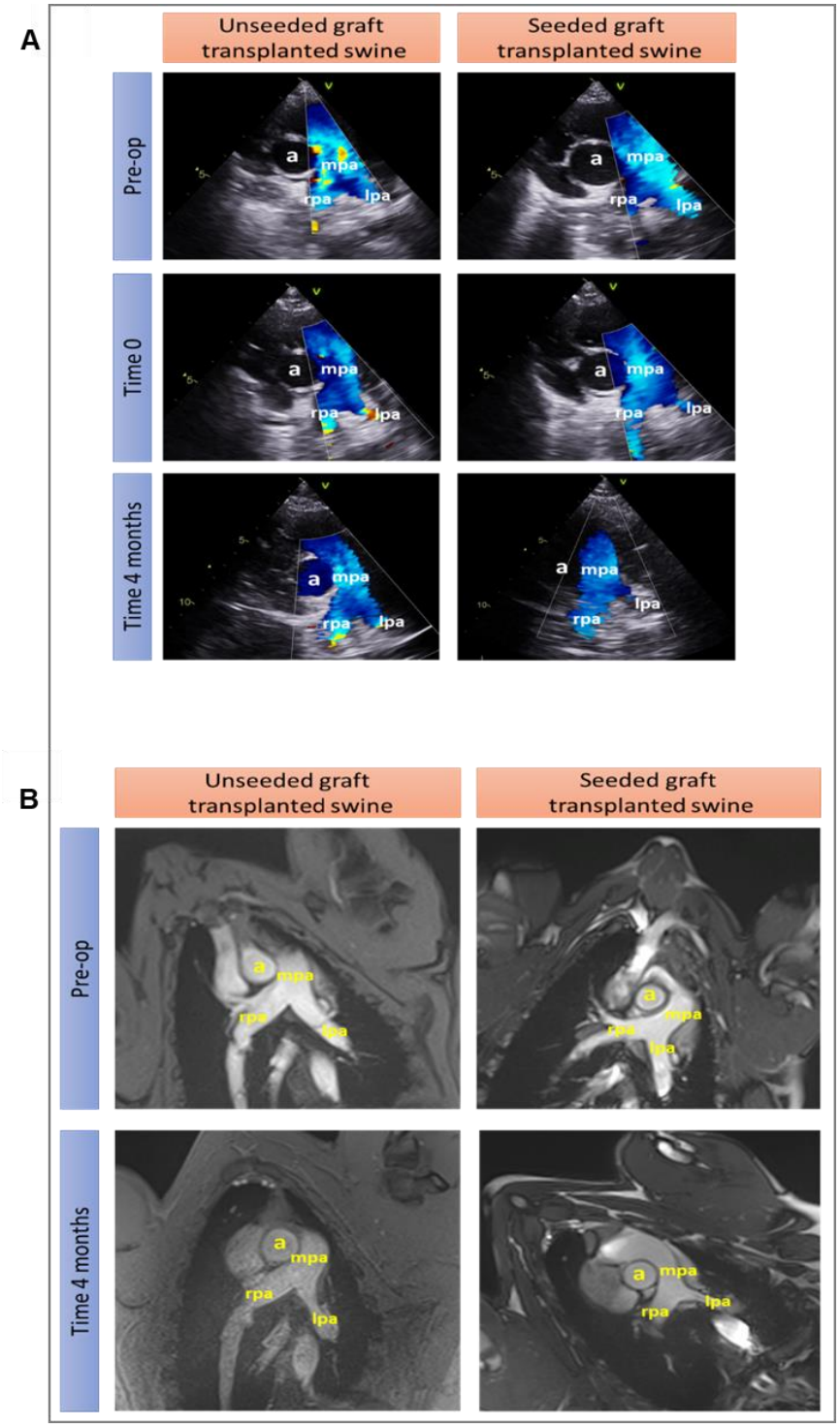

Figure 5-15. Imaging studies using Doppler Echocardiography (A) and cardiac MRI (B) of n=1 animal per group size. Vascular structures are typed in yellow colour: a= aorta; mpa= main pulmonary artery; rpa= right pulmonary artery; lpa= left pulmonary artery. Images were provided by the courtesy of institutional personnel of the Veterinary School in Langford (Bristol).

LPA	Unseeded	Seeded
Pre-op	0.86	1.23
Post-op	0.80	1.41
RPA		
Pre-op	1.33	0.93
Post-op	0.89	1.26
MPA		
Pre-op	1.04	1.33
Post-op	1.12	1.35

Table 5-1. Blood flow velocity measured by echocardio-Doppler. Values are mL/sec, n=1 per group size. *Abbreviations:* LPA= Left pulmonary artery; RPA= Right pulmonary artery; MPA= Main pulmonary artery; Pre-op= pre-operation; Post-op= Post-operation. Table was provided by the courtesy of institutional personnel from the Veterinary School in Langford (Bristol).

5.7 Immunohistochemical analysis of implanted grafts

H&E images show extensive nucleation throughout the structure of the proximal and distal seeded graft (**Figure 5-16A**). In both seeded and unseeded grafts, there were minimal levels of calcification which were detected in the suture area and in the adventitia of LPA and not in the implanted grafts, as assessed by Von Kossa staining method (**Figure 5-16B**). Elastin is the major component of the PA. In line with this, Von Gieson's staining displayed a consistent layer of organised elastin in the native tissue of the LPA. Elastin deposits were visible in the seeded graft attached to the proximal and distal LPA but less defined in the unseeded graft (**Figure 5-16C**). Collagen fibres (both interstitial and perivascular) were detected especially in the unseeded explant probably due to the formation of a fibrous scar tissue. In addition, new muscle tissue appeared in the LPA and in the perivascular area of the explants (**Figure 5-16D**). The IHC analysis showed an organised multilayer of smooth muscle cells (SMCs) populating the tunica media of the LPA. ECs identified by the CD31 antigen, were present at the luminal side of the artery and in the vessels within the adventitia (**Figure 5-17A**). Cells expressing NG2 were also found in the adventitia of the vessels. Notably, more organised vessel structures appeared in the seeded graft-adventitia compared to the unseeded one (**Figure 5-17B**). Positive staining controls, used in association with the main histological analyses of the grafts, are shown in **Figure 5-18**.

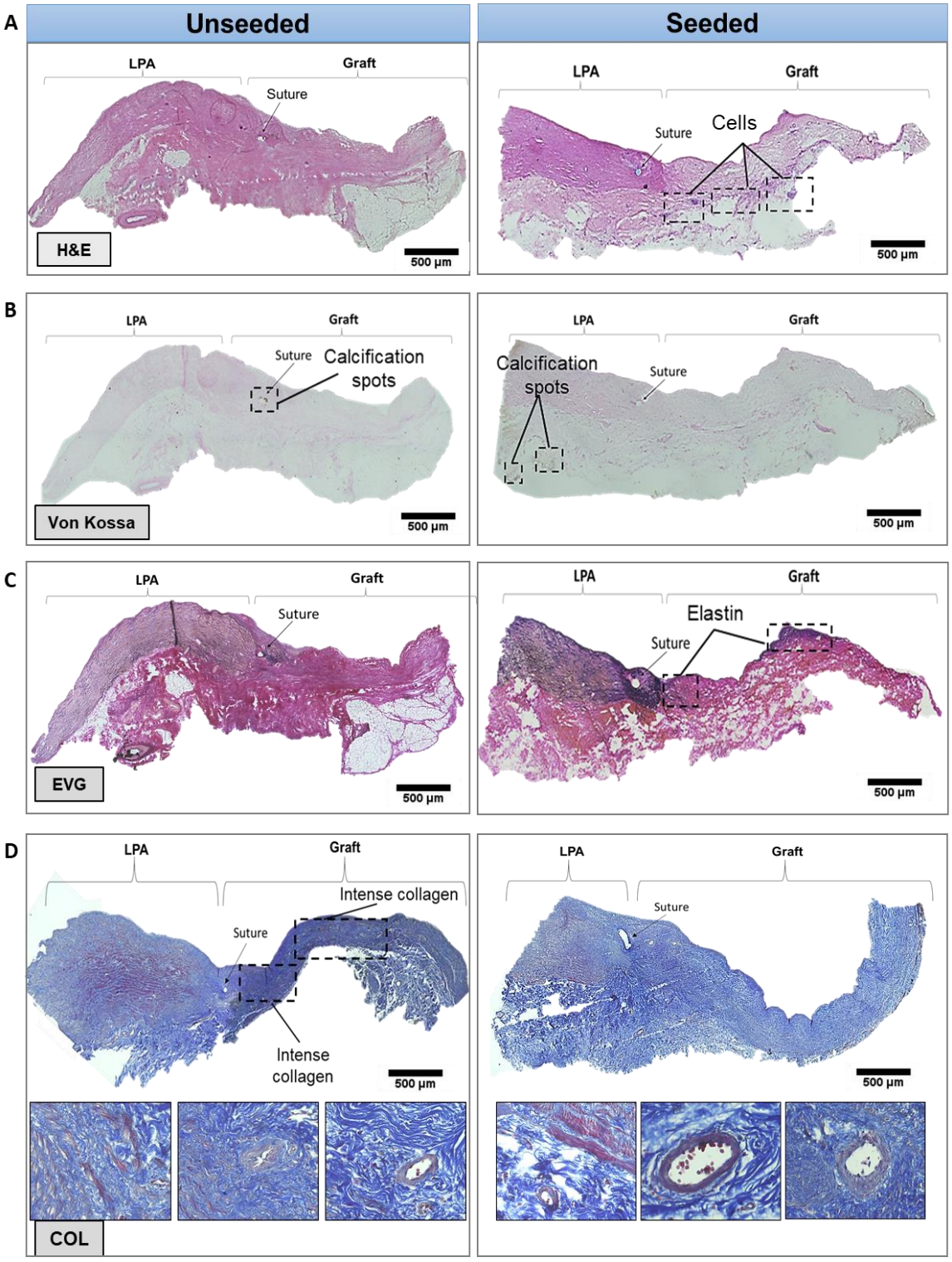

Figure 5-16. Histochemistry of the explanted grafts (LPA and Graft). A. H&E staining for cell identification of the unseeded and seeded grafts. B. Von Kossa staining for microcalcification detection. C. Von Gieson's staining for elastin evaluation. D. Azan Mallory staining for collagen and fibrosis assessment. Side panels showing at higher magnification muscle tissue in the PA and in the perivascular areas of the explants. Magnification x100, n=1 animal per group size,

scale bar= 500µm. *Abbreviations*: COL= Collagen; EVG= Elastic fibres Von Gieson's; H&E= Hematoxylin and Eosin; LPA= Left pulmonary artery.

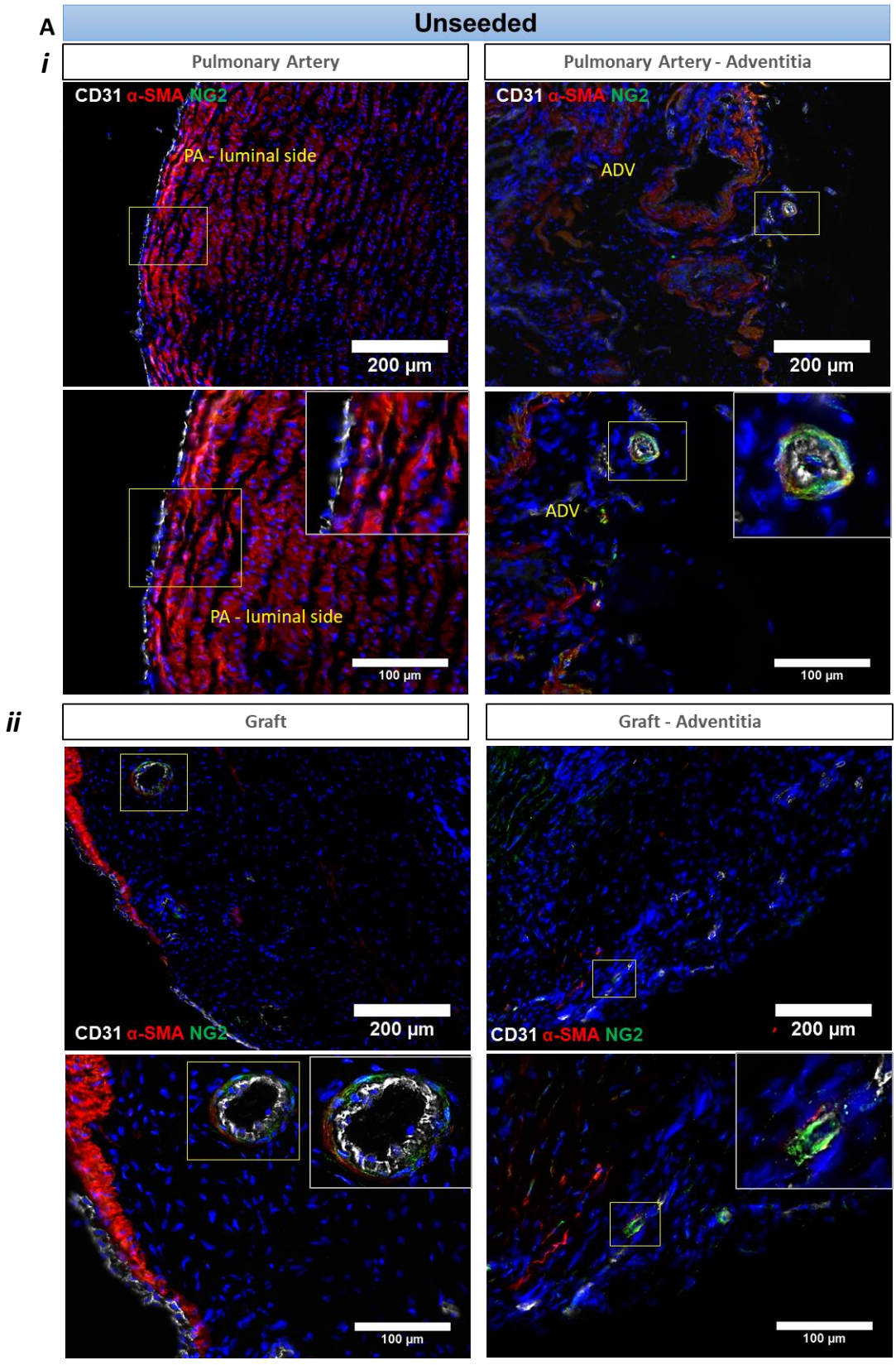

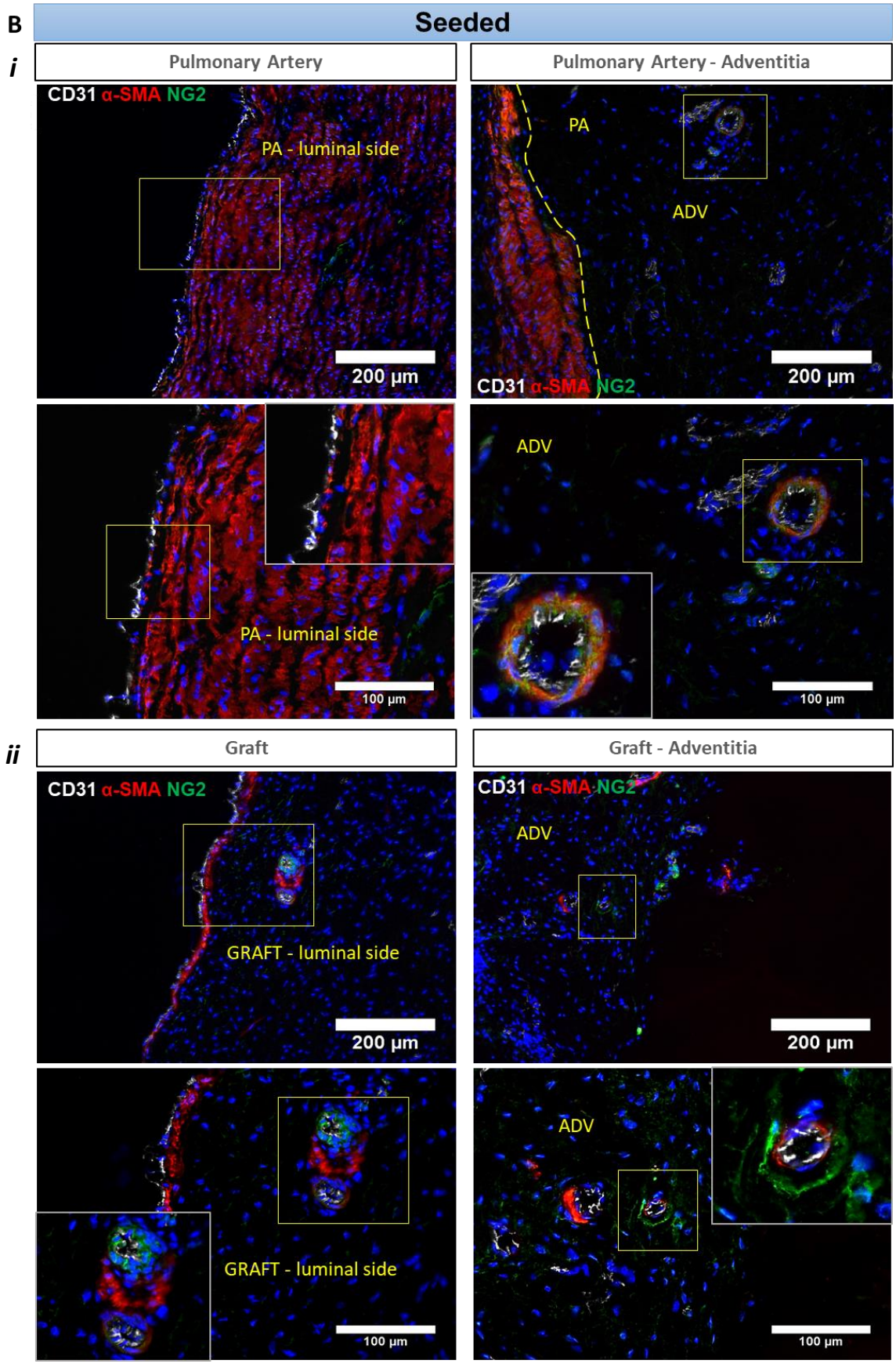
B
Seeded
i
Pulmonary Artery
Pulmonary Artery - Adventitia
CD31 α-SMA NG2
PA - luminal side
200 µm
PA
ADV
CD31 α-SMA NG2
200 µm
PA - luminal side
100 µm
ADV
100 µm
ii
Graft
Graft - Adventitia
CD31 α-SMA NG2
GRAFT - luminal side
200 µm
CD31 α-SMA NG2
ADV
200 µm
GRAFT - luminal side
100 µm
ADV
100 µm

Figure 5-17. Immunohistochemistry of the LPA and explanted grafts. A&B. IF images showing the PA with adventitia (i) and the graft with adventitia (ii) for unseeded (A) and seeded grafts (B). Cells expressing α-SMA (red) and CD31 (white) are present in the internal layer and luminal side of the native PA tissue and graft. In addition, NG2+ cells (green) are identified in the adventitia around the vasa vasorum. Magnification x100, n=1 animal per group size, scale bars= 100 µm. Merged channels are also shown at higher magnification in the panels. In yellow colour: PA= Pulmonary artery; ADV= Adventitia. *Abbreviations*: CD=cluster of differentiation; NG2= neural/glial antigen 2; SMA= smooth muscle actin.

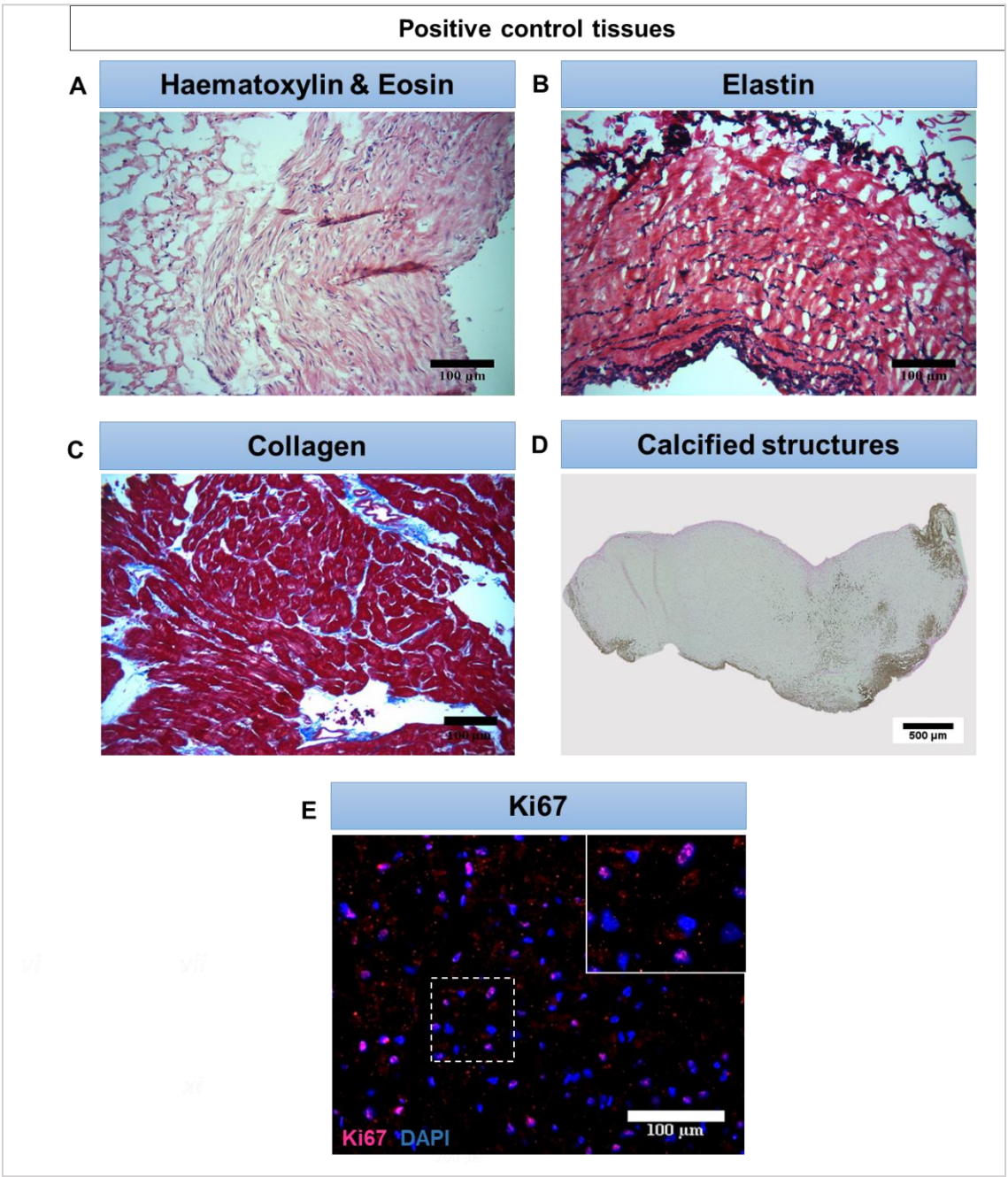

Figure 5-18. Positive control tissues for immunohistochemistry graft comparison. Swine saphenous vein showing H&E (A) and EVG staining (B) (cells and elastic fibres, respectively). Swine MI heart biopsy displaying Azan Mallory staining (Collagen) in the remote area (C). Aortic valve from swine MI model showing Von Kossa staining for the identification of microcalcifications (D). Swine health cardiac tissue stained with Ki67 for the cell proliferation. N=1 each control tissue.

6 Discussion

Quantitative and qualitative research studies from different investigators and with different animal models, species and methodologies, are important for a deep understanding of translational medicine. Neither the US FDA nor European Medicine Agency have provided specific guidelines about the TE cell therapy whether is tested in one or more animal species and how the data and results from different animal models and species should influence the begin of a clinical trial. In addition, there are different and contrasting views about the use of human cells in an animal model for preclinical studies because of their xenogeneic nature. Despite there are high immunological similarities among mammals, the presence of microorganisms and pathogens led mice and swine animals to differ in their immunity system so that it is not possible to compare and transfer the data and results between them (Bailey et al. 2013). Currently large animal models are gaining much interests in cardiovascular field for cell therapy with dispersed cells and for TE cardiac and vascular applications. For TE studies, swine animal becomes fundamental when testing an intracardiac or vascular graft (in forms of patches, conduits, valves or stents), and biomedical devices. The lack of similarity between human and mouse in vascular dimensions and hemodynamic parameters make these rodents poor models for TEVG evaluation.

Cell therapy and TE are gaining a lot of importance for the correction of CHD (Avolio et al. 2015a; Wehman and Kaushal 2015; Tsilimigras et al. 2017). Preclinical studies have demonstrated the utility of delivering different cell types, including skeletal myoblasts, cord blood stem cells, and mesenchymal stromal cells, either through intramyocardial or epicardial way to treat RV dysfunction and pulmonary artery hypertension induced by pressure or volume overload (Hoashi et al. 2009; Davies et al. 2010; Wehman et al. 2016). This experimental evidence was followed by clinical trials, some already concluded and other still ongoing, in patients with univentricular heart syndrome or HLHS. A more complex attempt aims to create cellularized conduits to correct severe cardiac defects, such as TOF, which are characterized by a constriction of the RVOT and PA. Initial evidence indicates that acellular grafts repopulated with ECs or BM cells are less susceptible to thrombosis or obstruction (Cebotari et al. 2010; Hibino et al. 2010; Dohmen et al. 2011). Recently, it has been demonstrated that swine intestinal submucosa, manufactured by CorMatrix® biotechnology company, and cellularized with thymus-MSCs (T-MSCs), could be implanted in a swine model for the reconstruction of the RVOT. After ~ 5 months from the implantation, more ECs, cardiomyocyte infiltration and reduction of collagen content were identified compared with the cellularized graft (Albertario et al. 2019). Furthermore, an

alternative approach has been developed where a swine CorMatrix® graft functionalized with umbilical mesenchymal stromal cell derived VSMCs was employed for replacement of the PA in piglets (Ghorbel et al. 2019). After 6 months from implantation, grafted arteries had developed a functional intima and media without evidence of aneurism formation. Using a similar strategy, we have now demonstrated the feasibility of employing CPs to generate living vascular conduits for reconstruction of the PA. The two approaches are mutually compatible and adaptable to the individual clinical condition and the time of diagnosis. We propose that sCPs are not employed in a future therapy as dispersed cells, but as a cell product to be seeded on top of an ECM and contribute to the homing of resident cells in the host tissue and confer structural capacities. The successful use of CorMatrix® in cardiovascular and CHD surgery derives from the perfect compatibility with the native tissue. Foetal stem-cells or umbilical cord stem cells isolated at the time of birth could be employed if CHD is diagnosed before birth. When diagnosis of CHD is made after birth or in babies who require a palliative intervention soon after birth, tissue specific cardiac cells, such as CPs, could be isolated from surgical cardiac leftovers to generate living conduits to be implanted at the occasion of the definitive correction (Avolio et al. 2015c).

Human pericytes represent the cell product to be ideally tested in preclinical safety/efficacy studies prior to a first-in-human clinical trial. However, their use in a xenogeneic piglet model is discouraged because of the adverse effects and confounding influence of immunosuppression to prevent rejection. The immunosuppression in these animals has been considered but it has some limitations. The isolation of the swine animal in the farms requires high costs and force the animal to live stressful conditions (Proudfoot and Habing 2015). In addition, it exposes the animal to high risk of infections and the duration of chronic immunosuppressive drug treatment requires the animal to reach the adult age. All these aspects would generate outcomes with misleading interpretations. Therefore, an equivalent animal cell product might be a sensible way forward to simulate an autologous or allogeneic transplantation at the preclinical stage before moving toward the clinical phase. Regulatory agencies are usually reluctant to allowing an animal equivalent product where possible, but, under these circumstances, the Medicines & Healthcare products Regulatory Agency (MHRA) has provided us with a favourable feedback for swine cells to be used in piglets for the model rather than human cells in swine. In addition, the MHRA's opinion is that the pulmonary artery reconstruction used here is an appropriate *in vivo* model to assess feasibility and efficacy of the cell engineered CorMatrix® conduit.

The equivalent cell product was validated through extensive characterization of antigenic markers, using *in situ* IHC, ICC and FACS. We also confirmed the clonogenic capacity of freshly processed or thawed single-sorted sCPs. The possibility of generating frozen stock of CPs

provides therapeutic flexibility for meeting the surgical schedule (i.e. surgery happening on a later time than the one required for the preparation of the graft) or multi-stage surgical corrections. In addition, swine and human pericytes share the ability to recruit endothelial cells and promote endothelial network formation through secretion of paracrine factors (Avolio et al. 2015c). Pericytes signal to endothelial cells through the binding of ANG1 to Tie2 results in the activation of pathways mediating survival, proliferation, migration and anti-inflammatory signals. Using a Tie2 antagonist, here we demonstrated that this signalling is instrumental to the recruitment of ECs by the sCP secretome. Our data indicate that sCPs promote the organization of sPAECs on Matrigel, likely through activation of migration and inhibition of degradation. This is in line with the well-known role of pericytes stabilizing the nascent vessels (von Tell et al. 2006; Armulik et al. 2011; Geevarghese and Herman 2014).

The use of extracellular matrix as a biological scaffold for tissue repair and regeneration is an established procedure within the clinical community. Commercial scaffolds manufactured from a range of ECM materials from different animals are available for use in cardiac surgery. CorMatrix®, the most used product of this type, is a decellularized porcine small intestinal submucosa product that has received approval by both the FDA and European authorities for cardiovascular applications. A recent meta-analysis assessing the results of clinical studies using CorMatrix® in pediatric populations indicates favourable outcomes (Mosala Nezhad et al. 2017). However, some of the claimed advantages of the material, such as the bio-inductive capacity to support the ingrowth of reparative cells from the host without inducing inflammatory reactions, have been questioned by several reports. Histological examination of failing grafts showed moderate to severe grade inflammation in the explant tissue without signs of regeneration or integration(Zaidi et al. 2014; Padalino et al. 2015; Rosario-Quinones et al. 2015). Interestingly, these reactions were not seen in swine models, thus suggesting the possibility that inflammation was a reaction to antigenic epitopes present in the swine intestine, but not in the humans (Rosario-Quinones et al. 2015). Moreover, ~ 90% of the CorMatrix® is made of collagen type I but contains little amounts of elastin (Badylak et al. 2009), which is instead a major component of a pulmonary artery and a determinant in maintaining vascular hemodynamic efficiency (Lammers et al. 2008)

Recellularization with stromal cells prior to *in vivo* implantation could overcome the inadequate constructive remodelling capacity and lack of elasticity of the native CorMatrix®. Confirming the data of our previous study on human pericytes (Avolio et al. 2015c), the present study shows that sCPs proliferate and engraft onto the CorMatrix® external surface, maintaining a high degree of viability and the original antigenic phenotype making the conclusion that the graft

does not alter the CP features. This is in line with the goal of creating a cellularized adventitial layer, from which, upon *in vivo* implantation, sCPs could exert paracrine recruiting effects on the recipient cells and timely remodelling of the matrix. Premature penetration of sCPs into the matrix core prior to *in vivo* implantation is not desirable. In fact, for this, the matrix should undergo degradation, which could weaken the scaffold making it unable to withstand the mechanical forces *in vivo*. The equilibrium between breakdown of the structure due to proteases and the production of ECM proteins plays a fundamental role in the stabilization and rearrangement of the graft as well as native blood vessel (Heydarkhan-Hagvall et al. 2006).

The *in vivo* study provided us with valuable data in preparation of a properly designed efficacy trial, but also highlighted the strengths and weaknesses of the swine model. We used Doppler and CMR imaging to measure the blood flow velocity and confirm the patency of the implanted graft. The values of blood flow velocity from the present study are consistent with a previous report (Ghorbel et al. 2019). A power calculation based on combined data from the two studies indicate that a minimum of 7 animal per group are necessary to detect a difference of 0.3 mL/min with a standard deviation of 0.2. Our previous studies confirmed that graft stenosis is a rare event in swine compared with humans, possibly due, as mentioned above, to a lower inflammatory reaction and to a product from the same species. Therefore, hemodynamic outcomes should be considered in combination with histological outcomes, such as matrix remodelling, endothelialization of the intima, and cellularization of the media and adventitia, as shown in the present study.

This work has generated many positive outcomes which are the proof of feasibility of using allogeneic organ-specific cells seeded on top of a natural prosthesis and implanted as cellularized small conduit interposed between the two branches of the LPA. The use of a swine model, which replicates the clinical scenario of ToF, represents the essential validation prior moving towards the first-in-man trial with sCPs. The use of sCPs and swine CHD model will help also the researchers and clinicians to deeply understand the challenges and issues of using them and to address the project to move forward in terms of efficacy and safety. The challenges occurred during the entire project were related to the *in vitro* and *in vivo* experimental studies. For the *in vitro* studies, some challenges occurred when moving from human to swine reagents. Translational Health Science has made many progresses to the use of swine reagents employed during *in vitro* studies. Many advances were also made in the immunology field where swine-specific antibodies were developed against antigens of hematopoietic cells of swine. In this work, I have isolated and expanded swine cells in EGM-2 media which contains human GFs and swine serum. The substitution of all these factors with swine components and a comparison

with xeno-factors would better clarify the similarities and differences in the cell phenotype and functional properties. Another challenge raised during TE procedures while working with a 3D-structure, such as CorMatrix®. Different distribution of the ECM layers and the long-time of culture may be also responsible of a high autofluorescence intensity signal during the IHC procedures. For instance, the in-situ evaluation of apoptotic sCPs seeded in the CorMatrix® detected a high autofluorescence signal generated by ECM fibres and this was more evident when the graft was exposed for 7- and 14-days static and dynamic culture. Furthermore, the cell apoptotic staining kit detected also native nucleic acid fragments in the graft left after the decellularization process, making difficult the exact quantification of the apoptotic bodies from the exogenous sCPs. Therefore, I attempted to perform the detachment of cells from the graft. The issues of this method can be that the enzymatic digestion may overestimate the number of apoptotic cells and leads misleading outcomes. CorMatrix® strongly retains exogenous cells, and a longer incubation time with the enzymes (trypsin/EDTA or Accutase) is required for the detachment from the graft. For future studies, a more accurate test would be ideal to assess the exact percentage of apoptotic sCPs, despite this was low after using the method described here. Sometimes the detached cells are not enough for the performance of different assays aimed to evaluate the characteristics of cells seeded onto graft. I attempted to detach cells from the graft which were further spun on top of the slides to perform an immunostaining for the apoptosis. However, I was unable to obtain cells and perform assays which require a higher number of cells, such as, FACS. Furthermore, another challenge occurred during the mechanical manipulation of the TEVG when moving from the static condition to the perfused flow in the bioreactor. The stitching procedure that simulates the formation of the engineered conduit may interfere with the cell viability. In addition, the suture sites may develop areas of aggregates of cells which may trigger calcification or formation of thrombi in the vasculature. For the *in vivo* studies, one challenge was to collect autologous swine heart sample using a cardio-biopsy catheter system instead of collecting tissue from a littermate swine after termination. The catheter system is a non-invasive procedure, different from the invasive open-chest surgical intervention that might be the gold standard to obtain small biopsies from the animal and from the human patients. This advanced procedure would translate into the clinical scenario to reduce the risks of collecting a small piece of cardiac tissue from a baby patient during an open-chest surgery for CHD.

The project is still ongoing and aimed to be completed by the middle of 2020. The completion of this study will provide additional information about the capacity of the TEVG to remodel the recipient heart in terms of structural and functional properties (ECM proteins and capillary and arteriole formation) and teratoma formation (calcification). In addition, a separate

biodistribution study will assess the localization of the sCPs, collected from a female donor animal, in the adventitia of the TEVG after the implantation in the male recipient animal.

7 Future perspectives

The outcomes of this project support the theory that sCPs can be used as an equivalent cell product of hCPs to engineer CorMatrix® conduits which are implanted in the LPA of swine model. An efficacy and safety study based on this technology and by recruiting more swine animals is currently ongoing and to be completed by the middle of 2020. This will provide a clear evidence of the advantages of using PEGs over the unseeded grafts in terms of structural and functional aspects. The 2015 NHS England review document indicates that CHD care was provided last year by 10 hospitals doing 3,700 operations and 2,000 procedures in children and by 25 hospitals performing 850 operations and 1,600 procedures in adults. This activity will expectedly increase by 14% in children and 67% in adult cardiac services during the next 10 years. If this trend is confirmed, the 2025/26 expenditure will be between £186 and 207 million, with cost increment being more remarkable in ACHD patients (21%) than in children patients (8%). Costs for repeated operations heavily impacts on these patients. NHS England and other analysts have previously calculated that there will be a mismatch between total NHS budget and patient needs of nearly £30 billion by 2020/21. Therefore, efficiency actions to increase quality and reduce expenditure growth will be essential in all services, including CHD. However, efficiency will not suffice without the introduction of innovative technologies offering a transformative impact on this unmet clinical field. The successful application of a TEVG system could reduce all these costs and improve the quality of life of these patients.

8 Conclusions

The work described in this study is part of the translational science programme which is developed at University of Bristol under the leadership of Prof *Paolo Madeddu* and Prof *Massimo Caputo.* The project has the ambition to generate new TE strategies for the correction of CHD employing swine CPs delivered with a TEVG after demonstrating the similarity with the human cells. I attempt to reach different objectives during my PhD course: the first one is to optimize all the methods required to manipulate cells in a different specie than human and to retrieve all information about the use of swine reagents and antibodies to grow and characterize with more specificity and selectivity CPs. However, the swine reagents have still limited availability and I have tried to overcome these limitations by using human reagents or antibodies which cross-react with swine animal. I have become confident with Uniprot, an online bioinformatic database which uses FASTA for the alignment of two protein sequences from different species and finds the percentage of homology between the human and swine molecules. I have encountered some issues related to the interaction between human and swine cells when cultured together *in vitro* to assess the their angiogenic capacity. Although swine CP-CM exerts a strong attractive action on human umbilical cord vein endothelial cells (HUVECs), no angiogenesis is observed when HUVECs are co-cultured with sCPs on Matrigel substrate, suggesting that there might be a physical obstacle when human and swine are seeded and cultured together (data not shown). Another goal is to face my first experience with TE techniques where I have used all the instruments requested to manipulate and maintain the non- and -cellularized grafts under static and dynamic culture environment (cell crowns and bioreactor). I have contributed to set up the bioreactor and the chambers for the position of a TEVG for culture conditions and I have learnt how the cells behave when exposed to a different material than a plastic dish. I attempt to refine some limitations of this project. Swine CP phenotype is assessed when cells are seeded into the plastic dishes and detached to obtain a cell suspension. We do not know whether their FACS phenotype changes in a different culture system. The characterization of neonatal sCPs seeded on CorMatrix® could have been improved. In order to evaluate these markers of cells seeded on the graft, $1x10^6$ cells are required at least. The enzymatic detachment by Trypsin/EDTA or Accutase is not enough to obtain this cell number as CorMatrix® has a high cell retention. Another limitation is to provide more quantitative results of implanted grafts in terms of antigens, ECM proteins, calcification. More animals are in the process of the surgical procedures and final termination for the harvest of tissue-grafts to allow the histological analysis.

At the beginning of my PhD studies, my knowledge and expertise were focused on cell biology, and joining to this laboratory has given me the possibility to apply my basic knowledge and build up biochemistry, molecular biology and basic TE techniques that are essential to the translational cardiovascular medicine. We have applied a swine CHD animal model to investigate how the seeded TEVG product interferes with and how it improves the host's response.

I also contributed to the publication of review article covering TE topics, such as, "*Perivascular cells and tissue engineering: Current applications and untapped potential*" (Avolio et al. 2017).

My first-author manuscript entitled "*Transplantation of allogeneic pericytes improves myocardial vascularization and reduces interstitial fibrosis in a swine model of reperfused acute myocardial infarction*" (Alvino et al. 2018) and published in Journal of American Heart Association (JAHA), aimed to demonstrate the emerging potential of delivering swine allogeneic APCs, which are perivascular progenitor cells, for the treatment of MI. I have performed *in vitro* experiments and analysed the data. Material, methods and results are reported in a small appendix section of the thesis.

My second manuscript "*In vitro and in vivo preclinical testing of pericyte-engineered grafts for the correction of congenital heart defects*" (Alvino et al. 2020), published in JAHA and reported in this thesis, has confirmed that it is possible to isolate pericytes from heart of neonatal swine and expand them to engineer an ECM scaffold. We provide an initial evidence of the feasibility of using PEGs for the reconstruction of swine LPA.

This studentship has projected me into a clinical scenario and fostered a great deal of interest and enthusiasm in medical science. I am very committed to persevere in this endeavour hoping to contribute in the fight of cardiac disease that affect many people in the UK and worldwide.

9 Appendix

9.1 Isolation and characterization of swine adventitial saphenous vein pericytes enabling the myocardial infarction therapy

Alongside the study of new-born sCPs which are employed for the repair of CHD, a similar *in vitro* approach has been used to derive and characterize sAPCs and use them in a preclinical swine model of acute MI. The reason of using swine cells has been previously explained. We have demonstrated that sAPCs show robust similarities with hAPCs and that finding has supported the validation of swine cell therapy in a swine MI model. This appendix aims to describe three different objectives: the first one encompasses sAPC isolation and expansion; the second one includes the identification of similarities according to antigenic profile and mesenchymal commitment; the third objective includes the similarity according to functions relevant to the designated therapeutic use. Here, I will explain and illustrate the material, methods and results of the experiments performed by myself before and after cell therapy with dispersed sAPCs in the swine MI model. The *in vivo* studies were performed by our research collaborators of the Centro Nacional de Investigaciones Cardiovasculares (CNIC) Carlos III in Madrid (Spain) under the leadership of Prof Borja Ibanez. Many other *in vitro* and *in vivo* studies were conducted by other colleagues and are not reported in this thesis. The entire project entitled "Transplantation of allogeneic pericytes improves myocardial vascularization and reduces interstitial fibrosis in a swine model of reperfused acute myocardial infarction" is published in JAHA (Alvino et al. 2018) (**Figure 9-1**).

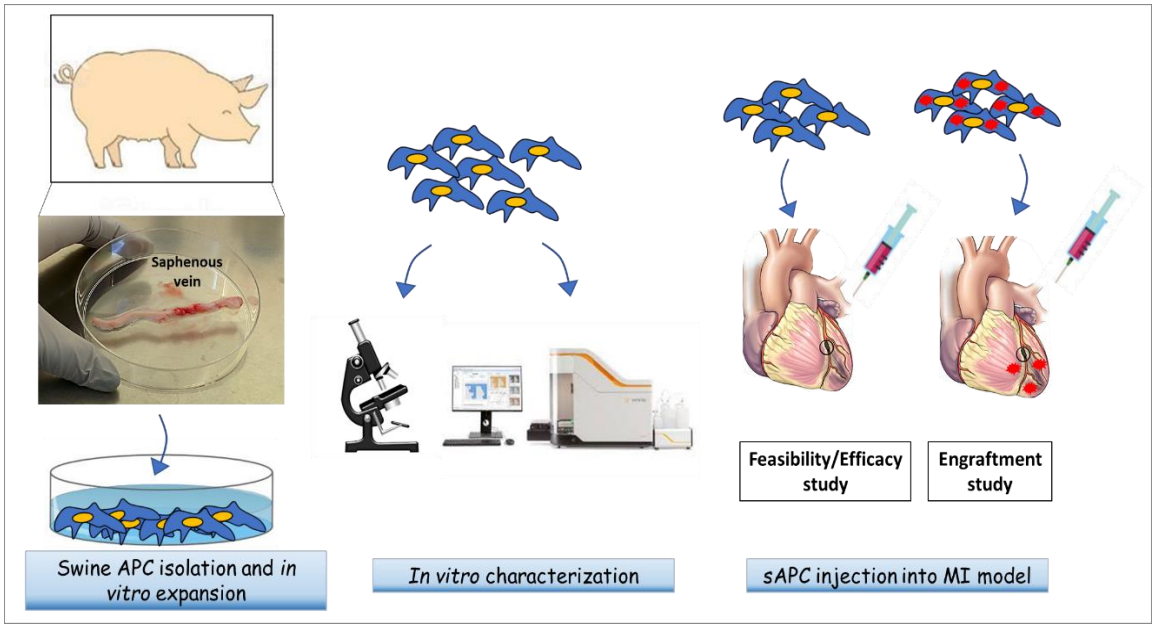

Figure 9-1. Cartoon showing the workflow of preclinical study with sAPCs. Cells are isolated from the adventitial saphenous vein of adult swine animal, expanded and characterized to validate the similarity with human counterpart. The in vitro studies are performed to feed the in vivo transplantation of allogeneic sAPCs in a swine MI model. Efficacy and engraftment studies are performed at different times. *Abbreviations*: MI= myocardial infarction; sAPC= swine adventitial saphenous vein pericyte.

10 Material and methods

10.1 Swine adventitial saphenous vein pericyte processing

Studies using human cells were covered by South West Central Bristol Research Ethics Committee, REC reference 06/Q2001/197.

All the procedures for swine tissue harvest, isolation and expansion of swine cells were previously described for hAPCs (Campagnolo et al. 2010; Katare et al. 2011). Here, I report all the in vitro experiments performed by myself and in which I have contributed.

Large-white swine (age, 3-4 months, UK registered breed), were terminally anesthetized for the collection of peripheral blood and saphenous vein (5-10 cm length and 1 g weight). **Figure 10-1** displays a schematic isolation procedure of sAPCs. The list of swine donors and the *in vitro* use of corresponding cell lines are listed in **Table 10-1**.

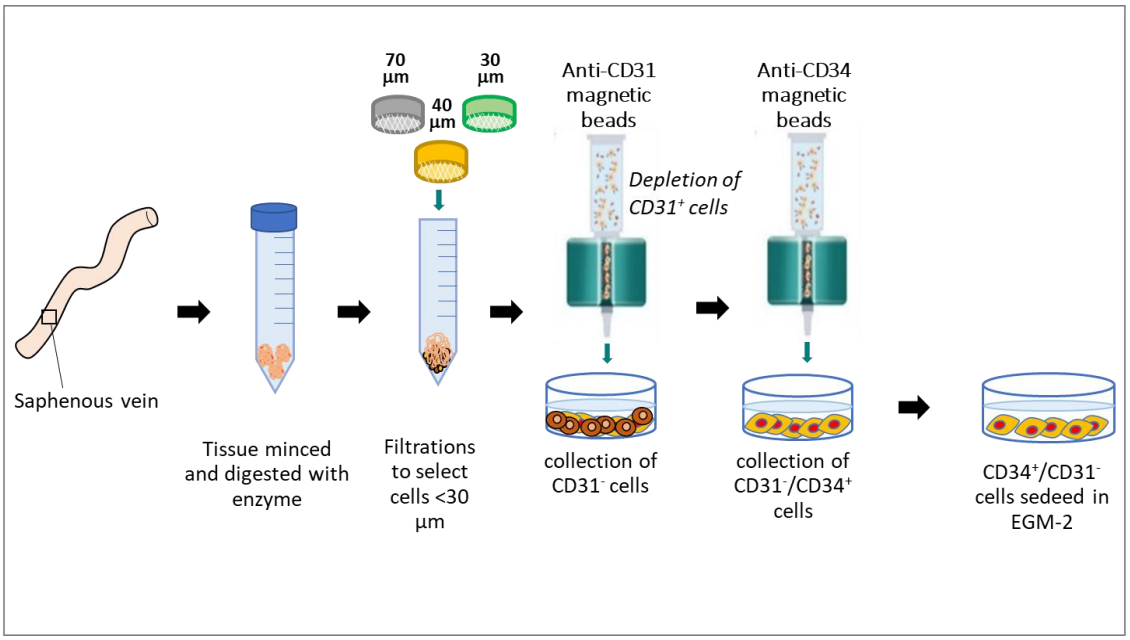

Figure 10-1. Scheme of swine APC isolation. Saphenous vein was manually minced, and the homogenate was incubated for 2 hours with 0.45 WU/mL/g Liberase enzyme and sequentially passed through 70 µm, 40 µm, and 30 µm cell strainers to ensure single cell suspension. Isolated cells were incubated with anti-CD31 and –CD34 conjugated microbeads to select a final population of CD31- and CD34+ cells. This cell fraction was cultured in a pre-coated dish and in EGM-2 media, supplemented with 10% heat-inactivated swine serum. *Abbreviations*: CD= cluster of differentiation; EGM-2= endothelial cell growth media.

Swine APC code	Line	*In vitro* use
020215 A	1	PCR, ICC, FACS, Differentiation, ELISA, WB
190515 A	2	PCR, ICC, FACS, Cell sizing, MATRIGEL, ELISA, WB
190515 B	3	PCR, ICC, FACS, Cell sizing, MATRIGEL, ELISA, WB
150615 B	4	ICC, FACS
290715 A	5	PCR, ICC, FACS, Cell sizing, Differentiation, Matrigel, ELISA
220116 A	6	Differentiation, Cloning
220116 B	7	Cloning, ELISA

Table 10- 1. Code of donor swine and specific use of corresponding sAPC lines. *Abbreviations*: ELISA= enzyme-linked immunosorbent assay; FACS= flow Activated Cell Sorting; ICC= immunocytochemistry; PCR= polymerase Chain Reaction; WB= western Blotting.

10.1.1 Antigenic characteristics of swine adventitial saphenous vein pericytes

A series of comparative experiments was performed to assess the purity of cells isolated from swine veins and to verify their similarities to hAPCs. The *in vitro* sAPC studies are equivalent to sCP studies and are not repeatedly explained in this appendix. The reader should refer to paragraph 4.3.2 in the Chapter 4, where the IF and FACS procedures and the use of reagents are described in detail.

10.1.2 Gene and protein expression

Quantitative PCR was performed on cells cultured following stimulation in normoxia (21% oxygen) or hypoxia (2% oxygen). For RNA extraction and RT-PCR, the reader should refer to paragraph 4.3.4 in the Chapter 4.

In addition, the expression of the T-box family transcription factor Tbx18 was tested in sAPCs and hAPCs by qPCR (Hs01385457_m1, Thermo fisher, UK) and western blot (WB, Santa Cruz, UK).

For protein extraction, 100 µL of lysis buffer (RIPA buffer, Thermo fisher, UK) were used per $1x10^6$ cells. Protease inhibitors were used at 1:100 and added to the ice-cold lysis buffer. Cell scraper was used to collect and transfer the cell lysate into the tubes and spun at 1500 rpm, for 10 minutes, at +4 °C. The supernatant was collected, and the cell pellet discarded. Bicinchoninic acid assay (BCA) was performed to determine the concentration of total proteins in the cell lysate. To reduce and denaturate the proteins, a hot block set up at 95 °C was used for 2 minutes. Total proteins were loaded (15 µg) with 6x Laemmli sample buffer into the wells of the sodium dodecyl sulphate-polyacrylamide gel electrophoresis (SDS-PAGE), alongside the molecular weight (MW) marker (ladder). The percentage of resolving/separating gel was 10% as Tbx18 size was 65 KDa. After running, polyvinylidene difluoride (PVDF) membrane of 0.2 µm pores was activated with 100% methanol and rehydrated with deionized H_2O. Then, the gel was transferred on the membrane at 250 mA, for 90 minutes using 1x transfer buffer. The transfer procedure was stopped, and the membrane rinsed in deionized H_2O. The transferred proteins to the membrane were checked with Ponceau S staining for 3-5 minutes. Then, the solution was removed, and the membrane was rinsed with 0.1% (v/v) Tris-buffered saline-0.1% Tween-20 (TBS-T) in deionized H_2O. The membrane was blocked with 5% milk diluted in 0.1% TBS-T for 1 hour, at RT following by an incubation with 1:100 anti-human Tbx18 primary antibody (Santa-cruz, UK) into the above blocking buffer, for 16 hours, at +4 °C. Membrane was washed in 0.1% TBS-T once and an anti-rabbit horseradish peroxidase secondary antibody was incubated in the blocking solution at 1:5000, for 1 hour, at RT, protected from light. After washes, ECL Prime WB Detection Reagent 1:1 (GE Healthcare, UK) was incubated on the membrane for 1 minute for the signal development. The excess of reagent was removed and the chemiluminescence image scanning was performed using ChemiDoc XRS+ system with Image Lab™ software (Biorad, UK). β-actin loading control (42KDa) was used as housekeeper.

10.1.3 Differentiation and clonogenic capacity

For the induction of osteogenesis, sAPCs (N=3) were cultured in Dulbecco's Modified Eagle Medium (DMEM, Life Technologies, UK) supplemented with L-Ascorbic acid 2-phosphate (50 µM – w/v), Dexamethasone (0.1 µM- w/v) and β-glycerol phosphate (10 mM – w/v). For adipogenic differentiation, cells (N=3) were cultured in DMEM supplemented with Dexamethasone (1 µM – w/v), Indomethacin (100 µM – w/v), Insulin (10 µg/mL – w/v) and 3-isobutyl-1-methyxanthine

(500 µM – w/v). The media was replaced every three days. Osteogenic differentiation was evaluated with Alizarin Red solution and adipogenic differentiation with Oil-Red-O solution (both from Sigma-Aldrich, UK). The staining protocol was performed according to the Manufacturer's instructions.

Single cell cloning of sAPCs was carried out according to the procedure described in the paragraph 4.3.3 of Chapter 4.

10.1.4 Vascular endothelial growth factor A and miR-132 secretion

The levels of VEGF-A protein and miR-132 were determined in the CM by an anti-human ELISA kit (R&D Systems, UK). To this aim, sAPCs (N=3) were cultured in EGM-2 complete media in a T25 flask and exposed to normoxia or hypoxia environment. The culture media was substituted with 2.5 mL freshly and serum-free EBM-2 for 48 hours. After 48 hours, the cell supernatant was collected and centrifuged at 400xg, at +4°C to remove any cell debris. The resulting CM was stored at -80°C until batch analysis. ELISA assay was performed following Manufacturer's instructions. In addition, a WB analysis was performed to detect the same protein in concentrated CM and UCM (EGM-2) using the Amicon® Ultra-2 Centrifugal Filter Devices (Merck Millipore, UK) to concentrate the samples.

10.1.5 Network formation

Swine PAECs were co-cultured with sAPCs at 1:4 ratio and following stimulation with sAPC-CM. The reader is referred to paragraph 4.3.6 for Matrigel assay protocol.

10.2 Transplantation of swine adventitial saphenous vein pericytes

10.2.1 Feasibility, efficacy and engraftment study

The in vivo study in 32 swine was carried out by the Investigators based at CNIC in Madrid. Two additional swine underwent the same MI protocol and then received an intramyocardial injection of fluorescent labelled sAPCs. The protocol is summarized in **Figure 10-2**.

Since this study was performed by Prof Borja Ibanez and his Research team, the reader should refer to the manuscript published in JAHA for the details (Alvino et al. 2018).

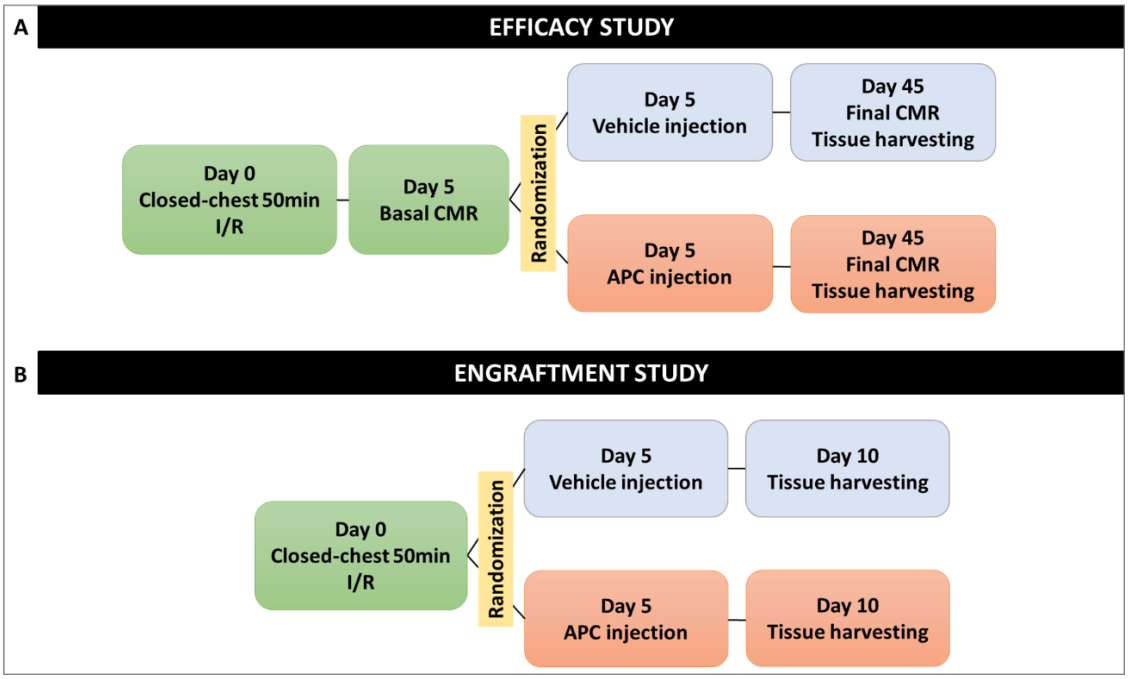

Figure 10-2. Study design. (A) In the efficacy study, swine were subjected to close-chest 50-minues balloon occlusion of the mid-LAD to induce acute MI. At 5 days post-MI, they underwent a comprehensive basal CMR study. Animals did not show a transmural infarction (at least 50% of the wall thickness infarcted) were excluded. Immediately after day 5-CMR, animals were randomised to receive intra-myocardial vehicle or sAPC injection. CMR was repeated at day 45 post-MI and hearts were harvested for histology assessment. (B) A similar protocol was used to assess cell engraftment with hearts being collected 5 days after vehicle and sAPC injection. *Abbreviations*: APC= adventitial saphenous vein pericyte; CMR= cardiovascular magnetic resonance; I/R= ischemia/reperfusion; LAD= Left Anterior Descending artery; MI= Myocardial Infarction. Figure source: Alvino et al., 2018, JAHA.

10.2.2 Cell preparation for transplantation in the swine myocardial infarction model

The expansion of sAPC lines was carried out in Bristol and synchronized with the scheduled MI induction in the laboratory of CNIC in Spain. Briefly, APCs were cultured and expanded to P6 to reach enough cells for the injection, then seeded into multilayer flasks (Hyperflasks M Cell Culture Vessels, Corning, UK), allowing complete cell adhesion for 48 hours and shipped to CNIC within 24 hours. In Madrid, our collaborators organized and performed the cell detachment and the injection in the MI animal model.

10.3 Histological assessment of swine hearts

Capillary and arteriole, interstitial fibrosis and cell engraftment staining procedures were performed and completed in Bristol. I have contributed to vessel and fibrosis stainings and quantifications and entirely assessed the persistence of DiI-labelled sAPCs in the swine hearts.

10.3.1 Capillary and arteriole density

For capillary density quantification, paraffin-embedded sections were incubated with biotinylated Griffonia Simplicifolia Isolectin B4 (1:200, Life Technologies, UK), overnight in a humidified chamber and at +4°C, followed by the incubation of Streptavidin Alexa Fluor 488-conjugated (1:200, Life Technologies, UK) for 1 hour, at +20°C, in the dark. For arteriole density quantification, the same sections were probed with anti-α-SMA antibody Cy3-conjugated (1:400, Sigma-Aldrich, UK). Capillaries and arterioles were calculated in 40 fields (at 200x magnification) in the peri-infarcted area of myocardium and the final data expressed as the number of capillaries or arterioles per square millimetre. The analysis was performed using the free software ImageJ. Adobe Photoshop v6 was utilized to compose and overlay the images.

10.3.2 Interstitial fibrosis

For the cardiac interstitial fibrosis, paraffin-embedded sections of peri-infarcted areas were stained with Azan Mallory solution according to the manufacturer's instructions.

10.3.3 Swine adventitial saphenous vein pericyte engraftment

For the assessment of the persistence and the location of DiI labelled sAPCs in different regions of swine hearts 5 days post-injection, 5 µm-thick sections were cut and antigen retrieval was performed after deparaffinization using 0.02M Citrate buffer, PH=6, for 30 minutes at 98°C. Sections were incubated with biotinylated Griffonia Simplicifolia Isolectin B4 (1:200) overnight in a humidified chamber and at +4°C, followed by the incubation of Streptavidin Alexa Fluor 488-conjugated (1:200) for 1 hour, at +20°C, in the dark. Cardiomyocytes were stained with a mouse monoclonal anti-α-sarcomeric actin primary antibody for 2 hours, at +20°C (1:200) followed by Alexa Fluor 647-conjugated goat anti-mouse IgM secondary antibody (1:200, Invitrogen, UK) for 1 hour, at +20°C, in the dark. Nuclei were labelled with 1:1000 (v/v) DAPI in 1xPBS. Sections were analysed at 200x magnification with Zeiss Observer.Z1 microscope (Carl Zeiss Microscopy, LLC,

US) and Zen pro software. Morphometric analyses were performed using the free software ImageJ.

11 Results

11.1 Isolation, expansion and characterization of swine adventitial saphenous vein pericytes

Having previously demonstrated the isolation and characterization of hAPCs (Campagnolo et al. 2010) and that the swine is not immune tolerant to hAPCs (Alvino et al. 2018), an equivalent cell product obtained from the adventitia of swine saphenous vein was evaluated. To this aim, a SOP, previously employed for the isolation and expansion of hAPCs, was adopted with the substitution of 2% (v/v) heat-inactivated FBS with 10% (v/v) heat-inactivated swine serum and the use of 1% (w/v) swine gelatin instead of 10 µg/mL gelatin (Sigma-Aldrich, UK)/fibronectin (Corning, UK) for the coating of the dishes. The gelatin/fibronectin solution triggered the formation of the clumps and cell death as assessed by Trypan blue exclusion method (data not shown). Cells were expanded from seven swine saphenous veins with a success of 100%.

11.1.1 Doubling time and cell sizing

Cells grew quickly in culture with an average DT of 2.5 days, reaching ~30x10^6 cells at P6 in 6 to 8 weeks (data not shown). Both hAPCs and saphenous vein-derived swine cells showed similar spindle-shape morphology at phase-contrast microscopy (**Figure 11-1A**) and similar sizes as assessed by the Tali™ image-based cytometer (hAPCs 16.2 µm±0.1; sAPCs 15.7 µm±0.4) (**Figure 11-1B**).

11.1.2 Immunocytochemical assessment

Next, ICC studies were performed to compare the two cell populations, using validated specie-specific primary antibodies as indicated in the **Table 4-2** of paragraph 4.3.2. The similarity of the two cell products was confirmed through a high expression of the lineage antigen NG2 (hAPCs 62±6%; sAPCs 99±1%), PDGFRβ (hAPCs 97.3±3%; sAPCs 100±1%) and Vimentin (hAPCs 95±5%; sAPCs 100±1%) (**Figure 11-1C**) and of the stemness markers GATA-4, SOX-2 and OCT-4 (**Figure 11-1D**). Both hAPCs and sAPCs were negative for endothelial markers CD31, VE-cadherin and expressed very low levels of CD146, whereas HUVECS and sPAECs (both positive controls) expressed these antigens (**Figure 11-1E**).

11.1.3 Tbx18 gene and protein expression in swine adventitial saphenous vein pericytes

The expression of the T-box family transcription factor Tbx18 was also verified. This protein is reportedly and selectively expressed by microvascular pericytes and VSMCs in the adult mouse (Cai et al. 2008; Birbrair et al. 2017). Results confirmed the Tbx18 gene was detected by qPCR for both cell populations (hAPCs Ct value=24.4; sAPCs Ct value=26.6, data not shown), with the expression being confirmed at the protein level by WB analysis of the cell lysates (**Figure 11-1F**).

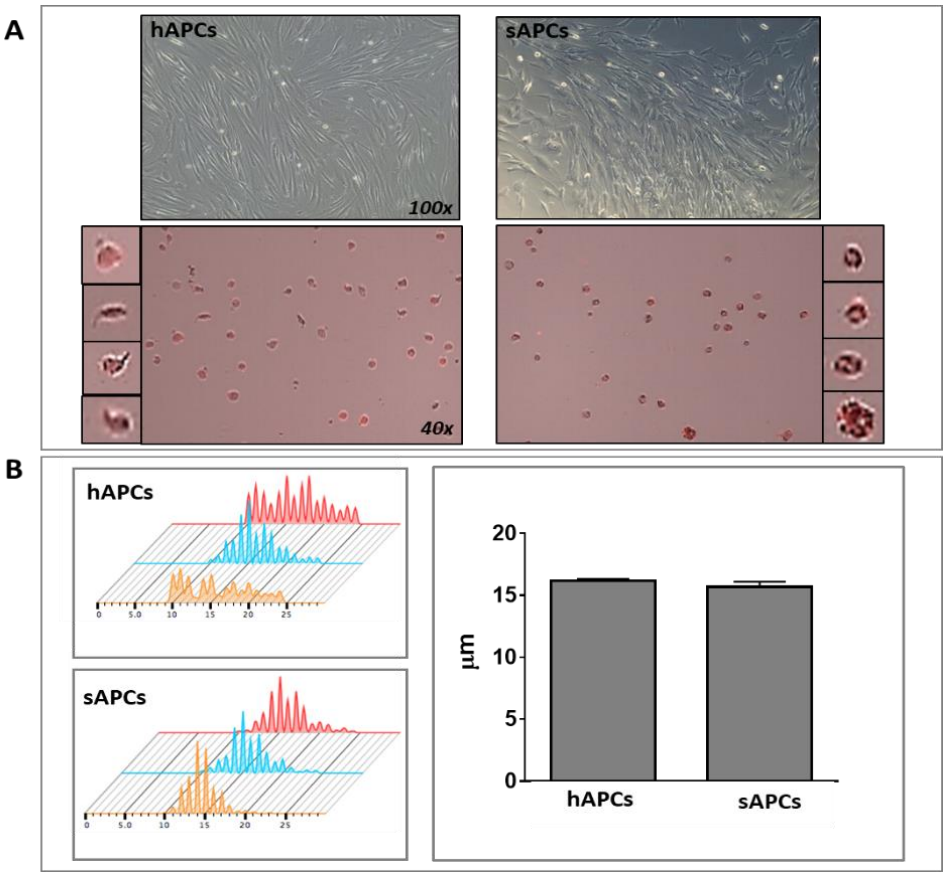

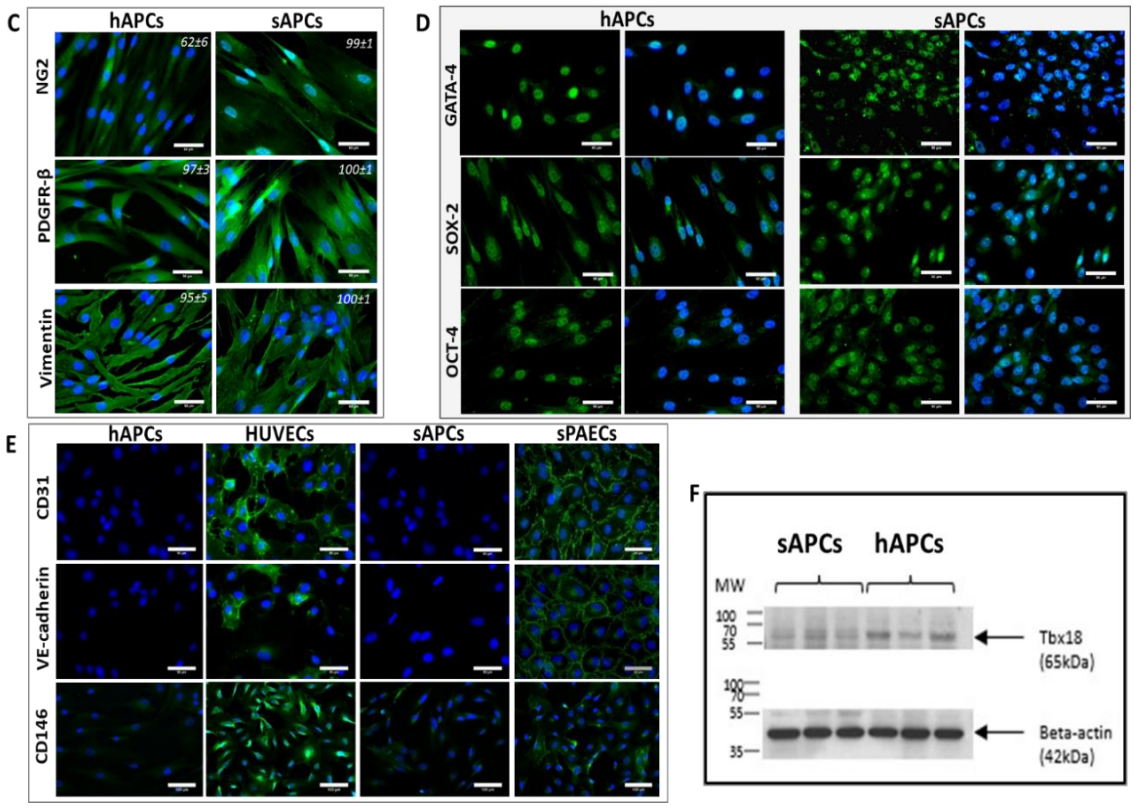

Figure 11-1. Comparison of APCs isolated from human and swine saphenous veins. A. Upper panels: phase-contrast microscopy images of human and swine cells displaying similar spindle-shape features (x100 magnification); Lower panels: cells shown in the contrast-phase microscopy images are stained with human and swine CD105 PE-conjugated (red fluorescence) for the measurement of cell size (x40 magnification). B. Left panels: cell size histograms calculated by Tali and Novocyte 3000. The X axis represents the cell size and the Y axis represents the number of cells counted (3 cell lines for each group). Right panel: the bar graph shows the mean and SEM which is similar between the two groups, though the range of cell size was wider for hAPCs. C. Representative IF microscopy images showing the expression of NG2, PDGFRβ and Vimentin. Values in each panel represent the mean±SEM of n=4 biological replicates. D. IF microscopy images displaying the expression of GATA-4, OCT-4 and SOX-2. Blue fluorescence DAPI recognizes the nuclei. Magnification x200 and x400, scale bar= 50 µm. E. IF images confirming these cells do not express endothelial antigens, at variance with HUVECs and sPAECs (positive controls). F. WB image showing Tbx18 protein corresponding to the 65 KDa Molecular Weight (MW) of n=3 sAPC and hAPC lines. *Abbreviations*: CD= cluster of differentiation; hAPCs= human adventitial saphenous vein pericytes; NG2= neural/glial antigen 2; OCT-4= octamer-binding factor 4; PDGFRβ= platelet-derived-growth factor beta; sAPCs= swine adventitial saphenous vein pericytes; SOX-2= sex determing region Y; VE-cadherin= vascular endothelial-cadherin.

11.1.4 Flow cytometry studies

Furthermore, FACS studies indicated that like hAPCs, sAPCs abundantly expressed the mesenchymal markers CD44 (hAPCs 99±6%; sAPC 97±1%), CD90 (hAPCs 88.3±5.6%; sAPCs 94±1%), CD105 (hAPCs 87.0±5.7%; sAPCs 97±1%) and PDGFRβ (hAPCs 86.2±5.7%; sAPCs 94±0.2%) but were negative for CD146 (hAPCs 0.1±0.03%; sAPCs 5±0.5%), CD31 (hAPCs 0.5±0.2%; sAPCs 0.6±0.3%) and the hematopoietic marker CD45 (hAPCs 1.8±0.4%; sAPCs 2±0.1%) (**Figure 11-2A-D**). Swine PB-MNCs and sPAECs were used as positive controls (**Figure 11-2E-F**). In addition, experiments were conducted to exclude the possibility that contamination of the vein extracts by circulating hematopoietic cells could have compromised the purity of the cell product. To this aim, MNCs were isolated from peripheral blood and cultured them using the APC-SOP, with or without initial immune-magnetic microbeads sorting for CD31/CD34. In both cases, no cells emerged during a 1-month-long culture in the incubator, thus providing a definitive confirmation that the adopted SOP was selective for APC isolation. Altogether these data indicated that the expanded swine cell product is a bona fide equivalent of hAPCs.

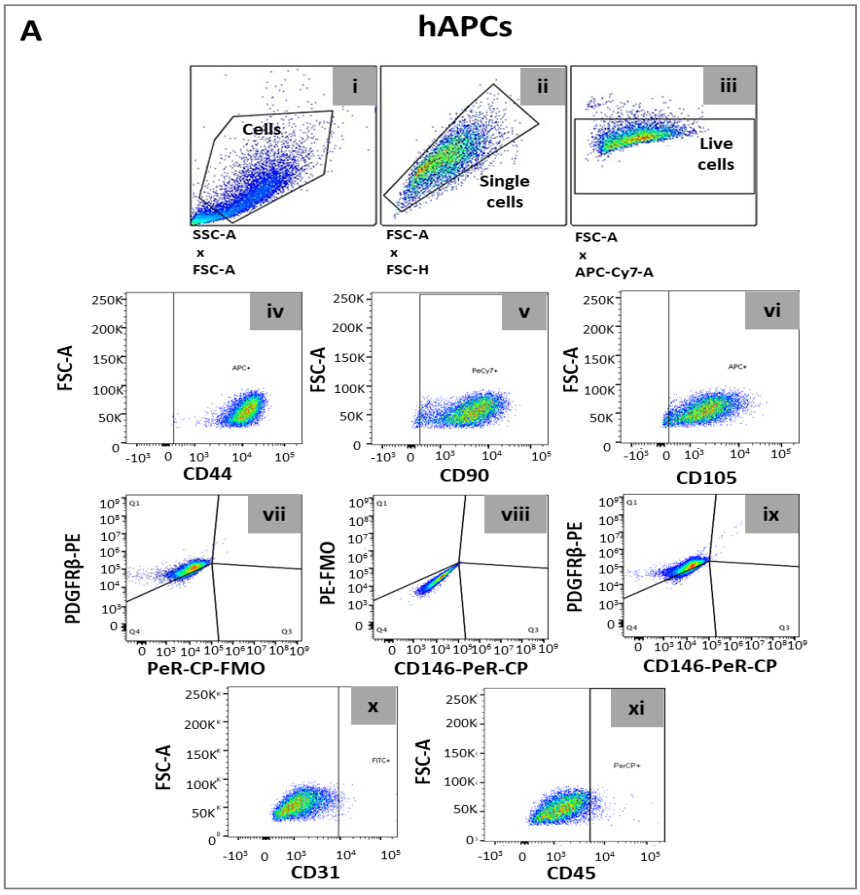

Figure 11-2 (continued).

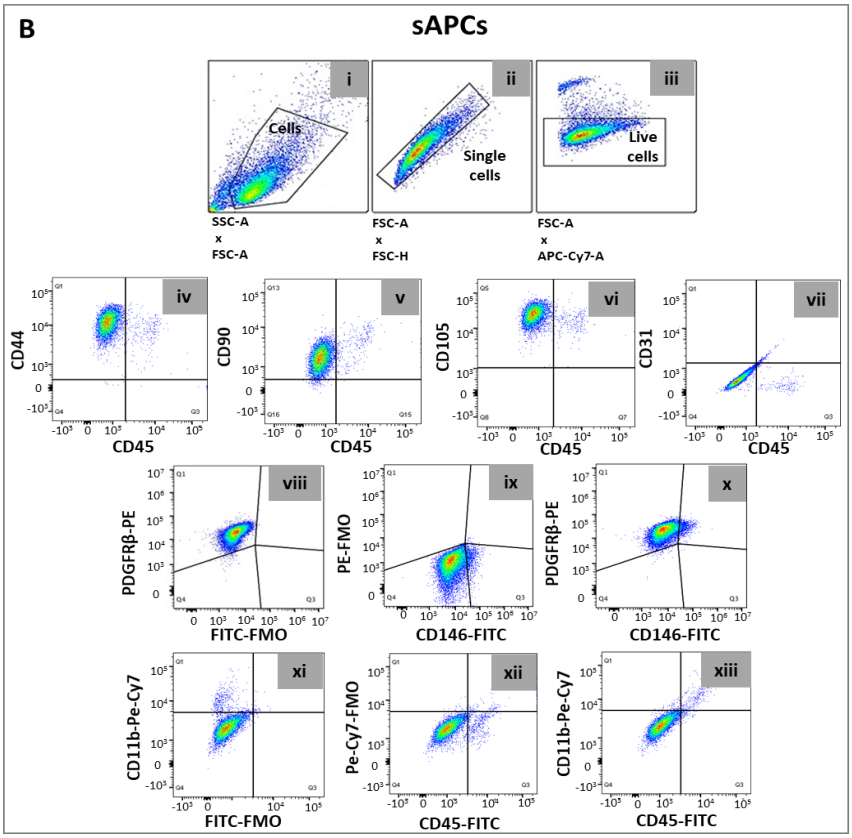

Figure 11-2 (continued).

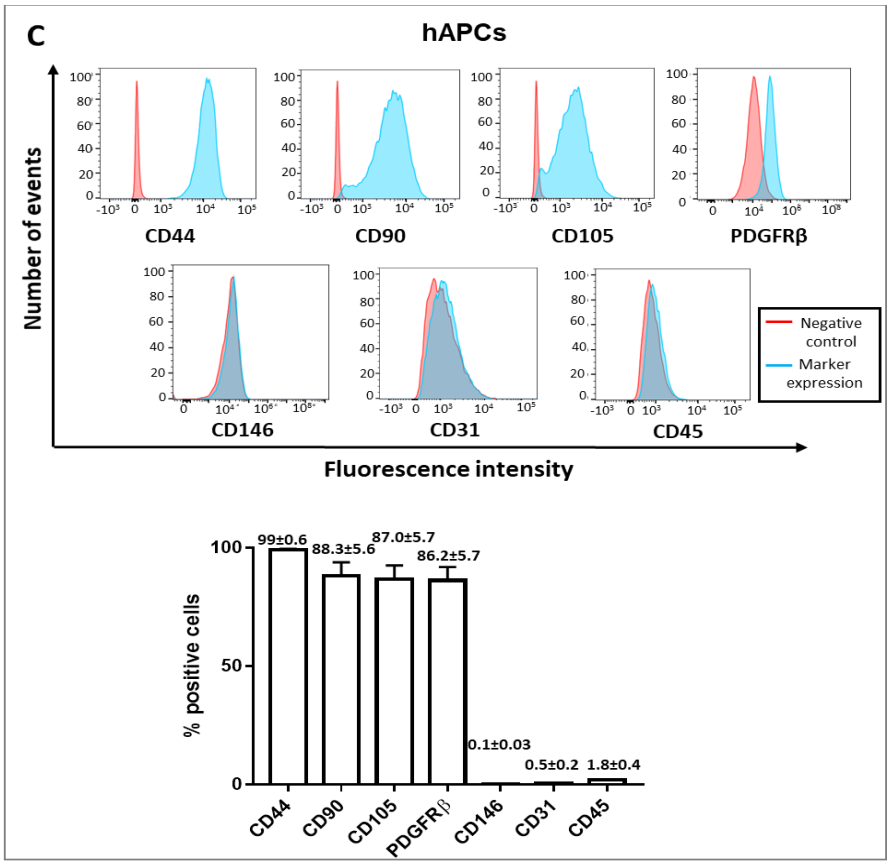

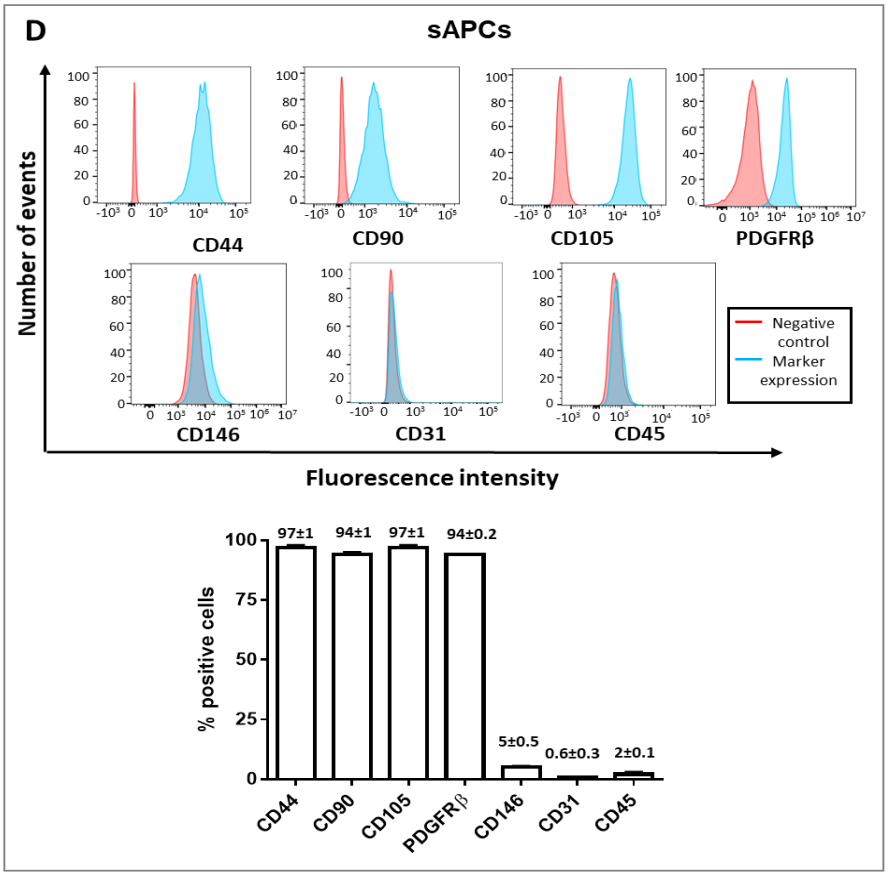

Figure 11-2 (continued).

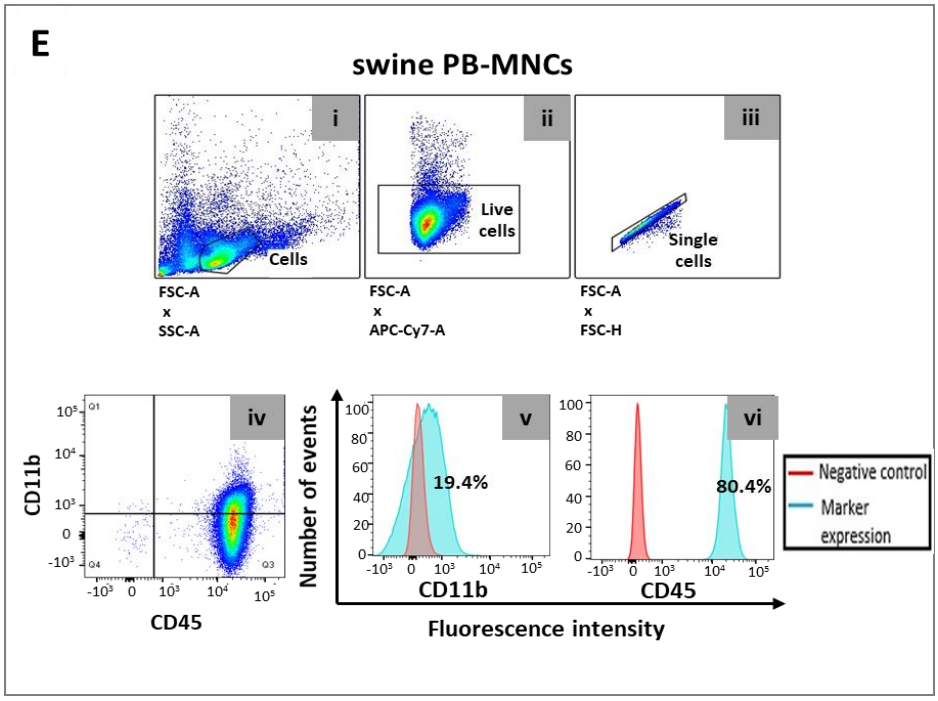

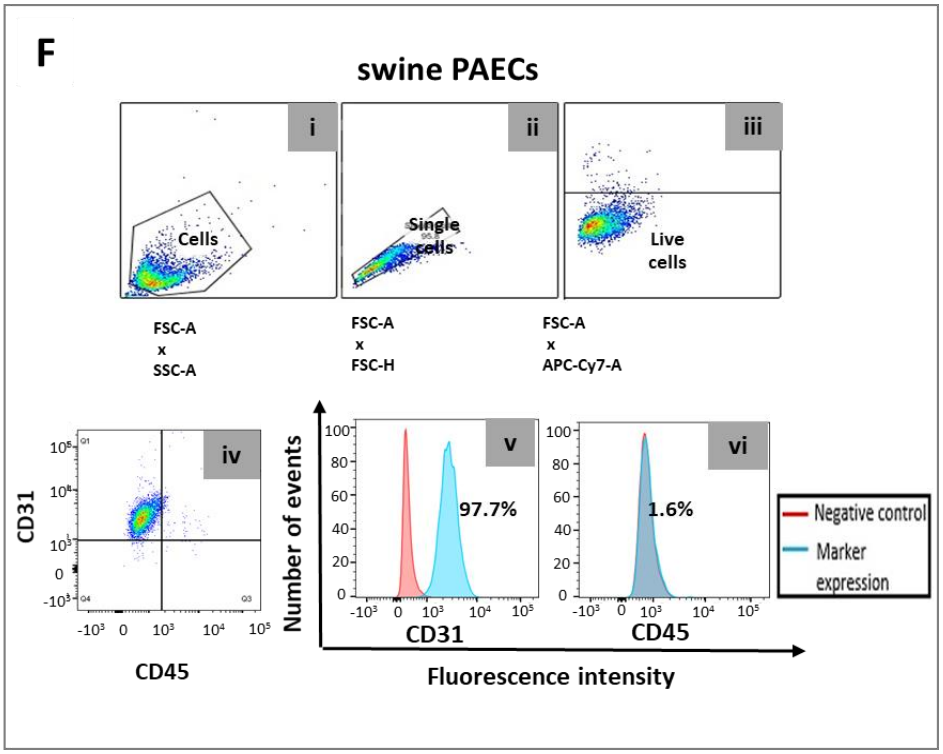

Figure 11-2. FACS analyses of APCs isolated from human and swine saphenous veins. A and B. Representative FACS gating procedure of hAPCs and sAPCs at P5. Total cell population and the single cells (singlets) were gated according to FSC-A vs. SSC-A and FSC-A vs. FSC-H parameters (i-ii). Viable cells were distinguished from dead cells using fixable viability dye eFluor780 (iii) and further gated for selected antigens (iv-xi and iv-xiii). Pericyte, mesenchymal, endothelial and hematopoietic markers were studied. The FMO control was used in the assessment and gating of CD146+ and PDGFRβ+ cells, owing to the use of multiple fluorochromes (vii-ix and viii-x). The same approach was used when studying the expression of CD45 and CD11b on sAPCs to exclude hematopoietic contamination in the cell culture system (xi-xiii). C and D. FACS histograms for each surface marker in representative hAPC (C) and sAPC lines (D) Negative control staining profiles are shown by the red histograms, whereas specific antibody staining profiles are shown by light blue histograms. Bar graphs shows the mean and SEM of n=3 human and swine APC lines. E and F. Gating and histograms of fresh isolated sPB-MNCs and sPAEC lines at P5 used as positive control for the staining of hematopoietic and endothelial markers, respectively. In both cell lines, the negative control staining profile is shown by fully red histograms, while the positive staining profile is shown by light blue histograms. *Abbreviations*: APCs= adventitial saphenous vein pericytes; APC =Allophycocyanin; APC-Cy7 =Allophycocyanin-7; CD= cluster of differentiation; FSC-A= Forward Scatter-Area; FSC-H= Forward Scatter-Height; FITC= Fluorescein isothiocyanate; FMO= fluorescence minus one; PAECs= pulmonary artery endothelial cells;

PDGFRβ= platelet-derived-growth factor beta; PE =Phycoerythrin; Pe-Cy7= Phycoerythrin-Cy7; SSC-A= Side Scatter-Area.

11.2 Clonogenic and differentiation capacity

11.2.1 Clonogenic assay of swine adventitial saphenous vein pericytes

Next, the similarity of functional grounds was confirmed. To investigate whether sAPCs could form clones, total cells from 2 biological replicates were sorted as single cell and cultured in 96-well plates. Two weeks later, 23% of cells from one sAPC line formed colonies (57 out of 240), while the other APC line gave rise to 27% of colonies (67 out of 240). Of these primary colonies, 9 and 14 could be further expanded in culture (data not shown).

11.2.2 Mesenchymal differentiation of swine adventitial saphenous vein pericytes

Next, 3 sAPC lines were exposed to differentiation stimuli for the derivation of mesenchymal lineages. All the cell lines showed the typical differentiation capacities, as denoted by the accumulation of fat droplets with Oil-Red-O staining solution in the adipogenesis assay and Alizarin Red and Alkaline Phosphatase staining in the osteogenesis assay (**Figure 11-3**). These results denote similarities with the reported clonogenic activity and *in vitro* differentiation properties of hAPCs.

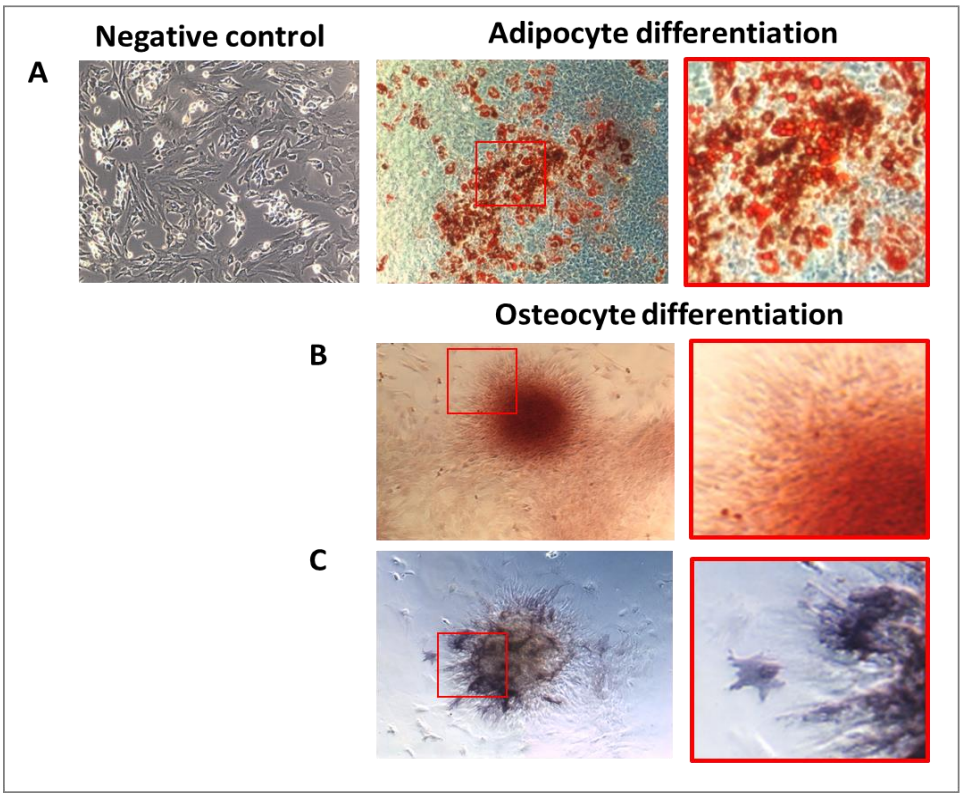

Figure 11-3. Osteogenic and adipogenic differentiation of sAPCs. Representative images showing the differentiation of one sAPC line towards mesodermal lineages. A. Lipid droplets were identified by Oil Red staining (red). B and C. Calcium deposits by Alizarin Red (red colour) and alkaline phosphatase (violet color) staining. Magnification x100, n=3 sAPC lines. Inserts show details of the positive staining. In A (upper-left panel), sAPCs maintained under normal culture medium are also shown (negative control).

11.3 Angiocrine properties

11.3.1 Angiocrine factors

Previous studies showed that hAPCs expressed and secreted a spectrum of angiogenic factors and microRNAs (Campagnolo et al. 2010; Katare et al. 2011; Avolio et al. 2015b). Following the exposure in normoxia and hypoxia environments, sAPCs expressed and secreted VEGF-A and the proangiogenic miR-132. By WB technique a 22 KDa MW and larger bands of VEGF-A protein were detected. The antibody detection of these bands suggested that either multiple molecules are bound together in a multimerized complex or that VEGF-A is bound to another molecule with the region bound by the antibody exposed/separated from the region bound the corresponding

molecule/receptor. Swine APCs also expressed the hypoxia-inducible factor miR-210, with levels being increased in response to hypoxia environment (**Figure 11-4**).

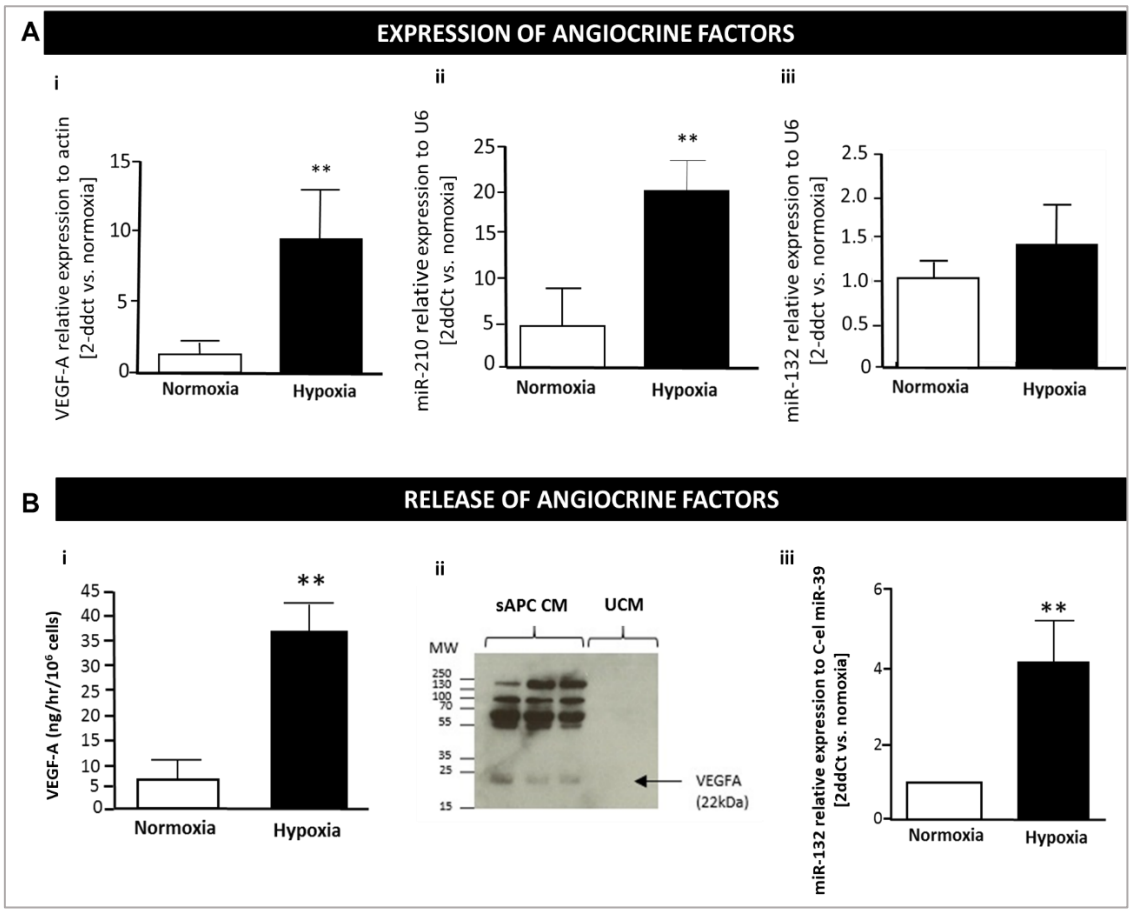

Figure 11-4. A-B. Bar graphs showing the expression of VEGF-A (i), miR-210 (ii) and miR-132 (iii) in sAPC lysate (n=4) and in sAPC-CM (n=3) under normoxia and hypoxia. WB image displays secreted VEGF-A with MW= 22 KDa and larger bands under normoxia condition (n=3) (ii). Values are mean±SEM; **p<0.01 vs normoxia. *Abbreviations*: APC-CM= adventitial saphenous vein pericyte-conditioned media; miR= microRNA; UCM=unconditioned media; VEGF-A= vascular endothelial growth factor-A.

11.3.2 Proangiogenic activity

One of important feature of hAPCs consisted of their ability to modulate the angiogenesis via direct contacts with, and transfer of paracrine GFs and mcroRNAs to ECs (Campagnolo et al. 2010; Katare et al. 2011; Caporali et al. 2017). Therefore, the ability of sAPCs to share similar properties by testing their capacity to promote endothelial cell network formation was investigated in a Matrigel – endothelial tube formation assay. Interestingly, preliminary

experiments showed that the sAPC-CM potentiated the network-forming capacity oh HUVECs, whereas the direct contact of sAPCs and HUVECs in co-culture inhibited the network formation (data not shown). This suggested that the physical interaction between co-cultured xenogeneic cells could override the proangiogenic activity of the sAPC secretome. To exclude any specie-specific incompatibility that may confound the interpretation of the results, commercial primary cells from swine, sPAECs, were used as an angiogenic target for sAPCs. In this setup, both sAPCs (**Figure 11-5A**) and their CM (**Figure 11-5B**) led to potentiation of the network-forming capacity of sPAECs. Moreover, the sAPC secretome exhibited a superior proangiogenic activity as compared with hAPC secretome (**Figure 11-5B**), with this difference being compatible with a higher specificity of the sAPC-derived paracrine factors for sPAECs.

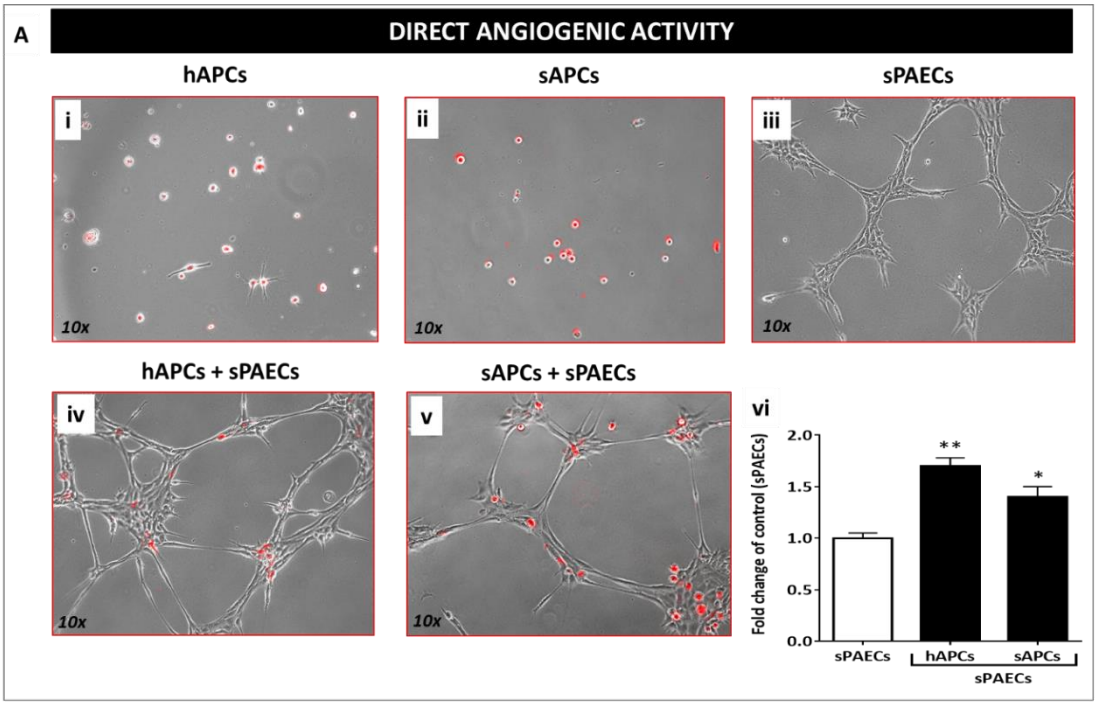

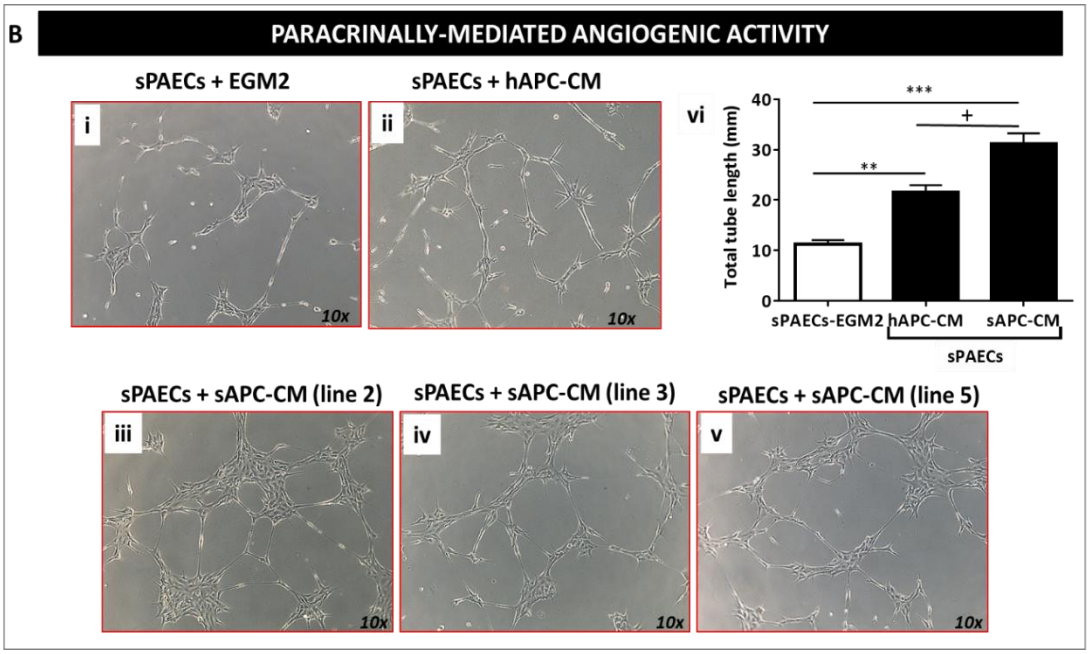

Figure 11-5. Endothelial tube formation assay (Matrigel). A. Representative phase-contrast and fluorescent images of hAPCs (Ai), sAPCs (Aii), and sPAECs (Aiii) alone or in combination (Aiv: hAPCs+sPAECs; Av: sAPCs+sPAECs at 1:4 ratio). APCs are stained with long cell tracker Dil (red fluorescence). (Avi) Graph bar showing the fold increase of cumulative tube length following the co-culture of APCs with sPAECs in two separate experiments, each including 3 APC lines per group. Data are represented as mean±SEM, **P<0.01 hAPCs and *P<0.05 sAPCs vs. sPAECs. B. Representative phase-contrast images of sPAEC networks formed in presence of EGM2 media (Bi) or human (Bii) or swine APC-CM on 3 cell lines (Biii-v). Magnification x100. (Bvi) Histograms summarise quantitative data of the tube length per field in an experiment including 3 APC lines per group. Data are represented as mean±SEM, **P<0.01 hAPC-CM and ***P<0.001 sAPC-CM vs. PAECs. +P<0.05 sAPC-CM vs. hAPC-CM. *Abbreviations*: CM= conditioned media; EGM2= endothelial cell growth media 2; hAPCs= human adventitial saphenous vein pericytes; sAPCs= swine adventitial saphenous vein pericytes.

11.4 Histological assessment of the cell therapy studies

11.4.1 Vascular density and fibrosis outcomes

The effects of sAPC therapy on microvascular, macrovascular and fibrosis outcomes were investigated. The injection of sAPCs increased the capillary density in the inferior segment of the peri-infarct zone (51%, **P=0.003 vs. vehicle) and the remote zone (34%, *P=0.04 vs. vehicle)

(**Figure 11-6A-B**). Arteriole density was not affected in any of the segment examined (**Figure 11-6C**).

Morphometric analysis of myocardial fibrosis in the infarct border zone indicates a beneficial effect of sAPC therapy (-26% reduction vs. vehicle, ***P<0.001) (**Figure 11-6D-E**).

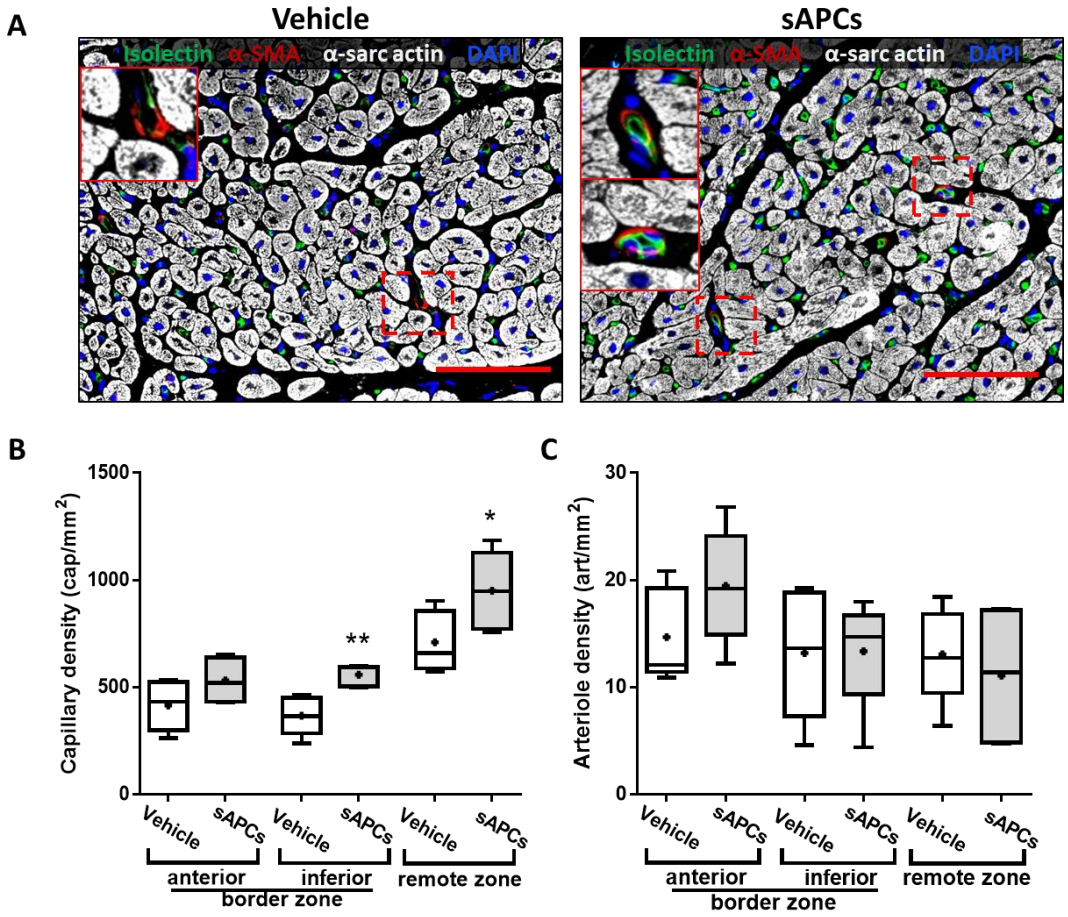

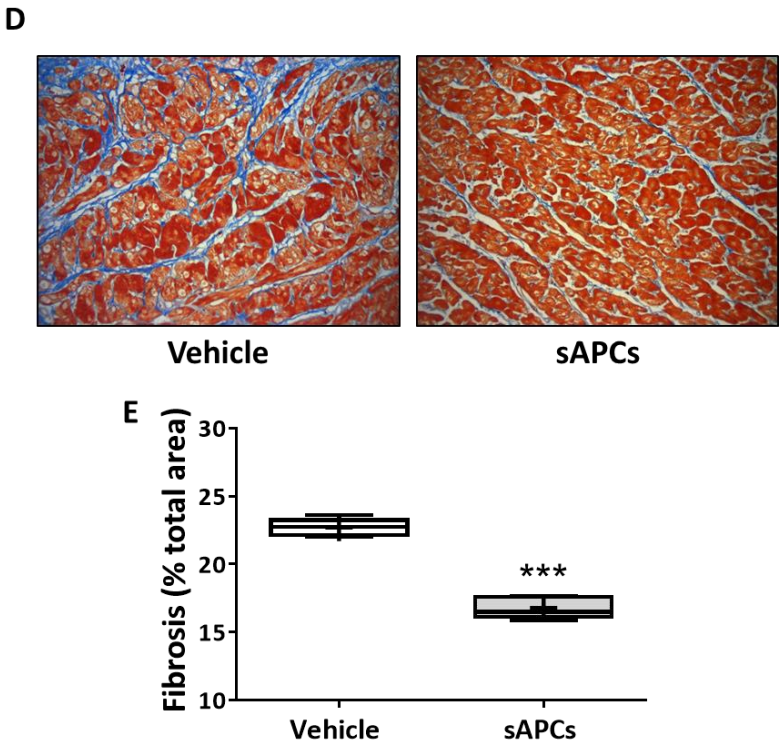

Figure 11-6. Benefit of sAPC therapy on micro/macrovascular density and fibrosis. A-C. Representative images (100x magnification; scale bar = 100 µm) (A) and bar graphs showing the effect of cell therapy with sAPCs on capillary (B) and arteriole density (C). Representative images refer to hearts injected with vehicle or sAPCs (donor swine cell line ID# 5). The inserts illustrate arterioles stained with α-SMA. Data are reported for two areas in the border zone and the remote zone. D. Illustrative microscopy images (total optical magnification x200) and (E) bar graph illustrating the quantification of the fibrotic myocardium in the infarct border zone of swine hearts injected with vehicle (n=5) or sAPCs (n=5) (donor swine cell line ID# 2, ***P<0.01 vs. vehicle). *Abbreviations*: sAPCs= swine adventitial saphenous vein pericytes; sarc-actin= sarcomeric actinin; SMA= smooth muscle actin.

11.4.2 Swine adventitial saphenous vein pericyte engraftment in the infarcted hearts

Immunohistochemistry of hearts collected from two additional swine indicates the presence of DiI-labelled swine cells in the infarct and peri-infarct border zone, with a few of them surrounding the isolectin-positive vascular profiles and others dispersed in the scar (**Figure 11-7A**). No signal from injected swine cells was detected in the remote zone (**Figure 11-7B**). As expected, controls hearts injected with vehicle did not show any staining for the labelling tracer

(**Figure 11-7C**). There was no evidence for the differentiation of injected cells into cardiomyocytes. The observed engraftment is in line with our previous study in mice, where DiI-labelled hAPCs were found located in the infarct and infarct border zone (Katare et al. 2011).

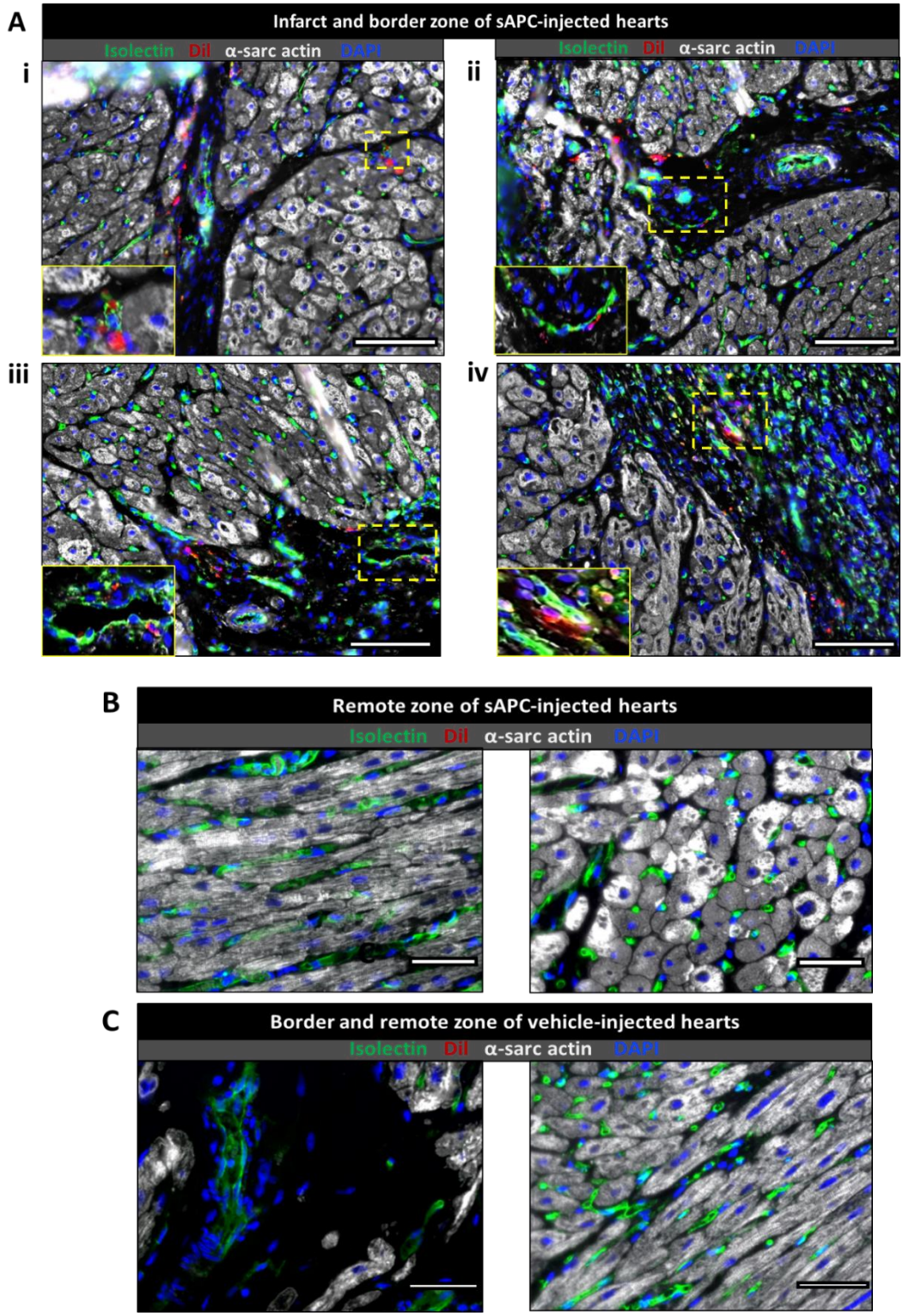

Figure 11-7. Engraftment of sAPCs in swine infarcted hearts. A. Representative immunofluorescence images showing engraftment of sAPCs in the infarct and nearby border zone (n=2). Four different areas of infarct and border zones of sAPC-injected heart (i-iv). Swine

APCs are recognized by the red fluorescence of the DiI cell tracker which stains cell membranes. In addition, anti-α-Sarc Actin (white) identifies cardiomyocytes. Anti-Isolectin B4 (green) has been used as a marker for ECs, while DAPI (blue) shows nuclei. Swine APCs can be appreciated at a higher magnification in the inserts placed on each image. B. Representative images showing absence of sAPCs to the remote zone. C. Images taken from a vehicle-injected heart as a negative control for the DiI staining. For all images, total optical magnification is x200. The scale bar in all images is 50µm. *Abbreviations*: sAPCs= swine adventitial saphenous vein pericytes; sarc-actin= sarcomeric actinin; SMA= smooth muscle actin.

12 Discussion

The sAPCs showed similar features with hAPCs as assessed by ICC, FACS, ELISA assay and cloning activity and functional studies (Matrigel assay). Swine cells represent an inestimable product thanks to the high request of using preclinical swine model as donor of cells prior transplantation. Human APCs express and release proangiogenic and antifibrotic factors, such as VEGF-A, leptin, and miR-132, and their secretion is increased following hypoxia environment (Campagnolo et al. 2010; Katare et al. 2011; Riu et al. 2017). In this study we have demonstrated by WB analysis that VEGF-A secreted in the sAPC-CM corresponded to the mature swine 22-KDa protein and that other VEGF-A bands were present. The antibody detection of these bands suggests that there are multiple molecules which are bound together in a multimerized complex. Also, VEGF-A may be bound to another molecule, such as secreted VEGF receptors, with the region bound by the antibody exposed/separate from the region bound by the corresponding molecule/receptor. Both possibilities are supported by previous evidences and the different isoforms of this huge molecule may have different effects in the heart that needs to be still determined. For instance, several isoforms could help to start a specific VEGF therapy which recognizes specific receptors in different cell types and exert their therapeutic activity (Herrera et al. 2009; Stachon et al. 2009). In this study, we have confirmed the presence of transplanted sAPCs by IHC after 10 days from the MI and after 5 days from the injection and the limitation of our study is that we are unable to track the persistence of the cells overtime. Moreover, in terms of efficacy and benefits, we have showed that allogeneic transplantation improved the microvascular angiogenesis and reduced the interstitial fibrosis and it was consistent with previous publications (Katare et al. 2011; Avolio et al. 2015b). The fact that the injected sAPCs have a role in the neovascularization and fibrosis has an important clinical meaning for the healing of an infarcted heart.

13 Conclusion

This appendix has demonstrated the possibility to generate swine APCs, which are surrogate of human counterpart, and to characterize them prior intramyocardial injection in a swine acute MI model. The equivalence with hAPCs was demonstrated. Feasibility and efficacy outcomes of the *in vivo* study were described to assess the proangiogenic and antifibrotic activities of the sAPCs after transplantation. These activities were confirmed by IHC assessment.

13.1 References

Al-Halees, Z., F. Pieters, F. Qadoura, M. Shahid, M. Al-Amri and F. Al-Fadley (2002). "The Ross procedure is the procedure of choice for congenital aortic valve disease." J Thorac Cardiovasc Surg **123**(3): 437-441; discussion 441-432 DOI: 10.1067/mtc.2002.119705.

Albertario, A., M. M. Swim, E. M. Ahmed, D. Iacobazzi, M. Yeong, P. Madeddu, M. T. Ghorbel and M. Caputo (2019). "Successful Reconstruction of the Right Ventricular Outflow Tract by Implantation of Thymus Stem Cell Engineered Graft in Growing Swine." JACC Basic Transl Sci **4**(3): 364-384 DOI: 10.1016/j.jacbts.2019.02.001.

Allen, B. S., C. El-Zein, B. Cuneo, J. P. Cava, M. J. Barth and M. N. Ilbawi (2002). "Pericardial tissue valves and Gore-Tex conduits as an alternative for right ventricular outflow tract replacement in children." Ann Thorac Surg **74**(3): 771-777 DOI: 10.1016/s0003-4975(02)03767-0.

Alvino, V. V., R. Fernandez-Jimenez, I. Rodriguez-Arabaolaza, S. Slater, G. Mangialardi, E. Avolio, H. Spencer, L. Culliford, S. Hassan, L. Sueiro Ballesteros, A. Herman, A. Ayaon-Albarran, C. Galan-Arriola, J. Sanchez-Gonzalez, H. Hennessey, C. Delmege, R. Ascione, C. Emanueli, G. D. Angelini, B. Ibanez and P. Madeddu (2018). "Transplantation of Allogeneic Pericytes Improves Myocardial Vascularization and Reduces Interstitial Fibrosis in a Swine Model of Reperfused Acute Myocardial Infarction." J Am Heart Assoc **7**(2) DOI: 10.1161/JAHA.117.006727.

Alvino, V. V., M. Kilcooley, A. C. Thomas, M. Carrabba, M. Fagnano, W. Cathery, E. Avolio, D. Iacobazzi, M. Ghorbel, M. Caputo and P. Madeddu (2020). "In Vitro and In Vivo Preclinical Testing of Pericyte-Engineered Grafts for the Correction of Congenital Heart Defects." J Am Heart Assoc **9**(4): e014214 DOI: 10.1161/JAHA.119.014214.

Ambastha, C., G. J. Bittle, D. Morales, N. Parchment, P. Saha, R. Mishra, S. Sharma, A. Vasilenko, M. Gunasekaran, M. T. Al-Suqi, D. Li, P. Yang and S. Kaushal (2018). "Regenerative medicine therapy for single ventricle congenital heart disease." Transl Pediatr **7**(2): 176-187 DOI: 10.21037/tp.2018.04.01.

Andersen, D. C., S. Ganesalingam, C. H. Jensen and S. P. Sheikh (2014). "Do neonatal mouse hearts regenerate following heart apex resection?" Stem Cell Reports **2**(4): 406-413 DOI: 10.1016/j.stemcr.2014.02.008.

Andersen, S., A. Andersen and J. E. Nielsen-Kudsk (2016). "The renin-angiotensin-aldosterone-system and right heart failure in congenital heart disease." Int J Cardiol Heart Vasc **11**: 59-65 DOI: 10.1016/j.ijcha.2016.03.013.

Anwar, S., G. K. Singh, J. Varughese, H. Nguyen, J. J. Billadello, E. F. Sheybani, P. K. Woodard, P. Manning and P. Eghtesady (2017). "3D Printing in Complex Congenital Heart Disease: Across a Spectrum of Age, Pathology, and Imaging Techniques." JACC Cardiovasc Imaging **10**(8): 953-956 DOI: 10.1016/j.jcmg.2016.03.013.

Armulik, A., A. Abramsson and C. Betsholtz (2005). "Endothelial/pericyte interactions." Circ Res **97**(6): 512-523 DOI: 10.1161/01.RES.0000182903.16652.d7.

Armulik, A., G. Genove and C. Betsholtz (2011). "Pericytes: developmental, physiological, and pathological perspectives, problems, and promises." Dev Cell **21**(2): 193-215 DOI: 10.1016/j.devcel.2011.07.001.

Avolio, E., V. V. Alvino, M. T. Ghorbel and P. Campagnolo (2017). "Perivascular cells and tissue engineering: Current applications and untapped potential." Pharmacol Ther **171**: 83-92 DOI: 10.1016/j.pharmthera.2016.11.002.

Avolio, E., M. Caputo and P. Madeddu (2015a). "Stem cell therapy and tissue engineering for correction of congenital heart disease." Front Cell Dev Biol **3**: 39 DOI: 10.3389/fcell.2015.00039.

Avolio, E. and P. Madeddu (2016). "Discovering cardiac pericyte biology: From physiopathological mechanisms to potential therapeutic applications in ischemic heart disease." Vascul Pharmacol **86**: 53-63 DOI: 10.1016/j.vph.2016.05.009.

Avolio, E., M. Meloni, H. L. Spencer, F. Riu, R. Katare, G. Mangialardi, A. Oikawa, I. Rodriguez-Arabaolaza, Z. Dang, K. Mitchell, C. Reni, V. V. Alvino, J. Rowlinson, U. Livi, D. Cesselli, G. Angelini, C. Emanueli, A. P. Beltrami and P. Madeddu (2015b). "Combined intramyocardial delivery of human pericytes and cardiac stem cells additively improves the healing of mouse infarcted hearts through stimulation of vascular and muscular repair." Circ Res **116**(10): e81-94 DOI: 10.1161/CIRCRESAHA.115.306146.

Avolio, E., I. Rodriguez-Arabaolaza, H. L. Spencer, F. Riu, G. Mangialardi, S. C. Slater, J. Rowlinson, V. V. Alvino, O. O. Idowu, S. Soyombo, A. Oikawa, M. M. Swim, C. H. Kong, H. Cheng, H. Jia, M. T. Ghorbel, J. C. Hancox, C. H. Orchard, G. Angelini, C. Emanueli, M. Caputo and P. Madeddu (2015c). "Expansion and characterization of neonatal cardiac pericytes provides a novel cellular option for tissue engineering in congenital heart disease." J Am Heart Assoc **4**(6): e002043 DOI: 10.1161/JAHA.115.002043.

Badylak, S. F., D. O. Freytes and T. W. Gilbert (2009). "Extracellular matrix as a biological scaffold material: Structure and function." Acta Biomater **5**(1): 1-13 DOI: 10.1016/j.actbio.2008.09.013.

Badylak, S. F., G. C. Lantz, A. Coffey and L. A. Geddes (1989). "Small intestinal submucosa as a large diameter vascular graft in the dog." J Surg Res **47**(1): 74-80 DOI: 10.1016/0022-4804(89)90050-4.

Bailey, M., Z. Christoforidou and M. C. Lewis (2013). "The evolutionary basis for differences between the immune systems of man, mouse, pig and ruminants." Vet Immunol Immunopathol **152**(1-2): 13-19 DOI: 10.1016/j.vetimm.2012.09.022.

Barron, D. J., M. D. Kilby, B. Davies, J. G. Wright, T. J. Jones and W. J. Brawn (2009). "Hypoplastic left heart syndrome." Lancet **374**(9689): 551-564 DOI: 10.1016/S0140-6736(09)60563-8.

Bergers, G. and S. Song (2005). "The role of pericytes in blood-vessel formation and maintenance." Neuro Oncol **7**(4): 452-464 DOI: 10.1215/S1152851705000232.

Bernstein, H. S. and D. Srivastava (2012). "Stem cell therapy for cardiac disease." Pediatr Res **71**(4 Pt 2): 491-499 DOI: 10.1038/pr.2011.61.

Bertipaglia, B., F. Ortolani, L. Petrelli, G. Gerosa, M. Spina, P. Pauletto, D. Casarotto, M. Marchini, S. Sartore and P. Vitalitate Exornatum Succedaneum Aorticum Labore Ingenioso Obtenibitur (2003). "Cell characterization of porcine aortic valve and decellularized leaflets repopulated with aortic valve interstitial cells: the VESALIO Project (Vitalitate Exornatum Succedaneum Aorticum Labore Ingenioso Obtenibitur)." Ann Thorac Surg **75**(4): 1274-1282 DOI: 10.1016/s0003-4975(02)04706-9.

Bhatt, A. B., E. Foster, K. Kuehl, J. Alpert, S. Brabeck, S. Crumb, W. R. Davidson, Jr., M. G. Earing, B. B. Ghoshhajra, T. Karamlou, S. Mital, J. Ting, Z. H. Tseng and C. American Heart Association Council on Clinical (2015). "Congenital heart disease in the older adult: a scientific statement

from the American Heart Association." Circulation **131**(21): 1884-1931 DOI: 10.1161/CIR.0000000000000204.

Birbrair, A., I. D. T. Borges, I. F. Gilson Sena, G. G. Almeida, L. da Silva Meirelles, R. Goncalves, A. Mintz and O. Delbono (2017). "How Plastic Are Pericytes?" Stem Cells Dev **26**(14): 1013-1019 DOI: 10.1089/scd.2017.0044.

Bittle, G. J., D. Morales, K. B. Deatrick, N. Parchment, P. Saha, R. Mishra, S. Sharma, N. Pietris, A. Vasilenko, C. Bor, C. Ambastha, M. Gunasekaran, D. Li and S. Kaushal (2018). "Stem Cell Therapy for Hypoplastic Left Heart Syndrome: Mechanism, Clinical Application, and Future Directions." Circ Res **123**(2): 288-300 DOI: 10.1161/CIRCRESAHA.117.311206.

Bouma, B. J. and B. J. Mulder (2017). "Changing Landscape of Congenital Heart Disease." Circ Res **120**(6): 908-922 DOI: 10.1161/CIRCRESAHA.116.309302.

Brennan, M. P., A. Dardik, N. Hibino, J. D. Roh, G. N. Nelson, X. Papademitris, T. Shinoka and C. K. Breuer (2008). "Tissue-engineered vascular grafts demonstrate evidence of growth and development when implanted in a juvenile animal model." Ann Surg **248**(3): 370-377 DOI: 10.1097/SLA.0b013e318184dcbd.

Bret-Zurita, M., E. Cuesta, A. Carton, J. Diez, A. Aroca, J. M. Oliver and F. Gutierrez-Larraya (2014). "Usefulness of 64-detector computed tomography in the diagnosis and management of patients with congenital heart disease." Rev Esp Cardiol (Engl Ed) **67**(11): 898-905 DOI: 10.1016/j.rec.2014.01.028.

Budts, W., J. Roos-Hesselink, T. Radle-Hurst, A. Eicken, T. A. McDonagh, E. Lambrinou, M. G. Crespo-Leiro, F. Walker and A. A. Frogoudaki (2016). "Treatment of heart failure in adult

congenital heart disease: a position paper of the Working Group of Grown-Up Congenital Heart Disease and the Heart Failure Association of the European Society of Cardiology." Eur Heart J **37**(18): 1419-1427 DOI: 10.1093/eurheartj/ehv741.

Butcher, J. T., G. J. Mahler and L. A. Hockaday (2011). "Aortic valve disease and treatment: the need for naturally engineered solutions." Adv Drug Deliv Rev **63**(4-5): 242-268 DOI: 10.1016/j.addr.2011.01.008.

Cabrera-Pérez, M. Á., M. B. Sanz, V. M. Sanjuan, M. González-Álvarez and I. G. Álvarez (2016). Importance and applications of cell- and tissue-based in vitro models for drug permeability screening in early stages of drug development. Concepts and Models for Drug Permeability Studies**:** 3-29.

Cai, C. L., J. C. Martin, Y. Sun, L. Cui, L. Wang, K. Ouyang, L. Yang, L. Bu, X. Liang, X. Zhang, W. B. Stallcup, C. P. Denton, A. McCulloch, J. Chen and S. M. Evans (2008). "A myocardial lineage derives from Tbx18 epicardial cells." Nature **454**(7200): 104-108 DOI: 10.1038/nature06969.

Camacho, P., H. Fan, Z. Liu and J. Q. He (2016). "Small mammalian animal models of heart disease." Am J Cardiovasc Dis **6**(3): 70-80.

Campagnolo, P., D. Cesselli, A. Al Haj Zen, A. P. Beltrami, N. Krankel, R. Katare, G. Angelini, C. Emanueli and P. Madeddu (2010). "Human adult vena saphena contains perivascular progenitor cells endowed with clonogenic and proangiogenic potential." Circulation **121**(15): 1735-1745 DOI: 10.1161/CIRCULATIONAHA.109.899252.

Caporali, A., A. Martello, V. Miscianinov, D. Maselli, R. Vono and G. Spinetti (2017). "Contribution of pericyte paracrine regulation of the endothelium to angiogenesis." Pharmacol Ther **171**: 56-64 DOI: 10.1016/j.pharmthera.2016.10.001.

Carrier, R. L., M. Papadaki, M. Rupnick, F. J. Schoen, N. Bursac, R. Langer, L. E. Freed and G. Vunjak-Novakovic (1999). "Cardiac tissue engineering: cell seeding, cultivation parameters, and tissue construct characterization." Biotechnol Bioeng **64**(5): 580-589 DOI: 10.1002/(sici)1097-0290(19990905)64:5<580::aid-bit8>3.0.co;2-x.

Cebotari, S., I. Tudorache, A. Ciubotaru, D. Boethig, S. Sarikouch, A. Goerler, A. Lichtenberg, E. Cheptanaru, S. Barnaciuc, A. Cazacu, O. Maliga, O. Repin, L. Maniuc, T. Breymann and A. Haverich (2011). "Use of fresh decellularized allografts for pulmonary valve replacement may reduce the reoperation rate in children and young adults: early report." Circulation **124**(11 Suppl): S115-123 DOI: 10.1161/CIRCULATIONAHA.110.012161.

Cebotari, S., I. Tudorache, T. Schilling and A. Haverich (2010). "[Heart valve and myocardial tissue engineering]." Herz **35**(5): 334-341 DOI: 10.1007/s00059-010-3355-x.

Chang, W. G., J. W. Andrejecsk, M. S. Kluger, W. M. Saltzman and J. S. Pober (2013). "Pericytes modulate endothelial sprouting." Cardiovasc Res **100**(3): 492-500 DOI: 10.1093/cvr/cvt215.

Cheema, F. H., G. Polvani, M. Argenziano and M. Pesce (2012). "Combining stem cells and tissue engineering in cardiovascular repair -- a step forward to derivation of novel implants with enhanced function and self-renewal characteristics." Recent Pat Cardiovasc Drug Discov **7**(1): 10-20 DOI: 10.2174/157489012799362403.

Chen, J. H. and C. A. Simmons (2011). "Cell-matrix interactions in the pathobiology of calcific aortic valve disease: critical roles for matricellular, matricrine, and matrix mechanics cues." Circ Res **108**(12): 1510-1524 DOI: 10.1161/CIRCRESAHA.110.234237.

Chen, W. C., J. E. Baily, M. Corselli, M. E. Diaz, B. Sun, G. Xiang, G. A. Gray, J. Huard and B. Peault (2015). "Human myocardial pericytes: multipotent mesodermal precursors exhibiting cardiac specificity." Stem Cells **33**(2): 557-573 DOI: 10.1002/stem.1868.

Chessa, M., H. Baumgartner, I. Michel-Behnke, F. Berger, W. Budts, A. Eicken, L. Sondergaard, J. Stein, M. Wiztsemburg and J. Thomson (2019). "ESC Working Group Position Paper: Transcatheter adult congenital heart disease interventions: organization of care - recommendations from a Joint Working Group of the European Society of Cardiology (ESC), European Association of Pediatric and Congenital Cardiology (AEPC), and the European Association of Percutaneous Cardiac Intervention (EAPCI)." Eur Heart J **40**(13): 1043-1048 DOI: 10.1093/eurheartj/ehy676.

Corselli, M., C. W. Chen, B. Sun, S. Yap, J. P. Rubin and B. Peault (2012). "The tunica adventitia of human arteries and veins as a source of mesenchymal stem cells." Stem Cells Dev **21**(8): 1299-1308 DOI: 10.1089/scd.2011.0200.

Covas, D. T., R. A. Panepucci, A. M. Fontes, W. A. Silva, Jr., M. D. Orellana, M. C. Freitas, L. Neder, A. R. Santos, L. C. Peres, M. C. Jamur and M. A. Zago (2008). "Multipotent mesenchymal stromal cells obtained from diverse human tissues share functional properties and gene-expression profile with CD146+ perivascular cells and fibroblasts." Exp Hematol **36**(5): 642-654 DOI: 10.1016/j.exphem.2007.12.015.

Crisan, M., M. Corselli, W. C. Chen and B. Peault (2012). "Perivascular cells for regenerative medicine." J Cell Mol Med **16**(12): 2851-2860 DOI: 10.1111/j.1582-4934.2012.01617.x.

Crisan, M., S. Yap, L. Casteilla, C. W. Chen, M. Corselli, T. S. Park, G. Andriolo, B. Sun, B. Zheng, L. Zhang, C. Norotte, P. N. Teng, J. Traas, R. Schugar, B. M. Deasy, S. Badylak, H. J. Buhring, J. P. Giacobino, L. Lazzari, J. Huard and B. Peault (2008). "A perivascular origin for mesenchymal stem cells in multiple human organs." Cell Stem Cell **3**(3): 301-313 DOI: 10.1016/j.stem.2008.07.003.

Dai, W., J. Dong, G. Chen and T. Uemura (2009). "Application of low-pressure cell seeding system in tissue engineering." Biosci Trends **3**(6): 216-219.

Dar, A., H. Domev, O. Ben-Yosef, M. Tzukerman, N. Zeevi-Levin, A. Novak, I. Germanguz, M. Amit and J. Itskovitz-Eldor (2012). "Multipotent vasculogenic pericytes from human pluripotent stem cells promote recovery of murine ischemic limb." Circulation **125**(1): 87-99 DOI: 10.1161/CIRCULATIONAHA.111.048264.

Darland, D. C., L. J. Massingham, S. R. Smith, E. Piek, M. Saint-Geniez and P. A. D'Amore (2003). "Pericyte production of cell-associated VEGF is differentiation-dependent and is associated with endothelial survival." Dev Biol **264**(1): 275-288 DOI: 10.1016/j.ydbio.2003.08.015.

Davies, B., N. J. Elwood, S. Li, F. Cullinane, G. A. Edwards, D. F. Newgreen and C. P. Brizard (2010). "Human cord blood stem cells enhance neonatal right ventricular function in an ovine model of right ventricular training." Ann Thorac Surg **89**(2): 585-593, 593 e581-584 DOI: 10.1016/j.athoracsur.2009.10.035.

Dayan, V., G. Yannarelli, P. Filomeno and A. Keating (2012). "Human mesenchymal stromal cells improve scar thickness without enhancing cardiac function in a chronic ischaemic heart failure model." Interact Cardiovasc Thorac Surg **14**(5): 516-520 DOI: 10.1093/icvts/ivs048.

De Backer, J., A. Bondue, W. Budts, A. Evangelista, P. Gallego, G. Jondeau, B. Loeys, M. L. Pena, G. Teixido-Tura, I. van de Laar, A. Verstraeten and J. Roos Hesselink (2019). "Genetic counselling and testing in adults with congenital heart disease: A consensus document of the ESC Working Group of Grown-Up Congenital Heart Disease, the ESC Working Group on Aorta and Peripheral Vascular Disease and the European Society of Human Genetics." Eur J Prev Cardiol: 2047487319854552 DOI: 10.1177/2047487319854552.

Dean, E. W., B. Udelsman and C. K. Breuer (2012). "Current advances in the translation of vascular tissue engineering to the treatment of pediatric congenital heart disease." Yale J Biol Med **85**(2): 229-238.

DeSimone, D. C., I. M. Tleyjeh, D. D. Correa de Sa, N. S. Anavekar, B. D. Lahr, M. R. Sohail, J. M. Steckelberg, W. R. Wilson and L. M. Baddour (2015). "Temporal trends in infective endocarditis epidemiology from 2007 to 2013 in Olmsted County, MN." Am Heart J **170**(4): 830-836 DOI: 10.1016/j.ahj.2015.07.007.

Di Filippo, S., F. Delahaye, B. Semiond, M. Celard, R. Henaine, J. Ninet, F. Sassolas and A. Bozio (2006). "Current patterns of infective endocarditis in congenital heart disease." Heart **92**(10): 1490-1495 DOI: 10.1136/hrt.2005.085332.

Dohmen, P. M., F. da Costa, S. Yoshi, S. V. Lopes, F. P. da Souza, R. Vilani, A. F. Wouk, M. da Costa and W. Konertz (2006). "Histological evaluation of tissue-engineered heart valves implanted in the juvenile sheep model: is there a need for in-vitro seeding?" J Heart Valve Dis **15**(6): 823-829.

Dohmen, P. M., A. Lembcke, S. Holinski, A. Pruss and W. Konertz (2011). "Ten years of clinical results with a tissue-engineered pulmonary valve." Ann Thorac Surg **92**(4): 1308-1314 DOI: 10.1016/j.athoracsur.2011.06.009.

Dohmen, P. M., A. Lembcke, H. Hotz, D. Kivelitz and W. F. Konertz (2002). "Ross operation with a tissue-engineered heart valve." Ann Thorac Surg **74**(5): 1438-1442 DOI: 10.1016/s0003-4975(02)03881-x.

Dottori, M., M. Familari, S. Hansson and K. Hasegawa (2012). "Stem cells as in vitro models of disease." Stem Cells Int **2012**: 565083 DOI: 10.1155/2012/565083.

Eckhauser, A. W., D. Hannon, M. Molitor, E. Scaife and P. J. Gruber (2013). "Repair of traumatic aortoinnominate disruption using CorMatrix." Ann Thorac Surg **95**(4): e99-e101 DOI: 10.1016/j.athoracsur.2012.09.060.

Epstein, S. E., D. Luger and M. J. Lipinski (2017). "Large Animal Model Efficacy Testing Is Needed Prior to Launch of a Stem Cell Clinical Trial: An Evidence-Lacking Conclusion Based on Conjecture." Circ Res **121**(5): 496-498 DOI: 10.1161/CIRCRESAHA.117.311562.

Erikssen, G., K. Liestol, E. Seem, S. Birkeland, K. J. Saatvedt, T. N. Hoel, G. Dohlen, H. Skulstad, J. L. Svennevig, E. Thaulow and H. L. Lindberg (2015). "Achievements in congenital heart defect surgery: a prospective, 40-year study of 7038 patients." Circulation **131**(4): 337-346; discussion 346 DOI: 10.1161/CIRCULATIONAHA.114.012033.

Fallahiarezoudar, E., M. Ahmadipourroudposht, A. Idris and N. Mohd Yusof (2015). "A review of: application of synthetic scaffold in tissue engineering heart valves." Mater Sci Eng C Mater Biol Appl **48**: 556-565 DOI: 10.1016/j.msec.2014.12.016.

Fallon, A., T. Goodchild, R. Wang and R. G. Matheny (2012). "Remodeling of extracellular matrix patch used for carotid artery repair." J Surg Res **175**(1): e25-34 DOI: 10.1016/j.jss.2011.11.001.

Ferland-McCollough, D., S. Slater, J. Richard, C. Reni and G. Mangialardi (2017). "Pericytes, an overlooked player in vascular pathobiology." Pharmacol Ther **171**: 30-42 DOI: 10.1016/j.pharmthera.2016.11.008.

Fuxe, J., S. Tabruyn, K. Colton, H. Zaid, A. Adams, P. Baluk, E. Lashnits, T. Morisada, T. Le, S. O'Brien, D. M. Epstein, G. Y. Koh and D. M. McDonald (2011). "Pericyte requirement for anti-leak action of angiopoietin-1 and vascular remodeling in sustained inflammation." Am J Pathol **178**(6): 2897-2909 DOI: 10.1016/j.ajpath.2011.02.008.

Geevarghese, A. and I. M. Herman (2014). "Pericyte-endothelial crosstalk: implications and opportunities for advanced cellular therapies." Transl Res **163**(4): 296-306 DOI: 10.1016/j.trsl.2014.01.011.

Geva, T., J. D. Martins and R. M. Wald (2014). "Atrial septal defects." Lancet **383**(9932): 1921-1932 DOI: 10.1016/S0140-6736(13)62145-5.

Ghorbel, M. T., H. Jia, M. M. Swim, D. Iacobazzi, A. Albertario, C. Zebele, D. Holopherne-Doran, A. Hollander, P. Madeddu and M. Caputo (2019). "Reconstruction of the pulmonary artery by a novel biodegradable conduit engineered with perinatal stem cell-derived vascular smooth muscle cells enables physiological vascular growth in a large animal model of congenital heart disease." Biomaterials **217**: 119284 DOI: 10.1016/j.biomaterials.2019.119284.

Gittenberger-de Groot, A. C., M. M. Bartelings, M. C. Deruiter and R. E. Poelmann (2005). "Basics of cardiac development for the understanding of congenital heart malformations." Pediatr Res **57**(2): 169-176 DOI: 10.1203/01.PDR.0000148710.69159.61.

Godbey, W. T., S. B. Hindy, M. E. Sherman and A. Atala (2004). "A novel use of centrifugal force for cell seeding into porous scaffolds." Biomaterials **25**(14): 2799-2805 DOI: 10.1016/j.biomaterials.2003.09.056.

Gubernator, M., S. C. Slater, H. L. Spencer, I. Spiteri, A. Sottoriva, F. Riu, J. Rowlinson, E. Avolio, R. Katare, G. Mangialardi, A. Oikawa, C. Reni, P. Campagnolo, G. Spinetti, A. Touloumis, S. Tavare, F. Prandi, M. Pesce, M. Hofner, V. Klemens, C. Emanueli, G. Angelini and P. Madeddu (2015). "Epigenetic profile of human adventitial progenitor cells correlates with therapeutic outcomes in a mouse model of limb ischemia." Arterioscler Thromb Vasc Biol **35**(3): 675-688 DOI: 10.1161/ATVBAHA.114.304989.

Harding, J., R. M. Roberts and O. Mirochnitchenko (2013). "Large animal models for stem cell therapy." Stem Cell Res Ther **4**(2): 23 DOI: 10.1186/scrt171.

He, W., A. Nieponice, L. Soletti, Y. Hong, B. Gharaibeh, M. Crisan, A. Usas, B. Peault, J. Huard, W. R. Wagner and D. A. Vorp (2010). "Pericyte-based human tissue engineered vascular grafts." Biomaterials **31**(32): 8235-8244 DOI: 10.1016/j.biomaterials.2010.07.034.

Hecker, L. and R. K. Birla (2007). "Engineering the heart piece by piece: state of the art in cardiac tissue engineering." Regen Med **2**(2): 125-144 DOI: 10.2217/17460751.2.2.125.

Henaine, R., F. Roubertie, M. Vergnat and J. Ninet (2012). "Valve replacement in children: a challenge for a whole life." Arch Cardiovasc Dis **105**(10): 517-528 DOI: 10.1016/j.acvd.2012.02.013.

Herrera, J. J., O. Nesic and P. A. Narayana (2009). "Reduced vascular endothelial growth factor expression in contusive spinal cord injury." J Neurotrauma **26**(7): 995-1003 DOI: 10.1089/neu.2008-0779
10.1089/neu.2008.0779.

Herskind, A. M., D. Almind Pedersen and K. Christensen (2013). "Increased prevalence of congenital heart defects in monozygotic and dizygotic twins." Circulation **128**(11): 1182-1188 DOI: 10.1161/CIRCULATIONAHA.113.002453.

Heydarkhan-Hagvall, S., M. Esguerra, G. Helenius, R. Soderberg, B. R. Johansson and B. Risberg (2006). "Production of extracellular matrix components in tissue-engineered blood vessels." Tissue Eng **12**(4): 831-842 DOI: 10.1089/ten.2006.12.831.

Hibino, N., E. McGillicuddy, G. Matsumura, Y. Ichihara, Y. Naito, C. Breuer and T. Shinoka (2010). "Late-term results of tissue-engineered vascular grafts in humans." J Thorac Cardiovasc Surg **139**(2): 431-436, 436 e431-432 DOI: 10.1016/j.jtcvs.2009.09.057.

Hoashi, T., G. Matsumiya, S. Miyagawa, H. Ichikawa, T. Ueno, M. Ono, A. Saito, T. Shimizu, T. Okano, N. Kawaguchi, N. Matsuura and Y. Sawa (2009). "Skeletal myoblast sheet transplantation improves the diastolic function of a pressure-overloaded right heart." J Thorac Cardiovasc Surg **138**(2): 460-467 DOI: 10.1016/j.jtcvs.2009.02.018.

Hsu, D. T., V. Zak, L. Mahony, L. A. Sleeper, A. M. Atz, J. C. Levine, P. C. Barker, C. Ravishankar, B. W. McCrindle, R. V. Williams, K. Altmann, N. S. Ghanayem, R. Margossian, W. K. Chung, W. L. Border, G. D. Pearson, M. P. Stylianou, S. Mital and I. Pediatric Heart Network (2010). "Enalapril in infants with single ventricle: results of a multicenter randomized trial." Circulation **122**(4): 333-340 DOI: 10.1161/CIRCULATIONAHA.109.927988.

Huang, R. L., E. Kobayashi, K. Liu and Q. Li (2016). "Bone Graft Prefabrication Following the In Vivo Bioreactor Principle." EBioMedicine **12**: 43-54 DOI: 10.1016/j.ebiom.2016.09.016.

Hussey, G. S., J. L. Dziki and S. F. Badylak (2018). "Extracellular matrix-based materials for regenerative medicine." Nature Reviews Materials **3**(7): 159-173 DOI: 10.1038/s41578-018-0023-x.

Iacobazzi, D., G. Mangialardi, M. Gubernator, M. Hofner, M. Wielscher, K. Vierlinger, C. Reni, A. Oikawa, G. Spinetti, R. Vono, E. Sangalli, M. Montagnani and P. Madeddu (2014). "Increased antioxidant defense mechanism in human adventitia-derived progenitor cells is associated with therapeutic benefit in ischemia." Antioxid Redox Signal **21**(11): 1591-1604 DOI: 10.1089/ars.2013.5404.

Ibrahim, A. G., K. Cheng and E. Marban (2014). "Exosomes as critical agents of cardiac regeneration triggered by cell therapy." Stem Cell Reports **2**(5): 606-619 DOI: 10.1016/j.stemcr.2014.04.006.

Iop, L., A. Bonetti, F. Naso, S. Rizzo, S. Cagnin, R. Bianco, C. Dal Lin, P. Martini, H. Poser, P. Franci, G. Lanfranchi, R. Busetto, M. Spina, C. Basso, M. Marchini, A. Gandaglia, F. Ortolani and G. Gerosa (2014). "Decellularized allogeneic heart valves demonstrate self-regeneration potential

after a long-term preclinical evaluation." PLoS One **9**(6): e99593 DOI: 10.1371/journal.pone.0099593.

Iop, L., T. Palmosi, E. Dal Sasso and G. Gerosa (2018). "Bioengineered tissue solutions for repair, correction and reconstruction in cardiovascular surgery." J Thorac Dis **10**(Suppl 20): S2390-S2411 DOI: 10.21037/jtd.2018.04.27.

Ishigami, S., S. Ohtsuki, S. Tarui, D. Ousaka, T. Eitoku, M. Kondo, M. Okuyama, J. Kobayashi, K. Baba, S. Arai, T. Kawabata, K. Yoshizumi, A. Tateishi, Y. Kuroko, T. Iwasaki, S. Sato, S. Kasahara, S. Sano and H. Oh (2015). "Intracoronary autologous cardiac progenitor cell transfer in patients with hypoplastic left heart syndrome: the TICAP prospective phase 1 controlled trial." Circ Res **116**(4): 653-664 DOI: 10.1161/CIRCRESAHA.116.304671.

Jone, P. N. and K. O. Schowengerdt, Jr. (2009). "Prenatal diagnosis of congenital heart disease." Pediatr Clin North Am **56**(3): 709-715, Table of Contents DOI: 10.1016/j.pcl.2009.04.002.

Jonsson, M. K., T. A. van Veen, J. Synnergren and B. Becker (2016). "Towards Creating the Perfect In Vitro Cell Model." Stem Cells Int **2016**: 3459730 DOI: 10.1155/2016/3459730.

Jover, E., M. Fagnano, G. Angelini and P. Madeddu (2018). "Cell Sources for Tissue Engineering Strategies to Treat Calcific Valve Disease." Front Cardiovasc Med **5**: 155 DOI: 10.3389/fcvm.2018.00155.

Kalfa, D. and E. Bacha (2013). "New technologies for surgery of the congenital cardiac defect." Rambam Maimonides Med J **4**(3): e0019 DOI: 10.5041/RMMJ.10119.

Katare, R., F. Riu, K. Mitchell, M. Gubernator, P. Campagnolo, Y. Cui, O. Fortunato, E. Avolio, D. Cesselli, A. P. Beltrami, G. Angelini, C. Emanueli and P. Madeddu (2011). "Transplantation of human pericyte progenitor cells improves the repair of infarcted heart through activation of an angiogenic program involving micro-RNA-132." Circ Res **109**(8): 894-906 DOI: 10.1161/CIRCRESAHA.111.251546.

Kaushal, S., B. Wehman, N. Pietris, C. Naughton, S. M. Bentzen, G. Bigham, R. Mishra, S. Sharma, L. Vricella, A. D. Everett, K. B. Deatrick, S. Huang, H. Mehta, W. A. Ravekes, N. Hibino, D. L. Difede, A. Khan and J. M. Hare (2017). "Study design and rationale for ELPIS: A phase I/IIb randomized pilot study of allogeneic human mesenchymal stem cell injection in patients with hypoplastic left heart syndrome." Am Heart J **192**: 48-56 DOI: 10.1016/j.ahj.2017.06.009.

Kenny, D. P. and Z. M. Hijazi (2017). "Current Status and Future Potential of Transcatheter Interventions in Congenital Heart Disease." Circ Res **120**(6): 1015-1026 DOI: 10.1161/CIRCRESAHA.116.309185.

Kilkenny, C., W. J. Browne, I. C. Cuthill, M. Emerson and D. G. Altman (2010). "Improving bioscience research reporting: the ARRIVE guidelines for reporting animal research." PLoS Biol **8**(6): e1000412 DOI: 10.1371/journal.pbio.1000412.

Kloesel, B., J. A. DiNardo and S. C. Body (2016). "Cardiac Embryology and Molecular Mechanisms of Congenital Heart Disease: A Primer for Anesthesiologists." Anesth Analg **123**(3): 551-569 DOI: 10.1213/ANE.0000000000001451.

Knowles, R. L., C. Bull, C. Wren and C. Dezateux (2012). "Mortality with congenital heart defects in England and Wales, 1959-2009: exploring technological change through period and birth cohort analysis." Arch Dis Child **97**(10): 861-865 DOI: 10.1136/archdischild-2012-301662.

Krause, K., C. Schneider, K. H. Kuck and K. Jaquet (2010). "Stem cell therapy in cardiovascular disorders." Cardiovasc Ther **28**(5): e101-110 DOI: 10.1111/j.1755-5922.2010.00208.x.

Lammers, S. R., P. H. Kao, H. J. Qi, K. Hunter, C. Lanning, J. Albietz, S. Hofmeister, R. Mecham, K. R. Stenmark and R. Shandas (2008). "Changes in the structure-function relationship of elastin and its impact on the proximal pulmonary arterial mechanics of hypertensive calves." Am J Physiol Heart Circ Physiol **295**(4): H1451-1459 DOI: 10.1152/ajpheart.00127.2008.

Lancaster, M. A. and M. Huch (2019). "Disease modelling in human organoids." Dis Model Mech **12**(7) DOI: 10.1242/dmm.039347.

Libby, P. (2015). "Murine "model" monotheism: an iconoclast at the altar of mouse." Circ Res **117**(11): 921-925 DOI: 10.1161/CIRCRESAHA.115.307523.

Liu, A. C., V. R. Joag and A. I. Gotlieb (2007). "The emerging role of valve interstitial cell phenotypes in regulating heart valve pathobiology." Am J Pathol **171**(5): 1407-1418 DOI: 10.2353/ajpath.2007.070251.

Liu, Y., B. Deng, Y. Zhao, S. Xie and R. Nie (2013). "Differentiated markers in undifferentiated cells: expression of smooth muscle contractile proteins in multipotent bone marrow mesenchymal stem cells." Dev Growth Differ **55**(5): 591-605 DOI: 10.1111/dgd.12052.

Long, C., H. Li, M. Tiburcy, C. Rodriguez-Caycedo, V. Kyrychenko, H. Zhou, Y. Zhang, Y. L. Min, J. M. Shelton, P. P. A. Mammen, N. Y. Liaw, W. H. Zimmermann, R. Bassel-Duby, J. W. Schneider and E. N. Olson (2018). "Correction of diverse muscular dystrophy mutations in human engineered heart muscle by single-site genome editing." Sci Adv **4**(1): eaap9004 DOI: 10.1126/sciadv.aap9004.

Mackie, A. S., G. R. Rempel, A. H. Kovacs, M. Kaufman, K. N. Rankin, A. Jelen, M. Yaskina, R. Sananes, E. Oechslin, D. Dragieva, S. Mustafa, E. Williams, M. Schuh, C. Manlhiot, S. J. Anthony, J. Magill-Evans, D. Nicholas and B. W. McCrindle (2018). "Transition Intervention for Adolescents With Congenital Heart Disease." J Am Coll Cardiol **71**(16): 1768-1777 DOI: 10.1016/j.jacc.2018.02.043.

Mahle, W. T., P. M. Kirshbom, K. R. Kanter and B. M. Kogon (2008). "Cardiac surgery in adults performed at children's hospitals: trends and outcomes." J Thorac Cardiovasc Surg **136**(2): 307-311 DOI: 10.1016/j.jtcvs.2008.04.020.

Mahler, G. J. and J. T. Butcher (2011). "Cardiac developmental toxicity." Birth Defects Res C Embryo Today **93**(4): 291-297 DOI: 10.1002/bdrc.20219.

Matsumura, G., N. Hibino, Y. Ikada, H. Kurosawa and T. Shin'oka (2003a). "Successful application of tissue engineered vascular autografts: clinical experience." Biomaterials **24**(13): 2303-2308 DOI: 10.1016/s0142-9612(03)00043-7.

Matsumura, G., S. Miyagawa-Tomita, T. Shin'oka, Y. Ikada and H. Kurosawa (2003b). "First evidence that bone marrow cells contribute to the construction of tissue-engineered vascular autografts in vivo." Circulation **108**(14): 1729-1734 DOI: 10.1161/01.CIR.0000092165.32213.61.

Mestas, J. and C. C. Hughes (2004). "Of mice and not men: differences between mouse and human immunology." J Immunol **172**(5): 2731-2738 DOI: 10.4049/jimmunol.172.5.2731.

Mitchell, S. C., S. B. Korones and H. W. Berendes (1971). "Congenital heart disease in 56,109 births. Incidence and natural history." Circulation **43**(3): 323-332 DOI: 10.1161/01.cir.43.3.323.

Miyamoto, S. D., B. L. Stauffer, S. Nakano, R. Sobus, K. Nunley, P. Nelson and C. C. Sucharov (2014). "Beta-adrenergic adaptation in paediatric idiopathic dilated cardiomyopathy." Eur Heart J **35**(1): 33-41 DOI: 10.1093/eurheartj/ehs229.

Moorman, A., S. Webb, N. A. Brown, W. Lamers and R. H. Anderson (2003). "Development of the heart: (1) formation of the cardiac chambers and arterial trunks." Heart **89**(7): 806-814 DOI: 10.1136/heart.89.7.806.

Morris, C. D., M. D. Reller and V. D. Menashe (1998). "Thirty-year incidence of infective endocarditis after surgery for congenital heart defect." JAMA **279**(8): 599-603 DOI: 10.1001/jama.279.8.599.

Mosala Nezhad, Z., A. Poncelet, L. de Kerchove, C. Fervaille, X. Banse, X. Bollen, J. P. Dehoux, G. El Khoury and P. Gianello (2017). "CorMatrix valved conduit in a porcine model: long-term remodelling and biomechanical characterization." Interact Cardiovasc Thorac Surg **24**(1): 90-98 DOI: 10.1093/icvts/ivw314.

Naito, Y., Y. Imai, T. Shin'oka, J. Kashiwagi, M. Aoki, M. Watanabe, G. Matsumura, Y. Kosaka, T. Konuma, N. Hibino, A. Murata, T. Miyake and H. Kurosawa (2003). "Successful clinical application of tissue-engineered graft for extracardiac Fontan operation." J Thorac Cardiovasc Surg **125**(2): 419-420 DOI: 10.1067/mtc.2003.134.

Nees, S., D. R. Weiss, A. Senftl, M. Knott, S. Forch, M. Schnurr, P. Weyrich and G. Juchem (2012). "Isolation, bulk cultivation, and characterization of coronary microvascular pericytes: the second most frequent myocardial cell type in vitro." Am J Physiol Heart Circ Physiol **302**(1): H69-84 DOI: 10.1152/ajpheart.00359.2011.

Nelson, J. S., A. Heider, M. S. Si and R. G. Ohye (2016). "Evaluation of Explanted CorMatrix Intracardiac Patches in Children With Congenital Heart Disease." Ann Thorac Surg **102**(4): 1329-1335 DOI: 10.1016/j.athoracsur.2016.03.086.

Neumann, A., S. Cebotari, I. Tudorache, A. Haverich and S. Sarikouch (2013). "Heart valve engineering: decellularized allograft matrices in clinical practice." Biomed Tech (Berl) **58**(5): 453-456 DOI: 10.1515/bmt-2012-0115.

Niiyama, H., N. F. Huang, M. D. Rollins and J. P. Cooke (2009). "Murine model of hindlimb ischemia." J Vis Exp(23) DOI: 10.3791/1035.

Niwa, K., M. Nakazawa, S. Tateno, M. Yoshinaga and M. Terai (2005). "Infective endocarditis in congenital heart disease: Japanese national collaboration study." Heart **91**(6): 795-800 DOI: 10.1136/hrt.2004.043323.

Norozi, K., A. Wessel, V. Alpers, J. O. Arnhold, S. Geyer, M. Zoege and R. Buchhorn (2006). "Incidence and risk distribution of heart failure in adolescents and adults with congenital heart disease after cardiac surgery." Am J Cardiol **97**(8): 1238-1243 DOI: 10.1016/j.amjcard.2005.10.065.

Nugraha, B., M. F. Buono, L. von Boehmer, S. P. Hoerstrup and M. Y. Emmert (2019). "Human Cardiac Organoids for Disease Modeling." Clin Pharmacol Ther **105**(1): 79-85 DOI: 10.1002/cpt.1286.

Ossa Galvis, M. M. and M. D. Mendez (2019). Cyanotic Heart Disease. StatPearls. Treasure Island (FL).

Oyen, N., G. Poulsen, H. A. Boyd, J. Wohlfahrt, P. K. Jensen and M. Melbye (2009). "Recurrence of congenital heart defects in families." Circulation **120**(4): 295-301 DOI: 10.1161/CIRCULATIONAHA.109.857987.

Padalino, M. A., C. Castellani, A. Dedja, M. Fedrigo, V. L. Vida, G. Thiene, G. Stellin and A. Angelini (2012). "Extracellular matrix graft for vascular reconstructive surgery: evidence of autologous regeneration of the neoaorta in a murine model." Eur J Cardiothorac Surg **42**(5): e128-135 DOI: 10.1093/ejcts/ezs462.

Padalino, M. A., A. Quarti, E. Angeli, A. C. Frigo, V. L. Vida, M. Pozzi, G. Gargiulo and G. Stellin (2015). "Early and mid-term clinical experience with extracellular matrix scaffold for congenital cardiac and vascular reconstructive surgery: a multicentric Italian study." Interact Cardiovasc Thorac Surg **21**(1): 40-49; discussion 49 DOI: 10.1093/icvts/ivv076.

Padgett, M. E., T. J. McCord, J. M. McClung and C. D. Kontos (2016). "Methods for Acute and Subacute Murine Hindlimb Ischemia." J Vis Exp(112) DOI: 10.3791/54166.

Pavcnik, D., J. Obermiller, B. T. Uchida, W. Van Alstine, J. M. Edwards, G. J. Landry, J. A. Kaufman, F. S. Keller and J. Rosch (2009). "Angiographic evaluation of carotid artery grafting with prefabricated small-diameter, small-intestinal submucosa grafts in sheep." Cardiovasc Intervent Radiol **32**(1): 106-113 DOI: 10.1007/s00270-008-9449-7.

Perloff, J. K. and C. A. Warnes (2001). "Challenges posed by adults with repaired congenital heart disease." Circulation **103**(21): 2637-2643 DOI: 10.1161/01.cir.103.21.2637.

Pibarot, P. and J. G. Dumesnil (2009). "Prosthetic heart valves: selection of the optimal prosthesis and long-term management." Circulation **119**(7): 1034-1048 DOI: 10.1161/CIRCULATIONAHA.108.778886.

Piterina, A. V., A. J. Cloonan, C. L. Meaney, L. M. Davis, A. Callanan, M. T. Walsh and T. M. McGloughlin (2009). "ECM-based materials in cardiovascular applications: Inherent healing potential and augmentation of native regenerative processes." Int J Mol Sci **10**(10): 4375-4417 DOI: 10.3390/ijms10104375.

Pok, S. and J. G. Jacot (2011). "Biomaterials advances in patches for congenital heart defect repair." J Cardiovasc Transl Res **4**(5): 646-654 DOI: 10.1007/s12265-011-9289-8.

Porrello, E. R., A. I. Mahmoud, E. Simpson, B. A. Johnson, D. Grinsfelder, D. Canseco, P. P. Mammen, B. A. Rothermel, E. N. Olson and H. A. Sadek (2013). "Regulation of neonatal and adult mammalian heart regeneration by the miR-15 family." Proc Natl Acad Sci U S A **110**(1): 187-192 DOI: 10.1073/pnas.1208863110.

Proudfoot, K. and G. Habing (2015). "Social stress as a cause of diseases in farm animals: Current knowledge and future directions." Vet J **206**(1): 15-21 DOI: 10.1016/j.tvjl.2015.05.024.

Quarti, A., S. Nardone, M. Colaneri, G. Santoro and M. Pozzi (2011). "Preliminary experience in the use of an extracellular matrix to repair congenital heart diseases." Interact Cardiovasc Thorac Surg **13**(6): 569-572 DOI: 10.1510/icvts.2011.280016.

Rao, P. S. (2019). "Management of Congenital Heart Disease: State of the Art; Part I-ACYANOTIC Heart Defects." Children (Basel) **6**(3) DOI: 10.3390/children6030042.

Rieder, E., M. T. Kasimir, G. Silberhumer, G. Seebacher, E. Wolner, P. Simon and G. Weigel (2004). "Decellularization protocols of porcine heart valves differ importantly in efficiency of cell removal and susceptibility of the matrix to recellularization with human vascular cells." J Thorac Cardiovasc Surg **127**(2): 399-405 DOI: 10.1016/j.jtcvs.2003.06.017.

Riu, F., S. C. Slater, E. J. Garcia, I. Rodriguez-Arabaolaza, V. Alvino, E. Avolio, G. Mangialardi, A. Cordaro, S. Satchell, C. Zebele, A. Caporali, G. Angelini and P. Madeddu (2017). "The adipokine leptin modulates adventitial pericyte functions by autocrine and paracrine signalling." Sci Rep **7**(1): 5443 DOI: 10.1038/s41598-017-05868-y.

Roh, J. D., R. Sawh-Martinez, M. P. Brennan, S. M. Jay, L. Devine, D. A. Rao, T. Yi, T. L. Mirensky, A. Nalbandian, B. Udelsman, N. Hibino, T. Shinoka, W. M. Saltzman, E. Snyder, T. R. Kyriakides, J. S. Pober and C. K. Breuer (2010). "Tissue-engineered vascular grafts transform into mature blood vessels via an inflammation-mediated process of vascular remodeling." Proc Natl Acad Sci U S A **107**(10): 4669-4674 DOI: 10.1073/pnas.0911465107.

Rosario-Quinones, F., M. S. Magid, J. Yau, A. Pawale and K. Nguyen (2015). "Tissue reaction to porcine intestinal Submucosa (CorMatrix) implants in pediatric cardiac patients: a single-center experience." Ann Thorac Surg **99**(4): 1373-1377 DOI: 10.1016/j.athoracsur.2014.11.064.

Ruzmetov, M., J. J. Shah, D. M. Geiss and R. S. Fortuna (2012). "Decellularized versus standard cryopreserved valve allografts for right ventricular outflow tract reconstruction: a single-institution comparison." J Thorac Cardiovasc Surg **143**(3): 543-549 DOI: 10.1016/j.jtcvs.2011.12.032.

Saha, P., P. Potiny, J. Rigdon, M. Morello, C. Tcheandjieu, A. Romfh, S. M. Fernandes, D. B. McElhinney, D. Bernstein, G. K. Lui, G. M. Shaw, E. Ingelsson and J. R. Priest (2019). "Substantial

Cardiovascular Morbidity in Adults With Lower-Complexity Congenital Heart Disease." Circulation **139**(16): 1889-1899 DOI: 10.1161/CIRCULATIONAHA.118.037064.

Said, S. M. and H. M. Burkhart (2014). "When repair is not feasible: prosthesis selection in children and adults with congenital heart disease." Semin Thorac Cardiovasc Surg Pediatr Card Surg Annu **17**(1): 22-29 DOI: 10.1053/j.pcsu.2014.01.002.

Sasai, Y. (2013a). "Cytosystems dynamics in self-organization of tissue architecture." Nature **493**(7432): 318-326 DOI: 10.1038/nature11859.

Sasai, Y. (2013b). "Next-generation regenerative medicine: organogenesis from stem cells in 3D culture." Cell Stem Cell **12**(5): 520-530 DOI: 10.1016/j.stem.2013.04.009.

Schmidt, D., U. A. Stock and S. P. Hoerstrup (2007). "Tissue engineering of heart valves using decellularized xenogeneic or polymeric starter matrices." Philos Trans R Soc Lond B Biol Sci **362**(1484): 1505-1512 DOI: 10.1098/rstb.2007.2131.

Schoen, F. J. (2008). "Evolving concepts of cardiac valve dynamics: the continuum of development, functional structure, pathobiology, and tissue engineering." Circulation **118**(18): 1864-1880 DOI: 10.1161/CIRCULATIONAHA.108.805911.

Scholl, F. G., M. M. Boucek, K. C. Chan, L. Valdes-Cruz and R. Perryman (2010). "Preliminary experience with cardiac reconstruction using decellularized porcine extracellular matrix scaffold: human applications in congenital heart disease." World J Pediatr Congenit Heart Surg **1**(1): 132-136 DOI: 10.1177/2150135110362092.

Shepro, D. and N. M. Morel (1993). "Pericyte physiology." FASEB J **7**(11): 1031-1038 DOI: 10.1096/fasebj.7.11.8370472.

Shin'oka, T., Y. Imai and Y. Ikada (2001). "Transplantation of a tissue-engineered pulmonary artery." N Engl J Med **344**(7): 532-533 DOI: 10.1056/NEJM200102153440717.

Shin'oka, T., G. Matsumura, N. Hibino, Y. Naito, M. Watanabe, T. Konuma, T. Sakamoto, M. Nagatsu and H. Kurosawa (2005). "Midterm clinical result of tissue-engineered vascular autografts seeded with autologous bone marrow cells." J Thorac Cardiovasc Surg **129**(6): 1330-1338 DOI: 10.1016/j.jtcvs.2004.12.047.

Simon, P., C. Aschauer, R. Moidl, M. Marx, F. P. Keznickl, E. Eigenbauer, E. Wolner and G. Wollenek (2001). "Growth of the pulmonary autograft after the Ross operation in childhood." Eur J Cardiothorac Surg **19**(2): 118-121 DOI: 10.1016/s1010-7940(00)00638-2.

Smit, F. E. and P. M. Dohmen (2015). "Cardiovascular tissue engineering: where we come from and where are we now?" Med Sci Monit Basic Res **21**: 1-3 DOI: 10.12659/MSMBR.893546.

Stachon, A., A. Aweimer, T. Stachon, A. Tannapfel, S. Thoms, B. Ubrig, M. Koller, M. Krieg and M. C. Truss (2009). "Secretion of soluble VEGF receptor 2 by microvascular endothelial cells derived by human benign prostatic hyperplasia." Growth Factors **27**(2): 71-78 DOI: 10.1080/08977190802709619.

Stephenson, M. and W. Grayson (2018). "Recent advances in bioreactors for cell-based therapies." F1000Res **7** DOI: 10.12688/f1000research.12533.1.

Stout, K. K., C. J. Daniels, J. A. Aboulhosn, B. Bozkurt, C. S. Broberg, J. M. Colman, S. R. Crumb, J. A. Dearani, S. Fuller, M. Gurvitz, P. Khairy, M. J. Landzberg, A. Saidi, A. M. Valente and G. F. Van Hare (2019). "2018 AHA/ACC Guideline for the Management of Adults With Congenital Heart Disease: A Report of the American College of Cardiology/American Heart Association Task Force on Clinical Practice Guidelines." J Am Coll Cardiol **73**(12): e81-e192 DOI: 10.1016/j.jacc.2018.08.1029.

Stratman, A. N., A. E. Schwindt, K. M. Malotte and G. E. Davis (2010). "Endothelial-derived PDGF-BB and HB-EGF coordinately regulate pericyte recruitment during vasculogenic tube assembly and stabilization." Blood **116**(22): 4720-4730 DOI: 10.1182/blood-2010-05-286872.

Sun, R., M. Liu, L. Lu, Y. Zheng and P. Zhang (2015). "Congenital Heart Disease: Causes, Diagnosis, Symptoms, and Treatments." Cell Biochem Biophys **72**(3): 857-860 DOI: 10.1007/s12013-015-0551-6.

Sutherland, F. W., T. E. Perry, Y. Yu, M. C. Sherwood, E. Rabkin, Y. Masuda, G. A. Garcia, D. L. McLellan, G. C. Engelmayr, Jr., M. S. Sacks, F. J. Schoen and J. E. Mayer, Jr. (2005). "From stem cells to viable autologous semilunar heart valve." Circulation **111**(21): 2783-2791 DOI: 10.1161/CIRCULATIONAHA.104.498378.

Swartz, D. D. and S. T. Andreadis (2013). "Animal models for vascular tissue-engineering." Curr Opin Biotechnol **24**(5): 916-925 DOI: 10.1016/j.copbio.2013.05.005.

Tattersall, I. W., J. Du, Z. Cong, B. S. Cho, A. M. Klein, C. L. Dieck, R. A. Chaudhri, H. Cuervo, J. H. Herts and J. Kitajewski (2016). "In vitro modeling of endothelial interaction with macrophages and pericytes demonstrates Notch signaling function in the vascular microenvironment." Angiogenesis **19**(2): 201-215 DOI: 10.1007/s10456-016-9501-1.

Tchervenkov, C. I., J. P. Jacobs, P. M. Weinberg, V. D. Aiello, M. J. Beland, S. D. Colan, M. J. Elliott, R. C. Franklin, J. W. Gaynor, O. N. Krogmann, H. Kurosawa, B. Maruszewski and G. Stellin (2006). "The nomenclature, definition and classification of hypoplastic left heart syndrome." Cardiol Young **16**(4): 339-368 DOI: 10.1017/S1047951106000291.

Teichert, M., L. Milde, A. Holm, L. Stanicek, N. Gengenbacher, S. Savant, T. Ruckdeschel, Z. Hasanov, K. Srivastava, J. Hu, S. Hertel, A. Bartol, K. Schlereth and H. G. Augustin (2017). "Pericyte-expressed Tie2 controls angiogenesis and vessel maturation." Nat Commun **8**: 16106 DOI: 10.1038/ncomms16106.

Tillet, E., D. Vittet, O. Feraud, R. Moore, R. Kemler and P. Huber (2005). "N-cadherin deficiency impairs pericyte recruitment, and not endothelial differentiation or sprouting, in embryonic stem cell-derived angiogenesis." Exp Cell Res **310**(2): 392-400 DOI: 10.1016/j.yexcr.2005.08.021.

Tleyjeh, I. M., J. M. Steckelberg, H. S. Murad, N. S. Anavekar, H. M. Ghomrawi, Z. Mirzoyev, S. E. Moustafa, T. L. Hoskin, J. N. Mandrekar, W. R. Wilson and L. M. Baddour (2005). "Temporal trends in infective endocarditis: a population-based study in Olmsted County, Minnesota." JAMA **293**(24): 3022-3028 DOI: 10.1001/jama.293.24.3022.

Triedman, J. K. and J. W. Newburger (2016). "Trends in Congenital Heart Disease: The Next Decade." Circulation **133**(25): 2716-2733 DOI: 10.1161/CIRCULATIONAHA.116.023544.

Tsang, H. G., N. A. Rashdan, C. B. Whitelaw, B. M. Corcoran, K. M. Summers and V. E. MacRae (2016). "Large animal models of cardiovascular disease." Cell Biochem Funct **34**(3): 113-132 DOI: 10.1002/cbf.3173.

Tsilimigras, D. I., E. K. Oikonomou, D. Moris, D. Schizas, K. P. Economopoulos and K. S. Mylonas (2017). "Stem Cell Therapy for Congenital Heart Disease: A Systematic Review." Circulation **136**(24): 2373-2385 DOI: 10.1161/CIRCULATIONAHA.117.029607.

Vacanti, C. A., K. T. Paige, W. S. Kim, J. Sakata, J. Upton and J. P. Vacanti (1994). "Experimental tracheal replacement using tissue-engineered cartilage." J Pediatr Surg **29**(2): 201-204; discussion 204-205 DOI: 10.1016/0022-3468(94)90318-2.

van der Bom, T., M. M. Winter, B. J. Bouma, M. Groenink, H. W. Vliegen, P. G. Pieper, A. P. van Dijk, G. T. Sieswerda, J. W. Roos-Hesselink, A. H. Zwinderman and B. J. Mulder (2013). "Effect of valsartan on systemic right ventricular function: a double-blind, randomized, placebo-controlled pilot trial." Circulation **127**(3): 322-330 DOI: 10.1161/CIRCULATIONAHA.112.135392.

Verheugt, C. L., C. S. Uiterwaal, E. T. van der Velde, F. J. Meijboom, P. G. Pieper, A. P. van Dijk, H. W. Vliegen, D. E. Grobbee and B. J. Mulder (2010). "Mortality in adult congenital heart disease." Eur Heart J **31**(10): 1220-1229 DOI: 10.1093/eurheartj/ehq032.

Vincentelli, A., F. Wautot, F. Juthier, O. Fouquet, D. Corseaux, S. Marechaux, T. Le Tourneau, O. Fabre, S. Susen, E. Van Belle, F. Mouquet, C. Decoene, A. Prat and B. Jude (2007). "In vivo autologous recellularization of a tissue-engineered heart valve: are bone marrow mesenchymal stem cells the best candidates?" J Thorac Cardiovasc Surg **134**(2): 424-432 DOI: 10.1016/j.jtcvs.2007.05.005.

von Tell, D., A. Armulik and C. Betsholtz (2006). "Pericytes and vascular stability." Exp Cell Res **312**(5): 623-629 DOI: 10.1016/j.yexcr.2005.10.019.

Wehman, B. and S. Kaushal (2015). "The emergence of stem cell therapy for patients with congenital heart disease." Circ Res **116**(4): 566-569 DOI: 10.1161/CIRCRESAHA.115.305821.

Wehman, B., N. Pietris, G. Bigham, O. Siddiqui, R. Mishra, T. Li, E. Aiello, G. Jack, W. Wang, S. Murthi, S. Sharma and S. Kaushal (2017). "Cardiac Progenitor Cells Enhance Neonatal Right Ventricular Function After Pulmonary Artery Banding." Ann Thorac Surg **104**(6): 2045-2053 DOI: 10.1016/j.athoracsur.2017.04.058.

Wehman, B., S. Sharma, N. Pietris, R. Mishra, O. T. Siddiqui, G. Bigham, T. Li, E. Aiello, S. Murthi, M. Pittenger, B. Griffith and S. Kaushal (2016). "Mesenchymal stem cells preserve neonatal right ventricular function in a porcine model of pressure overload." Am J Physiol Heart Circ Physiol **310**(11): H1816-1826 DOI: 10.1152/ajpheart.00955.2015.

Wiant, A., E. Nyberg and R. C. Gilkeson (2009). "CT evaluation of congenital heart disease in adults." AJR Am J Roentgenol **193**(2): 388-396 DOI: 10.2214/AJR.08.2192.

Witt, R. G., G. Raff, J. Van Gundy, M. Rodgers-Ohlau and M. S. Si (2013). "Short-term experience of porcine small intestinal submucosa patches in paediatric cardiovascular surgery." Eur J Cardiothorac Surg **44**(1): 72-76 DOI: 10.1093/ejcts/ezs638.

Woo, J. S., M. C. Fishbein and B. Reemtsen (2016). "Histologic examination of decellularized porcine intestinal submucosa extracellular matrix (CorMatrix) in pediatric congenital heart surgery." Cardiovasc Pathol **25**(1): 12-17 DOI: 10.1016/j.carpath.2015.08.007.

Woodward, C. S. (2011). "Keeping children with congenital heart disease healthy." J Pediatr Health Care **25**(6): 373-378 DOI: 10.1016/j.pedhc.2011.03.007.

Yap, K. H., R. Murphy, M. Devbhandari and R. Venkateswaran (2013). "Aortic valve replacement: is porcine or bovine valve better?" Interact Cardiovasc Thorac Surg **16**(3): 361-373 DOI: 10.1093/icvts/ivs447.

Yerebakan, C., E. Sandica, S. Prietz, C. Klopsch, M. Ugurlucan, A. Kaminski, S. Abdija, B. Lorenzen, J. Boltze, B. Nitzsche, D. Egger, M. Barten, D. Furlani, N. Ma, B. Vollmar, A. Liebold and G. Steinhoff (2009). "Autologous umbilical cord blood mononuclear cell transplantation preserves right ventricular function in a novel model of chronic right ventricular volume overload." Cell Transplant **18**(8): 855-868 DOI: 10.3727/096368909X471170.

Yuan, S. M. and H. Jing (2009). "Palliative procedures for congenital heart defects." Arch Cardiovasc Dis **102**(6-7): 549-557 DOI: 10.1016/j.acvd.2009.04.011.

Zaidi, A. H., M. Nathan, S. Emani, C. Baird, P. J. del Nido, K. Gauvreau, M. Harris, S. P. Sanders and R. F. Padera (2014). "Preliminary experience with porcine intestinal submucosa (CorMatrix) for valve reconstruction in congenital heart disease: histologic evaluation of explanted valves." J Thorac Cardiovasc Surg **148**(5): 2216-2214, 2225 e2211 DOI: 10.1016/j.jtcvs.2014.02.081.

Zaidi, S. and M. Brueckner (2017). "Genetics and Genomics of Congenital Heart Disease." Circ Res **120**(6): 923-940 DOI: 10.1161/CIRCRESAHA.116.309140.

Zuppinger, C. (2016). "3D culture for cardiac cells." Biochim Biophys Acta **1863**(7 Pt B): 1873-1881 DOI: 10.1016/j.bbamcr.2015.11.036.